IMPROVING ADOPTION OF AQUIFER STORAGE AND RECOVERY IN TEXAS

A Dissertation

by

WADE BENJAMIN SMITH

Submitted to the Office of Graduate and Professional Studies of
Texas A&M University
in partial fulfillment of the requirements for the degree of

DOCTOR OF PHILOSOPHY

Chair of Committee,	Gretchen R. Miller
Committee Members,	Bryan Boulanger
	Peter Knappett
	Zhuping Sheng
Head of Department,	Robin Autenrieth

May 2018

Major Subject: Civil Engineering

ABSTRACT

Only three aquifer storage and recovery systems (ASR) currently operate in Texas, and less than 2% of Texas' future water supplies are expected to come from ASR. Texas water utilities have avoided implementing ASR due to concerns with quality degradation, downgradient movement, and capture by nearby users that minimize recovery efficiency of injected water. This dissertation aims to identify locations for new ASR systems and offer suggestions for operational strategies that can minimize losses of injected water to these processes.

The first study identifies hydrogeologically feasible locations for ASR across the Gulf Coast and Carrizo-Wilcox aquifer systems in Texas, using transmissivity, hydraulic gradient, well density, depth to aquifer, and depth to groundwater using a GIS-based index. Corpus Christi, Victoria, San Antonio, Bryan, and College Station are identified as possible cities where ASR would be a useful water storage strategy.

In the second study, groundwater flow and solute transport models were developed to simulate movement and estimate recovery efficiency of injected water in a large scale (2.27×10^5 m^3/d), multi-well ASR system near San Antonio, Texas. Recovered fraction estimates ranged from 54-90% for the first 9.5 years of actual operations and from 48-84% over a 19 year hypothetical operations scenario depending on longitudinal dispersivity. The results suggest that the same well in which water was injected should also be used for recovery to maximize recovery efficiency, but hydraulic effects between the wells must be accounted for, as they can adversely shift injected plumes away from ideal recovery zones.

The final study altered a previously-developed regional groundwater flow model to simulate and estimate the regional effects of the same ASR system in San Antonio. Such ASR systems may have large hydraulic effects on the nearby aquifer (<=2 miles) over short time scales. Over long time scales (decades), such ASR systems can raise aquifer heads as much as 3 feet 10 miles away. Pumping operations at this ASR facility correlate with both precipitation and other regional aquifer pumping, but precipitation is found to not be the sole predictor of ASR pumping operations. Transport simulations indicate that injected waters do not migrate significantly offsite.

ACKNOWLEDGEMENTS

I would first like to thank my advisor, Dr. Gretchen Miller, for her support during my graduate study. It's been a long process, and I fully recognize that I have been far from the easiest graduate student to advise. However, Dr. Miller has continually encouraged me to press on, even when I considered quitting. She always insisted that my work was publishable and more importantly, valuable, even if I thought otherwise. I am especially grateful for her continuing to advise me as I pursued my doctorate "remotely" from Houston- that opportunity has been and will be important to my family for many years to come.

I would also like to thank my committee members, Dr. Sheng, Dr. Boulanger, and Dr. Knappett for their guidance and support throughout the course of this research. Each of them was always available when I had questions or concerns about research, graduate school, or life in general. They added value to my research and helped me through the entire process.

Many thanks to my fellow members of the Miller Ecohydrology Research Group: Jonathan Sanders, Cody Saville, Andrea Dumont, Courtney Merket, Boris Minot, Charles Bruc, Saheli Majumdar, Si Gou, Tayyab Mehmood, Matthew Ballard, Monica Long, Liting Tao, Jaeyoung Song, Erica Yarbrough, Ryan Andrews, Jingqiu Zhang, and Susana Gonzalez. They have improved my research through great dialogue and questioning. Special thanks to Jonathan Sanders for being a great friend and lab mate, for always inspiring me to think outside the box, and, along with his wife Dr. Adriana Pavia-Sanders, for opening their house to me whenever I needed a place to stay in College Station.

Thanks to Dr. Tony Cahill, Dr. Pete England, Dr. Kelly Brumbelow, Laura Byrd, Joyce Green, Mary Ann Urbanovsky, D'Anne Crain, and Crystal Faust for the conversations we've shared that have made my time in undergraduate and graduate school in the Department of Civil Engineering at Texas A&M such a great experience.

Thanks to all the teachers I've had throughout my life, especially Mrs. Moddrell, Dr. Kuban, Dr. Scheer, Mrs. Buckingham, Mrs. Anderson, Mrs. Millis, and Mr. Shih for instilling in me a passion for math and science. Special thanks also go to Sister Kay, Mrs. Strange, Mrs. Pereira, Mrs. Crook, Mrs. Pastusek, Ms. Strange, Mrs. Cihak, Mrs. Kindred, Mrs. Dickson, and Mrs. Hobgood.

Thanks to my Houston friends and Westbury UMC who have supported me, my family, and my research in many different ways over the last four years. Thanks specifically to the Lloyds, Brewers, Lemons, Heathcocks, Hannah Terry, Behrmans, Yangs, Weltys, Fuersts, Sanders, Patlans, and Tollefsons.

Thanks to my parents, Brad and Judy Smith, and my siblings, Kristen and Josh, for their continued support. The jokes and conversations we shared about my graduate school experience helped more than you know. Mom and Dad, thanks for your support of my education over more than 18 years, both financially and otherwise. You put us in the best schools possible, required us to do our best, and encouraged us to follow our strengths and passions. Without your support, I never would have started graduate school, much less finished it. Thanks to my in-laws, Tim, Elaine, Julie and Kyle for their support of my family and I as well.

Brenham (and any future children we may have), if you ever read this, I want you to know that you can follow your dreams and be whatever you want to be in life, but it will take hard work and sacrifice. Having someone by your side to support you makes it easier and worthwhile. Go hug your mother, and tell her thanks for the sacrifices she has made for Dad and our whole family. I love you and will support you in whatever you want to do in life.

But, most importantly, thank you to my wife, Rebecca. You never had a doubt that I would finish this, even though I never thought I would. Taking seven years to graduate was not my plan when I asked you to marry me, but you have happily stood by me and been my rock through this process. Sure, moving to Houston may have lengthened graduate school for me, but without you and your positive attitude, I never would have finished anyways. I love you and can only hope to repay the debt I owe you over a lifetime of love.

CONTRIBUTORS AND FUNDING SOURCES

This work was supervised by a dissertation committee consisting of Dr. Gretchen Miller [advisor] of the Department of Civil Engineering at Texas A&M University, Dr. Peter Knappett of the Department of Geology and Geophysics at Texas A&M University, Dr. Zhuping Sheng of the Texas A&M AgriLife Research and Extension Center at El Paso and the Department of Biological and Agricultural Engineering at Texas A&M University, and Dr. Bryan Boulanger of the Department of Civil and Environmental Engineering at Ohio Northern University. Matthew Ballard helped with data collection, entry, and analysis of the Carrizo-Wilcox aquifer in Section 2. All other work for the dissertation was completed independently by the student.

Graduate study was supported by a Graduate Merit Fellowship from Texas A&M University. The three projects in this dissertation were also supported by Texas A&M AgriLife Research and the Texas A&M Engineering Experiment Station through a grant from the program "Research, Engineering, and Extension: Creation and Deployment of Water-Use Efficient Technology Platforms."

NOMENCLATURE

Amsl	Above mean sea level
AR	Artificial recharge
ASR	Aquifer storage and recovery
ASTR	Aquifer storage transfer and recovery
CERP	Comprehensive Everglades Restoration Plan
DEM	Digital elevation model
EAA	Edwards Aquifer Authority
EPA	Environmental Protection Agency
EPWU	El Paso Water Utilities
GAM	Groundwater Availability Model
GCD	Groundwater conservation district
GIS	Geographic information system
GMS	Groundwater Modeling System (by Aquaveo, LLC.)
GWDB	Groundwater Database
HB	House Bill
MAE	Mean average error
MAR	Managed aquifer recharge
ME	Mean error
MGD	Million gallons per day
MNW2	Multi-Node Well 2 Package
MODFLOW	Groundwater flow modeling software published by USGS

MT3DMS	Modular, 3-dimensional multi-species transport modeling software
NOAA	National Oceanic and Atmospheric Administration
NS	Nash-Sutcliffe efficiency coefficient
PHREEQC	Geochemical modeling software published by USGS
PHT3D	Reactive transport modeling software
QCSP	Queen City and Sparta (aquifers)
RE	Recovery efficiency
RMSE	Root mean squared error
SAWS	San Antonio Water Supply
SCADA	Supervisory control and data acquisition
SPI	Standard Precipitation Index
TCEQ	Texas Commission on Environmental Quality
TWDB	Texas Water Development Board
UIC	Underground Injection Control (Program)
USDW	Underground source of drinking water
USGS	United States Geological Survey
USDM	United States Drought Monitor

TABLE OF CONTENTS

LIST OF FIGURES

FIGURE Page

LIST OF TABLES

1. INTRODUCTION AND LITERATURE REVIEW

1.1 Overview

Aquifer storage and recovery (ASR) is a water storage alternative applicable to a wide range of hydrogeologic conditions and climates. Historically, Texas water utilities have primarily used surface reservoirs to manage temporal differences in water supply and demand, despite significant evaporative losses. The 2012 Texas State Water Plan primarily prescribes increasing water storage capacity via the construction of additional surface reservoirs throughout the state. Despite the fact that ASR provides additional benefits beyond water storage, including minimized environmental damage and replenished aquifers, it is currently underutilized in Texas, and based on the 2012 water plan, is projected to be in the future as well (Malcolm Pirnie Inc. et al. 2011; TWDB 2012b). A state-commissioned report in 2011 by the Texas Water Development Board (TWDB) indicated that ASR in Texas has been hindered for legal and regulatory reasons and by water utilities' technical concerns, but also noted that these deterrents could likely be alleviated by generating new information and data on ASR and targeting the water community (utilities, lawmakers, consultants) with ASR-related educational opportunities (Malcolm Pirnie Inc. et al. 2011).

The research detailed here seeks to better inform management decisions about ASR by answering a number of existing questions about the hydrogeologic processes that impact ASR and the applicability of ASR in Texas. The first study develops a GIS-based index based on five hydrogeologic factors to identify locations in Texas likely to be conducive to successful ASR systems. The second study develops local groundwater flow and transport models of a large, multi-well ASR system in San Antonio to: assess the recovery efficiency of such ASR systems, determine how source and native waters mix in the spaces between the wells, and offer guidelines for operational decisions that may increase recovery efficiency in those systems. The final study also uses groundwater flow and transport modeling to quantify how a large multi-well ASR system affects the aquifer heads and water quality of the surrounding regional aquifer.

1.2 Aquifer storage and recovery background

Aquifer storage and recovery (ASR) has been shown to be a promising water storage alternative to more traditional methods such as surface reservoirs. ASR is a subset of artificial recharge (AR), which sometimes is also termed managed aquifer recharge (MAR), artificial aquifer recharge (AAR), or artificial recharge and recovery (ARR). According to the EPA, “AR is the enhancement of natural groundwater supplies using man-made conveyances such as infiltration basins or injection wells” (US EPA 2014b). ASR is essentially AR with the additional intention of later recovering some or all of the injected water for various uses. Aquifer storage and recovery systems consist of four main subsystems: storage space (aquifer), injection or recharge facilities (wells, infiltration basins, etc.), extraction or recovery facilities (wells), and source water. All four of these subsystems must work in coordination with each other for an ASR system to successfully store water for later use (Sheng 2005). Many definitions attempt to limit ASR beyond this. Some agencies, like the TWDB, define ASR as only using wells for injection and extraction (TWDB 2012a), while others further limit ASR to injection and extraction in the exact same well (Pyne 2005). These semantic limitations preclude options that can expand the applicability of ASR such as infiltration basins for injection or water movement between wells to facilitate natural aquifer treatment (Maliva and Missimer 2010). El Paso Water

Utilities (EPWU) has found, for instance, that infiltration basins actually are a simpler method of injection in their ASR system, due to both technical and regulatory reasons (Malcolm Pirnie Inc. et al. 2011). This work will consider ASR as the broad system defined by the EPA, even if most of the research only deals with injection and extraction via wells.

ASR, in certain situations, is a better storage alternative than surface reservoirs. Surface reservoirs are faced with challenges such as evaporative losses, sediment accumulation, land consumption, high cost, and ecological impact (National Research Council 2008). ASR systems, deep underground, experience little to no evaporative losses (Bouwer 2002). They also minimize environmental disturbances and land consumption, since they require only a few small facilities at the land surface like pumps, wellheads, and occasionally a treatment plant (Maliva and Missimer 2010). Current and proposed ASR systems indicate that usable storage on the order of 10^6 acre-feet may be attainable at the upper limit, which is comparable to many surface reservoirs in the United States (Maliva et al. 2006). In favorable hydrogeologic conditions, ASR tends to be significantly less expensive than constructing a new surface reservoir, as the main costs are those associated with infrastructure like wells, pumps, and additional distribution lines, as opposed to massive land acquisition, earth movement, and dam construction costs (Khan et al. 2008). However, ASR is not without its own shortcomings and inefficiencies, which will be covered in the next section.

ASR systems can potentially be used in many different settings and scenarios. Many types of aquifers can serve as the storage space, including aquifers that are shallow or deep, fresh or saline, thick or thin, sandstone or limestone, or any other of a number of aquifer classifications (Maliva and Missimer 2010). Furthermore, ASR is applicable in a wide range of climates, as indicated by its successful adoption across the world: arid deserts in the Middle East (Maliva et al. 2011), temperate grasslands and wetlands of the Netherlands (Antoniou et al. 2012), and subtropical wetlands of Florida (Jones and Pichler 2007). Aquifer storage and recovery has been used to provide water storage for a variety of purposes: drinking water supplies for municipalities, minimum environmental stream flows, and protection against seawater intrusion in freshwater aquifers among other uses (Pyne 2005). It also could be used to store water for industrial, agricultural, and energy uses (both for energy generation and oil and gas production purposes). It is important to note here that ASR is not a source of water. It is simply a method of water storage, and thus, excess or unused water supplies must be available. Depending on the intended water use, potentially any water source could be used. Treated or untreated surface water (or stormwater), treated wastewater, and treated or untreated groundwater can all potentially be used as source waters for injection into ASR systems (Sheng 2005). Previous research has shown that untreated municipal wastewater, or minimally treated wastewater, is very difficult to use in an ASR system because of the high potential for well clogging, which for now, precludes it as a feasible water source (Rinck-Pfeiffer et al. 2000). Industrial and oil and gas wastewaters are also likely unfeasible to use as source waters due to their high pollutant concentrations and associated pretreatment requirements.

1.3 Hindrances to aquifer storage and recovery implementation

Despite the many advantages listed above, ASR still has many potential limitations which can decrease the recovery efficiency (RE) of a system, which is defined as the ratio of the volume of usable water recovered to the volume of injected water (Maliva et al. 2006). In terms of surface reservoirs, RE can be thought of as the percentage of water remaining after evaporation and other inefficiencies. A successful ASR system, which is often defined as having a high RE, is dependent on a number of physical, infrastructure, regulatory, and economic factors. This section focuses generally on these issues, except where considerations for ASR systems in Texas differ significantly from the general considerations.

Physical factors that control the performance of an ASR system include, but are not limited to: transmissivity, aquifer thickness, hydraulic conductivity, hydraulic gradient, available aquifer storage capacity, aquifer mineralogical composition, native groundwater quality, and degree of mixing (National Research Council 2008; Maliva and Missimer 2010). Transmissivity (T) values that are too low indicate that volumetric rates for injection and extraction are unacceptably small, while values that are too high indicate potential difficulty storing injected water for significant amounts of time without it flowing out of the recovery zone of the well field. Flat hydraulic gradients are preferred to steep hydraulic gradients, which also indicate the potential for injected water to flow out of the recovery zone of the extraction well. However, thoughtful system design can overcome these factors by injecting into upgradient wells and extracting via separate wells downgradient. Confirming adequate available aquifer storage capacity is vital both to prevent flooding of the land surface in shallow aquifers and potential fracturing of the aquifer matrix via high piezometric heads, and to ensure the investments made in ASR infrastructure. Aquifer mineralogical composition and native water quality are important to determine beforehand, so that any potential adverse effects on recovered water quality or aquifer performance may be identified prior constructing an ASR system (Sheng 2005). A variety of adverse effects could result from mixing between the injected water and the aquifer and its native groundwater, since typically an injected water will not be in equilibrium with either. Biogeochemical reactions between the injected water and the aquifer can result in effects such as aquifer matrix dissolution, clogging, or release of trace elements, which is especially negative when those trace elements include arsenic (Wallis et al. 2011). Even simple mixing between high-quality injected water and lower quality water can lower recovered water quality below acceptable standards. The degree of mixing is itself controlled by several aquifer hydraulic properties including thickness, vertical hydraulic conductivity and leakance, degree and type of heterogeneity, dispersivity, and effective porosity. High degrees of mixing are undesirable when storing freshwater in aquifers with native water of significantly lower quality or where there is a potential for adverse chemical reactions between the source and native waters (Maliva and Missimer 2010). In systems where the source and native waters are chemically compatible and of similar quality, high degrees of mixing may be irrelevant to recovered water quality.

Infrastructure factors that control the performance of an ASR system include, but are not limited to: existing recovery facilities, distances from source and point of use, source water quality, pretreatment and post-treatment requirements, land acquisition, site accessibility, facility maintenance, and energy costs. The presence of existing recovery facilities, such as production wells, can potentially make a water utility's decision to explore ASR easier, since one of the four required subsystems is already in place. Also, existing recovery facilities indicates a water utility's familiarity with groundwater and wells, depending on how long ago the wells in use were drilled. On the other hand, a water utility that has little to no experience with groundwater or wells in general likely will have to overcome a significantly higher learning curve and greater uncertainties before exploring ASR options further. Distances from source waters for injection, and the distance to point-of-use, for recovered waters, drive energy costs and infrastructure requirements related to water transmission over those distances. Source water quality and pretreatment and post-treatment (or treatment after the water has been recovered) requirements all are tightly related to the previous discussion on aquifer mineralogical composition and the impacts of mixing injected and native waters on the quality of the recovered water. Potential for adverse quality effects on the recovered water may necessitate additional pretreatment or post-treatment, depending on the intended water use. Acquiring land is usually a necessary step before installing ASR facilities, but it is important to remember that significantly less land acquisition is required for ASR than for surface reservoirs. Site accessibility accompanies land acquisition and must be considered, but usually isn't one of the controlling factors in the feasibility of ASR systems. Facility maintenance and energy costs also must be evaluated beforehand, but generally aren't the most important factors in determining the success of an ASR system (Maliva and Missimer 2010).

Regulatory issues that control the performance of an ASR system include, but are not limited to: federal, state, and local regulations, nearby aquifer users, political and public support, and environmental, historical, or cultural impacts. Unlike the semantic limitations placed on ASR by its various definitions, different regulatory entities place limits on ASR systems that are backed by the law. At the federal level for example, the Class V Injection Well requirements of the Environmental Protection Agency's (EPA) Underground Injection Control (UIC) Program require that waters injected into or above underground sources of drinking water (USDWs) meet the minimum quality standards for public drinking water (US EPA 2014a). In Texas, this regulation is enforced by the Texas Commission on Environmental Quality (TCEQ), and the minimum standards that must be met are listed in 30 Texas Administrative Code § 290. In Texas, this results in the following working definition of ASR used for drinking water purposes: The injection of water, treated to drinking water standards, into an aquifer via wells or other injection facilities during times of excess, any subsequent storage periods, and the recovery of that water during times of need. Class V injection well requirements are usually very important in the development of ASR systems, as most systems are intended for drinking water purposes. However, non-potable users such as farmers, irrigators, or ranchers must still have a thorough understanding of all governing regulations regarding groundwater in their location.

For instance, since 1904 Texas groundwater law has followed the Rule of Capture doctrine, which colloquially is known as the “law of the biggest pump.” This doctrine states that landowners own the groundwater beneath them, and thus, can pump groundwater from beneath their land at will, with few exceptions. Historically, these exceptions have been limited to the following: pumping with the intent only to harm a neighbor, willful wasting of groundwater, causing land subsidence, pumping from a contaminated well, and trespassing onto another’s property to pump (AgriLife 2013). Potential users of ASR systems in Texas must take extra precautions to protect their valuable injected water from intentional, or unintentional capture by nearby aquifer users. In recent decades the Texas legislature has exercised increasing control over groundwater pumping in Texas to protect this natural resource. 98 Groundwater Conservation Districts (GCDs) exist in Texas, and while the first was created in 1951, 75 have been created since 1990. These entities can regulate both the spacing of and production from water wells, among other things. In certain districts, ASR projects must first apply for permits, and some of these GCDs have additional regulations regarding ASR. For instance, the Evergreen Underground Water Conservation District is not very conducive to ASR systems in that they are currently required to recover no more than 90% of their injected water, which effectively limits the RE of the system to a maximum of 90% (Malcolm Pirnie Inc. et al. 2011). Major aquifers in Texas could potentially also end up being regulated much like the Edwards Aquifer has been by the Edwards Aquifer Authority since 1993. The EAA strictly permits users to only pump certain volumes every year in order to maintain environmental stream flows downstream of the Edwards Aquifer’s springs.

Political and public support are extremely important to the success of ASR systems. Political support helps legislation keep up with technical advancements in ASR technology. Public support is often necessary for funding municipal ASR systems but is less important for private industrial or agricultural applications. In some cases, this support may be hard to gain from the citizens or from any of the public utility’s employees that may lack experience with or knowledge of groundwater usage and principles.

Environmental, historical, and cultural considerations in regards to ASR projects differ little from any other typical infrastructure project, such as determining the presence or absence of endangered species or important cultural artifacts, but still must be considered before selecting a suitable site for an ASR system.

1.4 Usage in Texas

The broad applicability of aquifer storage and recovery is very conceptually attractive to a state the size of Texas, with its wide variety of climates, land cover, land uses, and geologic formations. From a water demand standpoint, Texas’ projected population boom will require significant amounts of additional source waters and water storage capabilities. Based on Texas’ 2012 State Water Plan, new surface reservoirs capable of producing 1,500,000 acre-feet/year anticipated by 2060, while only 81,000 acre-feet/year of production via new ASR systems is anticipated (TWDB 2012b). The toll of worst one year drought in Texas’ history in 2011 is still fresh in the minds of many of its residents and especially its water planners. Surface water evaporation compounded the dramatic water shortages across the state. An estimated 6-8 million acre-feet of reservoir storage were lost to evaporation in 2011 in Texas, which accounted for 22-29% of Texas' total reservoir storage at the beginning of 2011 (Long et al. 2013). Apart from helping to solve Texas' water shortages, ASR also helps to replenish aquifers that have been depleted and overstressed for more than 100 years. Natural aquifer recharge rates are typically much lower than human extraction rates, and without artificial recharge, high quality, easily accessible groundwater in Texas will become increasingly rare.

As discussed before, ASR systems can make use of most types of source waters (excluding untreated wastewaters), which is exemplified in Texas' three operating ASR systems. San Antonio Water System (SAWS) stores excess groundwater from the Edwards aquifer when its permit exceeds its demand, Kerrville stores surface water from the Guadalupe River, and EPWU stores reclaimed wastewater from its Fred Hervey Water Reclamation plant (Malcolm Pirnie Inc. et al. 2011). This flexibility allows municipalities or other water users to tailor ASR systems to their specific situation.

Successful systems in these Texas cities show that ASR is feasible with current technology in today's regulatory environment. San Antonio, Kerrville, and El Paso operate ASR systems rated at 60 (third largest in the nation), 10, and 2.65 million gallons per day. Additionally, Midland once operated an ASR system for several years prior to 2002 and the Colorado River Municipal Water District operated another for 7 years from 1963 to 1970 (Malcolm Pirnie Inc. et al. 2011). However, despite the three current successes and the advantages of ASR listed above, adoption of ASR in Texas has lagged behind other states in the U.S. like Florida, Nevada, and California. The TWDB issued a report in 2011 regarding the past, present, and future use of ASR in Texas, entitled *An Assessment of Aquifer Storage and Recovery in Texas* (Malcolm Pirnie Inc. et al. 2011). Seventeen municipalities across the state with current or previous interest in ASR were polled as part of the report, in addition to the three municipalities currently operating ASR systems. The four most common concerns given for why municipalities have not implemented ASR as part of their water management portfolio include the following:

1. Physical ability to recover stored water
2. Quality of the recovered water
3. Cost-effectiveness of an ASR system
4. Potential for other pumpers to capture the utility's stored water.

Two likely causes for the first concern exist. First, other users could potentially extract water before the injecting water utility can extract it (the same as the fourth concern, likely due to questionnaire wording). Second, injected water could migrate offsite due to physical aquifer properties such as steep hydraulic gradients or large hydraulic transmissivities. Loss of injected water to nearby pumpers in Texas is a reality of the Rule of Capture (Malcolm Pirnie Inc. et al. 2011). Providing for some legal protection of injected water is the easiest solution, but in the absence of changing laws, technical solutions do exist. Such solutions range from simply acquiring more land around an ASR well field to prevent water capture from nearby users, to more complicated operational procedures. Acquired land can easily be leased back to users such as farmers or ranchers to recoup some land acquisition costs. On the other hand, the potential loss of injected water because of steep hydraulic gradients or too conductive formations is a more technical issue with several technical solutions. Using models such as the U.S. Geological Survey's (USGS) MODFLOW (along with a host of pre- and post-processing software that make the model more user-friendly), groundwater flow can be estimated based on parameters including aquifer hydraulic properties, aquifer interactions with surface water features, and inputs such as expected nearby pumping rates. However, accuracy of estimated groundwater flow can vary widely depending on the heterogeneity present in the aquifer. If non-ideal aquifer hydraulic conditions exist nearby, solutions range from simple injection upgradient and extraction downgradient to, again, more complicated operational procedures like altering injection and extraction rates and schedules. Tracer studies and monitoring of aquifer heads and chemical constituents can also help to understand how and where injected water may be moving. While not simple, techniques for keeping groundwater on-site do exist, and education of muncipalities' water departments is likely to help overcome this concern.

1.5 Purposes and objectives of the study

The overall purpose of this dissertation study seeks to increase knowledge of the processes that govern ASR performance as well as determine how ASR systems affect the regional aquifer around them. This dissertation assembles three related topics targeting different objectives of study. The first study, entitled "Assessing Aquifer Storage and Recovery Feasibility in the Gulf Coastal Plains of Texas" uses a GIS-based index to identify areas that are likely to be feasible for ASR implementation based on the hydrogeologic setting. The objectives of this study are three-fold: 1) to develop a method for rating the feasibility of aquifer storage and recovery at regional aquifer scales using commonly available data; 2) to compile a geospatial information system (GIS) database for the Gulf Coast and Carrizo-Wilcox aquifer systems of Texas; and 3) use the database to create feasibility maps suitable for use by regional water planners and other government entities. Areas with the greatest potential need, based on a drought index, and potential sources of water for ASR are also identified.

The second study, entitled “Assessing the Performance of a Large, Multi-Well Aquifer Storage and Recovery System Using a Transport Model” develops groundwater flow and transport models to simulate the complex hydrology of a multi-well ASR system in San Antonio in order to estimate recovery efficiency of the system over time. The objectives of this study include: to verify that large scale, multiple-well ASR systems can achieve high RE of injected waters, to determine the shape and character of the mixing zones within and around such a well field, and to offer guidelines for operational decisions that may help to increase RE in those systems.

The final study, entitled “Modeling the Regional Effects of a Large, Multi-Well Aquifer Storage and Recovery System” uses a regional groundwater flow model to quantify the effects and benefits an ASR system in San Antonio has on the regional aquifer around it. The objectives of this study include: determining any potential relationship between precipitation and ASR operations, evaluating the short-term and long-term effects of an ASR system on the surrounding aquifer heads, and evaluating any water quality effects the ASR system may have on the surrounding aquifer.

2. ASSESSING AQUIFER STORAGE AND RECOVERY FEASIBILITY IN THE GULF COASTAL PLAINS OF TEXAS*

2.1 Overview

Study Region: The Gulf Coast and Carrizo-Wilcox aquifer systems in the Gulf Coastal Plains of Texas.

Study Focus: Aquifer storage and recovery is a water storage alternative that is underutilized in Texas, a state with both long periods of drought and high intensity storms. Future water storage plans in Texas almost exclusively rely on surface reservoirs, which are subjected to high evaporative losses. This study seeks to identify sites where aquifer storage and recovery (ASR) may be successful, especially in recovery of injected waters, by analyzing publicly-available hydrogeologic data. Transmissivity, hydraulic gradient, well density, depth to aquifer, and depth to groundwater are used in a GIS-based index to determine feasibility of implementing an ASR system in the Gulf Coast and Carrizo-Wilcox aquifer systems.

New Hydrological Insights for the Region: Large regions of the central and northern Gulf Coast and the central and southern Carrizo-Wilcox aquifer systems are expected to be hydrologically feasible regions for ASR. Corpus Christi, Victoria, San Antonio, Bryan, and College Station are identified as possible cities where ASR would be a useful water storage strategy.

---

* Reprinted from original publication: Smith, W. Benjamin, Gretchen R. Miller, and Zhuping Sheng. 2017. Assessing aquifer storage and recovery feasibility in the Gulf Coastal Plains of Texas. *Journal of Hydrology: Regional Studies*. 14: 92-108.

2.2 Introduction

Aquifer storage and recovery (ASR) is a water storage alternative applicable to a wide range of hydrogeologic conditions and climates. ASR is a subset of managed aquifer recharge (MAR), which sometimes is also termed artificial recharge, artificial aquifer recharge, or artificial recharge and recovery (Dillon 2005; Sheng and Zhao 2015). For most purposes, aquifer storage and recovery systems consist of four main subsystems: storage space (aquifer), injection or recharge facilities (wells, infiltration basins, etc.), extraction or recovery facilities (wells), and source water. All four of these subsystems must work in coordination with each other for an ASR system to successfully store water for later use (Sheng 2005).

ASR has many advantages over surface reservoirs: little to no evaporative losses, minimized environmental disturbances and land consumption, and lower costs (Bouwer 2002; Khan et al. 2008; Maliva et al. 2006; Maliva and Missimer 2010; National Research Council 2008). ASR is highly adaptable and can be used in a variety of aquifer types (e.g., shallow or deep, fresh or saline, thick or thin, sandstone or limestone (Maliva and Missimer 2010)), in a wide range of climates (e.g., arid deserts (Maliva et al. 2011), temperate grasslands and wetlands (Antoniou et al. 2012), and subtropical wetlands (Jones and Pichler 2007)), and to provide storage for a range of applications (e.g., drinking water supplies for municipalities, minimum environmental stream flows, and protection against seawater intrusion in freshwater aquifers among other uses (Pyne 2005)).

Two primary methods for determining ASR site suitability have been used in recent years. The more common practice is to develop a qualitative suitability index that classifies factors relevant to ASR suitability and combines them in a weighted sum. For instance, CH2MHILL, an engineering consulting firm, created a tool to assess feasibility of ASR in South Florida for the St. John's River Water Management District (CH2MHILL 1997). The Comprehensive Everglades Restoration Project (CERP) created a site selection suitability index to evaluate the feasibility of potential ASR sites that could be used in the restoration of the Everglades. They implemented the suitability index in GIS (Brown et al. 2005). Eastwood and Stanfield (2001) also employed a qualitative approach while stressing the importance of environmental acceptability as the more important success factor compared to water quality considerations. They argued water quality can be "engineered out" to not be an absolute hindrance to ASR like potential environmental damage, noting the economics of ensuring high quality recovered water may still eventually render specific ASR projects unfeasible (Eastwood and Stanfield 2001). Most other published research focuses on estimating suitability for managed aquifer recharge projects, especially those involving surficial infiltration, as opposed to the injection and extraction via wells of aquifer storage and recovery (Fernandez Escalante et al. 2014; Ghayoumian et al. 2007; Malekmohammadi et al. 2012; Pedrero et al. 2011; Rahman et al. 2012; Rahman et al. 2013). Smith and Pollock's (2012) approach is interesting to note, as they applied an analytical model for managed aquifer recharge via infiltration over an area to identify feasible MAR locations in a more quantitative manner than the other multi-criteria decision methods. Bridging the gap between subsurface ASR systems and MAR surficial systems, Russo et al. (2015) estimated the feasibility of managed aquifer recharge sites in California by weighted sum of classified factors, accounting for both potential surface infiltration and subsurface injection systems.

More quantitative methods for estimating the feasibility of locations for ASR-specific systems have been developed as well. These methods involve deriving dimensionless parameters that describe a physical process governing the recovery efficiency of an ASR system. Bakker (2010) created a dimensionless parameter based on well discharge, hydraulic conductivity, aquifer thickness, and dimensionless density difference, and used it along with the relative lengths of injection, storage and recovery periods to evaluate potential feasibility of ASR in saltwater aquifers. Ward et al. (2009) developed four additional dimensionless parameters to describe three major governing factors of ASR recovery efficiency: lateral flow, density-driven flow, and dispersive mixing. They proposed that these parameters could be used to help identify suitable ASR sites if sufficient data were available. The dimensionless parameters of Bakker (2010) and Ward et al. (2009) were evaluated separately to assess their effectiveness at predicting ASR site suitability in a coastal area of the Netherlands using GIS, and both were shown to be effective at predicting successful ASR sites (Zuurbier et al. 2013). Characterization of suitable regions by parameters with real physical significance, instead of simple qualitative characterizations like 'very suitable,' 'suitable,' or 'unsuitable' can provide valuable information to water resource managers.

Historically, Texas water utilities have primarily used surface reservoirs to manage temporal differences in water supply and demand, despite significant evaporative losses. The 2012 Texas State Water Plan, published by the Texas Water Development Board (TWDB), primarily prescribes increasing water storage capacity via the construction of additional surface reservoirs throughout the state. Despite the fact that ASR provides additional benefits beyond water storage, including minimized environmental damage and replenished aquifers, it is currently underutilized in Texas, and based on the 2012 water plan, is projected to be in the future as well (Malcolm Pirnie Inc. et al. 2011; TWDB, 2012b) . ASR can never completely replace surface storage, as it cannot match some benefits of surface storage, especially in regards to storm water management. Surface and subsurface storage of freshwater provide complementary benefits to water providers, and both should be considered for future storage needs.

ASR, when implemented as part of a water storage portfolio, can help Texas achieve water security and replenish aquifers that have been depleted and overstressed for more than 100 years. Natural aquifer recharge rates are typically much lower than anthropogenic extraction rates, and without artificial recharge, groundwater as a readily accessible natural resource in Texas will become increasingly rare. A 2011 TWDB report on ASR use in Texas found that the biggest concerns of municipalities in regards to ASR were the ability to physically recover stored water and degradation of water quality during storage, both of which highlight the need for additional information on aquifer storage spaces across the state.

This work focuses on the potential feasibility of systems that both inject and extract water from an aquifer via wells. Previous ASR feasibility indices have required significant amounts of site-specific data to assess feasibility at specific locations, which make large, regional scale analyses difficult. The objectives of this study are three-fold: 1) to develop a method for rating the feasibility of aquifer storage and recovery at regional aquifer scales using commonly available data; 2) to compile a geospatial information system (GIS) database for the Gulf Coast and Carrizo-Wilcox aquifer systems of Texas; and 3) use the database to create feasibility maps suitable for use by regional water planners and other government entities. Specifically, we define ASR as both injection into and extraction from the aquifer occurring via wells. We also view ASR feasibility through the lens of a municipality seeking seasonal or long term water storage in an aquifer, such that locations which will likely minimize injected water losses, operational costs, and constructions costs are given the highest ratings. The mapping scales chosen are appropriate for use in selection of sites where pilot studies or more detailed engineering studies should be conducted. This mapping exercise is not a replacement for detailed investigations prior to the installation of an ASR system.

2.3 Materials and methods

2.3.1 Study areas

Both the Gulf Coast and Carrizo-Wilcox aquifer systems in Texas' Gulf Coastal Plains were evaluated for their feasibility of implementing ASR systems. The primary aquifers within the Gulf Coast system are the Chicot, Evangeline, and Jasper aquifers. The primary aquifers in the Carrizo-Wilcox system are the Carrizo, Middle Wilcox, and Simsboro aquifers. The Simsboro aquifer represents the middle unit of the Wilcox group in the central portion of the Carrizo-Wilcox, and is therefore treated as one "Wilcox" aquifer along with the Middle Wilcox unit from the northern and southern portions of the study area (Deeds et al. 2003; Dutton et al. 2003). While the TWDB readily provides each aquifer system's boundaries, as shown in Figure 2.1, each constituent aquifer's boundaries are less clear. In this study, aquifer boundaries were defined by the maximum geographic extent of the wells screened into each aquifer, based on the TWDB's Groundwater Database (GWDB) (TWDB, 2015). The GWDB primarily encompasses only the freshwater regions of these aquifers above their "brackish water lines," typically defined in Texas where the total dissolved solids concentration is equal to 3000 mg/L. Therefore, this study implicitly considers only freshwater aquifers when determining feasible locations for ASR.

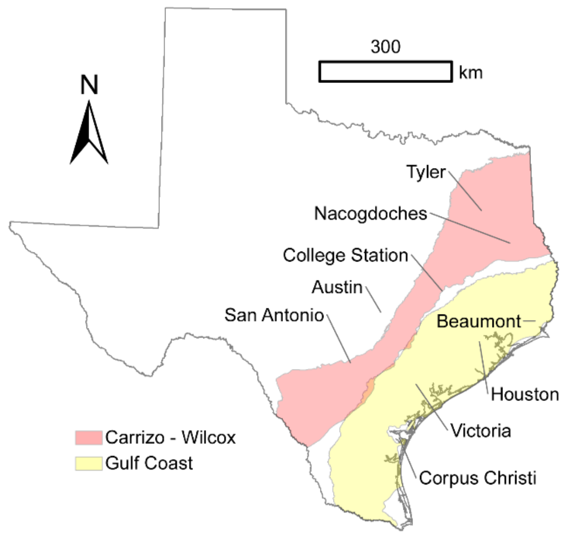

Figure 2.1: Aquifer systems in the region of interest with selected cities shown.

The Gulf Coast aquifer system's major units, as seen in Figure 2.2, are the Chicot aquifer, Evangeline aquifer, Burkeville confining unit, Jasper aquifer, and Catahoula confining unit (only in the northern portion of the aquifer system) (Kasmarek 2013). Changes in ancient sea levels and in deposited sediment flux and sources led to the discontinuous beds of sand, gravel, silt, and clay that comprise the three aquifer units. Subsidence of the depositional basin and rising land surfaces caused many of the units of the Gulf Coast aquifer to thicken downdip. These changes, along with growth faults in the area, contributed to the heterogeneity seen today in the strata of the Gulf Coast aquifer (Baker 1979).

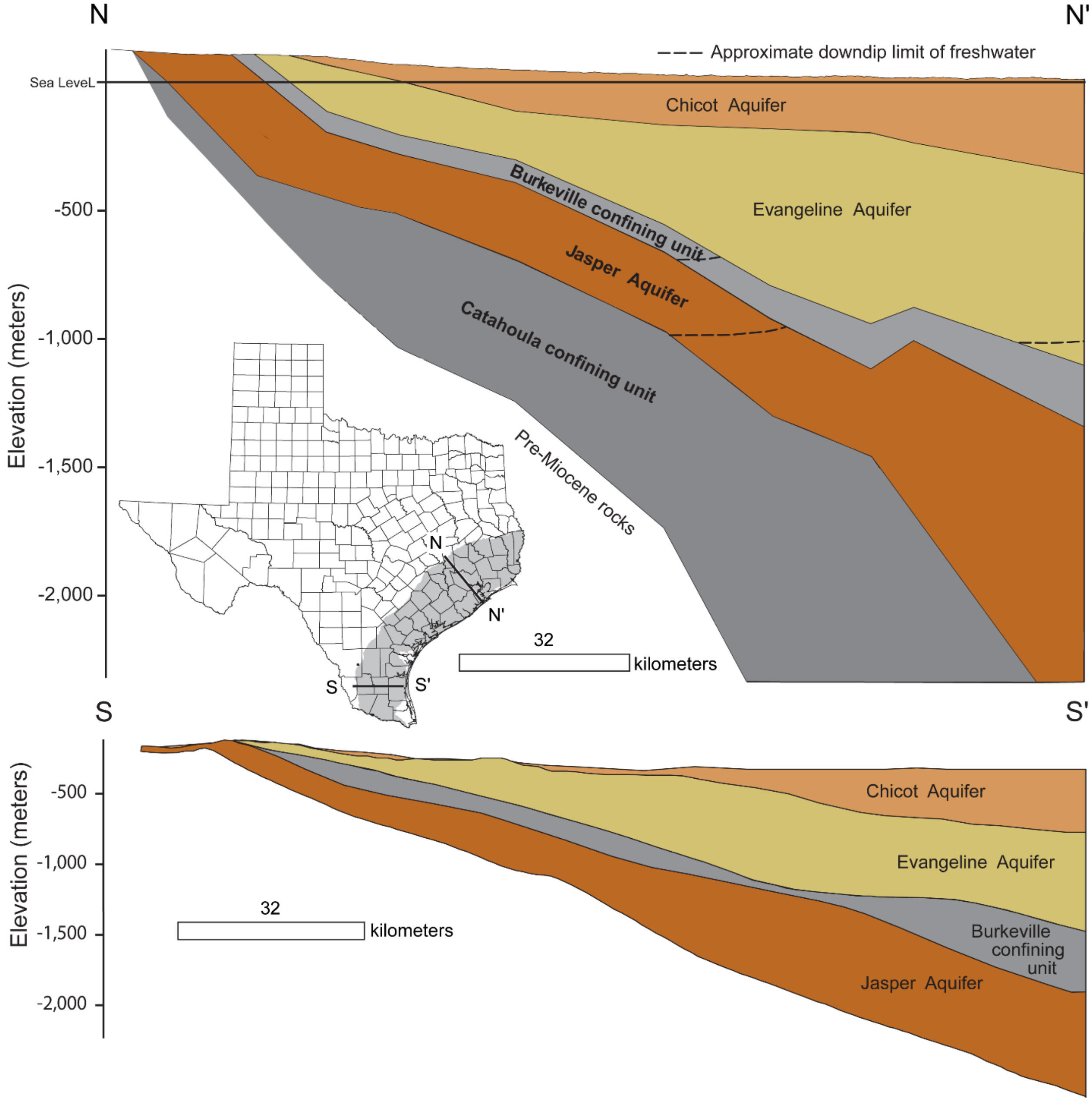

Figure 2.2: Structural cross sections of the Gulf Coast aquifer system (modified from George et al., 2011).

The Carrizo-Wilcox aquifer system is comprised of the Carrizo aquifer and the Wilcox group beneath it, both of which were deposited along the Gulf of Mexico between 50 and 60 million years ago, when the coastline was 240 – 320 kilometers inland relative to its current location (Mace et al. 2000). The Carrizo unit is overlain by the confining Reklaw, which itself is overlain by other layers including the Queen City and Sparta aquifers as shown in Figure 2.3. There are also some incomplete hydraulic barriers in the lower Carrizo and middle and upper Wilcox units (Mace et al. 2000). The aquifer is primarily sand or sandstone, but is locally interbedded with gravel, silt, clay, and lignite (George et al. 2011).

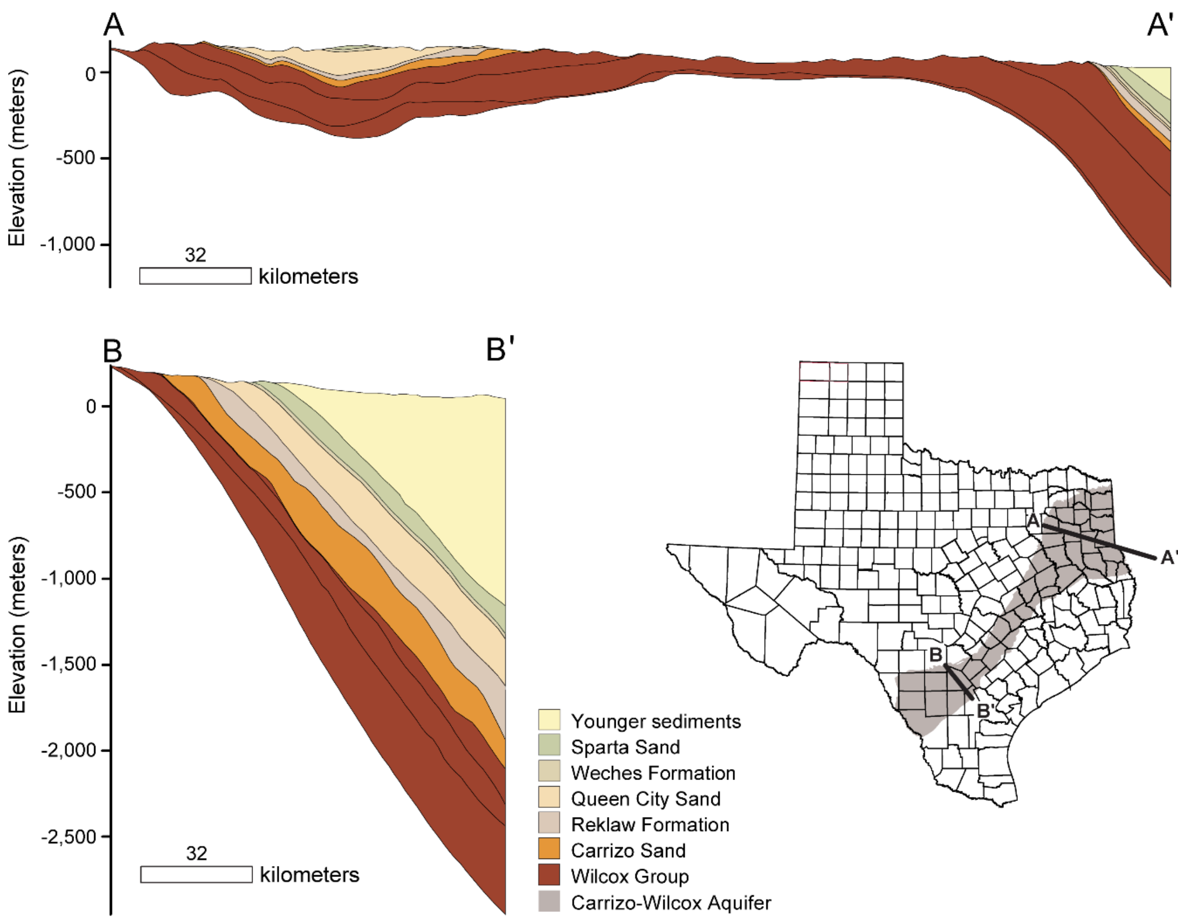

Figure 2.3: Structural cross sections of the Carrizo-Wilcox aquifer system (modified from George et al., 2011).

2.3.2 Determining ASR feasibility scores

Public data for Texas aquifers do not exist at the required resolution or scale to evaluate the more physically based factors of Bakker (2010) and Ward et al. (2009). Therefore, a classified and weighted factor analysis was used on factors that could be determined at useful scales and resolutions. In this study the relative feasibility of ASR across each of the five aquifers was estimated based on the following five hydrogeologic factors: transmissivity, hydraulic gradient, density of existing wells, depth to the potentiometric surface, and depth to the top of the aquifer formation. These factors were chosen based on both their potential to affect ASR feasibility and the existence of large scale datasets across each aquifer. The data used to map these factors came from several sources, including the TWDB Groundwater Database, TWDB Groundwater Availability Models data, and historical reports (Chowdhury and Mace 2007; Deeds et al. 2003; Dutton et al. 2003; Fryar et al. 2003; Kasmarek 2013; TWDB, 2015; Waterstone Inc. and Parsons Inc. 2003; Young et al. 2012). Based on the smallest scale of the datasets used in this study, a spatial resolution of 1.6 kilometers was used.

In order to standardize comparisons between the factors, data were reclassified based on a relative ranking system, with higher numbers indicating areas expected to be more feasible for ASR systems and zeros indicating that no data were available. The factors were then combined via weighted sum to determine an overall expected feasibility rating from 0 to 100 (Figure 2.4). The rationale for determining the weights and rankings for each hydrogeologic variable is described below and summarized in Figure 2.5.

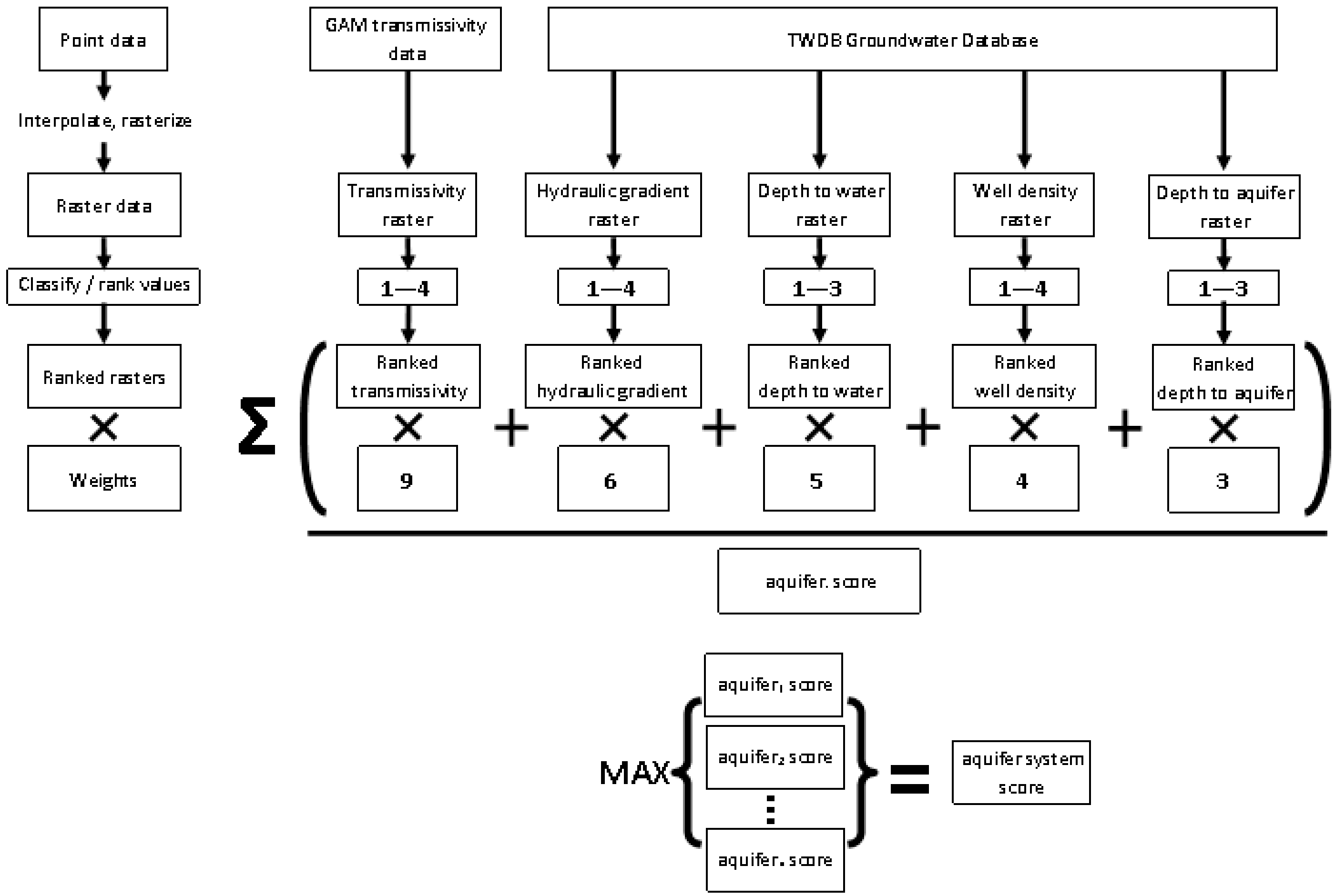

Figure 2.4: Process flow chart with relative weights and reclassification rankings for the five selected hydrogeologic factors.

All aquifers

Transmissivity (m^2/d)	
Class	Score
0 - 230	1
230 - 700	2
700 - 1160	3
1160 - 1630	4
1630 - 2550	3
2550 - 3950	2
> 3950	1

Well Density (wells/km^2)	
Class	Score
0	4
0.39	3
0.77	2
> 0.77	1

Hydraulic Gradient	
Class	Score
0 – 0.1	4
0.1 – 0.2	3
0.2 – 0.3	2
> 0.3	1

Gulf Coast aquifer system

Depth to Aquifer (m)	
Class	Score
< 57	3
57 - 138	2
> 138	1

Depth to Groundwater (m)	
Class	Score
< 12	3
12 - 26	2
> 26	1

Carrizo-Wilcox aquifer system

Depth to Aquifer (m)	
Class	Score
< 88	3
88 - 198	2
> 198	1

Depth to Groundwater (m)	
Class	Score
< 23	3
23 - 50	2
> 50	1

Figure 2.5: Reclassification ranges for each of the five selected hydrogeologic factors, with the respective ranges of the Gulf Coast aquifer system (GC) and Carrizo-Wilcox aquifer system (CW) for the depth to aquifer and depth to groundwater factors.

2.3.2.1 Transmissivity

Transmissivity is an important factor in determining the feasibility of ASR systems, as it affects both injection rates and retention of injected waters near recovery wells (Maliva and Missimer 2010). Aquifers with low transmissivities may not be able to inject, and thus store, water at usable rates, while aquifers with high transmissivities may allow too much migration of injected water out of the recoverable radius of wells. This depends also on regional hydraulic gradients. Transmissivity values were reclassified from 1-4 as shown in Figure 2.5, with both low and high values of transmissivity receiving the lowest possible score for the reasons described above. These classifications are based on previous ASR site suitability indices (Brown et al. 2005; CH2MHILL 1997). Transmissivity data were primarily sourced from the Groundwater Availability Models (GAMs) for each aquifer, commissioned by the TWDB (Chowdhury and Mace 2007; Deeds et al. 2003; Dutton et al. 2003; Fryar et al. 2003; Kasmarek 2013; Waterstone Inc. and Parsons Inc. 2003). When available in sufficient coverage and resolution, transmissivity data were used, otherwise the product of hydraulic conductivity and aquifer thickness from the GAMs were used. Aquifer thickness was derived from GAM source data first, and if not present or available, was digitized and interpolated from historical aquifer maps (Baker 1979). For both the Gulf Coast and Carrizo-Wilcox, three GAMs each were performed by various consultants, representing the Northern, Central, and Southern portions of each aquifer system. As the GAMs were completed by various consulting firms and agencies, the transmissivity datasets varied based on available sources and issues encountered during modeling. For instance, the central Gulf Coast GAM calculated layer transmissivities as the product of its estimated sand thicknesses and geometric mean hydraulic conductivity (Waterstone Inc. and Parsons Inc. 2003), while the northern Gulf Coast GAM used digitized transmissivity estimates from the literature (Baker Jr. 1986; Carr et al. 1985; Kasmarek 2013). Transmissivity data were preferentially used in the following order: historic values from the literature, values estimated in the GAM process, values calibrated in the GAM process, and finally values that were derived from GAM hydraulic conductivity estimates and thicknesses of the aquifer from other historical reports.

2.3.2.2 Hydraulic gradient

Hydraulic gradient is another important factor in the design of ASR systems as it affects the ability to keep injected water on site (Maliva and Missimer 2010). Steep regional gradients may move injected water out of recoverable zones, especially if storage times are long or transmissivities are high. Therefore, lower regional hydraulic gradients are seen as much more feasible for implementing an ASR system. Hydraulic gradient was reclassified from 1 – 4, as described in Figure 2.5, in part based on results from a simulated modeling study by Lowry and Anderson where recovery efficiency was related to regional hydraulic gradient (2006). The slope of each aquifer's estimated potentiometric surface was used to represent the regional hydraulic gradient. The elevation of the potentiometric surface was generated by kriging 15-year-average water levels. Only wells with sufficient water level data in the TWDB's Groundwater Database were used to calculate these 15-year-average water levels (TWDB, 2015). Sufficient water level data were defined as having one or more publishable, representative measurements (i.e. not during pumping or other disturbance) from 2000-2015, with the standard deviation of all such water levels in each well not exceeding 4.5 meters.

2.3.2.3 Depth to potentiometric surface

Depth to the potentiometric surface, simplified elsewhere in this text as depth to groundwater, is used as a proxy for energy usage required to extract water during recovery phases, with greater depths being deemed less feasible since more energy would be required to recover water. Depth to groundwater was reclassified from 1 – 3 based on the terciles of the depth to groundwater values for the GWDB wells in each aquifer system (TWDB, 2015). Depth was calculated as the difference between the digital elevation model (DEM) of the land surface and the potentiometric surface elevation, described in 2.3.2.2.

2.3.2.4 Depth to aquifer

Depth to aquifer is kriged from well depths in each aquifer. This factor is a proxy for construction ease and costs, where deeper wells would be more expensive or less feasible for an ASR system. Similar to depth to groundwater, depth to aquifer was reclassified from 1 – 3 based on the terciles of well depths within each aquifer system (Figure 2.5). The well depths are those given for the wells in the GWDB (TWDB, 2015). Thus, this factor attempts to indicate the typical depth at which each aquifer is being used in given area, instead of the depth to the top or middle of the aquifer.

2.3.2.5 Density of existing wells

Well density determines the potential for nearby wells to extract stored water or otherwise interfere with an ASR system’s performance (i.e. by increasing the regional hydraulic gradient or potentially polluting the aquifer). Wells were counted in each 2.6 square kilometer cell and reclassified from 1 – 4 according to Figure 2.5. Well density is based on the locations of all the wells defined in the GWDB for each aquifer (TWDB, 2015). The wells used to calculate this well density clearly do not include all wells screened in each aquifer, however, we assume that they are representative of the overall trend.

2.3.3 Limitations

Assumptions made in this analysis may not apply to every city in the region, so it is possible that the cities identified in the results are not the only locations where ASR is viable in the Gulf Coastal Plain. Other cities may expand their search radius for locations with high ASR feasibility scores or may have water sources or needs beyond what was considered in this study. This analysis is meant to serve as a starting point for identifying areas where ASR may be well suited. Clearly, more factors than the five identified here, such as storage capacity and compatibility of source and native waters, are important to the success of an ASR system. Factors were omitted from this study for one of two main reasons. First, many factors lacked adequate regional scale data. Second, other factors like compatibility of source and native waters, are highly complex, site-specific, and often dependent on design choices. Other non-physical factors also affect the feasibility of ASR systems. For example, laws and boundaries may sometime supersede physical factors when selecting ASR sites. These sociopolitical factors are not static; since this study began, Texas passed HB 655 in 2015 in order to make the permitting process easier for implementing ASR systems. GCDs, which have the power to regulate ASR systems, are still being created, with two new GCDs beginning in 2015 and another GCD yet to be confirmed via election.

2.4 Results and discussion

2.4.1 ASR feasibility scores

2.4.1.1 Scores for the Gulf Coast aquifer system

The estimated and reclassified, or ranked, values of each of the five factors are shown in Figure 2.6 for the three aquifers that comprise the Gulf Coast aquifer system. The influence of the greater Houston area on the Chicot and Evangeline aquifers can be seen in each of the three human-induced factors of hydraulic gradient, well density, and depth to groundwater in Figure 2.6. Significant numbers of wells in the area appears to have contributed to regional groundwater depressions, resulting in lower ranked scores for all three human-induced factors.

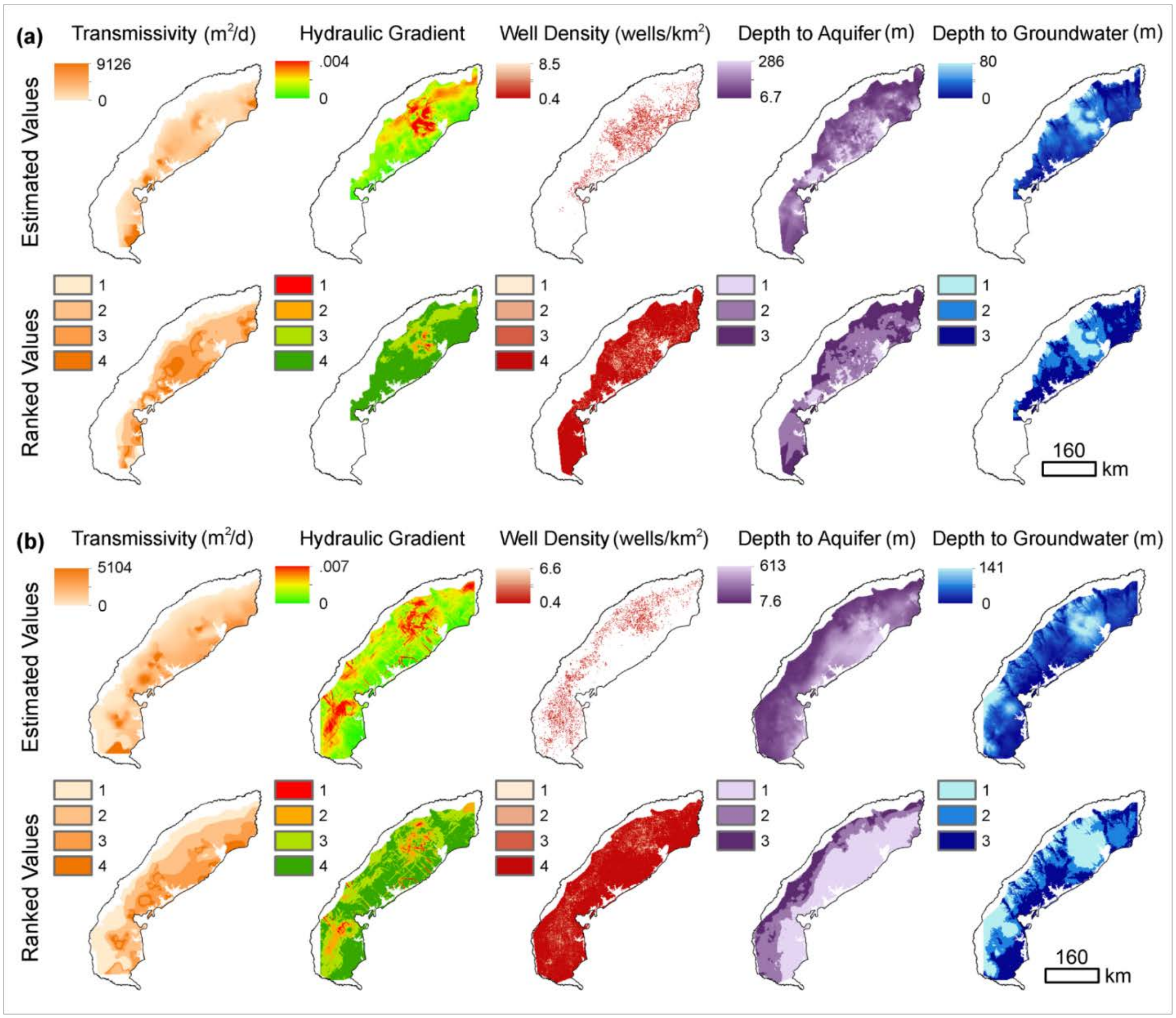

Figure 2.6: Maps of estimated and ranked values for transmissivity, hydraulic gradient, well density, depth to aquifer, and depth to groundwater for the Chicot (a), Evangeline (b), and Jasper (c) aquifers in the Gulf Coast aquifer system.

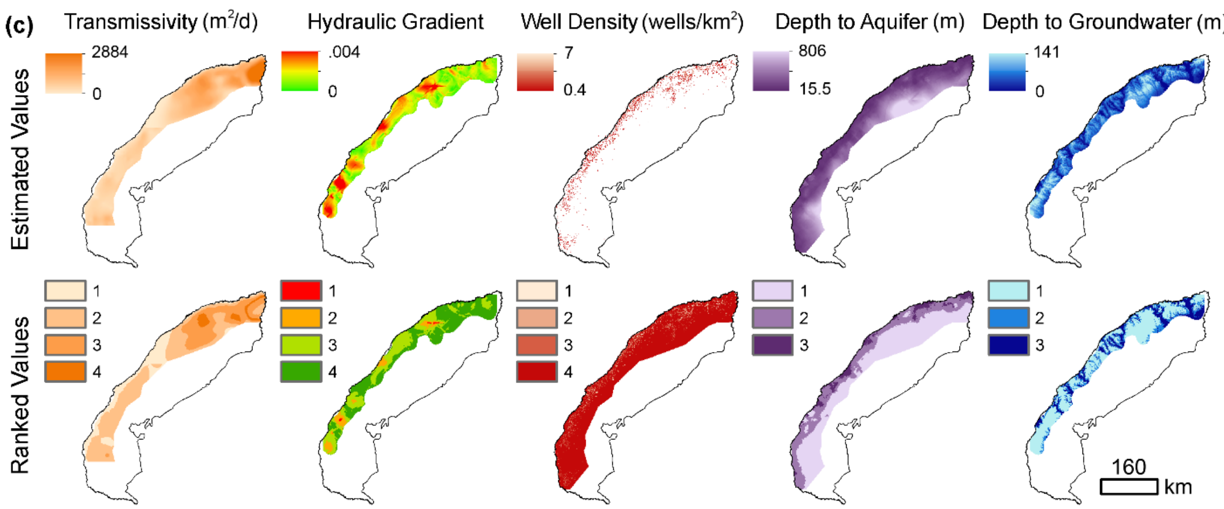

Figure 2.6: Continued.

Figure 2.7 represents the weighted-sum ASR feasibility score for each Gulf Coast aquifer, using the weights from Figure 2.4 and the ranked value datasets from Figure 2.6. The influence of the greater Houston area, seen in the human-induced factors in Figures 2.6a and 2.6b, is also apparent in these ASR feasibility scores for the Chicot and Evangeline aquifers. ASR feasibility scores in the greater Houston area are among the lowest in the areas with full data coverage for each factor. Lower scores do exist in some aquifer regions, but generally only on the edges of aquifers where some datasets do not exist.

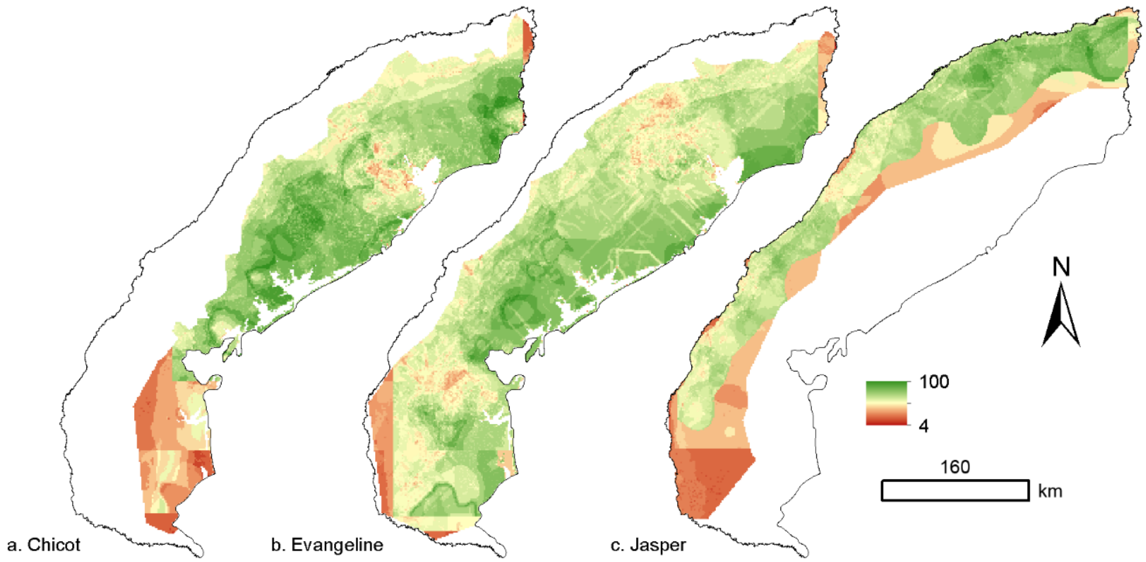

Figure 2.7 (a-c): ASR feasibility ratings for the Chicot, Evangeline, and Jasper aquifers in the Gulf Coast aquifer system.

The maximum ASR feasibility score from the set of the Chicot, Evangeline, and Jasper aquifers was determined for each location (Figure 2.8). Generally, it appears that the central and northern regions of the Gulf Coast aquifer system are the most feasible for ASR systems, especially around cities like Victoria and Beaumont. Areas south of Corpus Christi appear to be generally less feasible. These lower scores are partially due to a lack of water level data in the Chicot and Jasper aquifers in the southern region, but also because the primary aquifer in the region, the Evangeline, is characterized by lower groundwater levels, steeper regional hydraulic gradients, and small transmissivities.

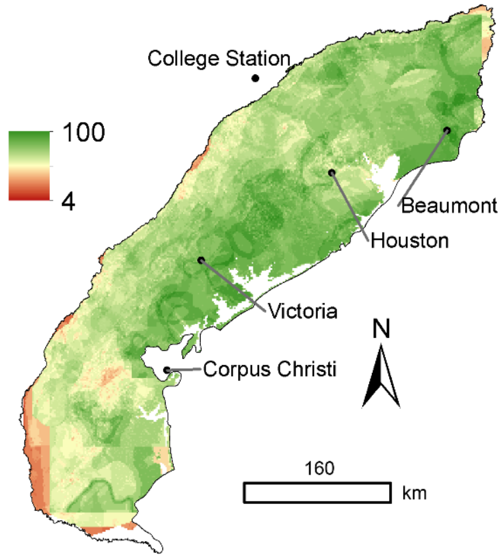

Figure 2.8: Maximum ASR feasibility ratings for the Gulf Coast aquifer system, as defined by the highest feasibility rating of the constituent aquifers (Chicot, Evangeline, or Jasper) in each location, with selected cities shown.

2.4.1.2 Scores for the Carrizo-Wilcox aquifer system

The estimated and reclassified, or ranked, values of each of the five factors are shown in Figure 2.9 for the Carrizo and Wilcox aquifers. Similar to the effects of Houston, the effects of groundwater usage around the cities of Nacogdoches and Tyler in the Carrizo aquifer are evident in the human-induced factors of hydraulic gradient and depth to groundwater. However, the areas around both of these cities also have low ranked values for transmissivity and depth to aquifer, which contribute to the significantly lower ASR feasibility scores (Figure 2.10) compared to most of the rest of the Carrizo aquifer. The wellfield for the Bryan/College Station metro area is slightly to its northwest in the Carrizo aquifer, but appears to show little human influence on the groundwater table or hydraulic gradient (Figure 2.9). This is most likely due to low density in this area of water level data from the TWDB’s Groundwater Database deemed suitable as described in Section 2.3.2. Previous studies (George et al. 2011) have indicated a significant drawdown cone near this area, which would decrease the ranked values for these two factors from those shown here. The high ranked values for transmissivity near Bryan/College Station and the rest of the Central Carrizo region (Figure 2.9) suggests the possibility of feasible ASR locations there (Figure 2.10).

The central and southern regions of the Carrizo-Wilcox appear to be the most feasible areas in either aquifer system (Figure 2.11), including near Bryan/College Station and San Antonio. We note that both Bryan and College Station are currently conducting ASR feasibility studies, while San Antonio is one of only three cities in Texas currently operating an ASR system.

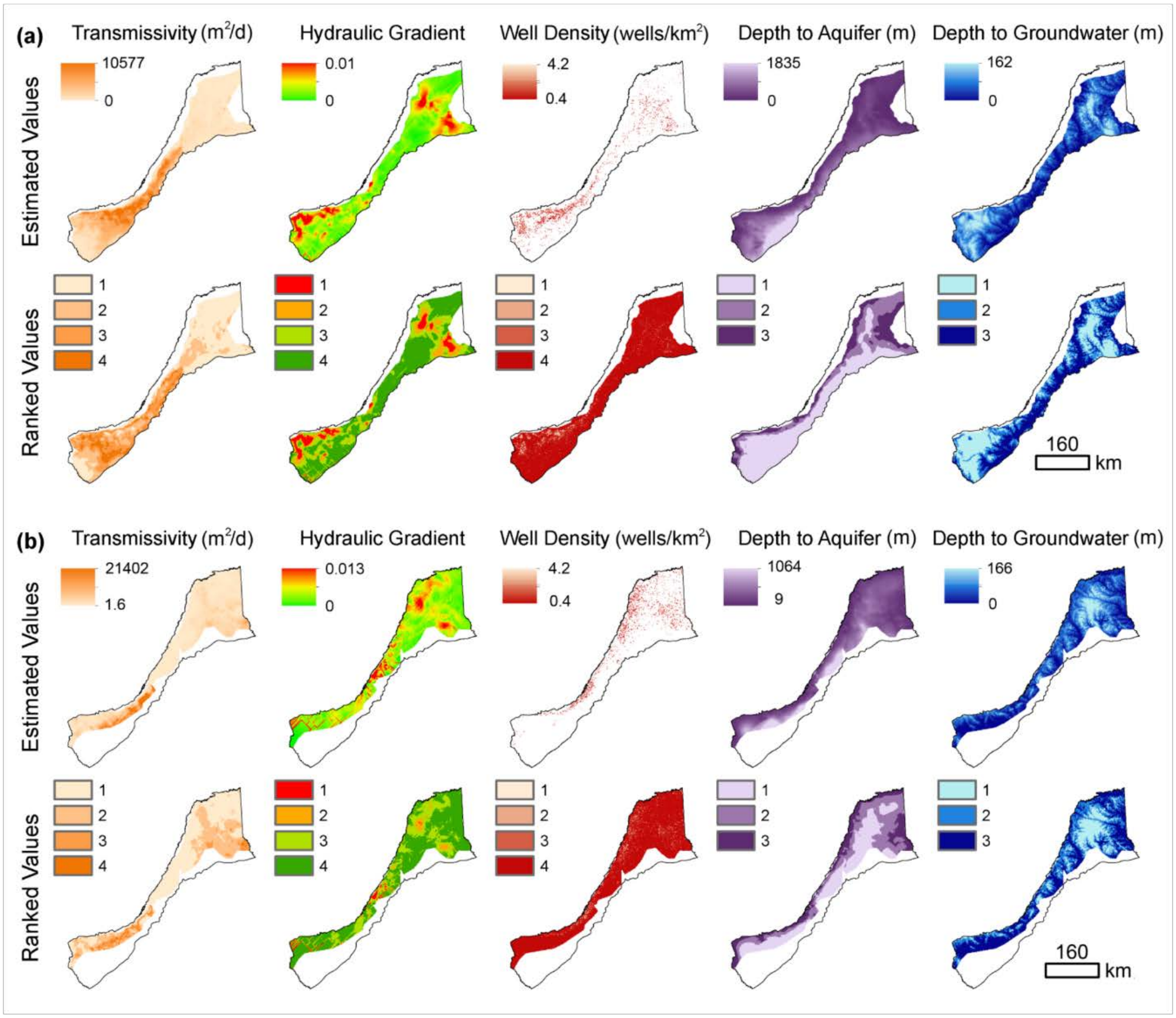

Figure 2.9 (a, b): Maps of estimated and ranked values for transmissivity, hydraulic gradient, well density, depth to aquifer, and depth to groundwater for the Carrizo (a) and Wilcox (b) aquifers in the Carrizo-Wilcox aquifer system.

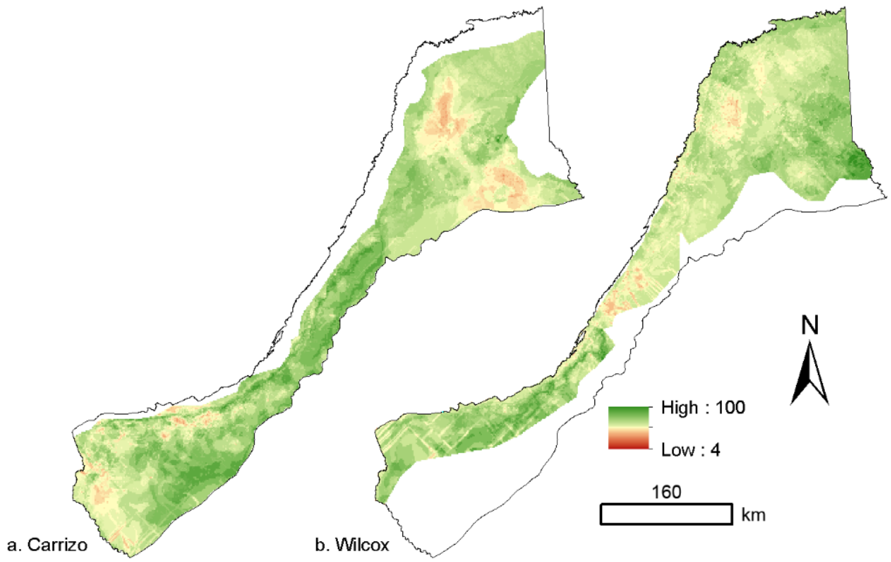

Figure 2.10 (a, b): Overall ASR feasibility ratings for the Carrizo and Wilcox aquifers in the Carrizo-Wilcox aquifer system.

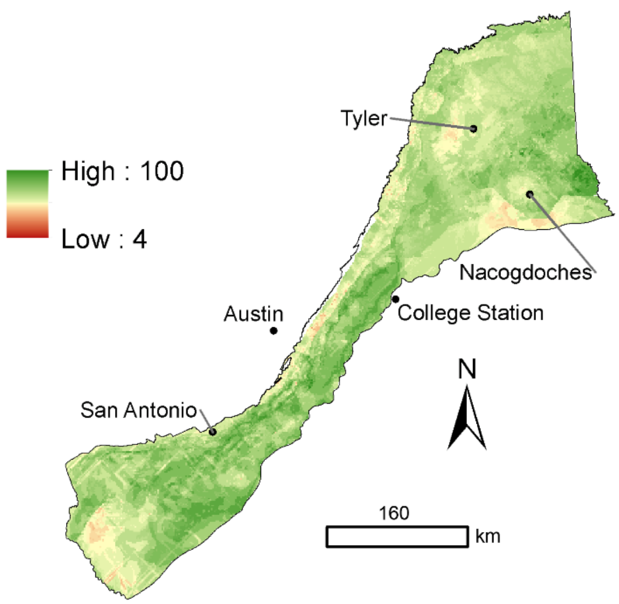

Figure 2.11: ASR feasibility ratings for the Carrizo-Wilcox aquifer system, as defined by the maximum feasibility rating of the constituent aquifers (the Carrizo or Wilcox) in each location, with selected cities shown.

2.4.2 Current ASR facilities in study area

San Antonio Water System (SAWS) opened the H2Oaks (formerly Twin Oaks) ASR facility, a multi-well ASR system south of the city in the Carrizo aquifer, in 2004 (CH2MHILL 2006). This 230 ML/d facility, with 29 dual purpose ASR wells, was developed to store Edwards aquifer water in order to fully utilize SAWS' annual Edwards aquifer water permit. The Edwards aquifer, governed by the Edwards Aquifer Authority, legally functions similarly to surface reservoirs in Texas. However, the Carrizo-Wilcox aquifer, which legally functions similarly to all other Texas aquifers, is still primarily governed by the Rule of Capture, allowing users to pump groundwater nearly unchecked, especially in areas without groundwater conservation districts (GCDs). Moving water from the Edwards to the Carrizo effectively allows SAWS long-term storage of their current valuable Edwards allotment for potential future needs, as long as it can prevent its injected waters from moving out of the recoverable range of its dual-purpose wells (Malcolm Pirnie Inc. et al. 2011). Figure 2.12 shows an inset of the Carrizo aquifer's ASR feasibility scores near the ASR wellfield.

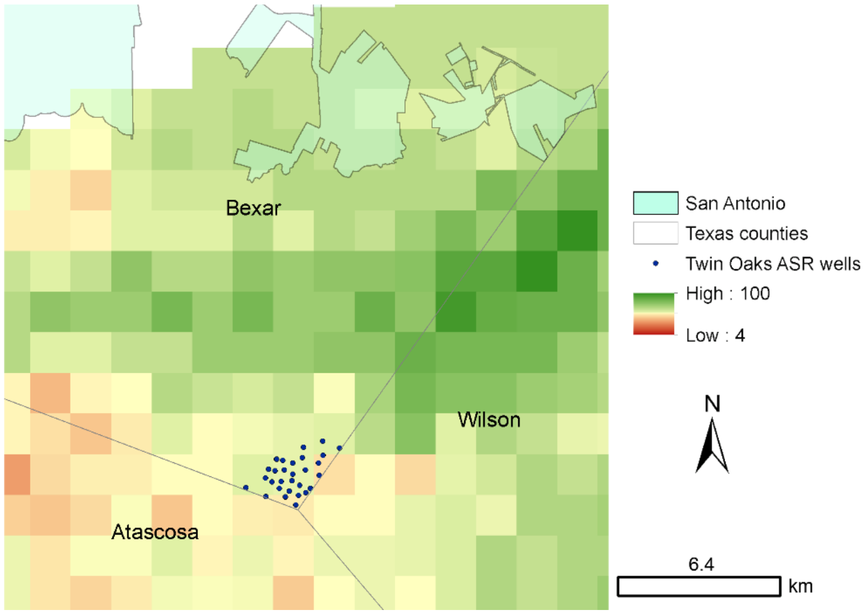

Figure 2.12: Carrizo aquifer feasibility, with H2Oaks ASR well locations and San Antonio depicted. Note how ASR wells are clustered at the bottom of Bexar County, where no GCD governs the Carrizo-Wilcox aquifer system, which the ASR wells are screened in.

Figure 2.12 represents the Carrizo score with the SAWS ASR wells omitted from the GWDB, to avoid artificially lowering the well density ranking. The mean score of the ASR wells is 53. An adjacent area in the Carrizo aquifer to the northeast appears to have a higher potential feasibility rating, but the influence of groundwater conservation districts (GCDs) in the area is apparent, as all of the ASR wells are clustered in the southern portion of Bexar County, where no GCD limits pumping or ASR activities in the Carrizo aquifer at this location. The H2Oaks ASR facility is surrounded to the south, east, and west by the Evergreen Underground Water Conservation District which does have regulations concerning groundwater withdrawals from ASR systems. This map illustrates the fact that placement of groundwater facilities such as ASR systems are influenced by more than just natural and anthropogenically-influenced hydrogeologic conditions. Existing infrastructure, available surface water rights, and sociopolitical considerations like regulatory boundaries and public support are just a few of the myriad considerations that go into selecting such a site. Those considerations are clearly pertinent and valid, but too innumerable and location-specific to consider in this study, which is meant to serve as a starting point for more in-depth feasibility assessments of ASR by municipalities and other water users in Texas.

2.4.3 Potential locations for future ASR development

2.4.3.1 Aquifers beneath the selected cities

ASR feasibility score statistics were calculated within the boundaries of cities with populations greater than 20,000 in the 2010 census. Populations of 20,000 or greater were chosen, as Kerrville, a city of about 22,000, currently operates one of the three ASR facilities in Texas. The 5 cities from each aquifer with the highest mean feasibility scores are shown in Table 2.1. The “count” column indicates how many of the feasibility score raster cells fall within a city’s boundaries, while the “variety” column indicates how many different score values occur within a city.

Table 2.1: ASR feasibility score statistics for 5 cities with the highest mean feasibility scores from each aquifer. Table for all cities with populations of 20,000+ can be found in Appendix A.

Aquifer	CITY	MEAN	MAX	MIN	COUNT	STDEV	VARIETY
Gulf Coast	Port Arthur	90.8	100	86	35	5.5	6
Gulf Coast	Beaumont	87.8	100	78	86	5.0	11
Gulf Coast	Lake Jackson	86.6	92	80	20	4.8	7
Gulf Coast	Victoria	79.7	87	73	35	3.2	8
Gulf Coast	Rosenberg	78.1	91	66	24	6.7	14
Carrizo-Wilcox	Bryan	88.3	94	80	32	4.8	3
Carrizo-Wilcox	College Station	81.1	85	76	7	4.5	2
Carrizo-Wilcox	Laredo	62.3	76	50	33	6.0	14
Carrizo-Wilcox	Longview	66.4	74	60	56	3.9	10
Carrizo-Wilcox	Lufkin	53.6	66	51	32	5.1	3

Table 2.1 emphasizes the high feasibility scores predicted for the Gulf Coast aquifer around Beaumont, as both it and nearby Port Arthur have high mean, maximum, and minimum feasibility scores within their boundaries. Lake Jackson, Bryan, and College Station also have high predicted ASR feasibility directly beneath their cities in the Gulf Coast and Carrizo-Wilcox, respectively. Such an ASR system would be similar to the system currently in place in Kerrville, Texas, which has ASR wells screened in the Trinity aquifer throughout its city limits (Malcolm Pirnie Inc. et al. 2011). In cities primarily surrounded by other cities, like those around Houston, such an ASR system developed in the aquifer directly below might be the only option, as nearby land acquisition costs are likely to be prohibitively large. Fewer cities have high feasibility scores in the Carrizo-Wilcox partly because only 11 cities overlap the aquifer, whereas 31 cities overlap the Gulf Coast aquifer, as seen in Figure 2.13.

Table 2.1 does not capture the ability of more remote cities to explore larger areas around their boundaries for hydrogeologic conditions more favorable for implementing ASR. Corpus

Christi, despite not appearing in Table 2.1, is near an area with feasibility scores as high as 95 just northwest of the city that should be explored further, as shown in Figure 2.8. Corpus Christi, it should be noted, is also currently conducting its own ASR feasibility study. Victoria and Huntsville are also near regions of high feasibility scores in the Gulf Coast. Almost no cities with populations greater than 20,000 exist in the high feasibility regions of the central and southern Carrizo-Wilcox. Despite this, San Antonio Water Supply purchased land for its ASR system south of its city limits where conditions were the most conducive for implementing ASR, as depicted in Figure 2.12. Nine cities from Austin to San Antonio are within 32 kilometers of the outcrop of the Carrizo-Wilcox and could follow San Antonio’s example by exploring ASR options in nearby high feasibility regions.

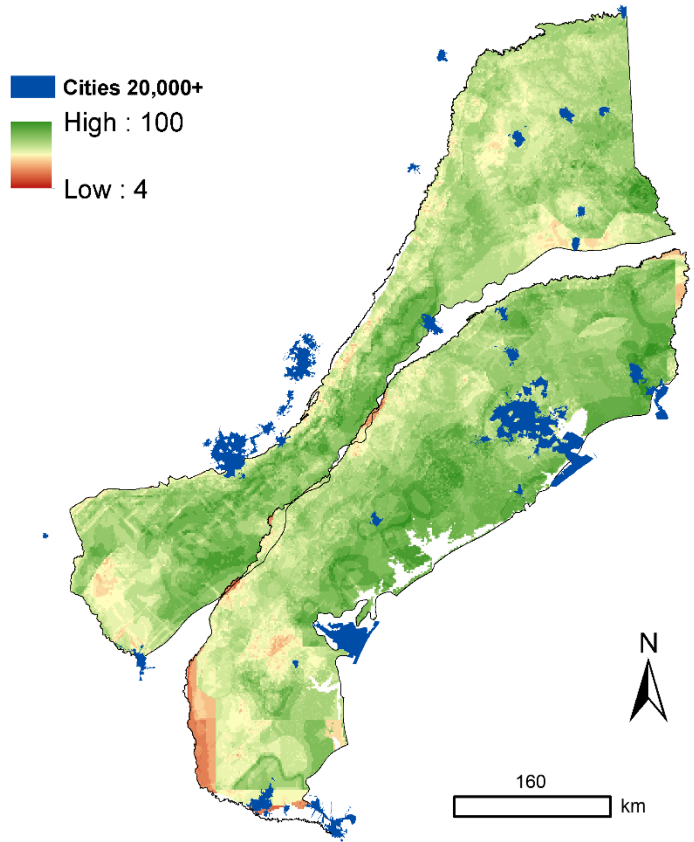

Figure 2.13: Gulf Coast and Carrizo-Wilcox ASR feasibility scores with boundaries of cities with populations greater than 20,000. Cities with boundaries within at least 32 kilometers of either aquifer are shown.

2.4.3.2 Areas with potential water supplies

In order to develop an ASR system, source water is required. As discussed in the introduction, ASR is an alternative approach for water storage, not a water source itself. An in-depth review of all potential water sources and associated water rights becomes excessively complex and is outside of the scope of this analysis. However, Figure 2.14 identifies regions that may have water sources available for ASR development, specifically areas within 32 kilometers of major surface reservoirs or wastewater treatment plants with average daily flow above 38 million liters.

Surface water in reservoirs can serve as a water source for an ASR system to take advantage of ASR’s primary benefit - no evaporative water losses. A municipality with water supply rights from a reservoir currently in excess of its demand (to plan for future growth, for instance) could take advantage of its current excess supply by storing it via ASR. The stored water could then be used at some point in the future. Water from a surface reservoir will most likely still need to be treated before injection in order to comply with relevant water quality regulations and avoid degrading the native groundwater quality.

Wastewater effluent from publicly owned wastewater treatment plants, despite the “ick factor” that still exists with some of the public, is another potential water source. Until it enters a stream, wastewater is still owned by the municipality, and has already received a significant level of treatment. Additional treatment may be required to satisfy legal requirements for injection into an aquifer (Sheng 2005). Additional filtration via the aquifer would also occur during ASR. This filtration by a natural system could potentially ease public concerns over using treated wastewater effluent as a source for ASR. These three attributes (minimal additionally required treatment, current ownership, and a potentially supportive public) make treated wastewater effluents a sensible potential water source for ASR systems.

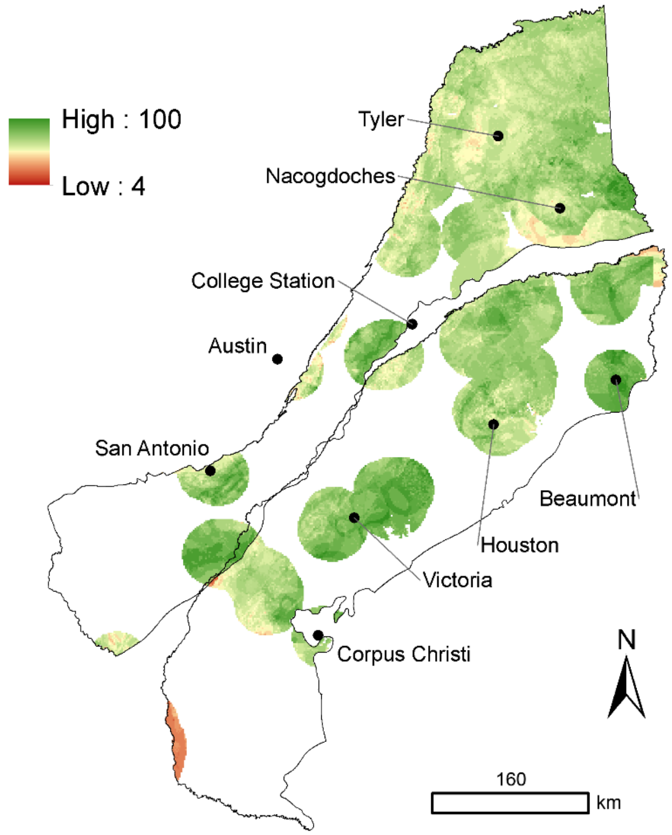

Figure 2.14: ASR feasibility scores highlighted in areas within 32 kilometers of potential water sources, specifically major surface reservoirs and publicly-owned wastewater treatment plants with average daily flow greater than 38 ML/d. In minor areas of overlap, Carrizo-Wilcox ASR feasibility scores are shown.

Surface reservoirs are primarily responsible for the highlighted areas northeast of the line between Houston and Austin, while the more sporadic highlights in the southwest come primarily, but not exclusively, from wastewater treatment plants. Lake Jackson is the only city with a mean score greater than 80 from Table 2.1 without a nearby large wastewater plant or reservoir, whereas Beaumont, Port Arthur, Bryan, and College Station all have potential water sources. Of the cities with nearby high feasibility regions, Corpus Christi, Victoria, Huntsville, and San Antonio have potential water sources; however, many of the cities between Austin and San Antonio do not.

2.4.3.3 Drought-prone regions

ASR can be used either for seasonal storage to ease peak demands, or for long term water storage to help alleviate water shortages during droughts. We determined which counties in the Gulf Coastal Plain have experienced the most Extreme Drought (as defined by the United States Drought Monitor), calculated as the 10-year average of the percent county area in USDM drought category D4. Figure 2.15 (b) varies the transparency of Figure 2.14 based on this calculated 10-year drought-prone index, with the most drought-prone counties being fully transparent and the least drought-prone counties being opaque.

This drought-prone index attempts to identify which counties have been most affected by extreme drought, and thus, could have been well-served with a drought-resistant water storage option like ASR in their water portfolio. This highlights the high feasibility region southeast of Austin in the central Carrizo-Wilcox, the high feasibility area northwest of Corpus Christi, which was also noted in both 2.4.3.1 and 2.4.3.2, and to a lesser extent, the high feasibility region around Victoria. Figure 2.16 overlays the varying-transparency drought layer on Figure 2.14, highlighting the cities with nearby ASR feasible regions, potential water sources, and significant experience with drought in recent history: Corpus Christi, San Antonio, Victoria, Bryan, and College Station.

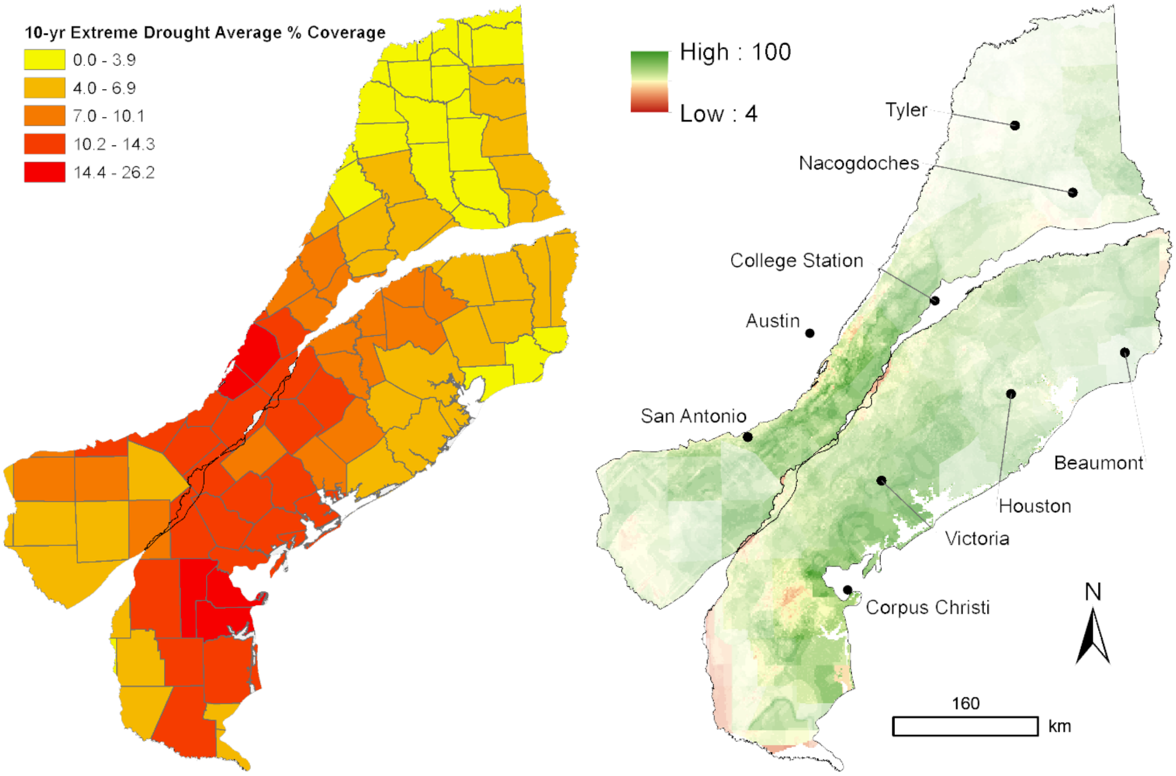

Figure 2.15: (a) The 10-year average of the U.S. Drought Monitor's % areal coverage in Extreme Drought, category D4. (b) ASR feasibility scores are progressively highlighted in areas more prone to drought by using the layer from (a) to vary transparency.

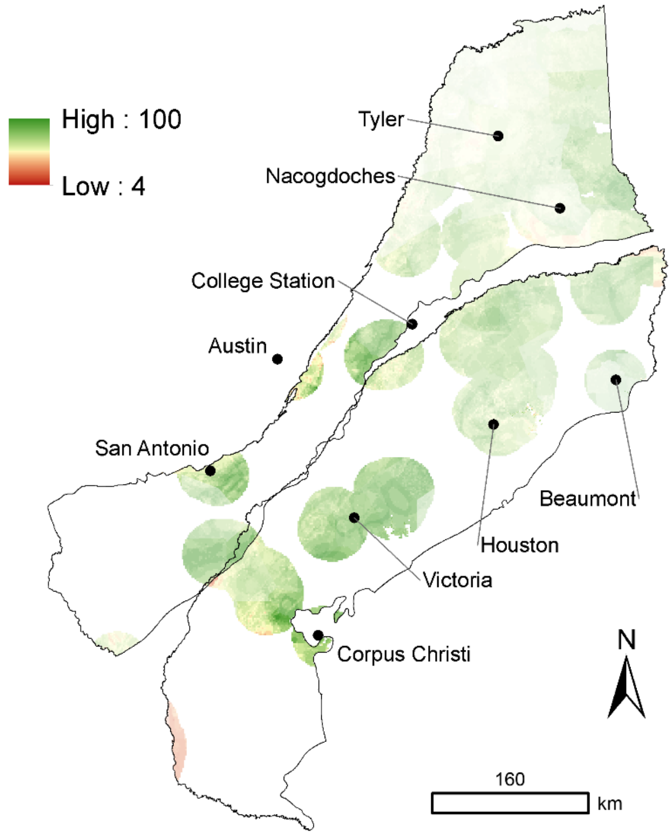

Figure 2.16: ASR feasibility scores in areas with potential ASR-compatible water sources, highlighted in the most drought-prone regions.

2.5 Conclusions

The classified and weighted factor analysis was used to assess ASR feasibility based on five hydrogeologic factors: transmissivity, hydraulic gradient, density of existing wells, depth to the potentiometric surface, and depth to aquifer (well depth). These factors were selected based on both their potential to affect ASR feasibility and the availability of large scale datasets across each aquifer. Some assumptions may limit the applicability of the method. Further study is recommended to enhance the score system by considering other factors.

Several cities of the northern Gulf Coast are in or near high feasibility regions with potential ASR-compatible water sources nearby, while cities between Austin and San Antonio are near high ASR feasibility regions in the Carrizo and have a need for drought-resistant water storage. But Corpus Christi, and to a lesser extent Victoria, San Antonio, Bryan, and College Station stand apart as areas that could be served well by implementing ASR. All these cities have nearby areas of high ASR feasibility, potential ASR-compatible water sources, and a need for drought-resistant water storage, as they have all been exposed to a higher frequency of extreme drought over the last decade relative to nearby areas. In fact, San Antonio operates one of the largest ASR facilities in the United States, and all of the other four cities currently have ongoing ASR studies.

Only a few cities sit directly in regions of high predicted ASR feasibility; most of the feasible regions exist between cities. In order to take advantage of these feasible regions, future ASR wells would most likely be installed away from cities and connected to them via transmission lines, similar to SAWS' H2Oaks system.

Regardless, ASR systems will be much more successful in areas with proper hydrogeologic conditions. This study identifies areas where ASR systems should be expected to perform well, and those areas should be studied further by local municipalities and water resources managers before implementation of ASR systems.

3. ASSESSING THE PERFORMANCE OF A LARGE SCALE, MULTI-WELL AQUIFER STORAGE AND RECOVERY SYSTEM USING A TRANSPORT MODEL

3.1 Overview

Recovery efficiency is one of the most important parameters to consider when designing and operating an aquifer storage and recovery system. In this study, groundwater flow and solute transport models were developed to simulate movement of injected water in and estimate the recovery efficiency of a large scale ($2.27*10^5$ m3/d), multi-well aquifer storage and recovery system near San Antonio, Texas. Recovered fraction estimates for the first 9.5 years of actual operations ranged from 54-90%. Using a hypothetical operations scenario for the next 9.5 years, recovered fraction estimates for the entire 19 year modeled period ranged from 48-84%. Plumes of injected water from separate wells remained fairly distinct from one another even after five years but were mostly coalesced after 9.5 years, although this was highly dependent on dispersivity. For our study site, the simulation results suggest that the same well in which water was injected should also be used for recovery of that water to maximize recovery efficiency. In addition, significant hydraulic effects between the wells must be accounted for, as they can adversely shift injected plumes away from ideal recovery zones. This study provides operational guidelines and strategies for maximizing recovery efficiency of multi-well systems.

3.2 Introduction

Aquifer storage and recovery (ASR), a subset of managed aquifer recharge (MAR), is a water storage alternative applicable to a wide range of hydrogeologic conditions and climates that primarily involves injection and extraction via wells. Unlike surface reservoirs, ASR systems experience little to no evaporative losses and minimize environmental disturbances and land consumption since they require only a few small facilities at the land surface like pumps, wellheads, and occasionally a treatment plant (Bouwer 2002; Maliva and Missimer 2010). Due to these benefits, ASR is being implemented on larger scales to meet the needs of municipalities especially in drier regions: Las Vegas Valley Water District, Calleguas Municipal Water District, and San Antonio Water System (SAWS) currently operate systems rated at 5.9×10^5, 2.6×10^5, and 2.3×10^5 m^3/d (157, 68, and 60 MGD), respectively (Malcolm Pirnie Inc. et al. 2011).

Originally, ASR was defined as a single well system with a dual-purpose injection/extraction well but today, ASR may refer to systems with a single well, multiple dual purpose wells, multiple separate injection and extraction wells, or even recharge basins and other traditional MAR recharge strategies (Pyne 2005; Maliva and Missimer 2010; Sheng 2005; Stuyfzand et al. 2017). Aquifer storage transfer recovery (ASTR) systems are very similar to multi-well ASR systems (and sometimes referred to as such), but additionally attempt to treat the injected water via transmission through the aquifer matrix between the injection and extraction wells (Miotlinski et al. 2014).

Despite its advantages, ASR still has potential limitations, such as low recovery efficiency (RE) of a system, which is defined as the ratio of the volume of usable water recovered to the volume of injected water (Maliva et al. 2006; Sheng et al. 2007). A successful ASR system with a high RE is dependent on an extensive list of factors, including: hydrogeologic properties like transmissivity, dispersivity, and aquifer thickness; operational parameters such as pumping rates and durations of injection, extraction, and storage periods; and even regulatory and economic considerations (Maliva and Missimer 2010; National Research

Council 2008). Significant research has been done in order to better understand how these hydrogeologic and operational factors affect ASR system performance in terms of RE. Ward et al. proposed dimensionless parameters from these factors to describe four major processes that govern RE of ASR systems in brackish aquifers: density effects during pumping, density effects during storage periods, and lateral drift and dispersion of the injected waters (Ward et al. 2009). Groundwater flow and transport modeling has been used extensively to understand the processes governing RE as well as to guide the operations and designs of actual ASR systems: Ringleb et al. (2016) estimates that of the 216 studies they found regarding modeling of MAR systems, ASR/ASTR systems accounted for more than 52% of those. These models have ranged from one-dimensional, axisymmetric models to a three-dimensional reactive transport model that explained the unexpected occurrence of arsenic in an ASR system in the Floridian aquifer (Wallis et al. 2011). However, nearly all of these studies, both modeling and otherwise, have primarily focused on single-well ASR systems, which may not address all of the concerns of municipalities and other water purveyors interested in large-scale ASR systems. Based on the capacities which some ASR systems currently operate at, it is likely that additional large scale ASR systems requiring multiple wells will be developed in the future, requiring further research to identify how well proximity and operational scenarios affect RE in such systems.

Very few published modeling studies have explored the performance of multi-well ASR systems. Miotlinski et al. (2014) demonstrated that detailed site characterization and solute transport modeling could be used to effectively guide the design and operation of a six well ASTR system in South Australia. Solute transport modeling was previously used for the same site to determine that a rhombic orientation was expected to maximize RE (Pavelic et al. 2004). Another study evaluated various hypothetical dual-purpose ASR well configurations (as many as five wells), and found that RE was approximately the same as if a single ASR well had been used (Yobbi 1997). Flow modeling was used at a site in the Netherlands to determine the performance of multiple-partially-penetrating dual-purpose wells screened at different depths within the same borehole in a brackish aquifer (Zuurbier et al. 2014). Flow rates in these studies were approximately 1.33 x 10^3 m^3/d, 1.54 x 10^4 m^3/d, and 38 m^3/d, which are significantly lower than the flow rates used by the large systems of Las Vegas, Calleguas, and San Antonio. One study modeled end-member mixing of the injected and native waters in the San Antonio ASR system using PHREEQC but did not include groundwater flow modeling and thus was uncertain as to how the waters mixed in the areas between wells (Azobu 2013).

The objectives of this study include: to verify that large scale, multiple-well ASR systems can achieve high RE of injected waters, to determine the shape and character of the mixing zones within and around such a well field, and to offer guidelines for operational decisions that may help to increase RE in those systems. We hypothesize that even after extensive operation periods (>5 years), native water will remain in the spaces between wells, and the plumes of water injected by individual wells will not completely coalesce. Further, the fraction of remaining native water will be dependent on the longitudinal dispersivity of the aquifer matrix, with higher dispersivities leading to greater coalescence and decreased recovery efficiency. Confirming this hypothesis will be important for future studies on the geochemical performance of such systems, which relies heavily on the extent of mixing and compatibility between native and injected waters.

3.3 Methods

3.3.1 Site description and hydrogeology

San Antonio Water System's (SAWS) H2Oaks Center aquifer storage and recovery (ASR) system, located at the southern tip of Bexar County approximately 21 miles south of San Antonio, is comprised of 29 dual-purpose ASR wells (referred to throughout the remainder of paper as the "ASR wells") and seven extraction-only wells ("extraction wells") screened in the Carrizo sand formation of the Carrizo-Wilcox aquifer system near its outcrop (Figure 3.1). The Carrizo aquifer is approximately 210 to 240 m thick and is underlain by the Wilcox aquifer and overlain by the confining Reklaw clay, which is 0 to 60 m thick. The Reklaw is overlain by the Queen City sand aquifer, which is 0-30 m thick in the area (CH2MHILL 2003; George et al. 2011). The Carrizo is primarily sand with interbedded deposits of clay and lignite, and has trace amounts of pyrite in its matrix. Its water is fresh, but may have elevated concentrations of iron and manganese (Pearson and White 1967; CH2MHILL 2003).

The ASR system is used to store water when the demand for SAWS water is lower than its permitted extraction rates from the nearby Edwards Aquifer. Formerly known as the Twin Oaks ASR system, the facility opened in June 2004 with 17 dual-purpose ASR wells. The remaining 12 dual-purpose ASR wells began their operation in February 2008, and the 7 extraction-only wells started pumping in late 2008. The 29 dual purpose wells and seven extraction only-wells have a total pumping capacity of 2.27×10^5 and 4.54×10^4 m^3/d, respectively. SAWS constructed a companion water treatment facility in order to lower levels of iron and manganese in recovered water, to be used as necessary if iron and manganese concentrations ever became elevated.

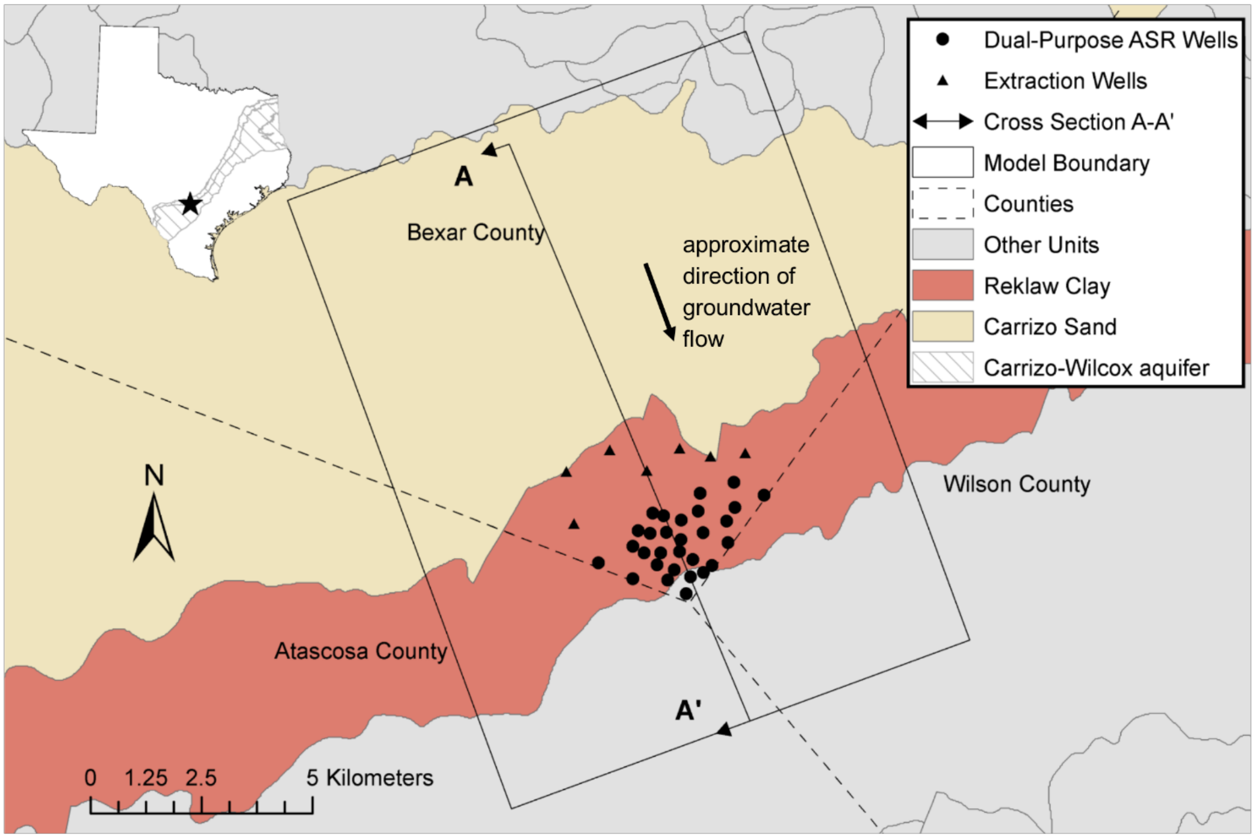

Figure 3.1: Map showing the location of the SAWS ASR system, the H2Oaks Center, in the Carrizo-Wilcox aquifer. Circles represent dual-purpose ASR wells, while triangles represent extraction-only pumping wells. Cross section A-A' is depicted in Figure 3.2.

3.3.2 Groundwater flow model development

3.3.2.1 Model grid configuration

MODFLOW-2005 was used to simulate the groundwater flow in the ASR system within the Aquaveo GMS environment (Harbaugh 2005; Harbaugh et al. 2013; Aquaveo 2017). The model was developed based on site specific information obtained from SAWS in the forms of project reports, raw data tables, and well logs, as well as results from the regional Southern Queen City and Sparta Groundwater Availability Model (GAM), which was based on the prior Southern Carrizo-Wilcox Groundwater Availability Model (CH2MHILL 1998; CH2MHILL

2006; CH2MHILL 2003; Morris et al. 2010; Deeds et al. 2003; Kelley et al. 2004). The GAM estimates for the area predict minimal changes in aquifer heads and regional gradients from 2000 to 2050. The model grid was oriented so that it corresponded with the expected direction of regional groundwater flow, which was also approximately in the downdip direction of the Carrizo aquifer. The upper model boundary corresponded with the updip limit of the Carrizo aquifer, and the lateral and downdip extents of the model were defined to be larger than estimated radius of influences from ASR wells.

Layer elevations for the 6 model layers were defined using data from geophysical logs of the ASR well boreholes provided by SAWS, source data for the regional GAM, and a digital elevation model of Texas. The geophysical borehole logs indicated the lower extent of the Reklaw as well as the elevations of clay lenses present in the ASR wellfield. The heterogeneous nature of the Carrizo aquifer was apparent: some borehole logs indicated no interbedded clay lenses, while others indicated 3 or more lenses. Based on our analysis of the borehole logs, our conceptual model included two lenses that appeared laterally continuous throughout most of the wellfield (Figure 3.2). These lenses were modeled in layers 3 and 5.

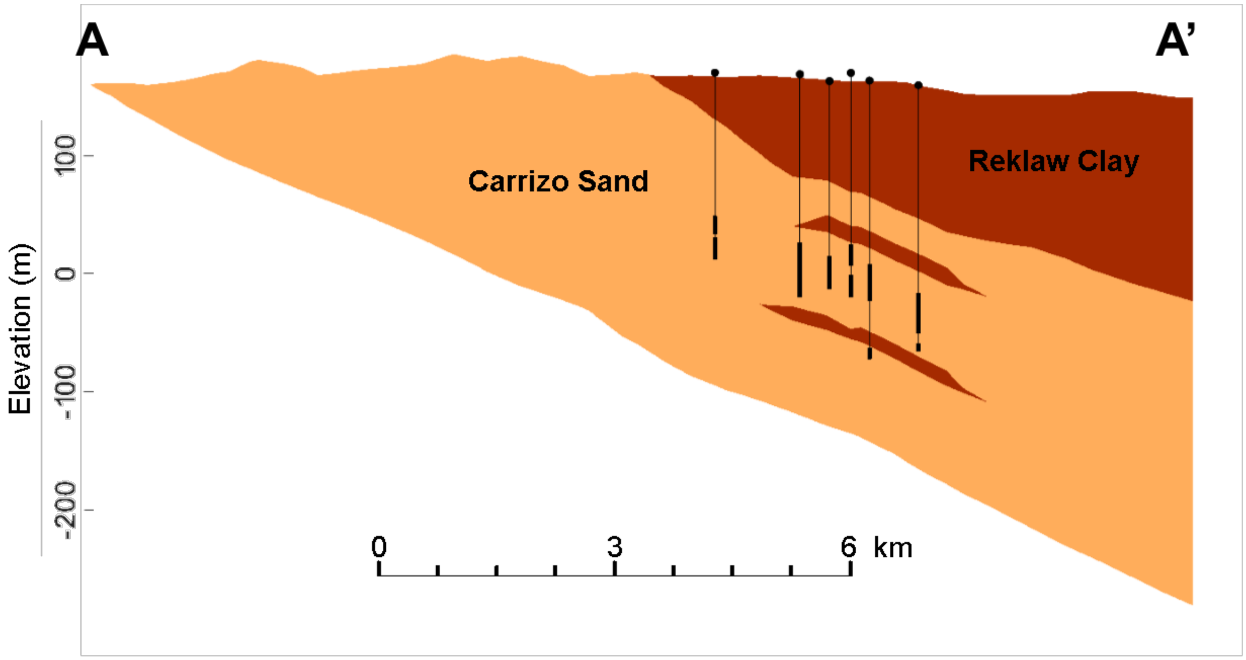

Figure 3.2: Conceptual hydrostratigraphy of the ASR system in the Carrizo Sand aquifer. Wells are located near the outcrop of the Carrizo, and are screened (thicker lines in figure) in multiple intervals to avoid low permeability clay lenses. Based on analysis of geophysical logs, only the two lenses that appeared the most laterally extensive throughout the wellfield were simulated – some wells are screened below the bottom lens, but most of the screens fall between the two lenses. The base of the Carrizo Sand is assumed to be a no-flow boundary.

Since the Queen City was not expected to affect groundwater flow in the ASR wellfield, it was omitted from the model and the Reklaw confining layer, represented in layer 1, was assumed to extend from the Reklaw/Carrizo interface to the land surface. The Reklaw/Carrizo interface elevations from the GAM source data appear to indicate that the updip limit of the Reklaw lies approximately between the 29 dual-purpose ASR wells and the 7 extraction-only wells. Presence and thickness of the Reklaw confining layer above the extraction-only wells are unclear from SAWS borehole data in four of those wells. In both our conceptual and numerical models, we assumed all wells were confined by the Reklaw. However, in each simulation of the numerical model many of the thin cells of the Reklaw layer near the 7 extraction wells became inactive as they went dry, effectively setting those wells in the unconfined outcrop of the Carrizo.

Layers 2-6 represented the Carrizo aquifer. Elevations for the Reklaw/Carrizo interface were defined by the boreholes in the wellfield and by the source data from the GAM outside of it. The bottom of the Carrizo aquifer was not clearly defined in the borehole data as they did not extend deep enough in most cases, and as such the bottom of the model was defined by the GAM source data for the Carrizo/Wilcox interface over the entire model domain. Outside of the ASR wellfield, layers 2-6 were vertically distributed approximately evenly. Within the wellfield, layers 3 and 5 become significantly thinner where they represent the interbedded clay lenses.

Our conceptual model assumed the Reklaw clay and clay lenses were relatively homogenous, so layer 1 and the clay lens portions of layers 3 and 5 used the same hydraulic parameters. The Carrizo sand was also assumed to be homogenous, so layers 2-6 all used another set of hydraulic parameters except for the clay lens portions of layers 3 and 5. Table 3.1 shows the source, initial, and calibrated values for the model's hydraulic and transport parameters. Data sources include values or ranges used in the regional GAM (Deeds et al. 2003), shown in column 1, along with values obtained from H2Oaks' constant-rate pump tests in the 29 dual-purpose ASR wells, shown in column 2 (CH2MHILL 2003; CH2MHILL 2006).

Table 3.1: Flow and transport model parameters.

	Southern Carrizo GAM Values	SAWS Constant-Rate Test Values	Initial Values	Calibrated Values
Reklaw / Clay lenses (Layers 1,3,5)				
Horizontal K (m/d)	0.91		0.263	0.86
Vertical Anisotropy (K_h/K_v)	1000		1000	1000
Specific Storage (1/m)	9.8×10^{-6}		3.3×10^{-8}	1.0×10^{-8}
Specific yield			0.03	0.01
Effective porosity			0.06	0.06
Longitudinal Dispersivity (α_L)			20	20
Carrizo (Layers 2-6)				
Transmissivity (m^2/d)		740 - 2410		
Horizontal K (m/d)	3 - 30	*3.5 - 11.5*	6	6.9
Vertical Anisotropy (K_h/K_v)	30		30	30
Storativity		8.4×10^{-5} - 4.1×10^{-4}		
Specific Storage (1/m)	9.8×10^{-6}	*4.0×10^{-7} - 1.9×10^{-6}*	9.8×10^{-7}	3.0×10^{-7}
Specific yield	.05 - .32		0.25	0.07
Effective porosity			0.3	0.3
Longitudinal Dispersivity (α_L)			25	25
All layers				
Horizontal Transverse Dispersivity / α_L			0.3	0.3
Vertical Transverse Dispersivity / α_L			0.05	0.05
Other Model Parameters				
Southeastern constant head boundary (m above mean sea level (amsl))	120		120	103
Recharge (mm/yr)	45.7		45.7	45.7

*Values in italics calculated from transmissivity and storativity tests, assuming a saturated thickness of 210 m.

The bottom of the model was treated as a no-flow boundary at the Carrizo-Wilcox interface. Since the model was oriented in the direction of expected regional groundwater flow (northwest to southeast), lateral model boundaries were also assumed to be no-flow boundaries. The southeast boundary was treated as a constant head boundary, and was initially estimated at approximately 120 meters amsl based on the predicted heads of the regional GAM for the years between 2000 and 2050 (Kelley et al. 2004). Recharge of 45.7 mm/yr was applied to the uppermost active grid cells based on previous studies in the region cited by the Southern Carrizo-Wilcox GAM report (Deeds et al. 2003). Daily well flows obtained from SAWS were implemented in the MNW2 (Multi-Node Well) package (Konikow et al. 2009). The MNW2 package was used to represent the ASR wells and extraction-only wells, since many of the ASR and extraction-only wells are screened in two or more intervals, and the well screens sometimes extend across multiple model layers.

Since spacing on some wells is as close as 250 meters, and the intent of the model is to understand transport processes between wells, a grid cell size of 50 m x 50 m was used in the vicinity of the wellfield, extending at least 1600 m in all directions from the dual-purpose wells (Figure 3.3). Beyond this, telescopic mesh refinement was used to increase the cell sizes to a maximum of 800 m x 800 m to minimize the model’s computational requirements. At each stage of grid refinement, adjacent cell sizes were varied by no more than 2x. The southeastern most row of the grid, where the constant head boundary was located, was set at 100 m wide.

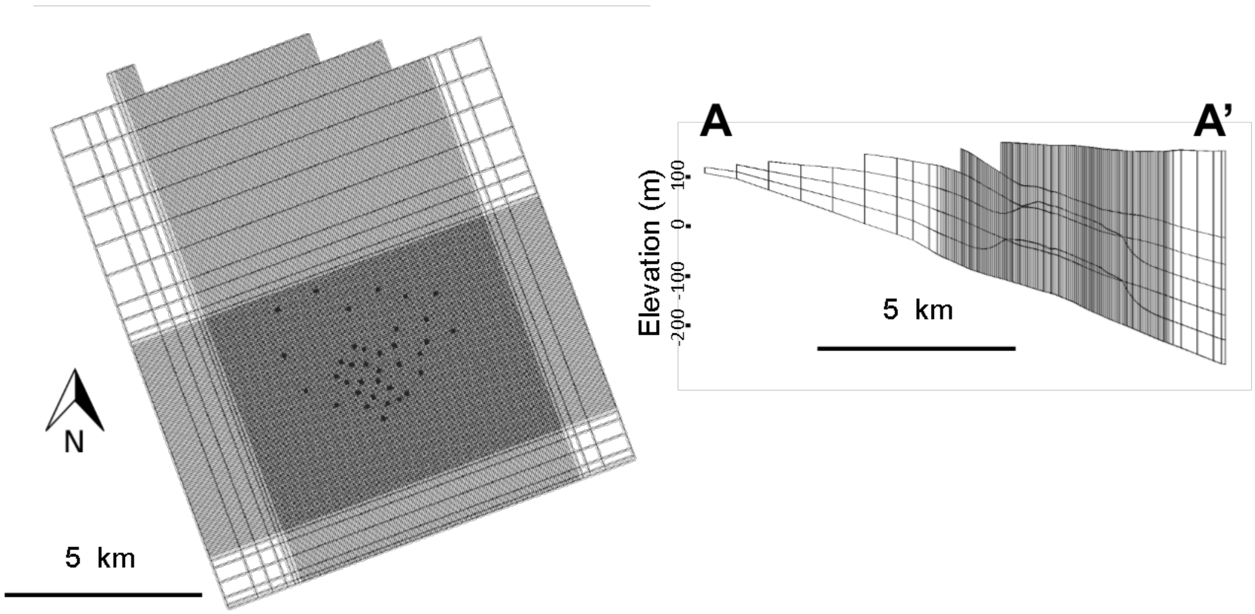

Figure 3.3: Plan and cross section views of the model grid, with locations of the 36 wells shown in plan view.

3.3.2.2 Temporal discretization

3.3.2.2.1 Period of actual operations

Well flows changed significantly enough on a daily basis to warrant temporally discretizing the model into daily stress periods. The model was developed based on pumping rates obtained from SAWS for the 9.5 year period between May 2004 and October 2013 (Figure 3.4c). The ASR wellfield primarily injected water over the first 9.5 years (Figure 3.4), but extracted water during periods of decreased rainfall and low aquifer levels in the Edwards aquifer (National Oceanic and Atmospheric Administration: National Centers for Environmental Information 2017b; Edwards Aquifer Authority 2017). The initial stress period of the model was set as steady-state so the model could equilibrate with the applied recharge. All remaining stress periods were further discretized into hourly time steps.

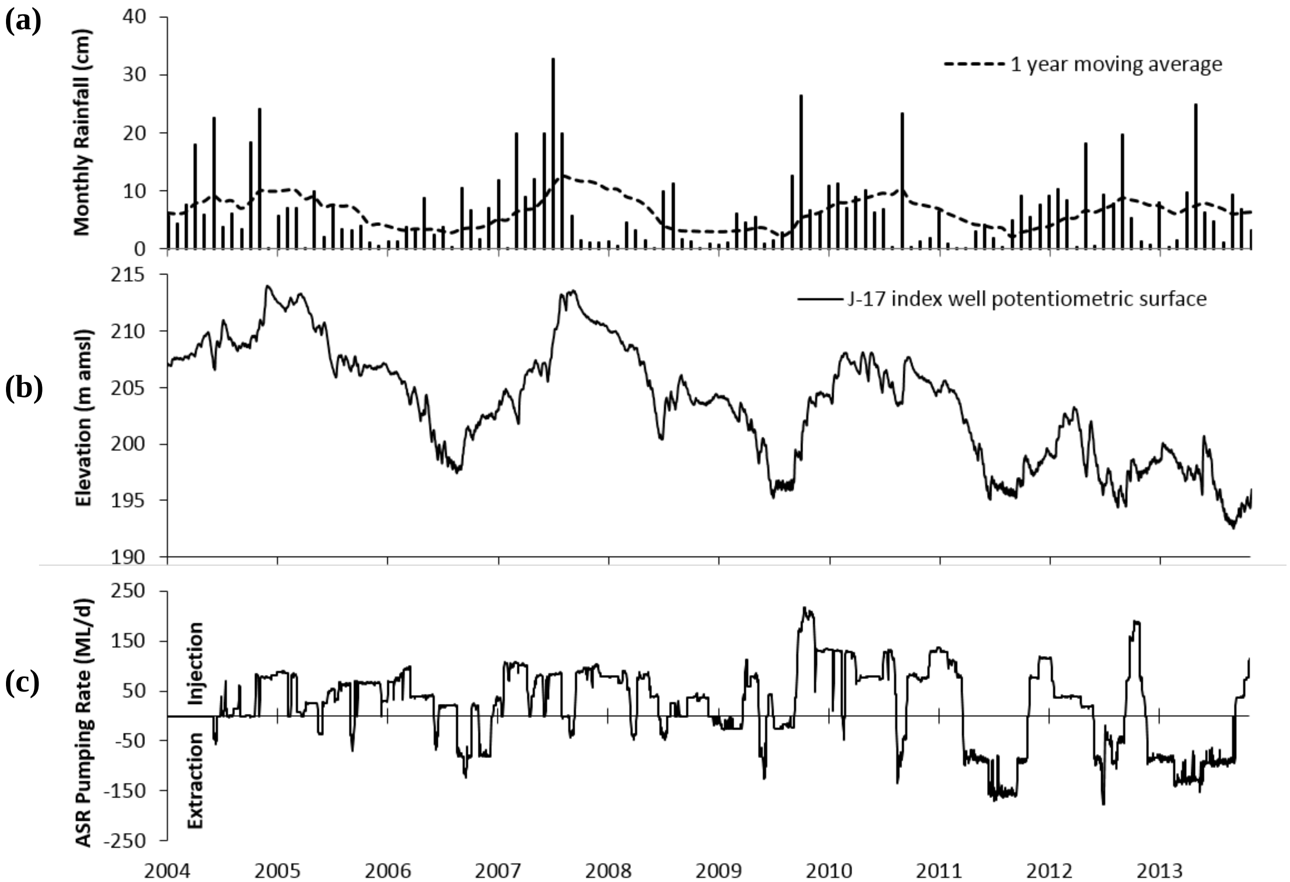

Figure 3.4: Areal rainfall, water level in Edwards aquifer index well J-17, and ASR pumping from 2004 through late 2013. The ASR wellfield pumping rate (c) tends to follow the patterns seen in San Antonio's rainfall (a) and elevation of the potentiometric surface of the Edwards aquifer (b). When rainfall is scarce and the Edwards aquifer level drops, as seen in the drought of 2011, the ASR system switches from its usual injection mode to extraction mode.

More than 65,500 raw, unedited water level observations, collected by pressure transducers in the supervisory control and data acquisition (SCADA) system, were obtained from SAWS to calibrate the MODFLOW model. Observations spanned from August 2007 through October 2013 and were available for each of the 29 ASR wells. These observations were taken daily in each well whether the well was injecting, extracting, or idle. The following data were excluded in order to produce usable observations by which to assess model performance:

observations taken while a well was pumping and 10 days afterwards; observations that were more than 2 standard deviations away from the mean in their respective well; data that was clearly incorrect due to maintenance, transducer error, or water levels dropping below a transducer. This last category of data included data spikes that were inconsistent with the typical variation in that well's transducer data. After implementing these quality control procedures, 33,638 observations remained by which to calibrate the model. For some wells, we were unable to obtain precise information about the elevation of the pressure transducer at a given point in time; these remain a potential source of unaccounted errors. The fit of the model to the observations heads was evaluated using the Nash-Sutcliffe efficiency coefficient (NS), mean error (ME), mean average error (MAE), and root mean squared error (RMSE) as described in detail by Anderson et al. (2015).

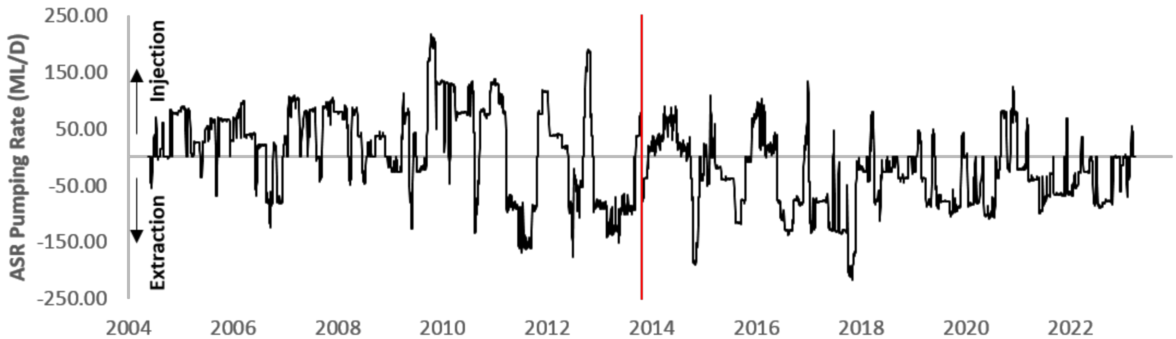

Figure 3.5: The ASR wellfield total pumping rate for both the period of actual operations (before the red line in late October 2013) and the period of hypothetical operations (after the red line).

3.3.2.2.2 Hypothetical period

Since SAWS recovered less than 36% of the total volume injected during the actual operations period, recovery efficiency estimates during this period were deemed insufficient to adequately assess the long-term performance of the ASR system. Instead, a hypothetical operational scenario for October 2013 to March 2023 was chosen that effectively reversed the first 9.5 years of ASR operations from June 2004 to October 2013 (Figure 3.5). Pumping rates for the dual-purpose ASR wells were reversed both in time and magnitude. For instance, the hypothetical extraction rates from the dual-purpose wells 1 month after late October 2013 match the magnitude of the injection rates 1 month prior. Since the extraction-only wells to the northwest of the ASR wellfield cannot be switched into injection mode, their pumping rates were only reversed in time. As a result of this, the flow rates in the hypothetical period are not always exactly inverse of the actual operations period (i.e. 2013 vs 2014, Figure 3.5), but generally are equal (when the extraction-only wells are idle). This hypothetical operational scenario was chosen primarily because it ensures that the recovered and injected volumes from the dual-purpose ASR wells are equivalent over the total modeled time domain, which simplifies calculation of overall recovery efficiency.

3.3.3 Transport model development

3.3.3.1 Injection of tracer into all wells

MT3DMS was used to estimate the transport of Edwards aquifer water injected into the Carrizo via the ASR wells during both the actual operations and hypothetical periods (Zheng and Wang 1999). The advection, dispersion, and source/sink mixing packages were included, but molecular diffusion and chemical reactions were not considered. Injected Edwards water was assumed to have an imaginary tracer with concentration of 100 mg/L, since insufficient data on conservative tracer concentrations were available from the ASR system. The imaginary tracer was set at 0 mg/L for the native Carrizo water. Longitudinal dispersivity (α_L) was assumed to be 25 meters in the Carrizo sand cells and 20 meters in the Reklaw and clay lens cells based on estimates from previous studies at similar scales in sand aquifers as well as empirical equations for predicting α_L (Gelhar et al. 1992; Lovanh et al. 2000; Schulze-Makuch 2005; Delgado, 2007). The ratios of transverse horizontal dispersivity to α_L and of vertical transverse dispersivity to α_L were assumed to be 0.3 and 0.05, respectively, for all model cells. The sensitivity of the modeled RE to α_L was analyzed by also modeling the transport of the tracer using α_L values of ranging from 0.5 m to 150 m for the Carrizo sand cells.

3.3.3.2 Injection of tracer into one well

In order to better understand the effects of injection of non-native waters in a single well on other wells in a multi-well system, a separate simulation was run where the tracer was injected into a single well. All other parameters for the flow and transport models, including injection and extraction rates and longitudinal dispersivity remained constant.

3.3.4 Recovery efficiency estimates

In this study, since cumulative injected volume is typically much larger than cumulative recovered volume for the first 9.5 years of operations, RE described as the ratio of usable recovered volume to injected volume does not adequately represent the performance of the system over time. Instead, RE was represented as the mixing fraction, *f* (expressed throughout this study in terms of percentage), similar to Miotlinski et al. (2014):

$$f = \frac{C_{rec} - C_{native}}{C_{injected} - C_{native}} * 100$$

where C_{rec} is the concentration of the tracer in the well, C_{native} = 0 mg/L, and $C_{injected}$ = 100 mg/L.

The performance of the entire ASR system as a whole is presented here as f_d:

$$f_d = \frac{\sum_{well=1}^{n} f_{well} * Q_{well,rec}}{\sum_{well=1}^{n} Q_{well,rec}}$$

where f_{well} is the recovered fraction in a well on a specific day, and $Q_{well,rec}$ is the flow recovered from that well on that day, so that f_d represents the total flow-weighted daily recovered wellfield fraction recovered from *n* wells. A cumulative flow weighted recovered fraction, f_{cum}, was also calculated as

$$f_{cum} = \frac{\sum_{t=1}^{m}\left(f_d * \sum_{well=1}^{n} Q_{well,rec}\right)}{\sum_{t=1}^{m}\left(\sum_{well=1}^{n} Q_{well,rec}\right)}$$

to assess the system's overall performance during the modeled periods, where t=1:m is the set of days where water was recovered from any wells in the wellfield.

In this study, f_d, the wellfield recovered fraction, is only calculated based on the injection and extraction in the dual-purpose ASR wells. The extraction-only wells to the northwest are upgradient and too distant to recover injected waters, and as such, inclusion of their pumping would artificially lower RE estimates, but they are included in the flow and transport model since they are still expected to influence the movement of the injected plumes.

3.4 Results

3.4.1 Calibration of the MODFLOW model

Groundwater flow model parameters were calibrated manually to determine the best fit to the head targets based on the NS and RMSE coefficients. The hydraulic conductivity in the Carrizo cells and the elevation of the constant head boundary on the southeast model boundary were the most sensitive parameters. Based on the transmissivity values estimated for the 29 ASR wells by constant-rate pumping tests and assuming an aquifer thickness of 210 m, the geometric mean of the hydraulic conductivity in the ASR wells was 7.4 m/d. The final calibrated value for the Carrizo horizontal hydraulic conductivity was 6.9 m/d. While groundwater flow-models are inherently non-unique, this agreement between the calibrated hydraulic conductivity and results of 29 constant-rate tests lends credence to the plausibility of this model. The initial estimate for the southeastern constant head boundary was 120 m amsl based on predictions from the GAM, but actual local aquifer heads were significantly lower, resulting in a final calibrated value of 103 m amsl.

The calibrated groundwater flow model reproduced 33,638 head observations from the entire wellfield with a NS coefficient of 0.58 and a RMSE of 10 m, or approximately 10% of the range of head observations from 60 m to 160 m as indicated in Figure 3.6. Results within individual wells were typically better than the overall model fit, as the median NS among the ASR wells was 0.70 in well 25 (Figure 3.7). The best-fitting well (# 13) had an NS of 0.89, while the worst-fitting well (# 16) had an NS of -6.8.

Well 16 was the only well where the modeled results fit worse than the mean of the observations (NS<0); the mean error of -31 m in well 16 indicates the possibility incorrect observations, likely due to uncertain information on the elevation of that well’s transducer, which affected the elevations of the head observations in the well. The changes in modeled heads vary approximately equally (1:1) with changes in the head targets in well 16, but do not pass through (0,0). Additionally, the NS of the two closest wells to well 16, both within 350 m, are 0.78 and 0.75. Figures and parameters including NS, ME, MAE, and RMSE that illustrate the fit in each of the 29 wells are presented in Appendix B. If the data from well 16 is excluded, the NS coefficient for the entire set of observations improves to 0.68.

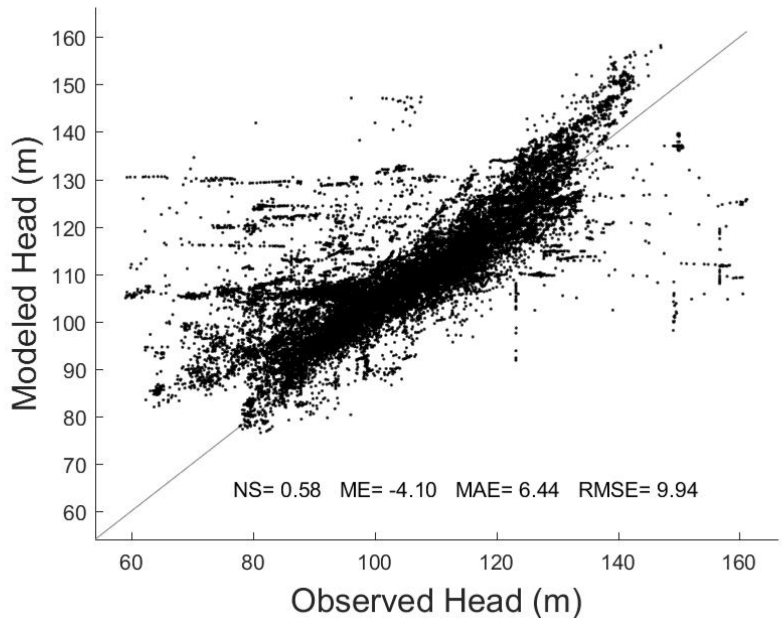

Figure 3.6: Modeled heads versus head targets for the entire ASR wellfield. A total of 33,638 head targets used, based on continuous monitoring by a SCADA system.

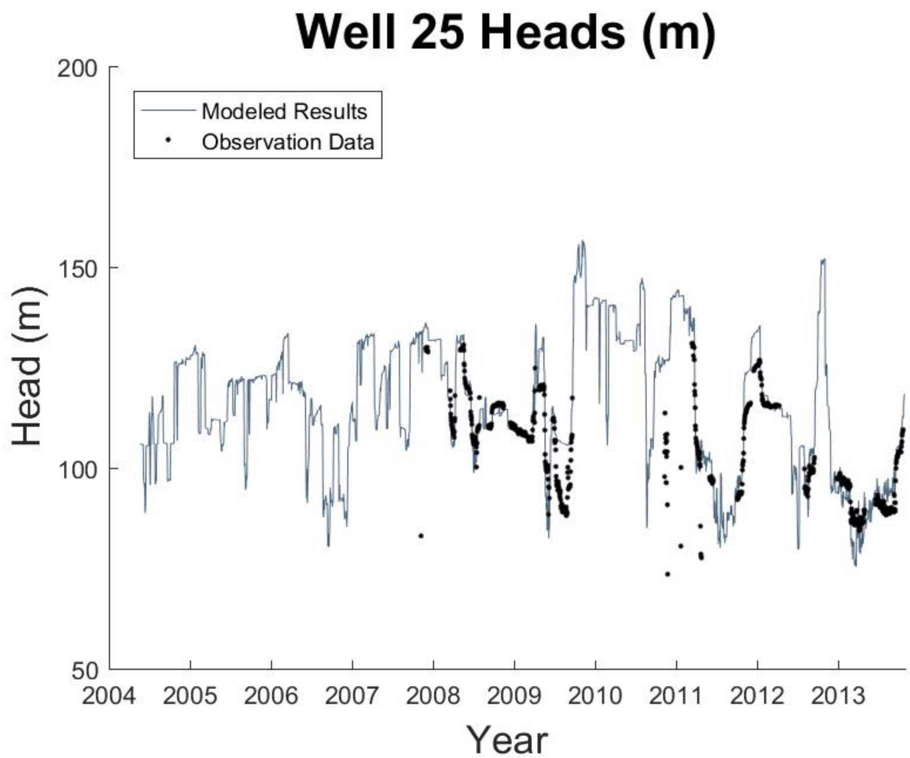

Figure 3.7: Modeled and observed head targets versus time in well 25, which has the median NS coefficient (0.70) for the 29 ASR wells. Figures for the remaining 28 wells (as well as figures of modeled heads vs head targets for all 29 wells) are available in the Appendix B.

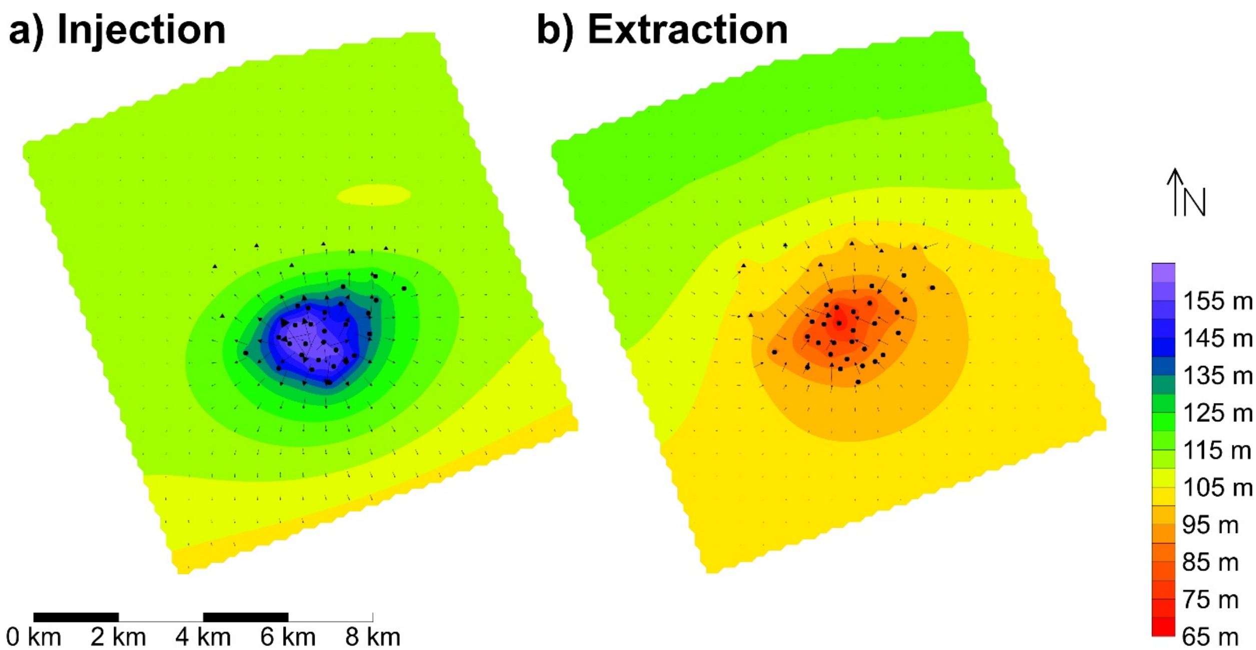

Figure 3.8: Contour plots of heads with velocity vectors during (a) a period of significant injection during October 2009 and (b) a period of significant extraction in September 2011.

As discussed in section 3.3.2.2.1, the ASR facility changes the total injection rate on a fairly frequent basis, often daily. Also, the wells are operated independently: not all 29 wells inject or extract at the same rate at one time. As such, the head contours and flow directions in the wellfield change frequently as well. Small cones of depression (or groundwater mounds) form around individual wells during extraction (or injection), coalescing into larger drawdown cones (or mounds) when several wells in close proximity extract (or inject) simultaneously for significant periods of time (Figure 3.8).

3.4.2 Recovery efficiency with MT3DMS solute transport model

The H2Oaks facility primarily injected water during the actual operations period, but there were two extended recovery periods: once from March through October 2011, during the worst one-year drought in Texas' history (Nielsen-Gammon 2011), and again from December

2012 through September 2013. The total wellfield recovered fraction f_d for these two periods decreases from nearly 100% at the start to less than 60% in 2011 and less than 45% in 2013 at the end of recovery operations (Figure 3.9a). However, f_d is highly erratic and non-monotonic during the actual operations period, including an increase of more than 25% during the 2013 recovery period. These variations in f_d are primarily due to operational changes which alternate between wells used for extraction as illustrated in the supplemental animation in Appendix C.

The recovered fraction is less erratic during the hypothetical period since the recovery wells do not change as often, which can be seen in the more stable extraction rates of the hypothetical period relative to the actual operations period. However, f_d continues to decrease throughout the hypothetical period to a low of 30%, especially near the end of recovery phases, as the cumulative stored volume in the aquifer decreases. In general, the mixing fraction f increases when a well injects water and decreases when a well extracts water, as expected (Figures 9b through 9d). However, f also changes during the idle periods, typically decreasing with the most dramatic decreases occurring in the distal wells. The changes in a well's f during its idle periods appears to be due to the operations of the other wells. For example, f in a distal well (Figure 3.9d), on the very southern tip of the wellfield, decreases in early 2010 during its idle period while the center and proximal wells (Figures 9b and 9c) are injecting water, suggesting that the injection operations in these wells (and other wells during this same period) creates a groundwater mound that moves the water injected in the distal well downgradient and away from that distal well.

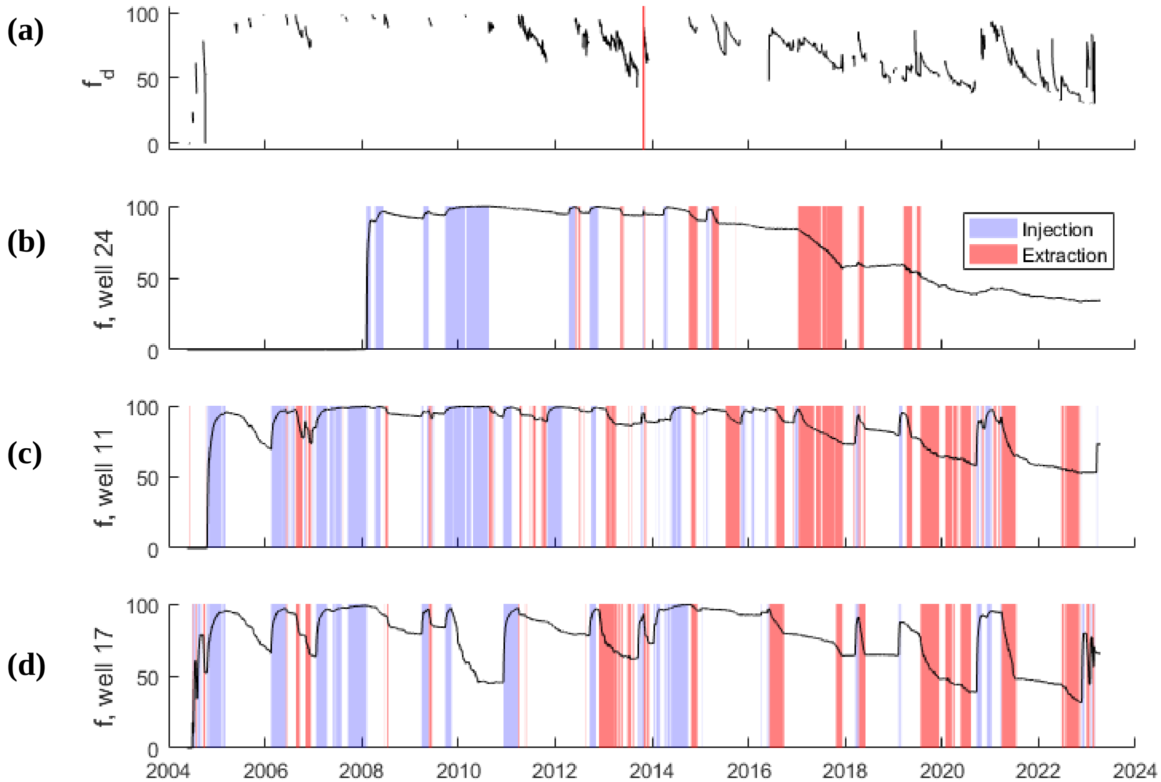

Figure 3.9: Recovered fraction of injected water f_d predicted by MT3DMS (a) and mixing fraction f in individual wells in the (b) center, (c) proximal, and (d) distal regions of the wellfield. Times before the red line (October 30, 2013) in (a) indicate the period of actual operations while times afterwards represent the hypothetical operational scenario used in the study. Blue and red bars indicate periods of injection and extraction, respectively, in that specific well. Figures of mixing fraction over time for the remaining 26 dual-purpose wells are also presented in Appendix D.

Contour plots of mixing fraction f (Figure 3.10) help illustrate the decreases in f_d during a well's idle periods (Figure 3.9a). Injection occurred at some point in each of the 29 dual-purpose ASR wells over the actual operations period, and the induced hydraulic gradients from these injections caused the plumes of injected water to migrate radially away from the center of the wellfield relative to their respective injecting wells, becoming more pronounced and moving from the northwest center to the distal edges of the wellfield in October 2013 (Figure 3.10a). High concentrations of native water ($f < 5\%$) are still present in the spaces between wells which have high injected water concentrations ($f > 90\%$ in one location) after nearly 5 years of operations in February 2009 (Figure 3.11). By October 2013, after 9.5 years of operation, the individual injected plumes have merged and are much less distinct, especially where the wells are spaced closer together on the western side of the wellfield (Figure 3.10a), and the mixing fraction along A-A' through the entire wellfield is much more uniform ($60\% < f < 85\%$, Figure 3.11). After 19 years of equal volumes of injected and recovered water from the dual-purpose ASR wells, the remaining plume of injected water appears to be nearly completely coalesced throughout the wellfield in April 2023 (Figure 3.10b). Additionally, the modeled operations of the hypothetical period, which essentially reversed the actual operations of the previous 9.5 years, is effective at undoing most of the outward migration of the injected plumes. The individual plumes appear to be mostly centered on their injecting wells, which allowed those wells to extract more of the high mixing fraction water in the center of those plumes.

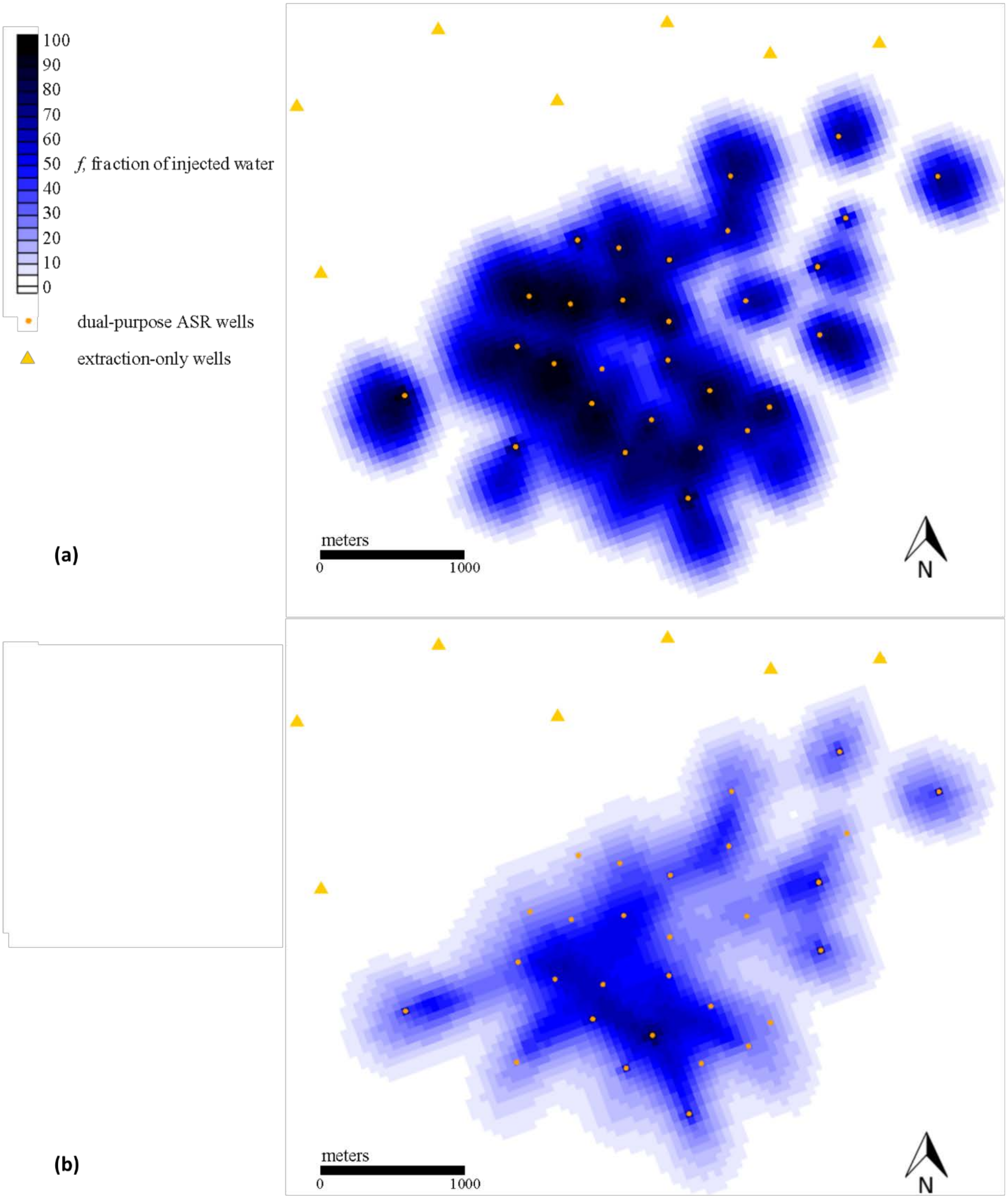

Figure 3.10: Estimated distribution of mixing fraction (f) in Layer 4 at the end of the actual operations period in October 2013 (a) and at the end of the hypothetical period in April 2023 (b).

The background hydraulic gradient shifts the centers of the injected plumes slightly downgradient of their respective wells (Figure 3.11). The pumping from the 7 extraction-only wells, which are updip and upgradient of the dual-purpose wells, is intended to minimize this downdip movement of the injected water.

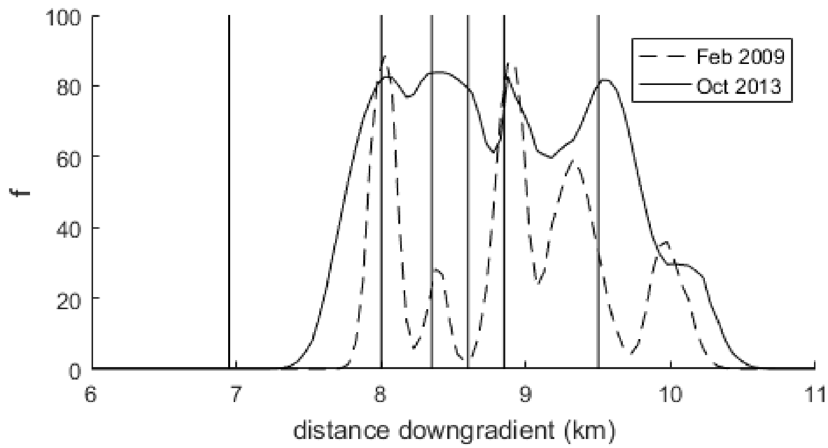

Figure 3.11: Cross section (A-A' as shown in Figures 3.1 and 3.2) of mixing fraction f in Layer 4 at the end of the actual operations period in October 2013 as depicted in Figure 3.8(a). Locations of wells along or near A-A' are depicted – only the two most downgradient wells are on A-A', while the four upgradient wells are laterally within 150m of A-A'.

Assuming a longitudinal dispersivity (α_L) of 25 meters, it takes more than 5 years for the injected waters to coalesce in most portions of the well field; prior to that, the injected plumes still appear fairly distinct from one another (Figure 3.11). This coalescing of the injected water plumes in the spaces between and around the wells occurs sooner when simulated with higher values of α_L. Since insufficient tracer data was available to constrain α_L, a sensitivity analysis of α_L (Figure 3.12) was used to identify the range of ASR system performance in terms of f_{cum} for actual operations during the actual operations period, hypothetical operations during the future

9.5 years, and for the operations of both periods combined. Estimates for f_{cum} during actual operations ranged from 53-90%, but when including the hypothetical operations, the f_{cum} estimates for the entire 19 year period drop to 46-84%.

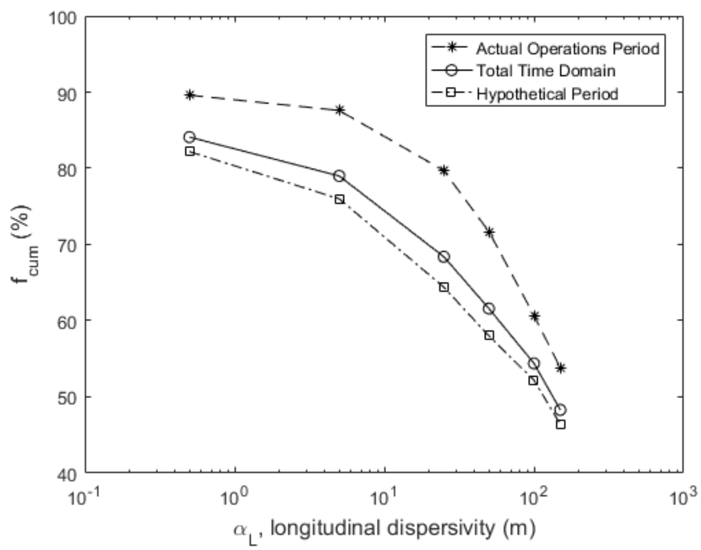

Figure 3.12: Sensitivity of cumulative recovered fraction, f_{cum}, to changes in α_L for the various modeled time domains: the first 9.5 years ("Actual Operations Period"), the second 9.5 years ("Hypothetical Period"), and the entire 19 modeled years ("Total Time Domain").

3.4.3 Examining extent of injected plumes with MT3DMS solute transport model

In order to better understand the movement of injected water, tracer was only injected into one well (Well 24) while still maintaining the same groundwater flow model. Well 24 was selected because the close proximity and orientation of nearby wells were ideal for estimating best case conditions for migration of injected waters to other wells for potential recovery. However, only minimal mixing fractions of injected water (<30%) reach other nearby wells

(Figure 3.13), suggesting that recovery of injected waters should occur from the same wells they were injected into.

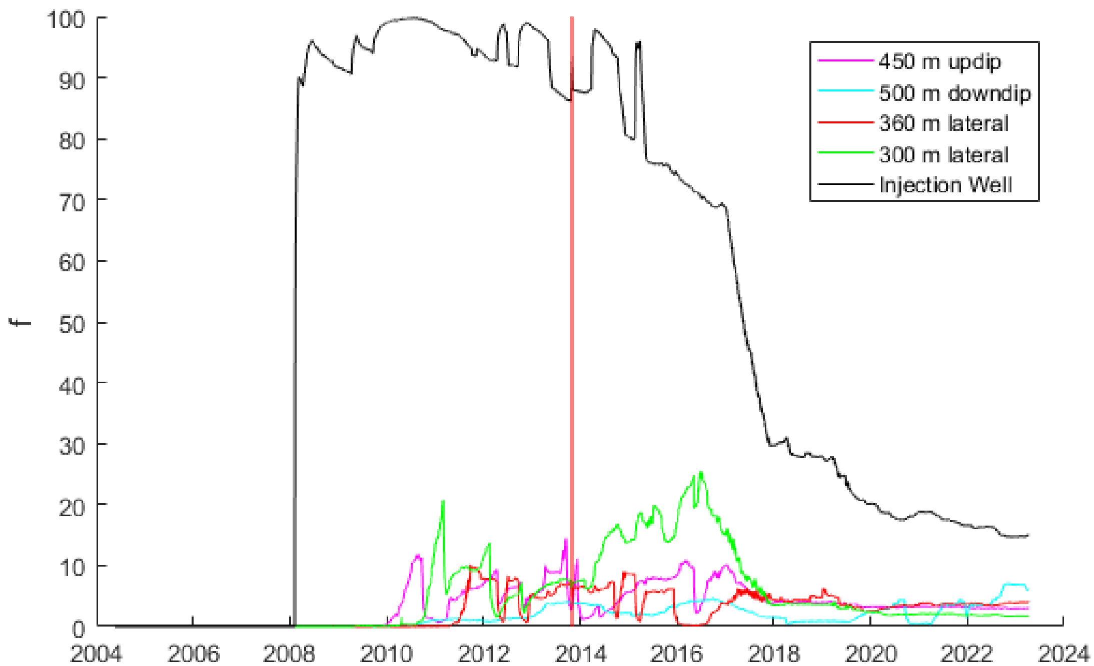

Figure 3.13: Mixing fractions in the injection well (black) and other nearby wells (magenta, aqua, red, and green) for the simulation where tracer was only injected into a single well, well 24.

3.5 Discussion

The results in this study provide several insights into ways to improve operations of large scale, multi-well ASR systems. The single-well simulation, where tracer was only injected into one well, suggests that each dual-purpose well should be operated individually given the specific hydrogeology and well spacing at the San Antonio ASR facility, meaning that water injected into one well should be recovered from that same well if maximum recovery efficiency is the ultimate goal of the ASR system. Neither dispersion, advection caused by well pumping, or advection caused by the regional background hydraulic gradient caused injected water to travel far enough in sufficient concentrations to warrant recovery in nearby wells. Dispersion and advection of injected water from pumping resulted in mixing fractions no higher than approximately 30% in nearby wells, while movement of injected water caused by background gradient was negligible compared to the distances between wells.

However, the results of the simulations where tracer was injected into all 29 dual-purpose wells suggest that each well clearly cannot be operated without considering the hydraulic effects of the other wells in the wellfield. Induced hydraulic gradients caused by pumping in other wells push and pull the injected plume of each well in different directions, but never far enough to be sufficiently recovered in any other wells. These hydraulic effects appear to be the most pronounced on the distal wells of the wellfield (Figures 9 and 10). Injected plumes in the central and proximal wells likely tend to stay more centered on their respective wells due to roughly equal induced gradients on all sides over time.

In this setting, it appears that the primary benefit of a multi-well system with this spacing is the large capacity of the facility and not the ability to operate the wells as a system, injecting water in one well and recovering in others. Closer well spacing could achieve this ability, while greater well spacing would lessen the hydraulic impacts between wells' injected plumes. However, many factors other than movement of injected plumes guide well spacing requirements, such as land acquisition costs and acceptable increases and decreases in the potentiometric surface.

Given the hypothetical recovery scenario and a reasonable range of dispersivity values (0.5 To 150 m), the cumulative recovered fraction (f_{cum}) of injected water over 19 years of operations would range between 48 and 84%. These ratios indicate that a large scale, multi-well ASR system like the H2Oaks center can be successful if placed in a hydrogeologically favorable settings. Aquifers with adverse conditions such as high regional hydraulic gradients, dispersivities, and heterogeneity would significantly decrease the recovered fraction through unrecoverable downgradient movement or excessive mixing. Thorough characterization of the storage aquifer is vital to ensure that these and other unfavorable conditions are accounted for and included in the design of the system in order to maximize recovery efficiency.

Even though the groundwater flow model reproduces heads fairly well over the 6 year observation period, it poorly predicts a drop in aquifer heads in July-September 2009 (Figure 3.7) across nearly all ASR wells. This corresponds to a period when all 29 ASR wells were idle and only the extraction wells to the north were actively pumping. We interpret this to indicate that the model underpredicts the influence of the extraction-only wells to the north and west of the ASR wells. Based on aquifer elevations used in the GAM and the boundaries of the Carrizo-Wilcox published by the TWDB, the extraction only wells are typically shown to be in the confined subcrop of the Carrizo (Figure 3.1), but only barely so. However, available borehole logs from SAWS for these wells are not clear as to the presence or absence of the Reklaw confining layer. Attempts to simulate the confining Reklaw in layer 1 above these seven wells were unsuccessful, as the cells in question always went dry due to their thinness caused by the vertical discretization of the model into 6 layers. We acknowledge this as a shortcoming of the model, but one that we consider minor due to both the small number of these wells relative to the number of ASR-dual purpose wells and the infrequent pumping from these wells across the 9.5 years modeled in this study.

Groundwater flow and transport models clearly add value to management of ASR operations. Without a transport model, it would to be difficult to envision or predict that injected plumes have moved radially outwards from the injection well (Figure 3.10), and thus would be difficult to know which wells provide for the most optimal recovery efficiency at any given time. Low values of f_d are caused by extraction from wells where the injected plume has had significant lateral movement relative to the well (supplemental animation, Appendix C). Well-developed, well calibrated, and frequently updated flow and transport models would allow development of recovery strategies that focus recovery in the most centered injected plumes of the wellfield, and could potentially raise f_{cum} calculated in this study by 5-10%. Such transport models would also help optimize future operations by evaluating several operations scenarios in regards to recovery efficiency. The results of this study suggest a hypothetical operations scenario that reverses the previous operations is an effective solution for optimizing recovery in multi-well ASR wellfields with dual-purpose wells. Some of the injected plumes in the outermost wells had migrated far from their injecting well, but running the system in reverse effectively re-centered the plumes so they could be accessed for effective extraction. However, this is only expected to be viable in aquifers without high background hydraulic gradients that can cause significant downgradient migration away from wells. In those cases, alternative measures such as upgradient injection followed by downgradient extraction would likely be more effective. Upgradient extraction from wells similar to the extraction-only wells in this study also could help offset the regional gradients.

At SAWS, the modeled recovered fractions obtained under non-optimized operations meet the goals of the system and indicate that the system is functioning successfully. Given that both the injected Edwards aquifer waters and native Carrizo sand aquifer water are of high quality and are generally chemically compatible, high recovery fractions are not critical. However, while optimization may not be cost-effective in this case, the results of this study have implications for other currently-operating multi-well ASR systems or water utilities considering large scale ASR as a water storage alternative. They are especially pertinent in locations where the native water quality is degraded or brackish or there is elevated potential for adverse geochemical reactions between the injected water and native aquifer water or matrix. For instance, oxidation of arsenian-pyrite in some ASR systems has mobilized arsenic in the recovered water. Groundwater flow and transport models can serve as valuable tools to maximize ASR operations. A well-calibrated model supported by thorough aquifer characterization and real-time data acquisition can be used to predict or track the approximate location of injected plumes when actual pumping rates are incorporated into the model, while multiple future pumping schemes can be evaluated to determine the most effective operation in terms of f_{cum}. Adding chemical reaction capabilities to a groundwater flow and transport model such as this, as in reactive transport models like RT3D and PHT3D, also would potentially open up the possibility of implementing ASR systems in aquifers with less than ideal geochemical compatibility, such as those where oxidation of arsenian-pyrite may be expected to mobilize arsenic, by tracking both the injected water and reactive fronts.

3.6 Conclusions

Well designed and properly calibrated flow and solute transport models are useful tools for assessing movement of injected water and transport of its chemical constituents. Such flow and transport models can also be used to evaluate different future operations scenarios to optimize recovery efficiency.

Large scale, multi-well ASR systems can be successful, as this study shows that recovery efficiencies ranging from 48-84% over 19 years may be possible depending on longitudinal dispersivity. Assuming a dispersivity of 25m, we estimate that the ASR system in this study achieved 82% recovery efficiency over its first 9.5 years of actual operations.

Operations of large, multi-well ASR systems appear to require different methods than those suggested for smaller multi-well systems, such as injection via one well and extraction via multiple wells. ASR systems like that of San Antonio's may have well spacing requirements due to the large capacity of the wells that preclude effective recovery from any well except the injecting well. However, while injection and recovery operations should be contained to the same well, each well cannot be operated completely independently of the others.

Hydraulic effects from other wells in the wellfield that cause injected waters to migrate around and sometimes away from their respective wells require strategies to maximize recovery efficiency. One strategy is to utilize the ASR wells and reverse the injection operations of the system during recovery operations to effectively reduce the hydraulic effects of injection amongst the wells.

4. MODELING THE REGIONAL EFFECTS OF A LARGE, MULTI-WELL AQUIFER STORAGE AND RECOVERY SYSTEM

4.1 Overview

A previously-developed regional groundwater flow model was modified to simulate and estimate the effects of a large, 74 MGD multi-well aquifer storage and recovery (ASR) system on the surrounding Carrizo-Wilcox aquifer near San Antonio, Texas. The large, multi-well ASR system has great hydraulic effects on the nearby aquifer (<=2 miles from the wellfield) over time scales less than a year, but beyond this, hydraulic effects are imperceptible relative to typical seasonal variations in aquifer heads. Over long time scales (i.e. decades), such ASR systems can potentially raise aquifer heads over large areas, as much as 3 feet at distances of 10 miles if the recovery is less than recharge. Transport simulations indicate that injected waters in these systems do not move significantly away from the wellfield, so no water quality effects are expected outside of the ASR wellfield itself. Finally, pumping operations at this ASR facility are correlated well with other aquifer users, likely explained by demand variations with precipitation. However, precipitation does not fully explain the variation in ASR pumping operations.

4.2 Introduction

Aquifer storage and recovery is a water storage system that can provide ancillary benefits to the regional aquifer around it. Current and proposed ASR systems indicate that usable storage on the order of 10^6 acre-feet may be attainable, which is comparable to many surface reservoirs in the United States (Maliva et al. 2006). In certain locations, like the warm and arid American southwest, ASR may be preferable to surface reservoirs. Deep underground, ASR systems experience little to no evaporative losses (Bouwer 2002). They also minimize environmental disturbances and land consumption, since they require only a few small facilities at the land surface like pumps, wellheads, and occasionally a treatment plant (Maliva and Missimer 2010). However, ASR is not limited to only arid locales. ASR is applicable in a wide range of climates, as indicated by its successful adoption across the world: arid deserts in the Middle East (Maliva et al. 2011), temperate grasslands and wetlands of the Netherlands (Antoniou et al. 2012), and subtropical wetlands of Florida (Jones and Pichler 2007). Additionally, many types of aquifers can serve as the storage space, including aquifers that are shallow or deep, fresh or saline, thick or thin, sandstone or limestone, or any other of a number of aquifer classifications (Maliva and Missimer 2010).

Aquifer storage and recovery has been used to provide water storage for a variety of purposes: drinking water supplies for municipalities, minimum environmental stream flows, and protection against seawater intrusion in freshwater aquifers among other uses (Pyne 2005; Shammas 2008). Municipalities may use ASR to provide long term water storage or to manage seasonal imbalances in water supply and demand (Pyne 2005; Maliva and Missimer 2010). Increased aquifer heads, subsidence mitigation, and improved water quality are some commonly mentioned benefits that ASR can provide to nearby users (Ros and Zuurbier 2017). One study in western Australia, which modeled an array of ASR wells over 70 square miles with a total capacity of 12 MGD, found that heads could be increased in localized areas by as much as 250 feet (Martin et al. 2012). Under the specific site hydrogeology, the modeling showed that injection via these ASR wells was capable of producing artesian conditions in the aquifer (Martin et al. 2012). However, not all ASR systems provide these benefits. Some systems in Florida have been plagued by releasing arsenic from the aquifer matrix into solution (Wallis et al. 2011; Neil et al. 2012). Since ASR systems also extract water, neighboring users may become concerned about decreased heads that may affect the water levels in their wells (Morris et al. 2010).

As ASR systems become more mainstream, they are also becoming larger. Water providers in Las Vegas, San Antonio, and near Los Angeles all currently operate multi-well ASR systems with capacities larger than 60 million gallons per day (MGD) (Malcolm Pirnie Inc. et al. 2011). Depending on their respective hydrogeological settings, these larger capacity systems may have increased effects on the regional aquifer around them. Two previous studies of the SAWS H2Oaks ASR system also indicate that during the first 7 years of operation, injected waters likely did not migrate far away from injection wells, and thus had a rather minimal effect on water quality in the surrounding region (Crow 2012; Otero and Petri 2010).

This study seeks to understand how an ASR system affects the heads and water quality of the regional aquifer around it, by specifically analyzing the H2Oaks ASR system and its surrounding hydrogeology. The objectives of this study include: determining any potential relationship between precipitation and ASR operations, evaluating the short-term and long-term effects of an ASR system on the surrounding aquifer heads, and evaluating any water quality effects the ASR system may have on the surrounding aquifer. We hypothesize that (1) effects of ASR pumping under future possible drought conditions can be adequately predicted by relating historic ASR pumping to precipitation, or more specifically the Standard Precipitation Index (SPI); (2) at a distance of 2 or more miles from the wellfield, the hydraulic effects of the ASR system won't exceed 150% of the maximum annual variation or 200% of the average annual variation in historic heads; (3) ASR operations could raise heads long-term by as much as 2 feet at a distance of 10 miles away from the system; and (4) lateral movement of water injected via the ASR system will be so minimal that no nearby wells would expect to see appreciable concentrations of a conservative tracer.

4.3 Methods

4.3.1 Site description

The San Antonio Water System's (SAWS) H2Oaks ASR system stores unused water from its Edwards Aquifer annual permit in the Carrizo sand formation of the Carrizo-Wilcox aquifer (CH2MHILL 2003). In operation since 2004, this system helps to mitigate both seasonal fluctuations in water supply and demand as well as provides long term water shortages during times of drought. The H2Oaks ASR system is comprised of 29 dual purpose injection-extraction wells and 7 additional extraction-only wells. The dual purpose wells are capable of a combined 64 MGD pumping capacity, with an additional 10 MGD from the extraction-only wells. As such, H2Oaks is the third largest ASR system in terms of pumping capacity in the United States. The ASR wells are screened in the Carrizo aquifer at the southern tip of Bexar County, in Texas, about 30 miles south of SAWS' source wells in the Edwards aquifer. These 36 wells are scattered over approximately 4.5 square miles (CH2MHILL 2006). Daily well flow data was obtained from SAWS for all 36 wells from the beginning of ASR operations in May 2004 through December 2013 (San Antonio Water System 2013).

The H2Oaks wells are just downdip of the Carrizo outcrop; the Carrizo is confined above by the Reklaw clay unit, and underlain by the Wilcox aquifer. The Carrizo aquifer in this area is about 700-800 feet thick, and primarily sand. Based on borehole logs of the ASR wells, some interbedded clay lenses exist throughout the area. Water quality tends to be slightly high in iron and manganese (CH2MHILL 1998).

4.3.2 Groundwater flow model development

4.3.2.1 Original model

In the late 1990s and early 2000s, the TWDB commissioned Groundwater Availability Models (GAMs) to estimate available future groundwater resources in order to facilitate water planning across the state. As such, these models are publicly available. All nine of the major aquifers in Texas have completed GAMs, and many of the state's minor aquifers do as well. The southern Queen City and Sparta (QCSP) GAM served as the regional model for this study.

The southern QCSP GAM, finished in 2005, added the Queen City and Sparta minor aquifers to the southern Carrizo-Wilcox GAM, previously completed in 2003 (Kelley et al. 2004; Deeds et al. 2003). The model simulates 8 layers from the Sparta aquifer down to the Lower Wilcox unit from 1975 through 2050; the Carrizo aquifer comprises layer 5 in the model. The QCSP GAM used the MODFLOW-96 code, which was the TWDB standard when it was commissioned to maintain consistency across all aquifer GAMs, but this study used MODFLOW-2000 (Harbaugh et al. 2000; Harbaugh et al. 2010). The GAM simulates 76 annual stress periods over 1 square mile cells; the 36 ASR wells are contained in 8 GAM grid cells as shown in Figure 4.1. Several sets of input files are available for the southern QCSP GAM that allow the user to simulate the Texas drought-of-record in a selected decade (i.e., 2000s, 2010s, 2020s, 2030s, 2040s) or not at all. In the original model, the drought of record conditions were simulated only by altering the recharge to the aquifer. The results of the GAM indicated that almost no change in water levels (outside of minor changes near the thin, updip recharging areas) was evident due to changing recharge in any of the drought of record simulations, so the no-drought-of-record simulation was used as the base model in this study (Kelley et al. 2004).

This study only varied well pumping rates in the MODFLOW model; other parameters such as hydraulic conductivity, storage coefficients, and recharge were left untouched. The model was used to determine the ASR system's effects on the regional aquifer during both historic operations as well as hypothetical future operations in Sections 4.3.2.2 and 4.3.2.3. Some of the results in this report are depicted in terms of net heads, which represent the head differences between simulations that incorporate new well pumping and the original unaltered GAM simulation.

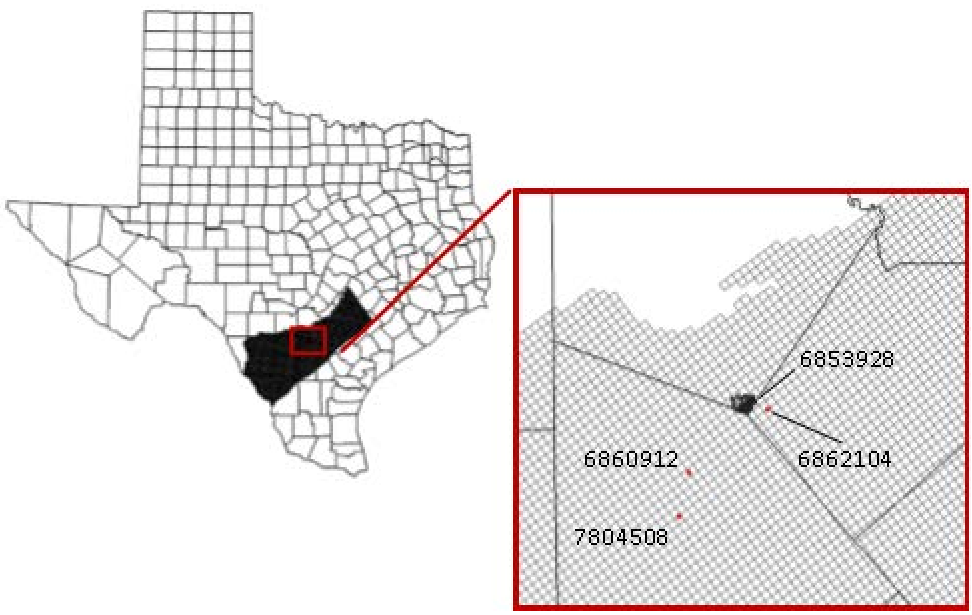

Figure 4.1: Outline of the Southern Carrizo-Wilcox GAM, with inset showing the location of the H2Oaks ASR wells (black) and nearby monitoring wells (red) relative to the regional model cells, with Texas county lines for reference. ASR wells are at the southern end of Bexar County. Model cells are 1 mi x 1 mi.

4.3.2.2 Simulations of historic operations

The H2Oaks ASR operations for the first 10 years were simulated to analyze its regional effects on the aquifer. The pumping rates of the ASR system varied significantly on a daily basis (Figure 4.2). To adequately account for this pumping variability in the model, the input files were altered to use daily stress periods during ASR operations from June 2004 through December 2013 instead of the annual stress periods that were used in the original model. Three distinct simulations with refined stress periods and time steps were run: a baseline simulation without any altered pumping scheme, a simulation with SAWS ASR pumping incorporated, and a simulation with SAWS ASR and other regional pumping data incorporated. The daily ASR pumping rates (Figure 4.2) were superimposed onto existing well pumping rates already in the GAM for the eight Carrizo cells encompassing the H2Oaks facility (located in layer 5). Other regional pumping was estimated using raw monthly data from the Texas Water Development Board's Groundwater Use Surveys for 2004-2013 (2017). A brief overview of the process used to generate appropriate well pumping boundary conditions from this raw data is presented here (see Appendix E for additional details).

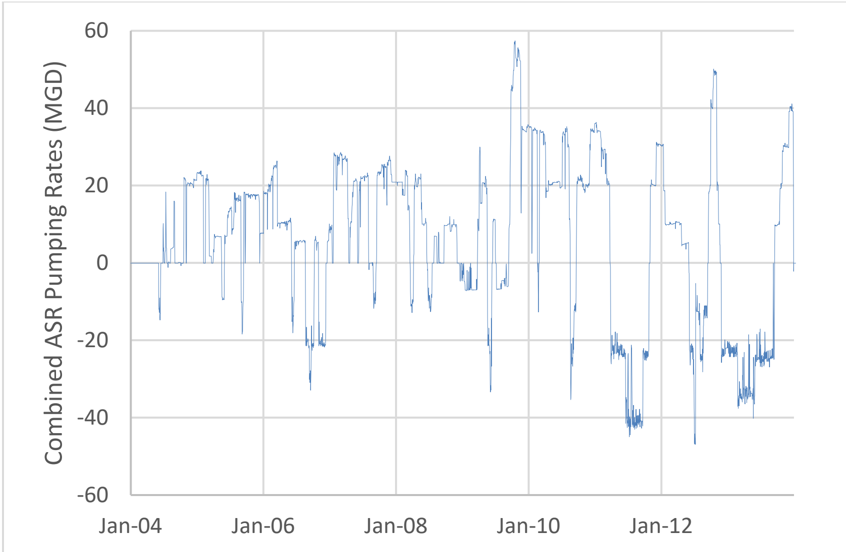

Figure 4.2: Combined pumping rates for the eight cells that contain H2Oaks ASR wells: positive rates indicate injection while negative rates indicate recovery/extraction. Daily pumping rates are used from June 2004 through December 2013; GAM-defined annual pumping rates are used before and after, but are negligible relative to the ASR pumping rates.

Pumping rates are voluntarily reported by some but not all groundwater users: however, it is assumed that the majority of the large water users are included in these surveys, and as such, account for the majority of aquifer drawdowns. For some responding users, only annual pumping rates were available, so monthly distributions of those rates were estimated from the average distributions of other nearby users based on the following categories in the following order depending on which categories had data: county-river basin-user type-year, county-river basin-year, county-year, and year. Well locations (which were not included in survey data) were estimated for users by linking name/owner fields between the Groundwater Use Surveys and the TWDB's Groundwater Database (GWDB), which does include well locations. Some inconsistencies between the name/owner fields in the Surveys and GWDB required some users to be manually linked. Finally, if no well records in the GWDB existed for a user from the

Groundwater Use Surveys, well locations for that user was estimated using web searches. If multiple wells were present for a user, reported groundwater pumping was distributed equally across those wells. Locations could not be found or estimated for all users, but users without identified locations only accounted for 2% of the pumping across the entire southern GAM area and less than 5 small users were unaccounted for in the counties immediately surrounding the ASR facility. Wells identified from the GWDB were assigned to model layers that corresponded to the actual aquifer formations listed for those wells in the GWDB. Model layers for locations identified from web searches were assigned by assuming their aquifer formations matched that of the nearest well from the GWDB using Theissen polygons. Once the appropriate grid cells were determined for each well, those monthly pumping rates were superimposed onto the rates used in the simulation with ASR pumping already incorporated.

Water level measurements, described in Table 4.1, from four monitoring wells surrounding the H2Oaks ASR wellfield (Figure 4.1), were collected from the TWDB's Groundwater Database for comparison to modeled results (Texas Water Development Board 2015). Two of these monitoring wells, 6853928 and 6862104, were used by the USGS to monitor head near the ASR facility. Correlations between observed heads in the monitoring wells and modeled heads were calculated to determine how closely the model reproduces trends and amplitudes of head changes at various distances from the ASR wellfield.

Table 4.1: Monitoring wells used in study.

Well	Distance to wellfield center (mi)	Observation dates	# of observations during historic operations
6853928	1.3	2009 - current	40
6862104	3.0	2003 - current	213
6860912	10.7	1992-2008	100
7804508	15.9	2008 - current	131

4.3.2.3 Predicted future operations

4.3.2.3.1 Relationship between ASR operations and precipitation

In order to help make predictions about future ASR operations during future potential drought conditions, the ASR pumping rates from June 2004 through December 2013 were compared to historic precipitation during the same period. Standardized Precipitation Index (SPI) is a probability index that represents a location's relative wetness or dryness and is based on monthly precipitation values. SPI can be calculated for a region or a specific sites, and can be calculated for one to 36 months. Several SPI datasets from NOAA for various relevant locations and time periods were analyzed for correlation with H2Oaks monthly total pumping rates (National Oceanic and Atmospheric Administration: National Centers for Environmental Information 2017a).

In order to adequately assess this relationship, the ASR pumping rates were summed by month to match the monthly values for SPI. Additionally, since the ASR system has had three phases of well construction, the total possible wellfield flow has increased over time. To account for this, ASR monthly pumping values were converted to a ratio from 0 to 1, where 0 represented the maximum possible extraction capacity of the system and 1 represented the maximum possible injection capacity of the system at any particular time (since these are not always equal, due to the 7 extraction-only wells).

4.3.2.3.2 Simulations of predicted future operations

Three simulations of predicted operations were analyzed in this study in order to assess potential future regional effects of the H2Oaks system. For these simulations, the yearly stress periods from the original model were preserved. To account for this, the daily ASR well flows used in the previous simulations were averaged by calendar year. Table 4.2 indicates the average annual flow rates for the entire ASR multi-well system.

Table 4.2: Annual average daily flow rates at H2Oaks facility.

Year	2004	2005	2006	2007	2008	2009	2010	2011	2012	2013
Average wellfield flow (MGD)	4.2	11.2	2.4	17.6	8.5	11.4	20.9	-6.7	2.6	-20.7

At the end of operations in 2013, the ASR facility had stored approximately 18,750 million gallons (MG) of water in the Carrizo aquifer. Using the maximum yearly extraction rate of 20.7 MG/day (MGD) observed at the H2Oaks system through the end of 2013, it would take about 2.5 years to withdraw the stored volume of water. Therefore, the first predicted operations scenario, such as might be used during an extended drought, simulated actual ASR operations from 2004 to 2013, followed by a 3 year period of extraction at the maximum observed pumping rate of 20.7 MGD. A second predicted operations scenario, similar to the first, simulated actual ASR operations from 2004 to 2013, followed by a 1 year period of extraction at the facility's maximum possible pumping rate of 74 MGD. At this pumping rate, it would take about 0.7 years to fully extract the stored volume from the Carrizo. The maximum pumping rate of 74 MGD is based on the pumping capacity of the wells in the ground –pipelines and other infrastructure at the surface actually prevent SAWS from extracting and pumping back to the city at this full capacity, but this scenario assumes all infrastructure is in place to take advantage of the full well-pumping capacity. A third scenario simulated the same pumping rates in the ASR wellfield from 2004-2013 consecutively every ten years until the end of the model in 2050 in order to assess the potential regional effects of decades-long ASR operations. Results are shown in terms of the difference in heads between the altered simulations and the baseline GAM.

4.3.3 Development of solute transport model

A solute transport model was developed using the MT3DMS code to simulate transport of Edwards aquifer water injected into the Carrizo via the ASR wells (Zheng and Wang 1999). Only the advection, dispersion, and source/sink mixing packages were included. An imaginary tracer with a concentration of 100 mg/L in Edwards water and 0 mg/L in native Carrizo water was used. Longitudinal dispersivity (α_L) was assumed to be 500 feet. The ratios of transverse horizontal dispersivity to α_L and of vertical transverse dispersivity to α_L were assumed to be 0.1 and 0.01, respectively, for all model cells. The solute transport model was developed using the annual stress period groundwater flow model described in the previous section.

4.4 Results and discussion

4.4.1 Simulations of historic operations

Of the monitoring wells near the ASR facility with significant water level records, only one had significant records before the ASR system went into operation. That well (6860912), which is more than 10 miles southwest of the ASR system, clearly exhibits seasonal variation in water levels (Figure 4.3). From 1992 to 2003, the average annual variation in water levels was 33 feet, with a maximum variation of 47 feet in 1998. This variation is assumed to represent the variation in aquifer heads for the area surrounding the H2Oaks system before it went in to operation in 2004. Model results are compared later to these values to determine how the ASR system affects heads relative to this pre-ASR variation.

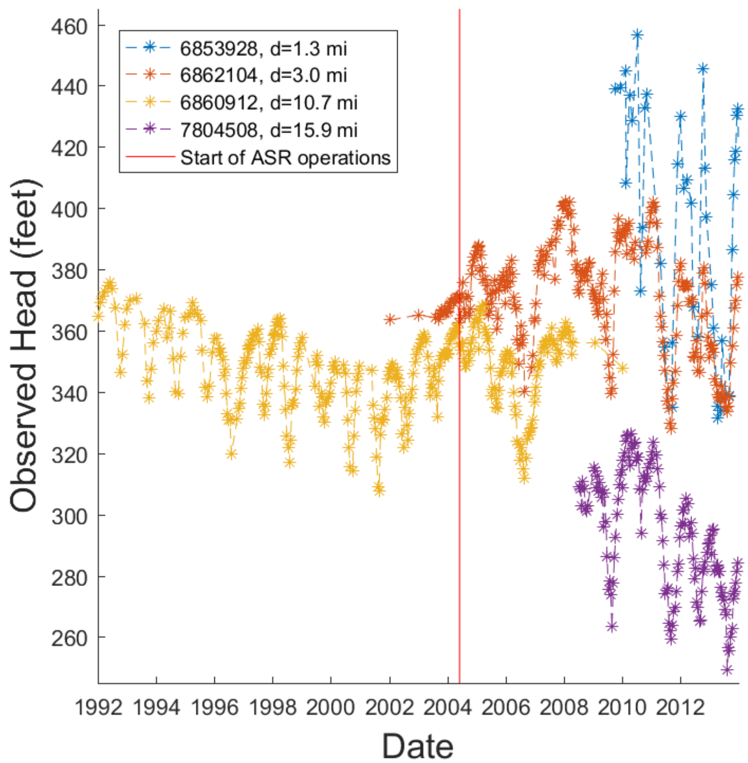

Figure 4.3: Observed heads in the four monitoring wells around the ASR facility.

Changes in water levels appear very similar across the various wells both in amplitude and trend, independent of distance from the ASR wellfield. The monitoring wells 3 and 10 miles away from the center of the ASR wellfield show nearly identical water level changes from the start of operations in 2004 through 2008. After that, the monitoring well 15 miles away from the wellfield closely mimics the changes in the monitoring well 3 miles away. The closest monitoring well, at 1.3 miles, follows the same trend as the 3 and 15 mile wells, but with clearly larger amplitude differences. These results suggest three distinct possibilities: the ASR wells are influencing all of the wells, the ASR wells are influencing none of the wells, or the operation of the ASR wells may be correlated with the operations of other wells across the rest of the aquifer. The correlations between the simulated heads and the observed heads (Figure 4.4) help to clarify the regional effects of the ASR wellfield.

Correlations between modeled and observed heads for each of the three simulations (baseline GAM simulation, GAM with superimposed ASR pumping simulation, and GAM with ASR and other regional user pumping simulation) are presented for all four monitoring wells. As expected, no correlation exists between the baseline GAM simulation heads and the observed heads in any of the four wells, since the original GAM during this time period is based on relatively steady predicted pumping rates. However, very strong correlations exist for both simulations with ASR pumping in monitoring wells 6853928 and 6862104 which are 1.3 and 3.0 miles from the approximate center of the wellfield, respectively. The very similar correlations between the ASR simulation and ASR with regional pumping simulation indicate that the ASR wells govern the heads in these two wells with minimal influence from other aquifer users. The ASR simulation, however, shows weak correlation in wells 6860912 and 7804508, which are 10.7 and 15.9 miles from the center of the wellfield, indicating that the effects of the ASR pumping at these distances are minimal.

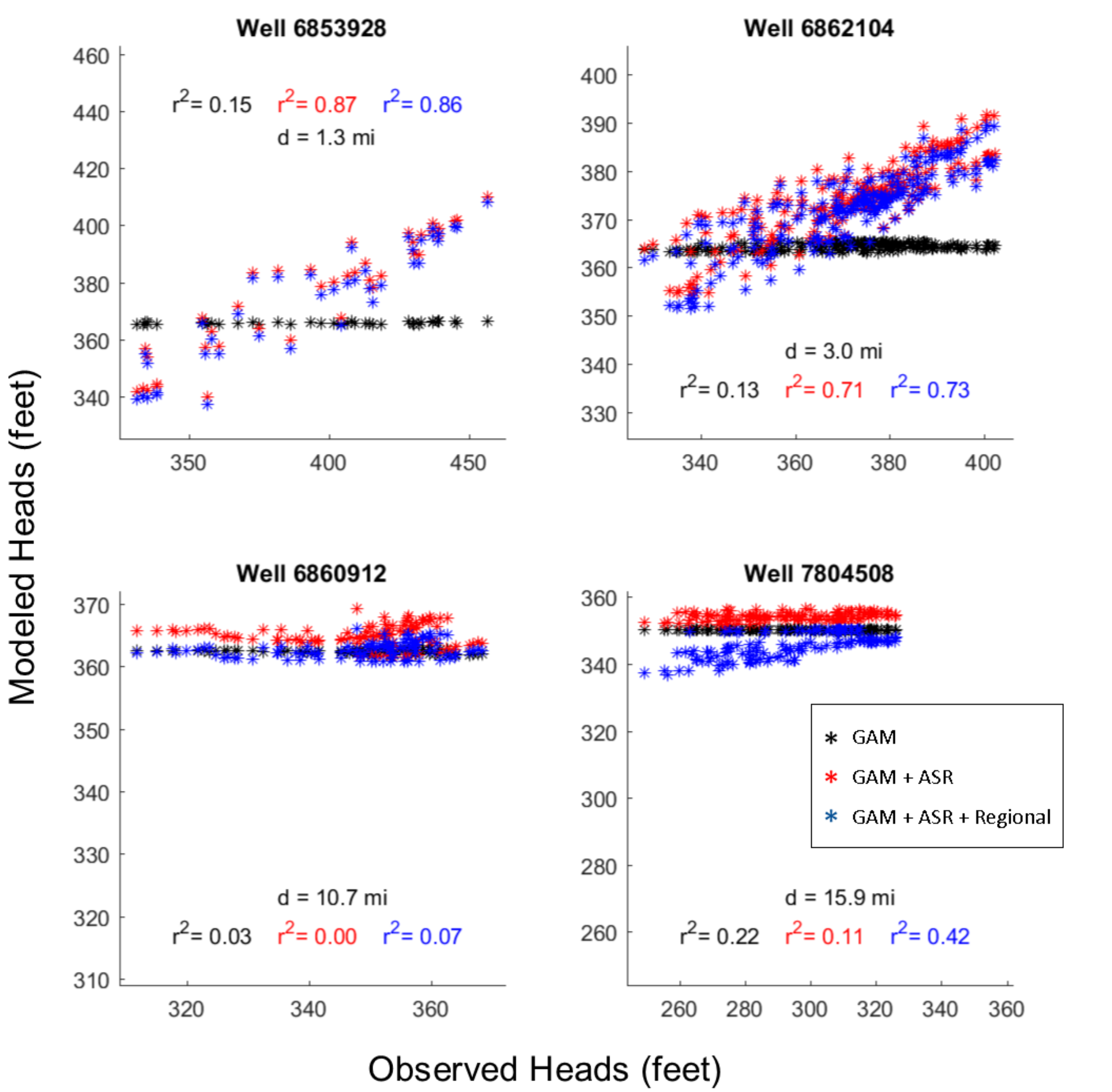

Figure 4.4: Modeled versus observed heads for the four monitoring wells near the ASR facility. Modeled heads are presented for each of the three historic operations simulations: black points represent heads from the base GAM model, red points represent heads from the GAM with superimposed ASR well pumping, and blue points represent heads from the GAM with superimposed ASR and other regional well pumping included.

Table 4.3: Parameters for regression equations for modeled/observed head correlations.

	m	b	r^2	M	b	r^2
	Well 6853928			Well 6862104		
GAM only	364	0.004	0.15	359	0.015	0.13
GAM + ASR	184	0.487	0.87	235	0.376	0.71
GAM + ASR + Regional	182	0.488	0.86	227	0.393	0.73
	Well 6860912			Well 7804508		
GAM only	364	-0.005	0.03	351	-0.003	0.22
GAM + ASR	368	-0.01	0	349	0.019	0.11
GAM + ASR + Regional	354	0.026	0.07	309	0.124	0.42

In well 7804508, the farthest well from the ASR wellfield, a stronger correlation exists for the simulation that includes both ASR pumping and other regional pumping relative to the ASR-only simulation, indicating that the other regional users pumping included is primarily responsible for the water level changes in this monitoring well. These results suggest the possibility of similar operations between the ASR wells and other aquifers users in the region is plausible. The possibility of similar operations is further supported by a correlation of monthly well flows for the ASR system and for all other aquifer users added to the model (Figure 4.5). Despite the fact that the ASR system can inject water while other aquifer users can only extract water, there is still an apparent trend between the ASR system’s pumping and all other users pumping. When relatively little extraction is happening elsewhere in the aquifer, the ASR system tends to be injecting more water, and when the most extraction is happening in the aquifer, the ASR system tends to switch into recovery mode. This correlation could be due to rainfall in the region. Under normal or abundant rainfall conditions, springs from SAWS’ source of water, the Edwards aquifer, provide more than the demand its users, and SAWS injects water into the Carrizo via its ASR wells. Similarly, other aquifers users appear to extract less water during these times, possibly accessing other surface water resources. During times of decreased rainfall and even drought, such as during Texas' worst one-year drought in 2011, SAWS clearly begins recovering water from its ASR wells (Figure 4.2), and other aquifer users also extract at higher rates. The relationship between precipitation and ASR operations is explored further in the following sections.

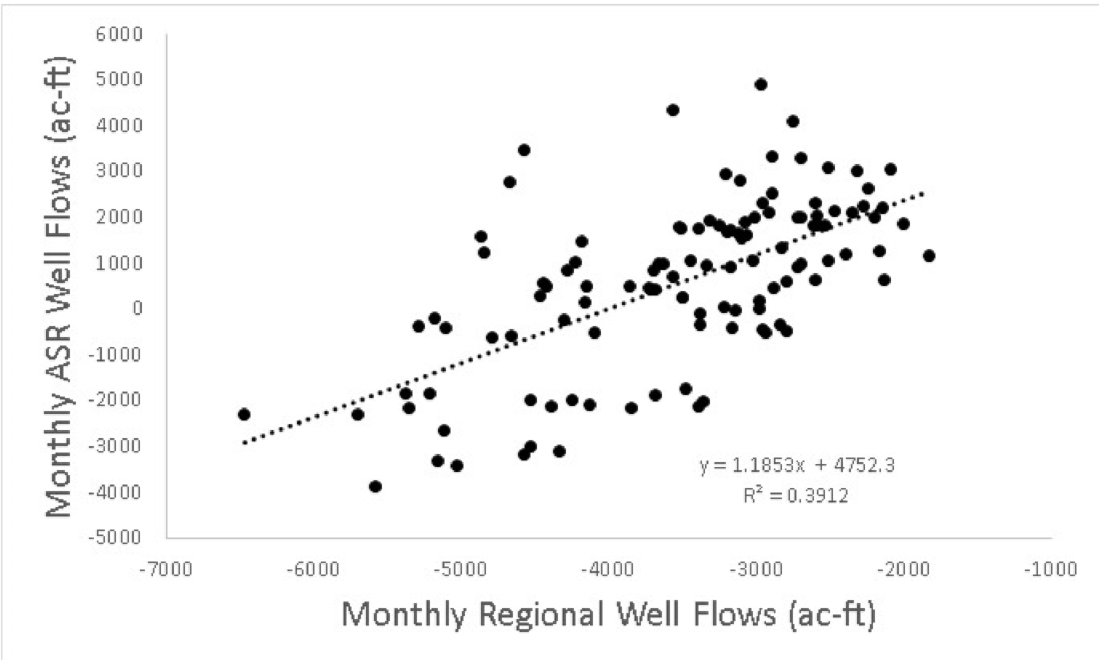

Figure 4.5: Correlation plot of the monthly total flows for the ASR facility and all other aquifer users implemented in the model, as taken from the TWDB's Groundwater Use Surveys. Even though the ASR facility is the only one in the region capable of injecting water, the positive correlation of these monthly pumping volumes helps explain the similar head trends seen at various distances from the ASR wellfield.

The model generally underpredicts the changes in heads caused by the superimposed pumping from the ASR system and the other aquifer users. At the closest monitoring well (6853928), the ASR pumping model only predicts approximately 49% of the actual head changes seen in the well, despite representing 87% of the head variation ($r^2 = 0.87$), while at monitoring well 6862104 3 miles away, it only predicts 37% of the observed head changes but represents 71% of the head variation. These high r^2 values indicate that the ASR system is the dominant cause of head changes near these two close monitoring wells. We expect that these underpredictions are due to the overestimated hydraulic conductivity values (40-70 ft/d) in the model that likely don't accurately reflect the local hydraulic conductivity. Previous studies have indicated that the hydraulic conductivity in and around the wellfield may actually be closer to 20-25 ft/d (CH2MHILL 2006; CH2MHILL 2003; Smith et al. 2018).

The model predicts head rises of up to 20 feet and declines as much as 30 feet during 2011 and 2013 at a distance of 2 miles from the wellfield near monitoring well 6862104 (Figure 4.6). Both drawdowns correspond to periods when the H2Oaks ASR system was extracting- the 2011 drawdown occurred during Texas' worst one year drought on record. The modeled drawdowns are less than both the average (33 feet) and maximum (47 feet) annual variations in aquifer heads previously stated. However, since the model may only predict approximately 38% of the head changes near well 6862104, the actual drawdowns at this location could potentially be as high as 79 feet (Figure 4.3), which does slightly exceed both 200% of the average variation (66 feet) and 150% of the maximum variation (70 feet).

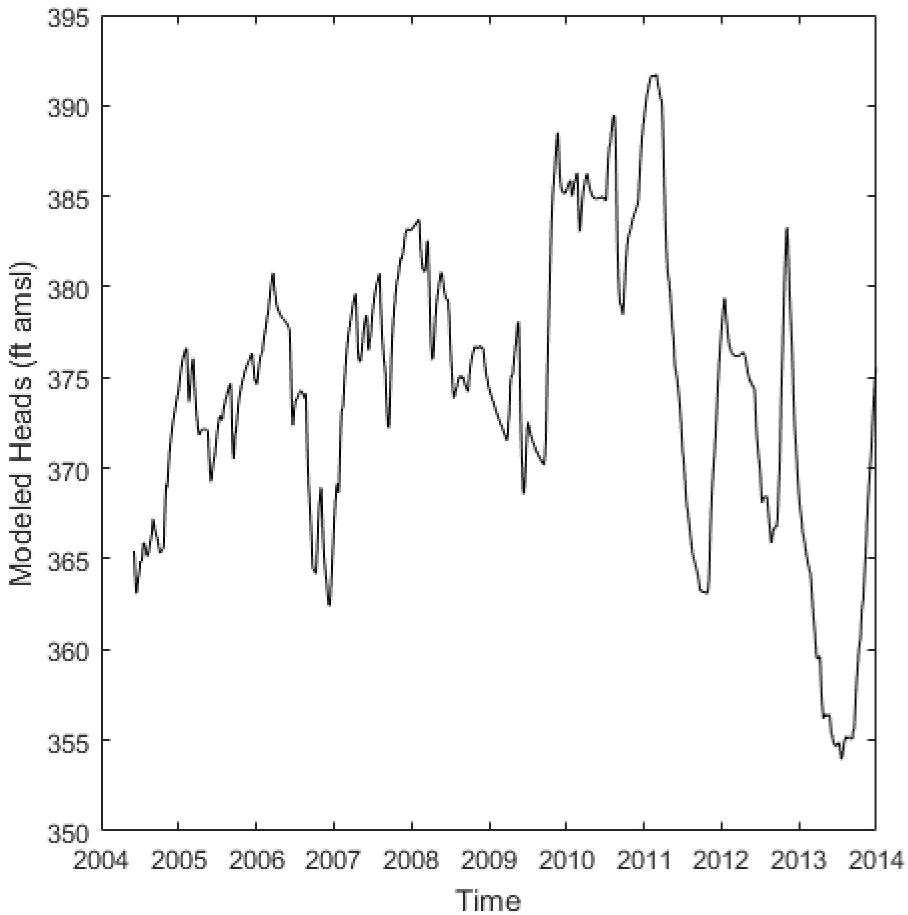

Figure 4.6: Head changes over time in monitoring well 6862104, approximately 3 miles from the center of the wellfield and 2 miles from the eastern edge of the wellfield.

4.4.2 Predicted future operations

4.4.2.1 Relationship between ASR operations and precipitation

Many variations of SPI were analyzed for correlation with monthly H2Oaks pumping values, presented here as a ratio from 0 to 1 (0 representing maximum extraction capacity and 1 representing maximum injection capacity at any given time). SPI values for 1, 3, 6, 9, 12, and 24 month time scales were analyzed for Texas climate divisions 6 and 7 as well as a handful of specific station locations near the H2Oaks facility. The best correlation ($r^2 = 0.24$) came from the 12 month SPI for climate division 6 (Edwards Plateau), which encompasses the source aquifer for H2Oaks, the Edwards aquifer (Figure 4.7). This SPI dataset indicates how unusually wet (positive SPI) or dry (negative SPI) the previous 12 months were relative to all other 12 month periods over the entire dataset in terms of standard deviation (going back to 1895). The data clearly indicates a generally positive relationship between wetness and injection (and dryness/extraction). However, the relatively weak correlation indicates that there are likely several variables other than precipitation that affect how much SAWS decides to inject or extract via the H2Oaks system. Such factors could include evapotranspiration, user demand for water, and availability of other SAWS sources. While the Edwards is still the primary and most vital water source for SAWS, it is not the only one (San Antonio Water System 2017).

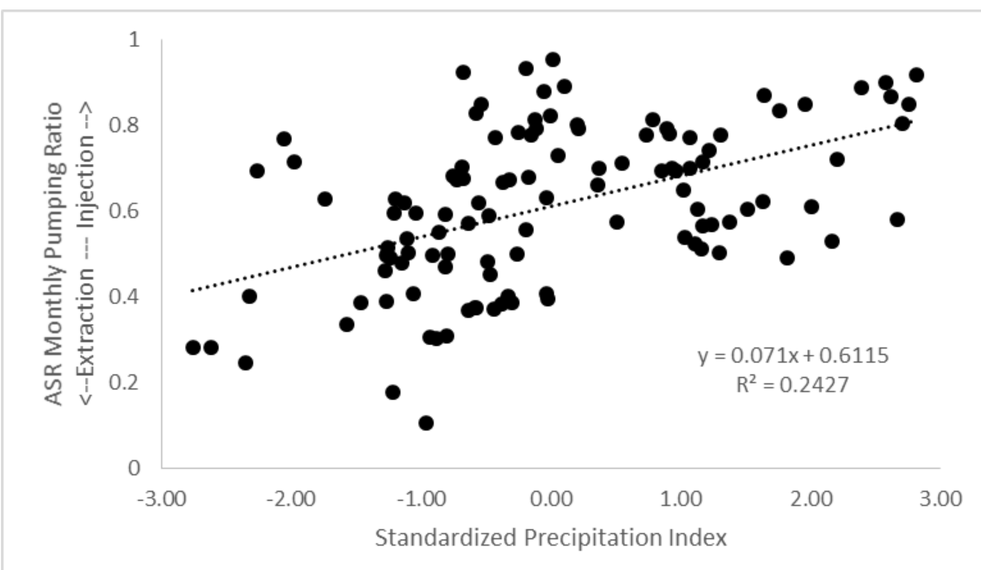

Figure 4.7: Correlation plot of monthly H2Oaks ASR pumping to the Standardized Precipitation Index. Monthly pumping is presented as a ratio from 0 to 1, where 0 is the maximum extraction capacity and 1 is the maximum injection capacity at any given time due to the phased nature of well construction at H2Oaks.

4.4.2.2 Simulations of predicted future operations

Since the relationship between precipitation and pumping rates was not strongly correlated for the H2Oaks ASR system, predictions for future operations scenarios were instead related to the maximum extraction rate used between 2004 and 2013 and the facility's overall maximum possible extraction rate.

The first predicted scenario simulates the H2Oaks system's operations under several consecutive dry years. Under this scenario, the ASR system would recover slightly more than its total volume of stored water from 2014-2016. Continuous recovery of 20.7 MGD for four years from 2013 through 2016 causes maximum drawdowns of 35 feet near the wellfield and ten feet at a distance of 8.5 miles of the center of the wellfield (Figure 4.8a). This drawdown 8.5 miles downdip would decrease from ten to five feet over a time of approximately two years in this aquifer if ASR operations were to cease all together. Since ASR operations would be unlikely to cease all together, this drawdown would likely decrease much quicker once injection began again in the wells.

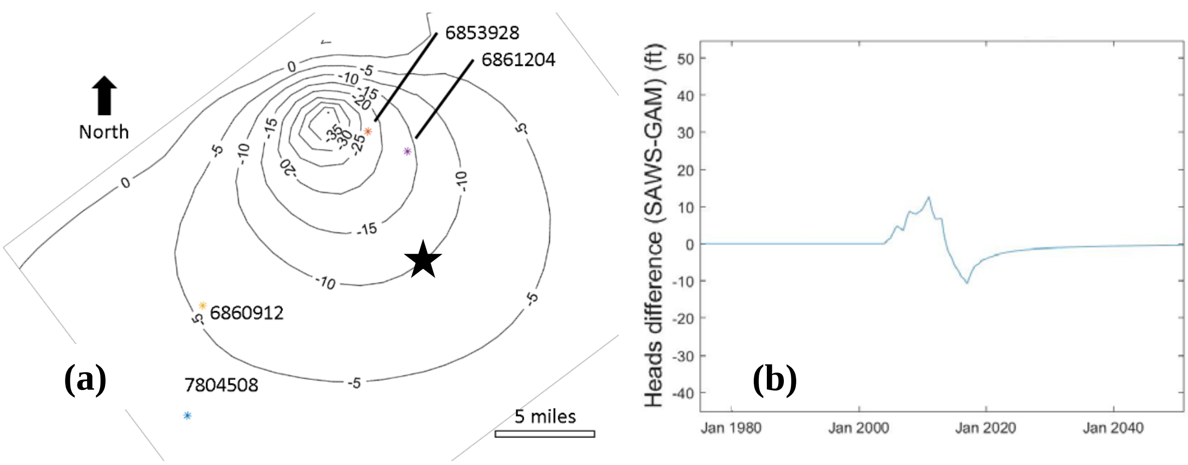

Figure 4.8: (a) Contours of drawdown caused by ASR pumping at the end of 2016 for the first predictive simulation, when the ASR wells extract for 3 years at the highest rate used during the first 10 years of actual operations. (b) Head differences expected at the indicated location 8.5 miles downdip of the ASR wellfield.

The second scenario simulates a much more intense one-year drought to determine the potential effects of the system to recovering its stored water at its maximum design capacity in 2014. The one-year drawdown scenario causes maximum drawdowns in excess of 90 feet around the wellfield and 22 feet at a distance of 8.5 miles downdip (Figure 4.9a). Drawdown would decrease from 22 to 11 feet at this location within one year of cessation of ASR operations (Figure 4.7b), but would decrease even faster once injection likely started again.

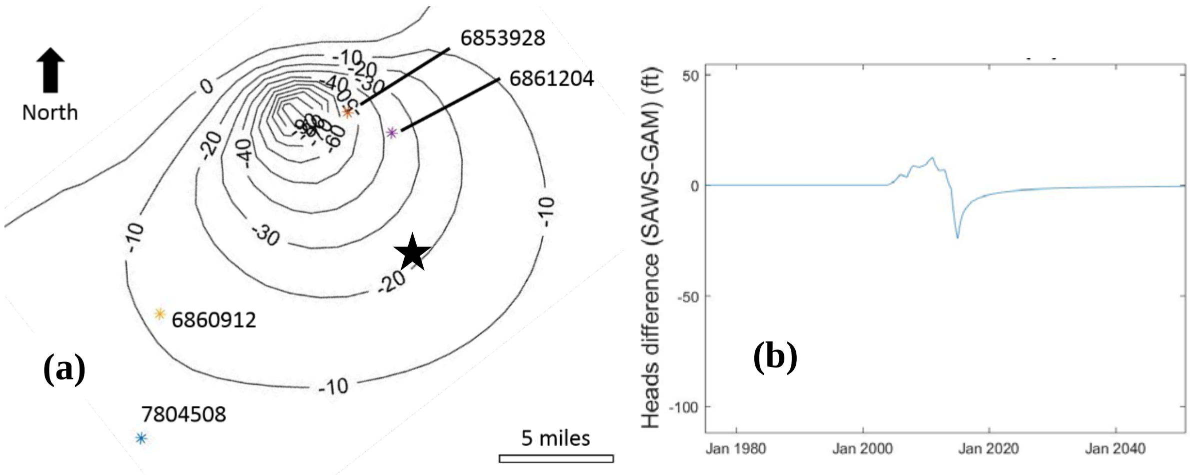

Figure 4.9: (a) Contours of drawdown caused by ASR pumping at the end of 2014, when the ASR wells were simulated to extract at maximum design capacity for 1 year. (b) Head differences expected at the indicated location 8.5 miles downdip of the ASR wellfield.

The third predictive simulation repeats the ASR operations from 2004-2013 each subsequent ten years afterwards until the end of the model in 2050. The net heads through 2050 caused by ASR operations essentially match the head trends from the first 10 years. However, the net injection of 18,750 MG of Edwards water in each ten year period also increases the head approximately 3 feet from 2010 to 2050 at a distance of 10 miles downdip of the center of the wellfield (Figure 4.10). This suggests that the H2Oaks system may be able to help raise regional aquifer heads at fairly large distances over long periods of time, even if only slightly.

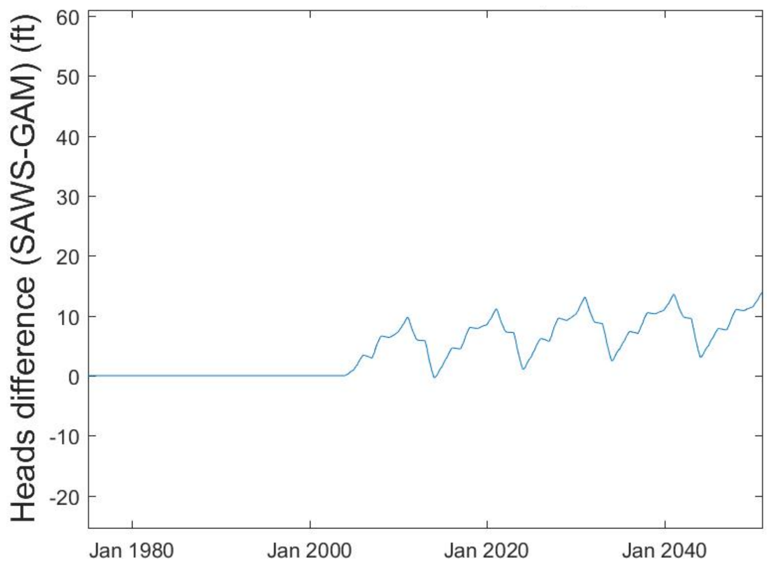

Figure 4.10: Net heads predicted in scenario 3, where ASR operations from the first 10 years repeat each following decade, approximately 5 miles downdip of the center of the ASR wellfield. This scenario predicts that the ASR facility would effectively raise heads about 3 feet at this distance from 2010-2050 due to the net storage of water over this period.

The contour plots presented in this section also indicate that most of the effects of the ASR pumping are focused downdip since the system is located so close to the outcrop of the Carrizo sand formation. As shown in the results from the simulations of historic operations, the model underpredicts the effects of the ASR wells. However, we believe this is offset by the fact that the predictive simulations use annual stress periods which overestimates the effects of the ASR wells on neighboring aquifer users. The H2Oaks ASR system typically varies its flow rates on much shorter timescales than 1 year (Figure 4.1), so effects of a pumping rate (i.e. a high injection rate) used by the ASR system is not expected to propagate too far through the aquifer before a different pumping rate (i.e. a low recovery rate) begins, which would help to offset high levels of mounding or drawdown at long distances from the aquifer. Therefore, we expect these results to be fairly approximate estimates for the range of heads that could be seen within 10 miles of the ASR wellfield, but would not expect the low or high heads discussed here to be experienced by neighboring users for too long of a period based on the operations of the system in its first 10 years.

4.4.3 Transport simulation results

A solute transport model was developed with the annual stress-period groundwater flow models, to determine the potential water quality effects the ASR system has on the regional aquifer around it. The model simulated injection of a 100 mg/L tracer representing Edwards aquifer water into native Carrizo water where the tracer concentration is 0. The transport model simulated that almost no injected Edwards water is expected to travel outside of the wellfield or H2Oaks ASR property boundary by the end of 2013 (Figure 4.11). The transport model was very insensitive to changes in longitudinal dispersivity (α_L). The maximum extent of Edwards water was almost identical whether α_L was 500 feet or 2000 feet. The transport model predicts that the injected water will form a large, coalesced bubble in the center of the wellfield, in contrast to a previous study (Smith et al. 2018). However, this is primarily due to the very coarse, 1 mile grid cells. This study does indicate however, that no neighboring wells would expect to see water quality evidence of injected Edwards water during the first ten years of ASR operations and likely for many years after that as well.

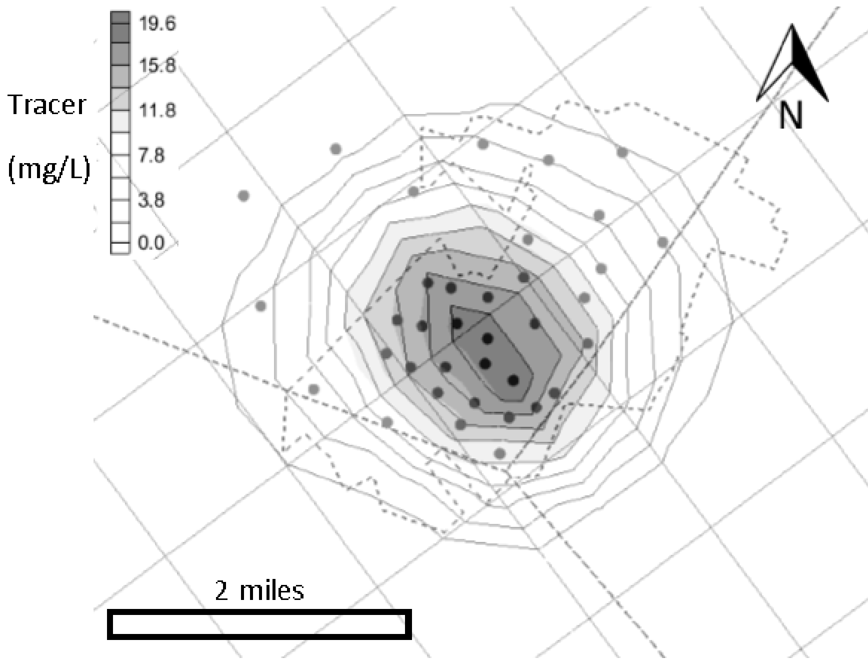

Figure 4.11: Extent of conservative tracer representing injected Edwards aquifer water near the end of 2013.

4.5 Conclusions

This study altered a regional groundwater model to study the extent of the hydraulic and water quality effects of an ASR system had on its surrounding aquifer. The results of this study are clearly specific to the location studied, but help to provide some clarity about potential benefits and drawbacks of ASR in general.

Over a small area (less than 2 miles from the wellfield) and short time scales (less than a year), large multi-well ASR systems like SAWS H2Oaks system may have hydraulic effects that are significantly greater than the typical variation in aquifer heads. Such ASR systems may cause significant drawdown during recovery operations, but they also likely elevate aquifer heads beneficially more frequently than they draw them down. At distances of around ten miles, hydraulic effects of the ASR system are imperceptible against the normal seasonal variation in the aquifer. However, if ASR systems are operated over long time scales (40-50 years), depending on how much they inject, they can potentially raise heads long-term across wider areas (as much as 2 feet even ten miles away).

In contrast to evidence of hydraulic effects reaching several miles beyond the ASR wellfield, transport simulations show that water quality effects are primarily confined to the ASR wellfield. Lateral or downgradient movement of injected water due to advection or dispersion is negligible.

Pumping operations of ASR systems correlate with the pumping operations of aquifer users around them, even though other users can only extract from the aquifer. This correlation is likely due to changes in precipitation –i.e. as rainfall increases, the ASR system moves to injection while other users may use less or even no groundwater, but as rainfall decreases, groundwater extraction for both ASR systems and other users' increases. However, attempting to predict effects of future ASR operations based on expected drought of record conditions is more complicated than simply relating precipitation to historic ASR pumping values, at least in the case of SAWS H2Oaks system. There is clearly a relationship between precipitation and pumping operations at the ASR facility, but other factors seem to contribute as well. Future studies should explore the natural and human processes that influence ASR operations to provide better estimates for how ASR systems may affect the aquifers around them under changing future climatic conditions, either beneficially or negatively.

5. SUMMARY

Aquifer storage and recovery is becoming an increasingly hot topic in water policy and management circles for solving a region's water issues: this is especially true in Texas, where both cities and politicians (local and state) have expressed interest in the technology. However, the state water plans of 2012 and 2017 both suggest that less than 2% of new Texas water supplies in the coming decades will actually come from aquifer storage and recovery systems due in part to water managers' fears and concerns related to storing freshwater underground. In order to address the water manager's concerns, three separate aspects of ASR were studied using both GIS and groundwater modeling. This dissertation aimed to improve understanding of where to preferentially locate ASR facilities, how to manage and operate them to maximize recovery efficiency, and how they may beneficially or adversely affect the larger aquifers around them.

In Section 2, a novel GIS-based index, based on commonly-available data, was created to estimate the hydraulic feasibility of locations across an entire aquifer for implementing aquifer storage and recovery. Previous ASR feasibility indices required significant amounts of data and were generally intended for determining feasibility at one or a few specific sites. Transmissivity, hydraulic gradient, depth to groundwater surface, depth to aquifer, and well density were used to estimate feasibility, while the presence or absence of potential source waters and a location's propensity for drought were used to identify locations that could or should, respectively, explore ASR implementation further. Most of the feasible regions for ASR in the Gulf Coast and Carrizo Wilcox aquifers existed between large cities, suggesting that future ASR systems would need to be installed outside city limits and connected to distribution systems via transmission lines, much like SAWS' H2Oaks system. Corpus Christi, Victoria, San Antonio, Bryan, and College Station all were cities that were identified as possible candidates for ASR systems due to nearby areas of high ASR feasibility, potential ASR-compatible water sources, and a need for drought-resistant water storage.

Section 3 presented groundwater flow and transport models used to estimate recovery efficiency of a multi-well ASR system for the first time, as previous studies had only focused on single ASR well systems. These models allowed retroactive analysis of operations at the SAWS H2Oaks facility over the first 10 years. Additionally, they can be used to evaluate which future potential operational schemes maximize recovery efficiency, recovered water quality, or other metric deemed important by facility managers. Large multi-well ASR systems were shown to be successful, achieving recovery efficiencies as high as 84% over 19 years of operations in suitable aquifers with low longitudinal dispersivities. We showed that operating a multi-well ASR system as a collection of individual wells (i.e. recovering injected waters from the same well they were injected in) is much more likely to result in higher recovery efficiencies relative to operating the wells as a system (recovering injected waters from other wells than the injection well), depending on the well spacing and hydraulic properties of the aquifer. Operations of the wells are not independent, however, so well designed and properly calibrated flow and solute transport models are useful tools for assessing the movement of injected water and transport of the associated chemical constituents due to the interfering effects of multiple wells, as well as for optimizing future strategies that maximize recovery efficiency of injected waters.

In Section 4, a Texas Water Development Board-commissioned regional Groundwater Availability Model was altered in order to examine the beneficial and adverse impacts of the H2Oaks system on the regional Carrizo-Wilcox aquifer around it. Large, multi-well ASR systems can dramatically increase and decrease heads, but only within a relatively small area (within a couple of miles of their wellfields) and affecting few other aquifer users. Outside of that small area, hydraulic effects from ASR systems are no larger than the typical seasonal variations seen before the ASR system began operations. Long term operations of ASR systems could result in appreciable increases in aquifer heads even ten miles away. Similar changes in head trends and amplitudes in monitoring wells both near and far from the ASR system were shown to be due to correlated operations between the ASR system and other aquifer users. While these correlated operations are suspected to be related to precipitation, detailed analysis suggested that operations of the H2Oaks ASR system are based on more than just historical precipitation.

The work presented in this dissertation suggests several topics that should be explored in future research endeavors. First, the GIS feasibility index should be explored across the remaining seven major aquifers in Texas (Trinity, Edwards-Trinity, Edwards, Ogallala, Hueco-Mesilla Bolsons, Seymour, and Pecos Valley) to determine ASR-feasible locations across the remainder of the state. Second, the effectiveness of the novel GIS index at identifying feasible ASR locations should be explored, since only one operating ASR system was available in the study area (H2Oaks in the Carrizo Wilcox) to provide an indication of the performance of the index. Smaller scale studies, such as at the county level, should be undertaken within the Gulf Coast or Carrizo-Wilcox aquifers with finer resolution and additional factors to estimate whether the coarse-scale, five-factor feasibility index is an effective tool for identifying large areas worthy of future study. Third, long term chemistry data on conservative tracers (i.e. chloride, stable isotopes) should be collected from multi-well ASR systems in order to calibrate and validate future solute transport models of multi-well ASR systems. Finally, chemical reaction capabilities should be added to the flow and transport models of multi-well ASR systems presented in this dissertation. Using reactive transport models like PHT3D, which add the capabilities of the chemical equilibrium model PHREEQC to the MODFLOW groundwater flow and MT3DMS solute transport models, to model multi-well ASR systems would be immensely helpful in understanding the fate and transport of sensitive constituents like iron, manganese, or arsenic that may be caused by reactions between the injected waters and native waters or aquifer matrix are concerns in recovered water quality. Reactive transport models of multi-well ASR systems could serve as useful design aids and operational tools when combined with pertinent data collection on conservative tracers and relevant non-conservative chemical species.

REFERENCES

AgriLife. Texas water: Basics of groundwater law | Texas agriculture law. 2013 [cited 10/27/2014]. Available from http://agrilife.org/texasaglaw/2013/10/22/texas-water-basics-of-groundwater-law/ (accessed 10/27/2014).

Anderson, Mary P., William W. Woessner, and Randall J. Hunt. 2015. *Applied groundwater modeling: Simulation of flow and advective transport*. 2nd ed. Elsevier Science.

Antoniou, E. A., B. M. van Breukelen, B. Putters, and P. J. Stuyfzand. 2012. Hydrogeochemical patterns, processes and mass transfers during aquifer storage and recovery (ASR) in an anoxic sandy aquifer. *Applied Geochemistry* 27, (12): 2435-52.

Aquaveo. 2017. *Groundwater modeling system, GMS v10.2.4*. Provo, Utah.

Azobu, Joshua Osamudiame. 2013. Using geochemical modeling (PHREEQC) to determine Edwards volume fraction in mixed groundwaters from the Edwards and Carrizo aquifers at saws aquifer storage and recovery (ASR) site, Bexar county Texas. M.S., Department of Geological Sciences, University of Texas at San Antonio.

Baker Jr., E. T. 1986. *Hydrology of the jasper aquifer in the southeast Texas coastal plain.* Austin, TX: Texas Water Development Board, 295.

Baker, Jr, E.T. 1979. *Stratigraphic and hydrogeologic framework of part of the coastal plain of Texas.* Austin, TX: Texas Department of Water Resources, 236.

Bakker, Mark. 2010. Radial Dupuit interface flow to assess the aquifer storage and recovery potential of saltwater aquifers. *Hydrogeology Journal* 18, (1): 107-15.

Bouwer, H. 2002. Artificial recharge of groundwater: Hydrogeology and engineering. *Hydrogeology Journal* 10, (1): 121-42.

Brown, Chris J., Rebecca Weiss, Steve Sutterfield, Robert Verrastro, Peter Kwiatkowski, Steve Schubert, and Yvette Alger. 2005. Development of an aquifer, storage and recovery (ASR) site selection suitability index in support of the comprehensive everglades restoration project. *Journal of Environmental Hydrology* 13, (20).

Carr, Jerry E., Walter R. Meyer, William M. Sandeen, and Ivy R. McLane. 1985. *Digital models for simulation of ground-water hydrology of the Chicot and Evangeline aquifers along the gulf coast of Texas.* Austin, TX: Texas Department of Water Resources, 289.

CH2MHILL. 2006. *Final report: South Bexar county aquifer storage and recovery phase II well construction and testing.* San Antonio, TX: San Antonio Water System.

CH2MHILL. 2003. *Final report: South Bexar county aquifer storage and recovery well construction and testing.* San Antonio, Texas: San Antonio Water System.

CH2MHILL. 1998. *Aquifer storage and recovery preliminary investigation and feasibility analysis, step 1 report.* San Antonio Water System and Bexar Metropolitan Water District.

CH2MHILL. 1997. *Water supply needs and sources assessment; alternative water supply strategies investigation; A tool for assessing the feasibility of aquifer storage recovery.* Palatka, FL: St. Johns River Water Management District, SJ97-SP4.

Chowdhury, Ali, and Robert E. Mace. 2007. *Groundwater resource evaluation and availability model of the Gulf Coast aquifer in the lower Rio Grande valley of Texas.* Austin, TX: Texas Water Development Board, 368.

Crow, Cassi L. 2012. *Water-level altitudes and continuous and discrete groundwater quality at and near an aquifer storage and recovery site, Bexar, Atascosa, and Wilson counties, Texas, June 2004-september 2011*. U.S. Geological Survey, Scientific Investigations Report 2012-5260.

Deeds, Neil, Van Kelley, Dennis Fryar, Toya Jones, Art J. Whallon, and Kirk E. Dean. 2003. *Final report: Groundwater availability model for the southern-Carrizo Wilcox aquifer.* Austin, TX: Texas Water Development Board.

Delgado, J M P Q. 2007. *Longitudinal and transverse dispersion in porous media*. Vol. 85.

Dillon, P. 2005. Future management of aquifer recharge. *Hydrogeology Journal* 13, (1): 313-6.

Dutton, Alan R., Bob Harden, Jean-Philippe Nicot, and David O'Rourke. 2003. *Groundwater availability model for the central part of the Carrizo-Wilcox aquifer in Texas.* Austin, TX: Texas Water Development Board.

Eastwood, J. C., and P. J. Stanfield. 2001. Key success factors in an ASR scheme. *Quarterly Journal of Engineering Geology and Hydrogeology* 34: 399-409.

Edwards Aquifer Authority. J-17 data. 2017. (accessed September 19, 2017).

Fernandez Escalante, Enrique, Rodrigo Calero Gil, San Miguel Fraile, Maria A, and Fernando Sanchez Serrano. 2014. Economic assessment of opportunities for managed aquifer recharge techniques in Spain using an advanced geographic information system (GIS). *Water* 6, (7) (JUL): 2021-40.

Fryar, Dennis, Rainer Senger, Neil Deeds, John Pickens, Toya Jones, Art J. Whallon, and Kirk E. Dean. 2003. *Final report: Groundwater availability model for the northern Carrizo-Wilcox aquifer.* Austin, TX: Texas Water Development Board.

Gelhar, Lynn W., Claire Welty, and Kenneth R. Rehfeldt. 1992. A critical review of data on field-scale dispersion in aquifers. *Water Resources Research* 28, (7): 1955-74.

George, Peter G., Robert E. Mace, and Rima Petrossian. 2011. *Aquifers of Texas.* Austin, TX: Texas Water Development Board, 380.

Ghayoumian, J., M. Mohseni Saravi, S. Feiznia, B. Nouri, and A. Malekian. 2007. Application of GIS techniques to determine areas most suitable for artificial groundwater recharge in a coastal aquifer in southern Iran. *Journal of Asian Earth Sciences* 30, (2): 364-74.

Harbaugh, A. W. 2005. *MODFLOW-2005, the U.S. geological survey modular ground-water model -- the ground-water flow process: U.S. geological survey techniques and methods 6-A16.*

Harbaugh, A. W., E. R. Banta, M. C. Hill, and M. G. McDonald. 2010. *MODFLOW-2000 version 1.19.01, the U.S. geological survey modular ground-water model: U.S. geological survey software release*.

Harbaugh, A. W., E. R. Banta, M. C. Hill, and M. G. McDonald. 2000. *MODFLOW-2000, the U.S. geological survey modular ground-water model -- user guide to modularization concepts and the ground-water flow process: U.S. geological survey open-file report 00-92.*

Harbaugh, A. W., C. D. Langevin, J. D. Hughes, R. N. Niswonger, and L. F. Konikow. 2013. *MODFLOW-2005 version 1.11.00, the U.S. geological survey modular ground-water model: U.S. geological survey software release*.

Jones, Gregg W., and Thomas Pichler. 2007. Relationship between pyrite stability and arsenic mobility during aquifer storage and recovery in southwest central Florida. *Environmental Science & Technology* 41, (3): 723-30.

Kasmarek, Mark C. 2013. *Hydrogeology and simulation of groundwater flow and land-surface subsidence in the northern part of the gulf coast aquifer system, Texas 1891 - 2009.* Austin, TX: Texas Water Development Board.

Kelley, Van A., Neil E. Deeds, Dennis G. Fryar, Jean-Philippe Nicot, Toya L. Jones, Alan R. Dutton, Gabe Bruehl, Tanya Unger-Holtz, and James L. Machin. 2004. *Final report: Groundwater availability models for the queen city and Sparta aquifers.* Austin, TX.

Khan, Shahbaz, Shahbaz Mushtaq, Munir A. Hanjra, and Juergen Schaeffer. 2008. Estimating potential costs and gains from an aquifer storage and recovery program in Australia. *Agricultural Water Management* 95, (4): 477-88.

Konikow, L. F., G. Z. Hornberger, K. J. Halford, and R. T. Hanson 2009. 2009. *Revised multi-node well (MNW2) package for MODFLOW ground-water flow model: U.S. geological survey techniques and methods 6–A30.*

Long, Di, Bridget R. Scanlon, Laurent Longuevergne, Alexander Y. Sun, D. Nelun Fernando, and Himanshu Save. 2013. GRACE satellite monitoring of large depletion in water storage in response to the 2011 drought in Texas. *Geophysical Research Letters* 40, (13): 3395-401, http://dx.doi.org/10.1002/grl.50655.

Lovanh, Nanh, You-Kuan Zhang, Richard C. Heathcote, and Pedro J. J. Alvarez. 2000. *Guidelines to determine site-specific parameters for modeling the fate and transport of monoarmomatic hydrocarbons in groundwater.* West Des Moines, IA: Iowa Comprehensive Petroleum Underground Storage Tank Fund Board.

Lowry, Christopher S., and Mary P. Anderson. 2006. An assessment of aquifer storage recovery using ground water flow models. *Ground Water* 44, (5) (September 1,): 661-7 (accessed Feb 1, 2017).

Mace, Robert E., Rebecca C. Smyth, Liying Xu, and Jinhuo Liang. 2000. *Transmissivity, hydraulic conductivity, and storativity of the Carrizo-Wilcox aquifer in Texas.* Austin, TX: Texas Water Development Board.

Malcolm Pirnie Inc., ASR Systems LLC, and Jackson, Sjoberg, McCarthy & Wilson, LLP. 2011. *An assessment of aquifer storage and recovery in Texas.* Austin, TX: Texas Water Development Board, 0904830940.

Malekmohammadi, Bahram, Majid Ramezani Mehrian, and HamidReza Jafari. 2012. Site selection for managed aquifer recharge using fuzzy rules: Integrating geographical information system (GIS) tools and multi-criteria decision making. *Hydrogeology Journal* 20, (7): 1393-405.

Maliva, Robert G., Weixing Guo, and Thomas M. Missimer. 2006. Aquifer storage and recovery: Recent hydrogeological advances and system performance. *Water Environment Research* 78, (13): 2428-35.

Maliva, Robert G., and T. M. Missimer. 2010. *Aquifer storage and recovery and managed aquifer recharge using wells: Planning, hydrogeology, design, and operation*. Sugar Land, TX: Schlumberger.

Maliva, Robert G., Thomas M. Missimer, Frank P. Winslow, and Rolf Herrmann. 2011. Aquifer storage and recovery of treated sewage effluent in the Middle East. *Arabian Journal for Science and Engineering* 36, (1): 63-74.

Martin, R. R., B. Barnett, C. Pittman, C. Kaufmann, A. Swiatnik, and C. Burgess. 2012. Modelling the regional impacts of multiple MAR schemes on the Northern Adelaide Plains. Paper presented at Symposium ISMAR 7.

Miotlinski, Konrad, Peter J. Dillon, Paul Pavelic, Karen Barry, and Sarah Kremer. 2014. Recovery of injected freshwater from a brackish aquifer with a multiwell system. *Ground Water* 52, (4): 495-502.

Morris, Tom, Roberto Macias, and R. David G. Pyne. 2010. 2. Design, installation, and operation challenges of large-scale aquifer storage and recovery wells in San Antonio, south Texas. In *Effects of urbanization on groundwater: An engineering case-based approach for sustainable development*. Ni-Bin Chang, 25. Reston, Va.: Environmental and Water Resources Institute, American Society of Civil Engineers.

National Oceanic and Atmospheric Administration: National Centers for Environmental Information. Drought indices and data. 2017a. Available from https://www.ncdc.noaa.gov/temp-and-precip/drought/nadm/indices (accessed December 2017).

National Oceanic and Atmospheric Administration: National Centers for Environmental Information. San Antonio, Texas area precipitation. 2017b [cited September 19, 2017]. Available from https://www.ncdc.noaa.gov/ghcnd-data-access (accessed September 19, 2017).

National Research Council. 2008. *Prospects for managed underground storage of recoverable water*, ed. Committee on Sustainable Underground Storage of Recoverable Water, Water Science and Technology Board. Washington, D.C.: National Academies Press.

Neil, Chelsea, Y. J. Yang, and Young-Shin Jun. 2012. Arsenic mobilization and attenuation by mineral □“water interactions: Implications for managed aquifer recharge. *Journal of Environmental Monitoring* 14, (7): 1772-88.

Nielsen-Gammon, John W. 2011. *The 2011 Texas drought.* College Station, TX: Office of the State Climatologist, College of Geosciences, Texas A&M University

Otero, Cassi L., and Brian L. Petri. 2010. *Quality of groundwater at and near an aquifer storage and recovery site, Bexar, Atascosa, and Wilson counties, Texas, June 2004 - August 2008.* U.S. Geological Survey, Scientific Investigations Report 2010-5061.

Pavelic, Paul, Peter Dillon, and Neville Robinson. 2004. *Groundwater modelling to assist well-field design and operation for the ASTR trial at Salisbury, South Australia.* Adelaide, South Australia: CSIRO Land and Water.

Pearson, F. J., and D. E. White. 1967. Carbon 14 ages and flow rates of water in Carrizo sand, Atascosa County, Texas. *Water Resources Research* 3, (1): 251-61, http://dx.doi.org/10.1029/WR003i001p00251.

Pedrero, Francisco, António Albuquerque, Helena Marecos do Monte, Victor Cavaleiro, and Juan José Alarcón. 2011. Application of GIS-based multi-criteria analysis for site selection of aquifer recharge with reclaimed water. *Resources, Conservation and Recycling* 56, (1): 105-16.

Pyne, R. David G. 2005. *Aquifer storage recovery: A guide to groundwater recharge through wells*. Gainesville, FL: ASR Systems.

Rahman, M. Azizur, Bernd Rusteberg, R. C. Gogu, J. P. Lobo Ferreira, and Martin Sauter. 2012. A new spatial multi-criteria decision support tool for site selection for implementation of managed aquifer recharge. *Journal of Environmental Management* 99, (MAY): 61-75.

Rahman, Mohammad Azizur, Bernd Rusteberg, Mohammad Salah Uddin, Annegret Lutz, Muath Abu Saada, and Martin Sauter. 2013. An integrated study of spatial multicriteria analysis and mathematical modelling for managed aquifer recharge site suitability mapping and site ranking at northern Gaza coastal aquifer. *Journal of Environmental Management* 124, (JUL 30): 25-39.

Rinck-Pfeiffer, S., S. Ragusa, P. Sztajnbok, and T. Vandevelde. 2000. Interrelationships between biological, chemical, and physical processes as an analog to clogging in aquifer storage and recovery (ASR) wells. *Water Research* 34, (7): 2110-8.

Ringleb, Jana, Jana Sallwey, and Catalin Stefan. 2016. Assessment of managed aquifer recharge through modeling--A review. *Water (20734441)* 8, (12): 1-31.

Ros, Steven Eugenius Marijnus, and Koen Gerardus Zuurbier. 2017. *The impact of integrated aquifer storage and recovery and brackish water reverse osmosis (ASRRO) on a coastal groundwater system*. Vol. 9.

Russo, Tess A., Andrew T. Fisher, and Brian S. Lockwood. 2015. Assessment of managed aquifer recharge site suitability using a GIS and modeling. *Groundwater* 53, (3): 389-400.

San Antonio Water System. 2017. *2017 water management plan.* San Antonio, Texas.

San Antonio Water System. 2013. *ASR well flows and water quality observations from 2004 - 2013*. San Antonio, Texas.

Schulze-Makuch, Dirk. 2005. Longitudinal dispersivity data and implications for scaling behavior. *Ground Water* 43, (3): 443-56.

Shammas, Mahaad I. 2008. The effectiveness of artificial recharge in combating seawater intrusion in Salalah coastal aquifer, Oman. *Environmental Geology* 55, (1): 191-204.

Sheng, Z. P. 2005. An aquifer storage and recovery system with reclaimed wastewater to preserve native groundwater resources in El Paso, Texas. *Journal of Environmental Management* 75, (4): 367-77.

Sheng, Zhuping, Jonathan Arthur, Jorge Restrepo, and Richelle Allen-King. 2007. On recovery efficiency of managed underground storage of recoverable water systems, *Proceedings of the 6th Biennial International Symposium on Managed Aquifer Recharge*. Phoenix, Arizona, USA, October 29 – November 2: 84-95.

Sheng, Zhuping, and Xuan Zhao. 2015. Special issue on managed aquifer recharge: Powerful management tool for meeting water resources challenges. *Journal of Hydrologic Engineering* 20, (3).

Smith, Anthony J., and Daniel W. Pollock. 2012. Assessment of managed aquifer recharge potential using ensembles of local models. *Ground Water* 50, (1): 133-43.

Smith, W. Benjamin, Gretchen R. Miller, and Zhuping Sheng. 2018. *Assessing the performance of a large scale, multi-well aquifer storage and recovery system using a transport model*. unpublished.

Stuyfzand, Pieter J., Ebel Smidt, Koen G. Zuurbier, Niels Hartog, and Mohamed A. Dawoud. 2017. Observations and prediction of recovered quality of desalinated seawater in the strategic ASR project in Liwa, Abu Dhabi. *Water (20734441)* 9, (3): 1-25.

Texas Water Development Board. 2017. *Raw monthly data from groundwater use surveys: 2000-2013*. Austin, TX.

Texas Water Development Board. 2015. *Groundwater database reports.* Austin, TX.

Texas Water Development Board. Aquifer storage and recovery. 2012a [cited 3/4 2015]. Available from http://www.twdb.texas.gov/innovativewater/asr/ (accessed 3/4/2015).

Texas Water Development Board. 2012b. *Water for Texas 2012 state water plan.* Austin, TX.

US EPA. Aquifer recharge (AR) and aquifer storage & recovery (ASR) | underground injection control | US EPA. 2014a [cited 10/24/ 2014]. Available from http://water.epa.gov/type/groundwater/uic/aquiferrecharge.cfm (accessed 10/24/2014).

US EPA. Discharge monitoring report (DMR) pollutant loading tool. 2014b. Available from http://cfpub.epa.gov/dmr/adv_search.cfm (accessed 8/28/2014).

Wallis, Ilka, Henning Prommer, Thomas Pichler, Vincent Post, Stuart B. Norton, Michael D. Annable, and Craig T. Simmons. 2011. Process-based reactive transport model to quantify arsenic mobility during aquifer storage and recovery of potable water. *Environmental Science & Technology* 45, (16): 6924-31.

Ward, James D., Craig T. Simmons, Peter J. Dillon, and Paul Pavelic. 2009. Integrated assessment of lateral flow, density effects and dispersion in aquifer storage and recovery. *Journal of Hydrology* 370, (1–4): 83-99.

Waterstone Inc., and Parsons Inc. 2003. *Groundwater availability of the central gulf coast aquifer: Numerical simulations to 2050, central gulf coast, Texas.* Austin, Texas: Texas Water Development Board.

Yobbi, D. K. 1997. *Simulation of subsurface storage and recovery of effluent using multiple wells, St. Petersburg, Florida.* Tallahassee, Fla: U.S. Dept. of the Interior, U.S. Geological Survey.

Young, Steve C., Tom Ewing, Scott Hamlin, Ernie Baker, and Daniel Lupton. 2012. *Updating the hydrogeologic framework for the northern portion of the gulf coast aquifer.* Austin, Texas: Texas Water Development Board, CR-1004831113.

Zheng, Chunmiao, and P. Patrick Wang. 1999. *Mt3DMS: A modular three-dimensional multispecies transport model for simulation of advection, dispersion, and chemical reactions of contaminants in groundwater systems*. Vol. v5.3. University of Alabama.

Zuurbier, Koen G., Mark Bakker, Willem Jan Zaadnoordijk, and Pieter J. Stuyfzand. 2013. Identification of potential sites for aquifer storage and recovery (ASR) in coastal areas using ASR performance estimation methods. *Hydrogeology Journal* 21, (6) (SEP): 1373-83.

Zuurbier, Koen G., Willem Jan Zaadnoordijk, and Pieter J. Stuyfzand. 2014. How multiple partially penetrating wells improve the freshwater recovery of coastal aquifer storage and recovery (ASR) systems: A field and modeling study. *Journal of Hydrology* 509: 430-41.

APPENDIX A

ALL STATISTICS FOR CITIES WITH POPULATION GREATER THAN 20,000

Aquifer	CITY_NM	MEAN	MAX	MIN	COUNT	STD	VARIETY
Carrizo-Wilcox	Bryan	88.3	94	80	32	4.8	3
Carrizo-Wilcox	College Station	81.1	85	76	7	4.5	2
Carrizo-Wilcox	Laredo	62.3	76	50	33	6.0	14
Carrizo-Wilcox	Longview	66.4	74	60	56	3.9	10
Carrizo-Wilcox	Lufkin	53.6	66	51	32	5.1	3
Carrizo-Wilcox	Marshall	69.1	77	63	29	3.8	6
Carrizo-Wilcox	Nacogdoches	60.8	65	54	27	3.3	3
Carrizo-Wilcox	San Antonio	61.2	79	50	65	6.3	12
Carrizo-Wilcox	Seguin	64.0	82	52	12	9.8	8
Carrizo-Wilcox	Texarkana	66.7	73	56	19	5.0	9
Carrizo-Wilcox	Tyler	62.6	66	51	57	5.1	6
Gulf Coast	Port Arthur	90.8	100	86	35	5.5	6
Gulf Coast	Beaumont	87.8	100	78	86	5.0	11
Gulf Coast	Lake Jackson	86.6	92	80	20	4.8	7
Gulf Coast	Victoria	79.7	87	73	35	3.2	8
Gulf Coast	Rosenberg	78.1	91	66	24	6.7	14
Gulf Coast	Missouri City	75.9	89	63	27	6.2	14
Gulf Coast	Sugar Land	74.2	84	61	31	7.0	12
Gulf Coast	Texas City	73.6	87	41	71	7.2	12
Gulf Coast	Conroe	73.5	76	64	57	2.4	6
Gulf Coast	Corpus Christi	73.0	82	54	33	7.1	7
Gulf Coast	Huntsville	68.8	84	53	40	7.0	10
Gulf Coast	Baytown	68.6	83	47	39	7.9	10
Gulf Coast	Deer Park	68.4	78	58	15	4.8	9
Gulf Coast	Houston	67.6	92	48	597	7.3	36
Gulf Coast	Alvin	67.0	75	60	14	4.5	4
Gulf Coast	Friendswood	65.4	66	60	21	1.8	2
Gulf Coast	Pearland	64.8	71	57	46	4.2	8
Gulf Coast	Edinburg	64.5	77	59	39	7.9	4
Gulf Coast	Pasadena	64.0	79	47	47	8.6	18
Gulf Coast	La Porte	63.9	69	55	19	3.7	8
Gulf Coast	League City	63.0	69	47	50	3.9	7
Gulf Coast	Kingsville	62.0	71	54	14	5.7	6
Gulf Coast	San Juan	52.6	59	26	7	11.2	3
Gulf Coast	McAllen	49.7	77	26	49	15.3	5
Gulf Coast	Mission	48.9	59	26	30	15.0	3
Gulf Coast	Weslaco	48.0	54	42	2	6.0	2
Gulf Coast	Pharr	39.7	59	26	18	15.4	3
Gulf Coast	Harlingen	31.0	31	31	3	0.0	1

APPENDIX B

ADDITIONAL HEAD PLOTS

For each ASR well, plots of:

- modeled and observed heads vs time

- modeled versus observed heads

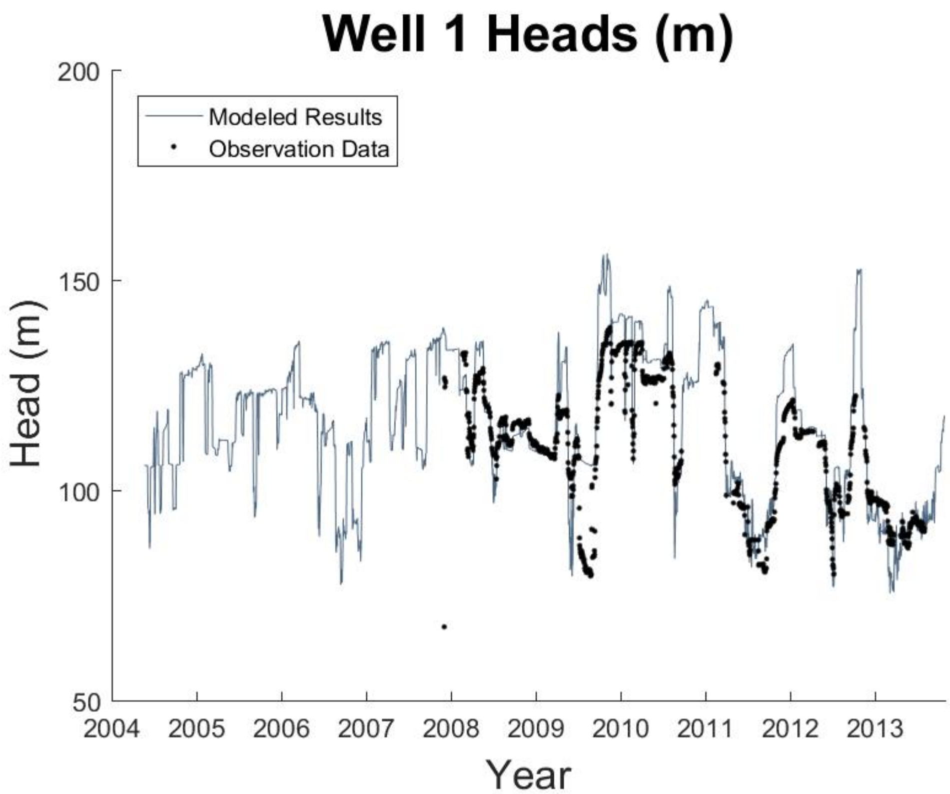
Well 1 Heads (m)
Modeled Results
Observation Data
Head (m)
Year
200
150
100
50
2004
2005
2006
2007
2008
2009
2010
2011
2012
2013

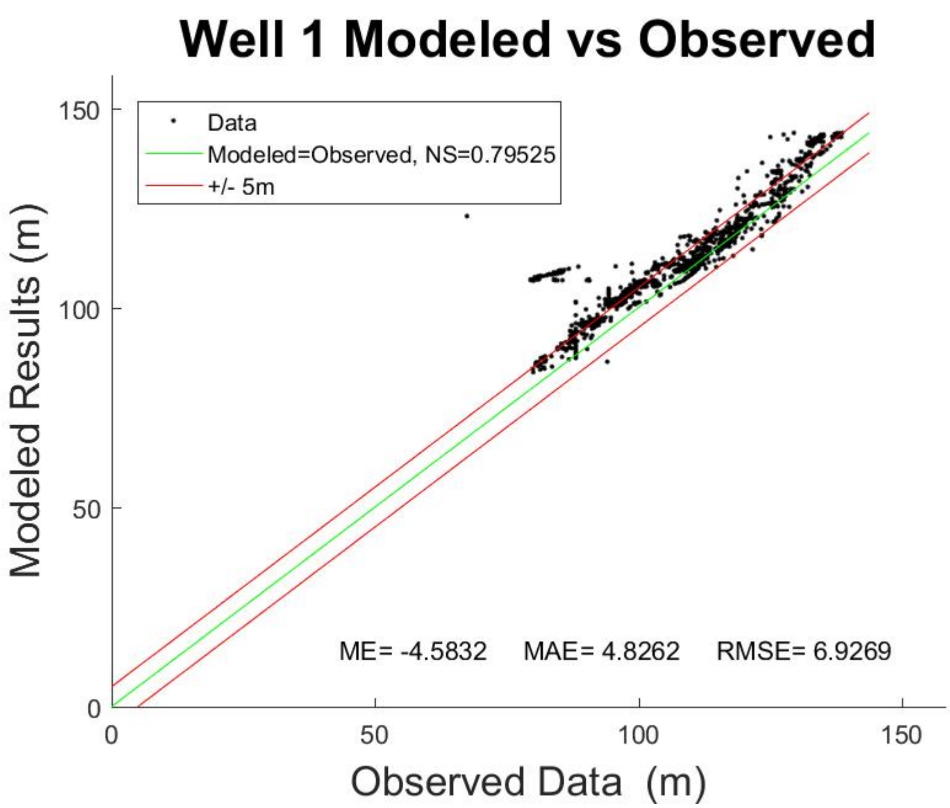
Well 1 Modeled vs Observed
Data
Modeled=Observed, NS=0.79525
+/- 5m
ME= -4.5832
MAE= 4.8262
RMSE= 6.9269
Modeled Results (m)
Observed Data (m)
150
100
50
0
0
50
100
150

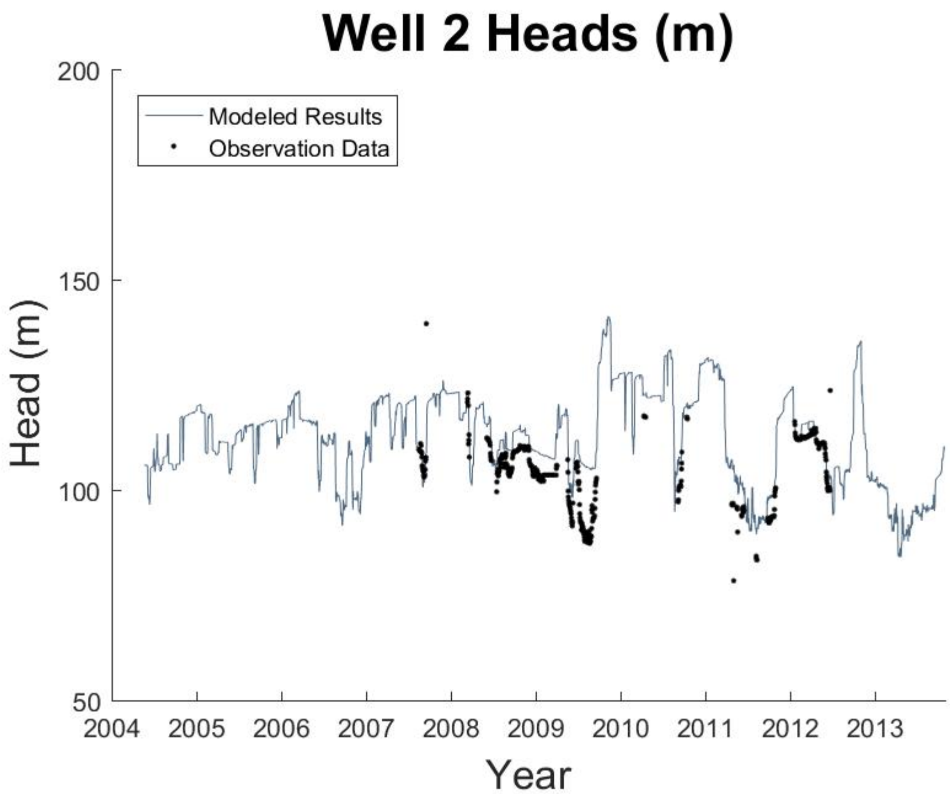
Well 2 Heads (m)
Modeled Results
Observation Data
Head (m)
200
150
100
50
2004
2005
2006
2007
2008
2009
2010
2011
2012
2013
Year

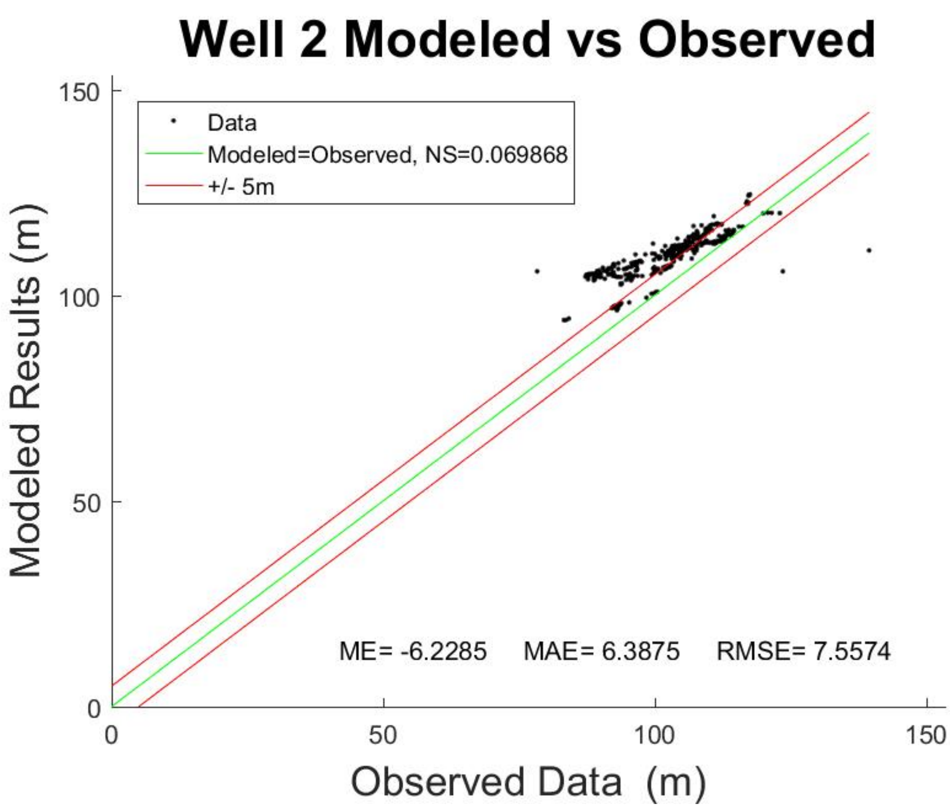
Well 2 Modeled vs Observed
Data
Modeled=Observed, NS=0.069868
+/- 5m
ME= -6.2285
MAE= 6.3875
RMSE= 7.5574
Modeled Results (m)
150
100
50
0
Observed Data (m)

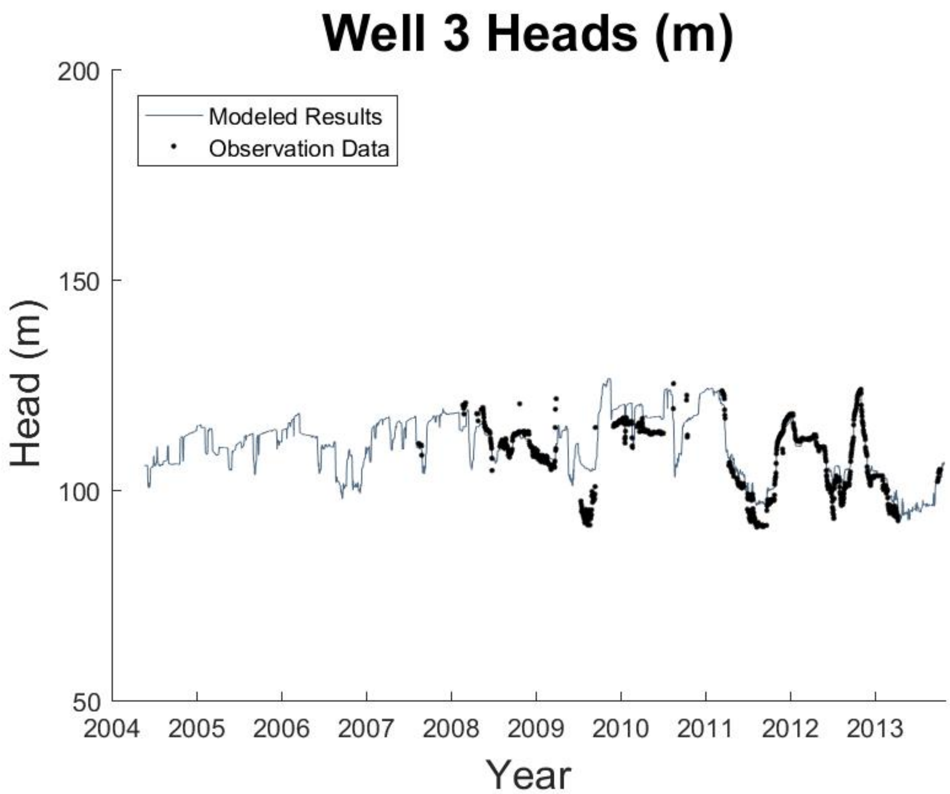
Well 3 Heads (m)
Modeled Results
Observation Data
Head (m)
200
150
100
50
2004
2005
2006
2007
2008
2009
2010
2011
2012
2013
Year

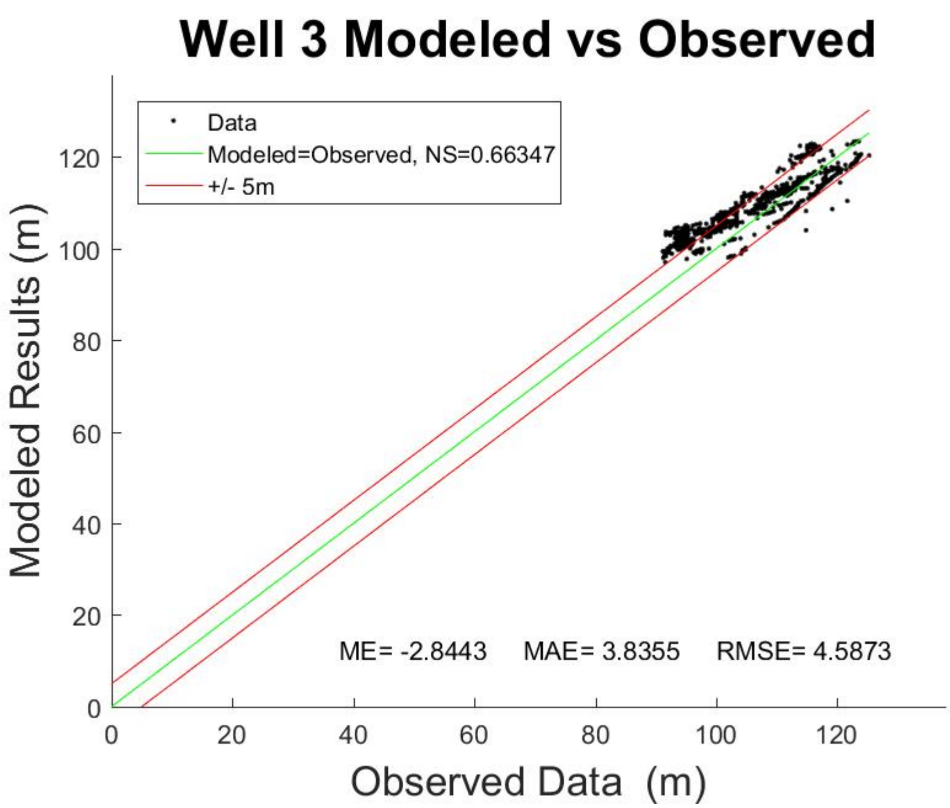
Well 3 Modeled vs Observed
Data
Modeled=Observed, NS=0.66347
+/- 5m
Modeled Results (m)
ME= -2.8443
MAE= 3.8355
RMSE= 4.5873
0
20
40
60
80
100
120
Observed Data (m)

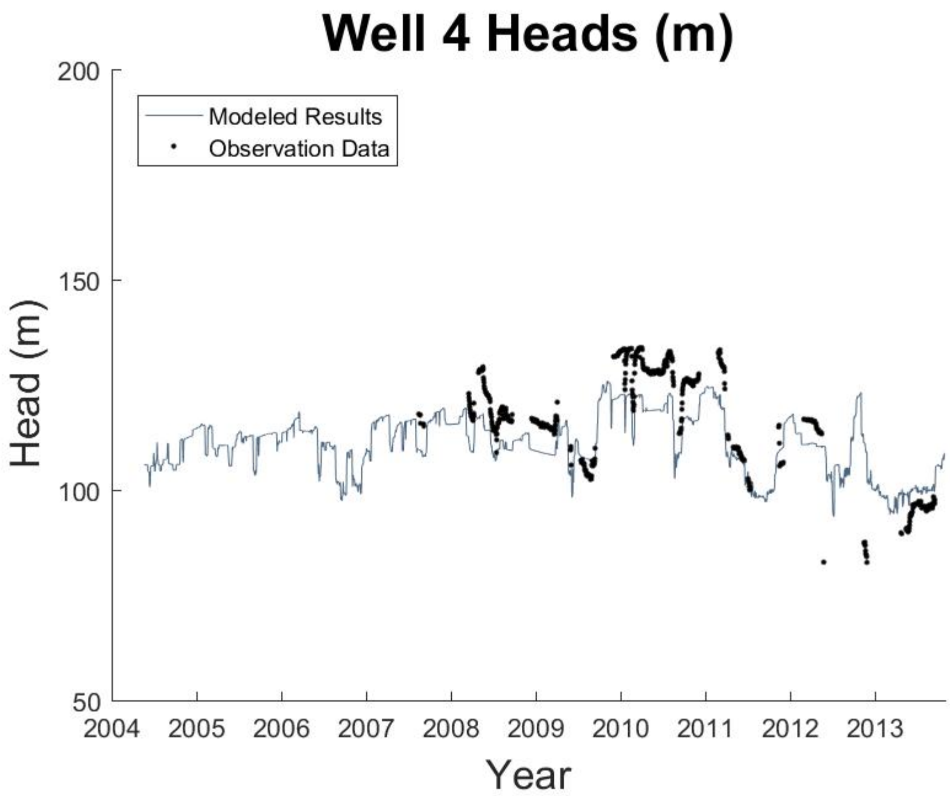
Well 4 Heads (m)
Modeled Results
Observation Data
Head (m)
Year
200
150
100
50
2004
2005
2006
2007
2008
2009
2010
2011
2012
2013

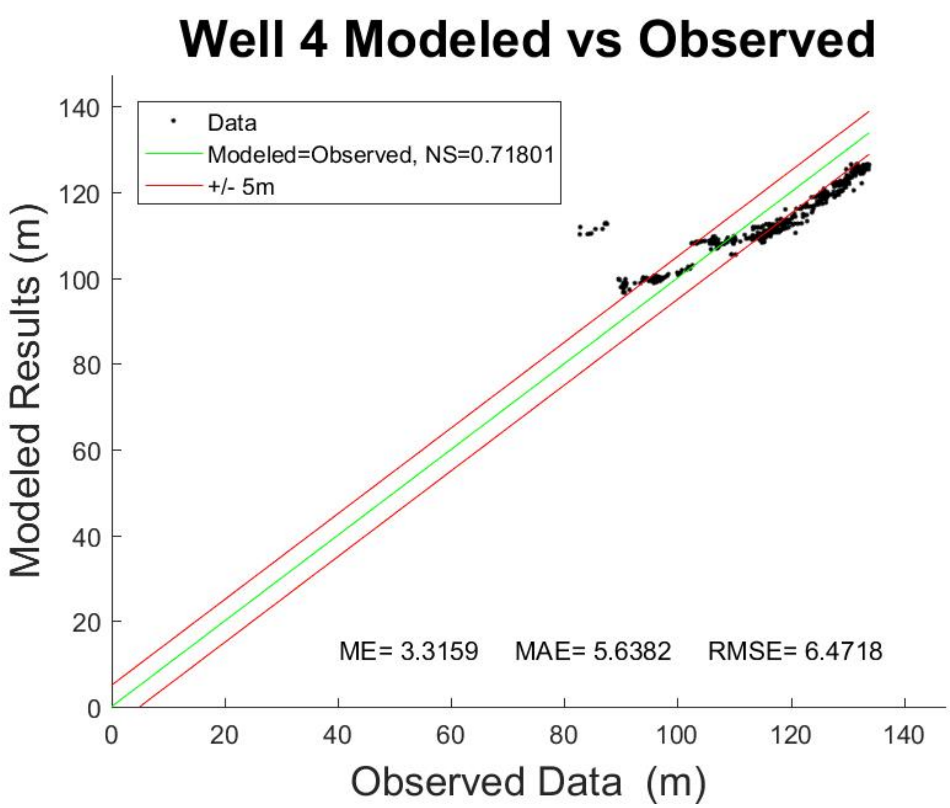
Well 4 Modeled vs Observed
Data
Modeled=Observed, NS=0.71801
+/- 5m
ME= 3.3159
MAE= 5.6382
RMSE= 6.4718
Modeled Results (m)
Observed Data (m)
140
120
100
80
60
40
20
0
0
20
40
60
80
100
120
140

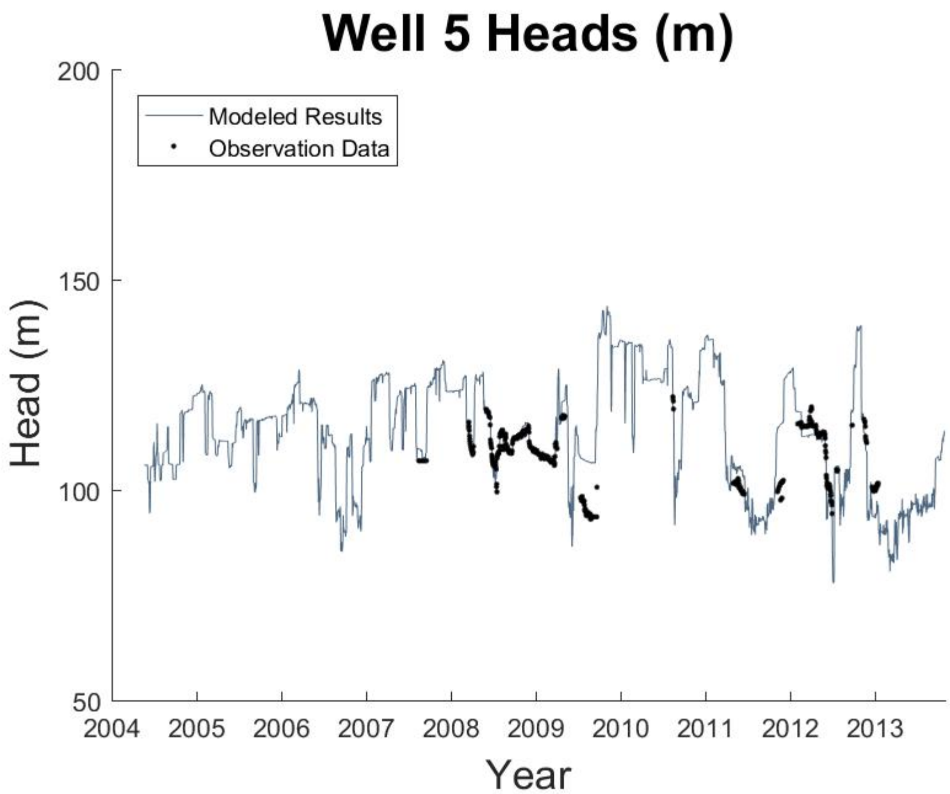
Well 5 Heads (m)
Modeled Results
Observation Data
Head (m)
200
150
100
50
2004
2005
2006
2007
2008
2009
2010
2011
2012
2013
Year

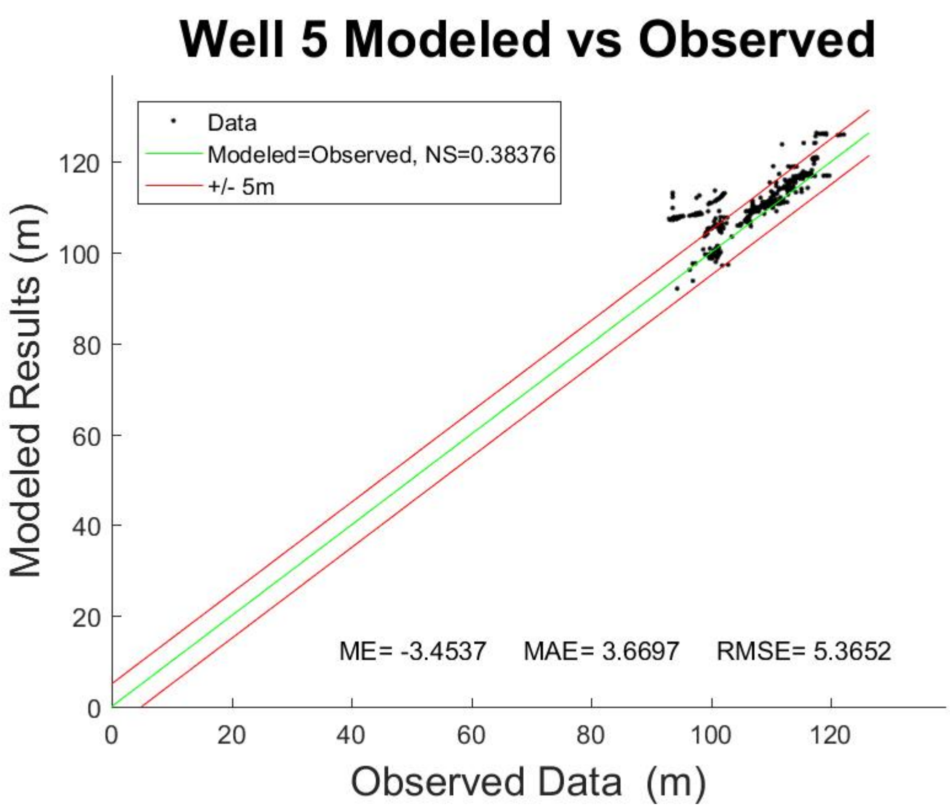
Well 5 Modeled vs Observed
Data
Modeled=Observed, NS=0.38376
+/- 5m
Modeled Results (m)
120
100
80
60
40
20
0
ME= -3.4537
MAE= 3.6697
RMSE= 5.3652
0
20
40
60
80
100
120
Observed Data (m)

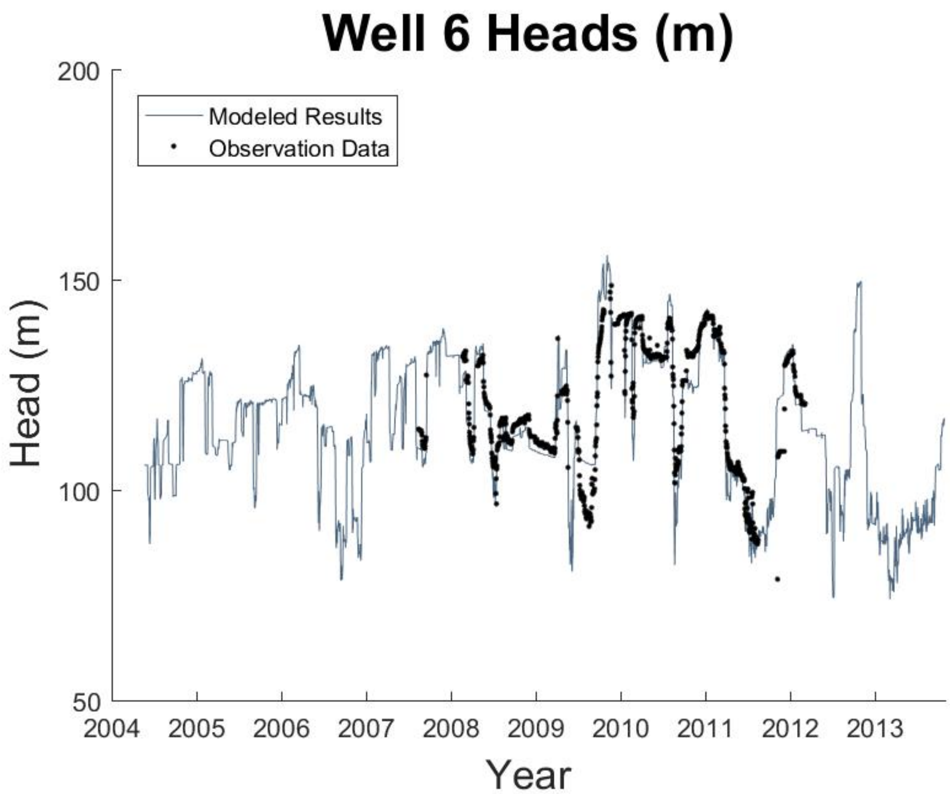
Well 6 Heads (m)
Modeled Results
Observation Data
Head (m)
200
150
100
50
2004
2005
2006
2007
2008
2009
2010
2011
2012
2013
Year

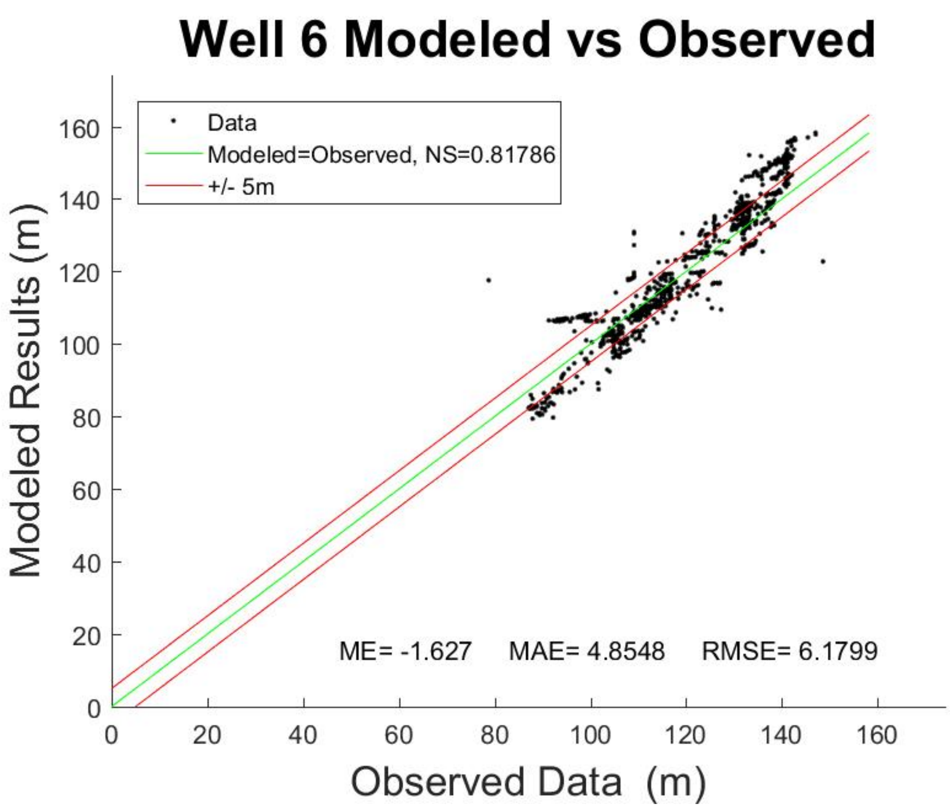
Well 6 Modeled vs Observed
Data
Modeled=Observed, NS=0.81786
+/- 5m
Modeled Results (m)
ME= -1.627
MAE= 4.8548
RMSE= 6.1799
0
20
40
60
80
100
120
140
160
Observed Data (m)

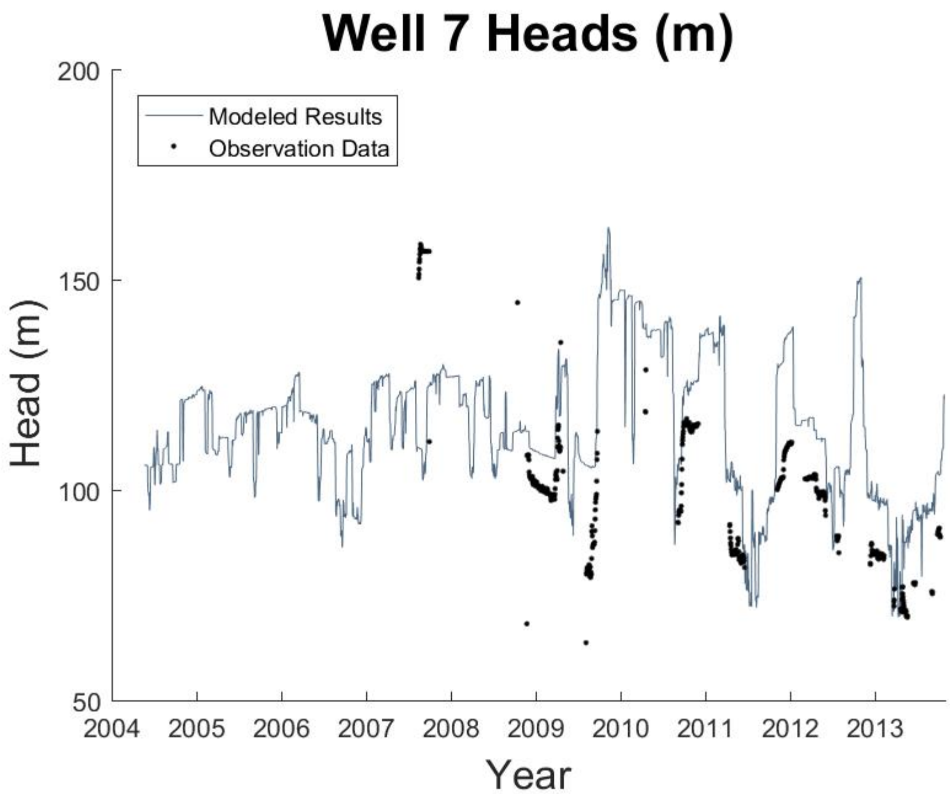
Well 7 Heads (m)
Modeled Results
Observation Data
Head (m)
Year
200
150
100
50
2004
2005
2006
2007
2008
2009
2010
2011
2012
2013

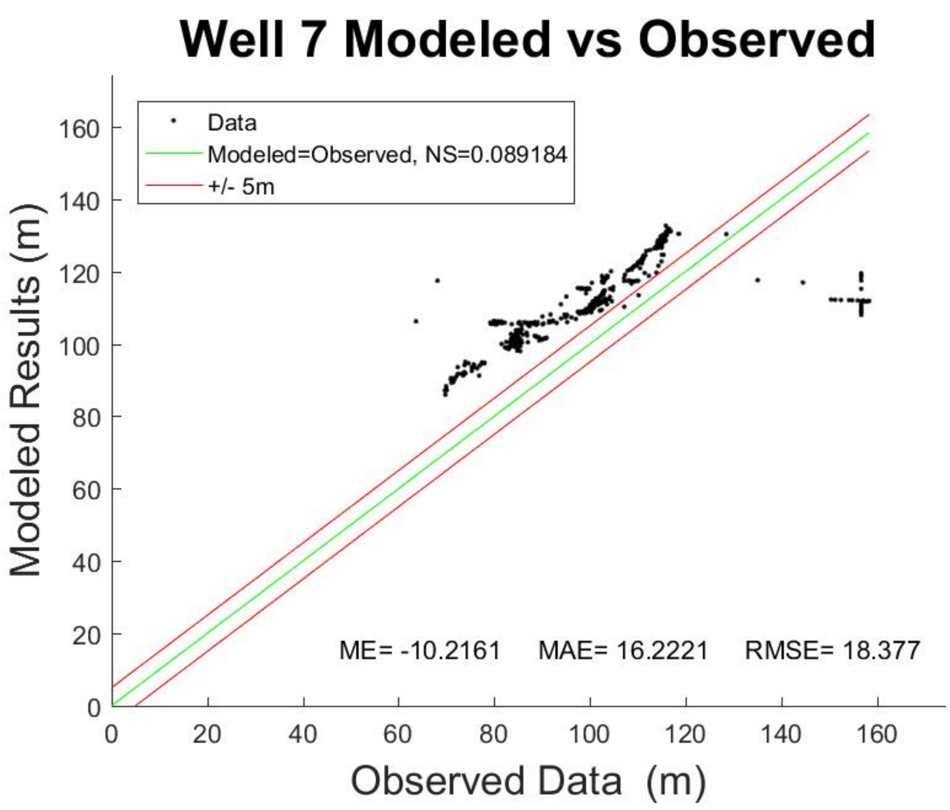
Well 7 Modeled vs Observed
Data
Modeled=Observed, NS=0.089184
+/- 5m
Modeled Results (m)
Observed Data (m)
ME= -10.2161
MAE= 16.2221
RMSE= 18.377
0
20
40
60
80
100
120
140
160

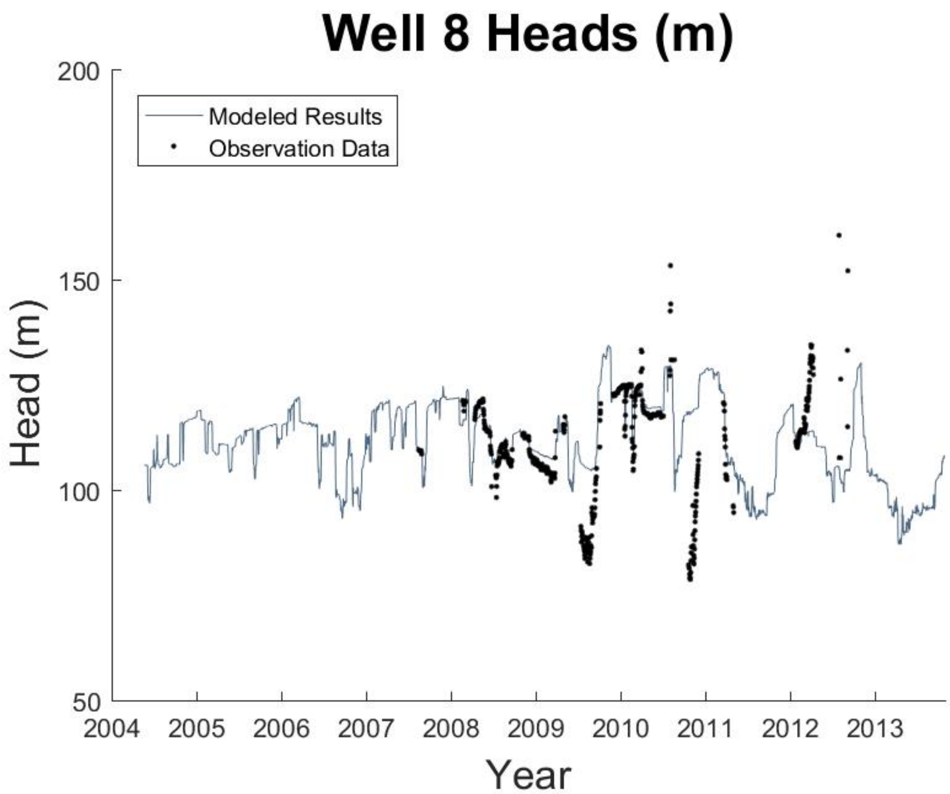
Well 8 Heads (m)
Modeled Results
Observation Data
Head (m)
200
150
100
50
2004
2005
2006
2007
2008
2009
2010
2011
2012
2013
Year

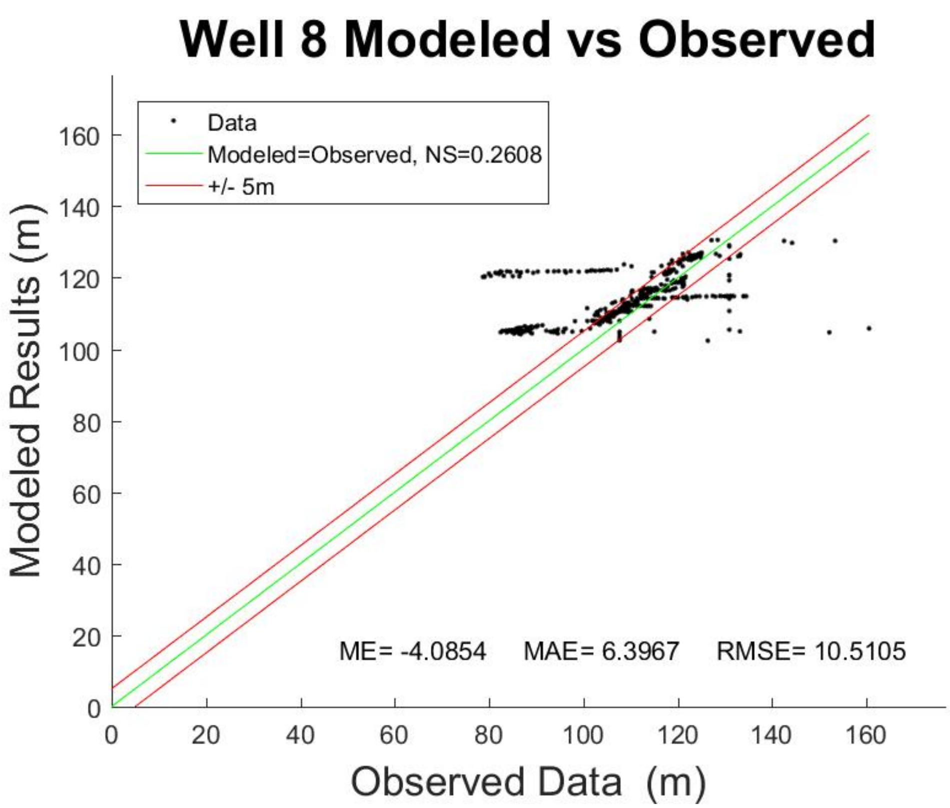
Well 8 Modeled vs Observed
Data
Modeled=Observed, NS=0.2608
+/- 5m
Modeled Results (m)
160
140
120
100
80
60
40
20
0
ME= -4.0854
MAE= 6.3967
RMSE= 10.5105
0
20
40
60
80
100
120
140
160
Observed Data (m)

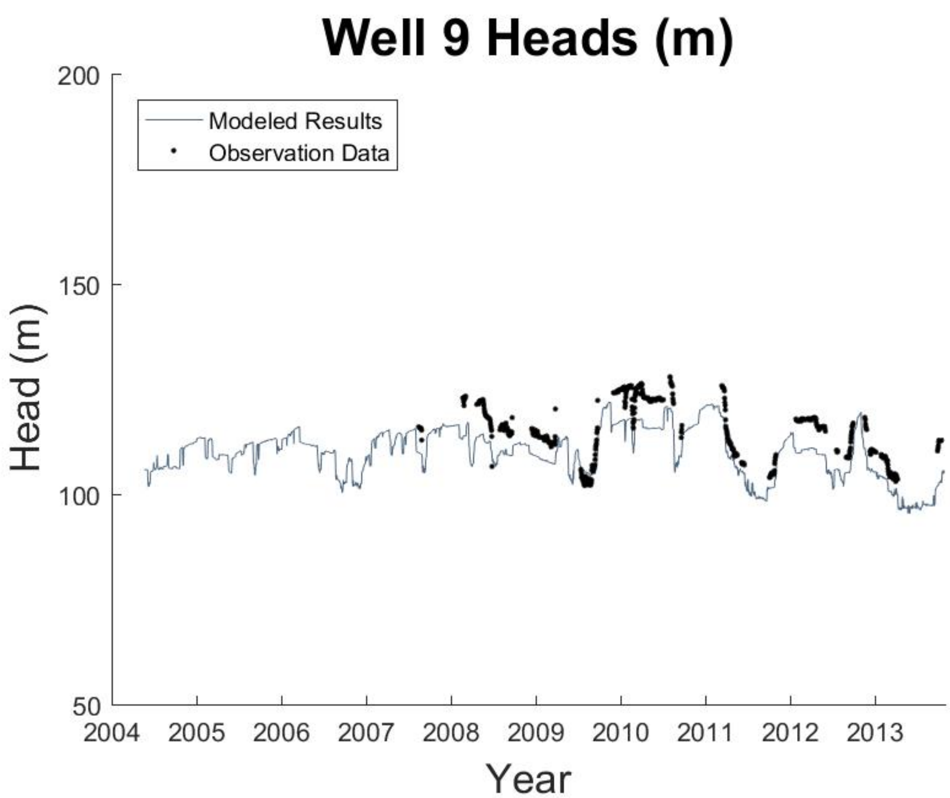

Well 9 Heads (m)
Modeled Results
Observation Data
Head (m)
200
150
100
50
2004
2005
2006
2007
2008
2009
2010
2011
2012
2013
Year

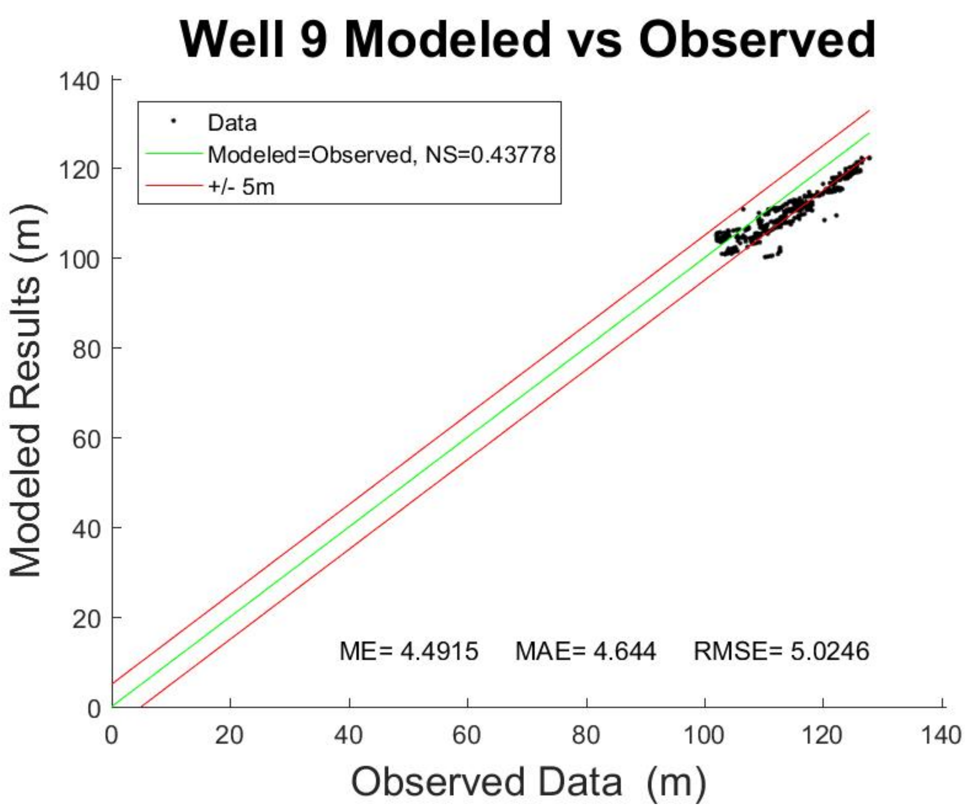

Well 9 Modeled vs Observed
Data
Modeled=Observed, NS=0.43778
+/- 5m
ME= 4.4915
MAE= 4.644
RMSE= 5.0246
Modeled Results (m)
140
120
100
80
60
40
20
0
0
20
40
60
80
100
120
140
Observed Data (m)

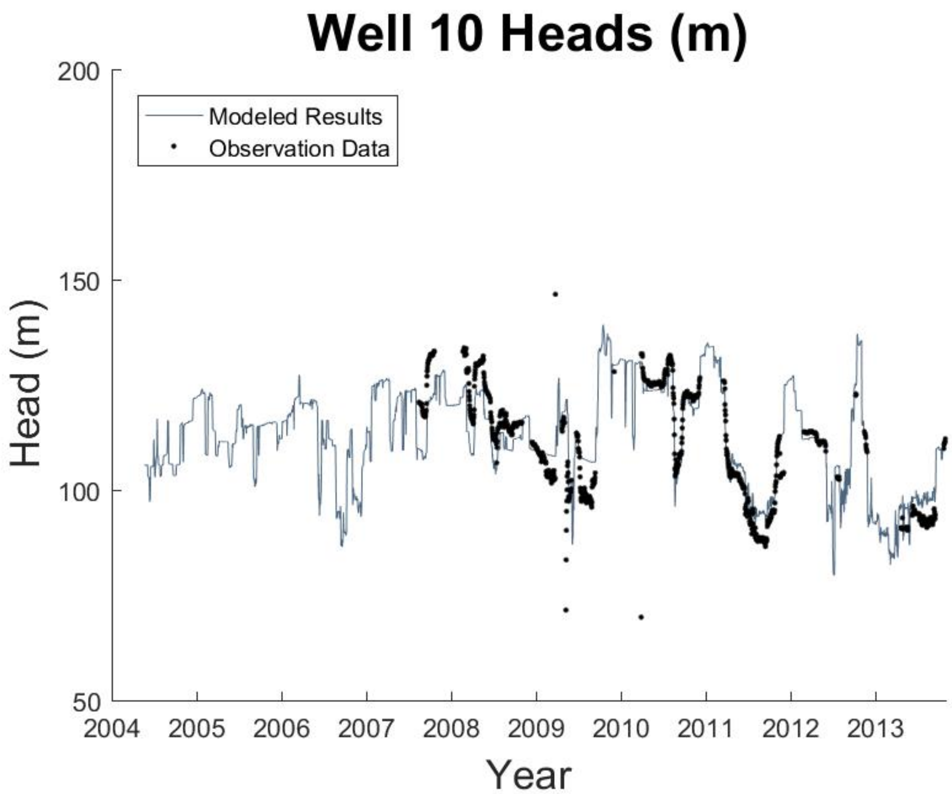
Well 10 Heads (m)
Modeled Results
Observation Data
Head (m)
Year
200
150
100
50
2004
2005
2006
2007
2008
2009
2010
2011
2012
2013

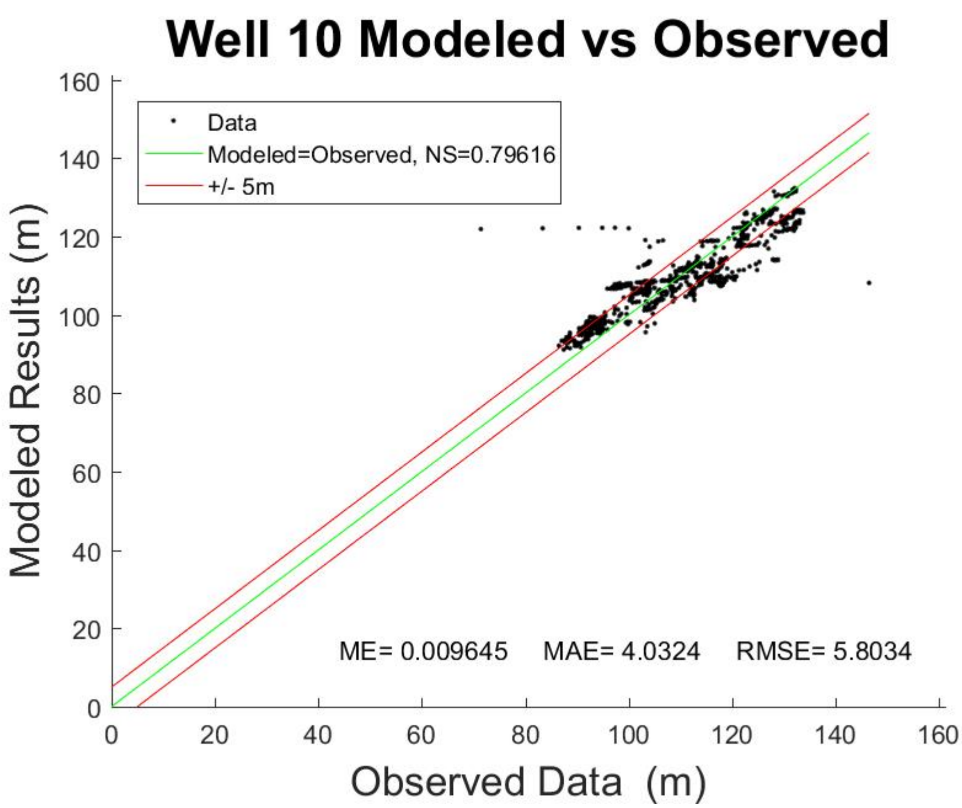
Well 10 Modeled vs Observed
Data
Modeled=Observed, NS=0.79616
+/- 5m
ME= 0.009645
MAE= 4.0324
RMSE= 5.8034
Modeled Results (m)
Observed Data (m)
0
20
40
60
80
100
120
140
160

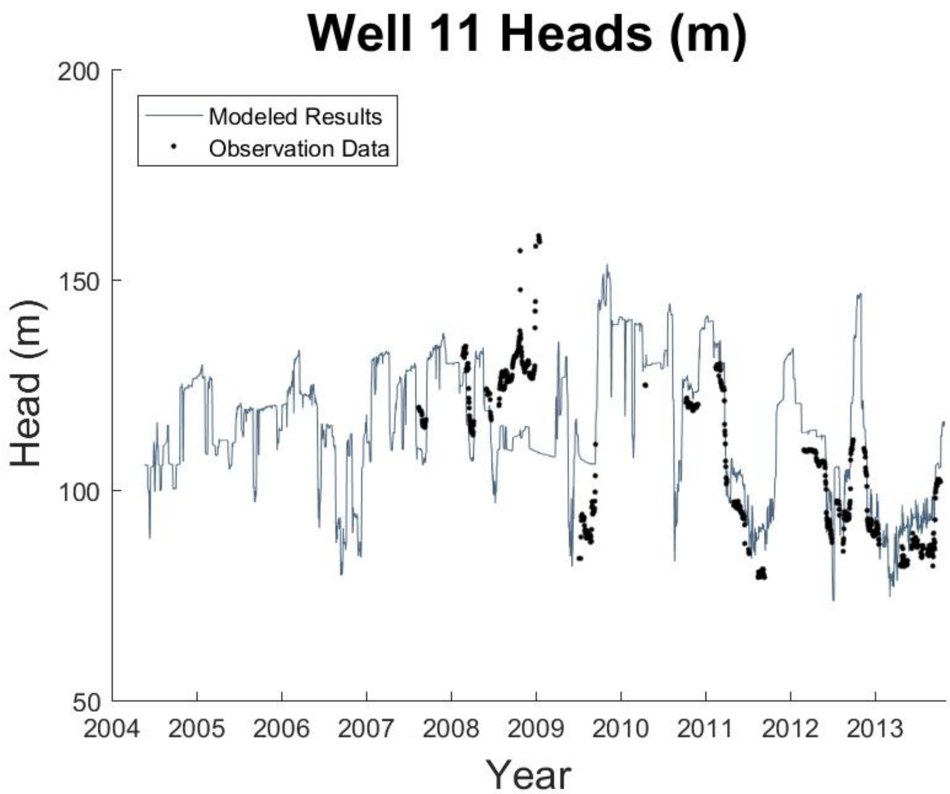
Well 11 Heads (m)
Modeled Results
Observation Data
Head (m)
200
150
100
50
2004
2005
2006
2007
2008
2009
2010
2011
2012
2013
Year

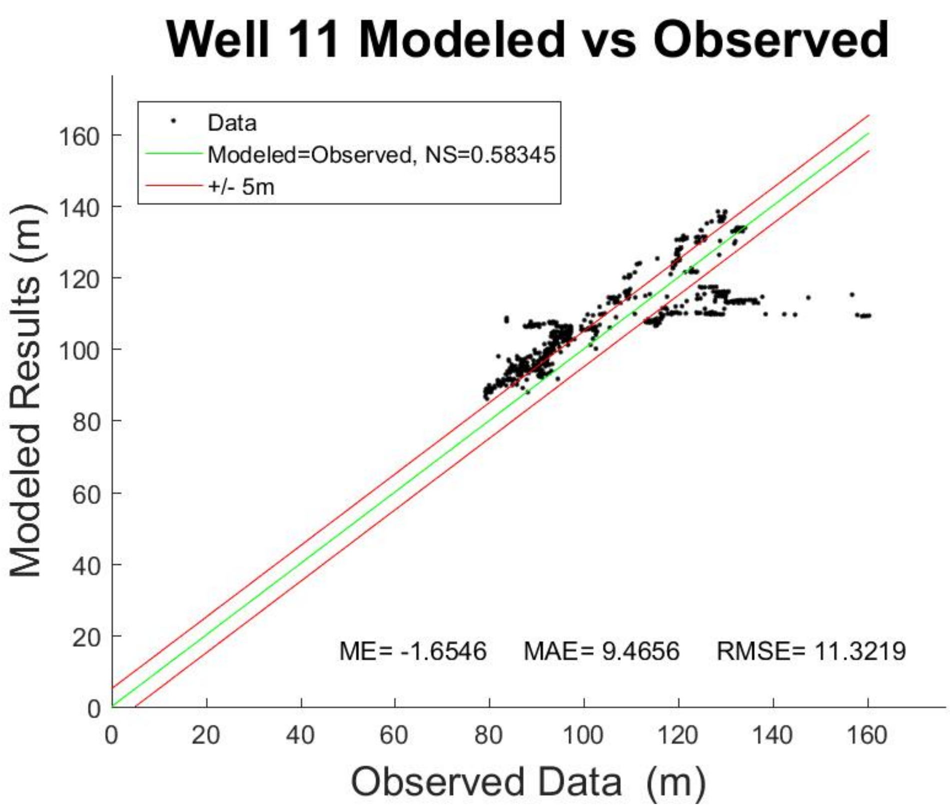
Well 11 Modeled vs Observed
Data
Modeled=Observed, NS=0.58345
+/- 5m
Modeled Results (m)
ME= -1.6546
MAE= 9.4656
RMSE= 11.3219
0
20
40
60
80
100
120
140
160
Observed Data (m)

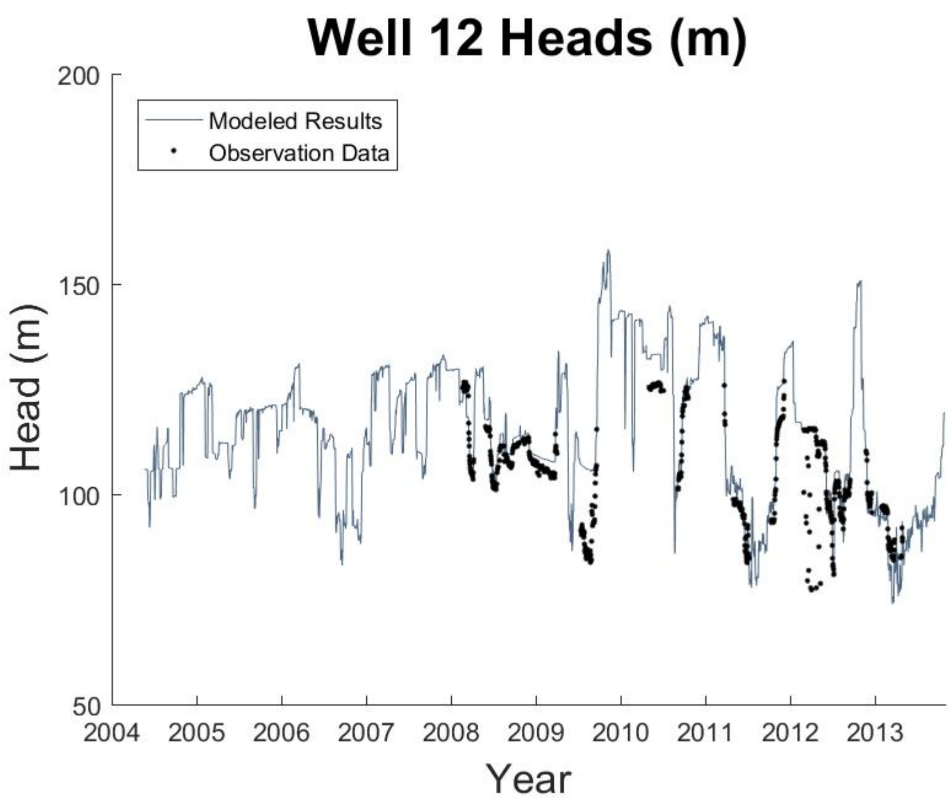

Well 12 Heads (m)
Modeled Results
Observation Data
Head (m)
Year
200
150
100
50
2004
2005
2006
2007
2008
2009
2010
2011
2012
2013

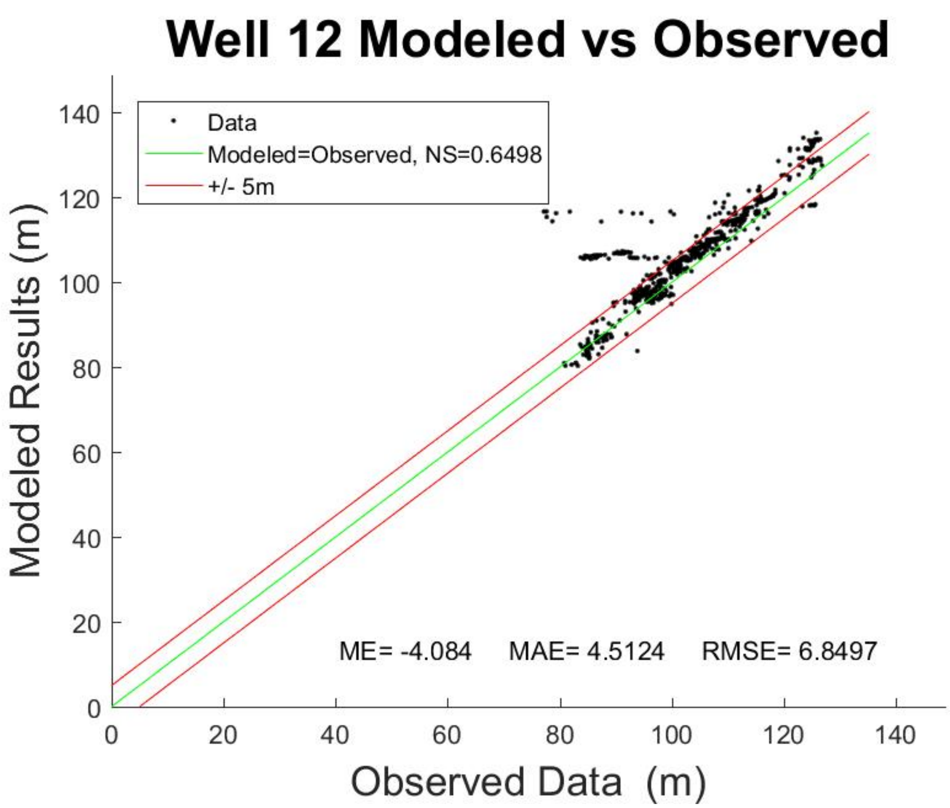

Well 12 Modeled vs Observed
Data
Modeled=Observed, NS=0.6498
+/- 5m
ME= -4.084 MAE= 4.5124 RMSE= 6.8497
Modeled Results (m)
Observed Data (m)
0
20
40
60
80
100
120
140

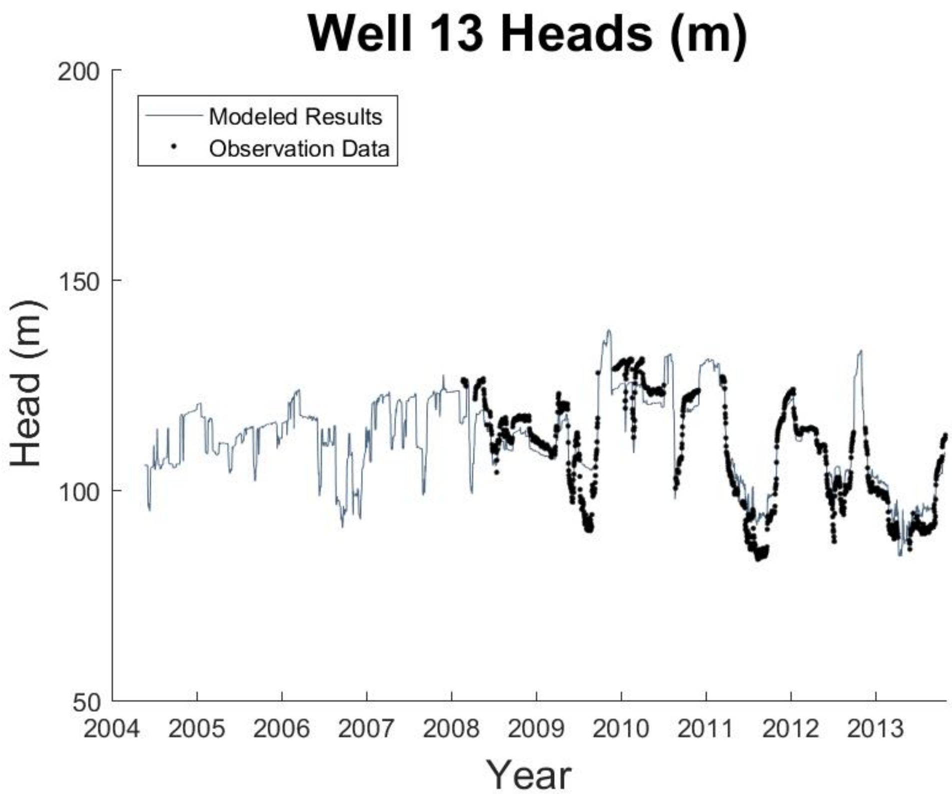

Well 13 Heads (m)
Modeled Results
Observation Data
Head (m)
Year
200
150
100
50
2004
2005
2006
2007
2008
2009
2010
2011
2012
2013

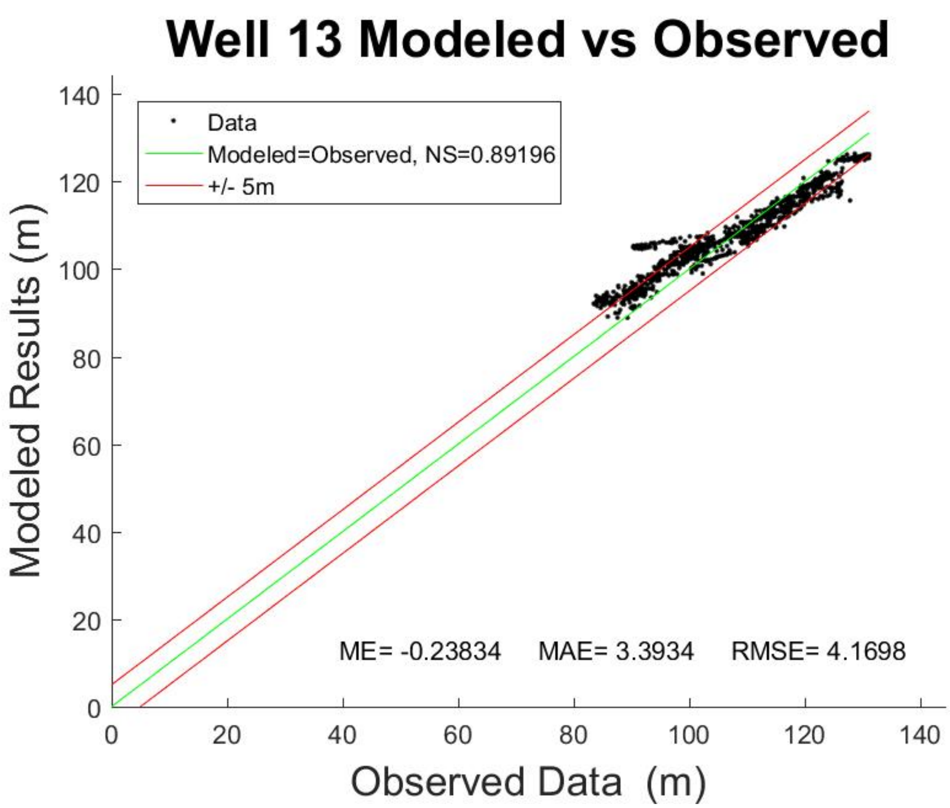

Well 13 Modeled vs Observed
Data
Modeled=Observed, NS=0.89196
+/- 5m
ME= -0.23834
MAE= 3.3934
RMSE= 4.1698
Modeled Results (m)
Observed Data (m)
0
20
40
60
80
100
120
140

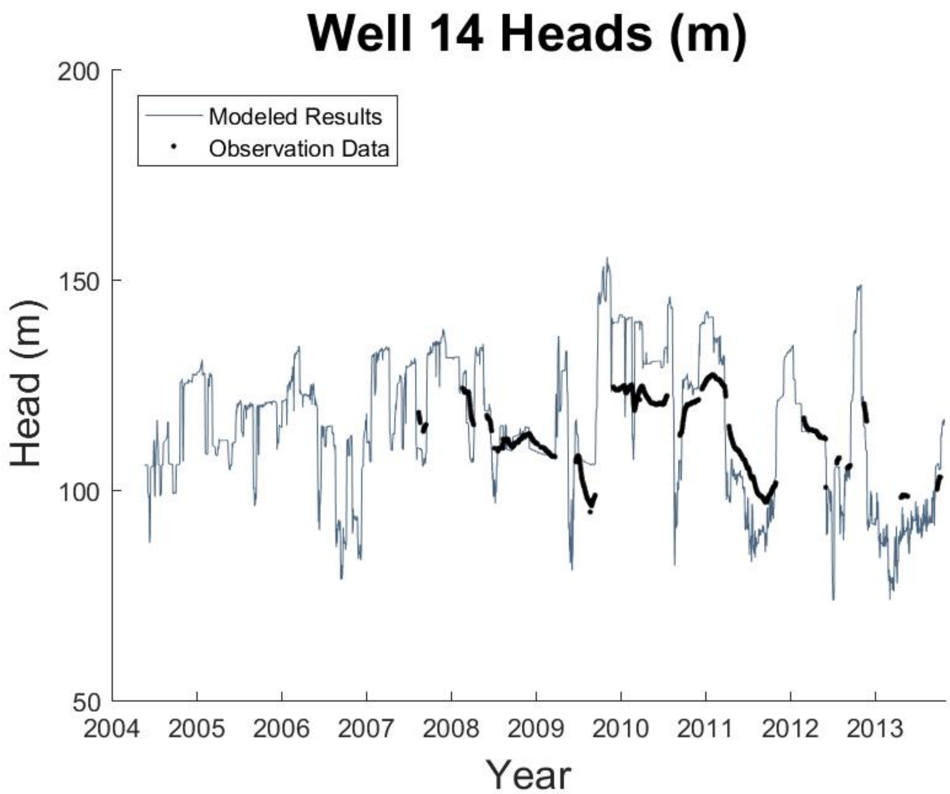
Well 14 Heads (m)
Modeled Results
Observation Data
Head (m)
200
150
100
50
2004
2005
2006
2007
2008
2009
2010
2011
2012
2013
Year

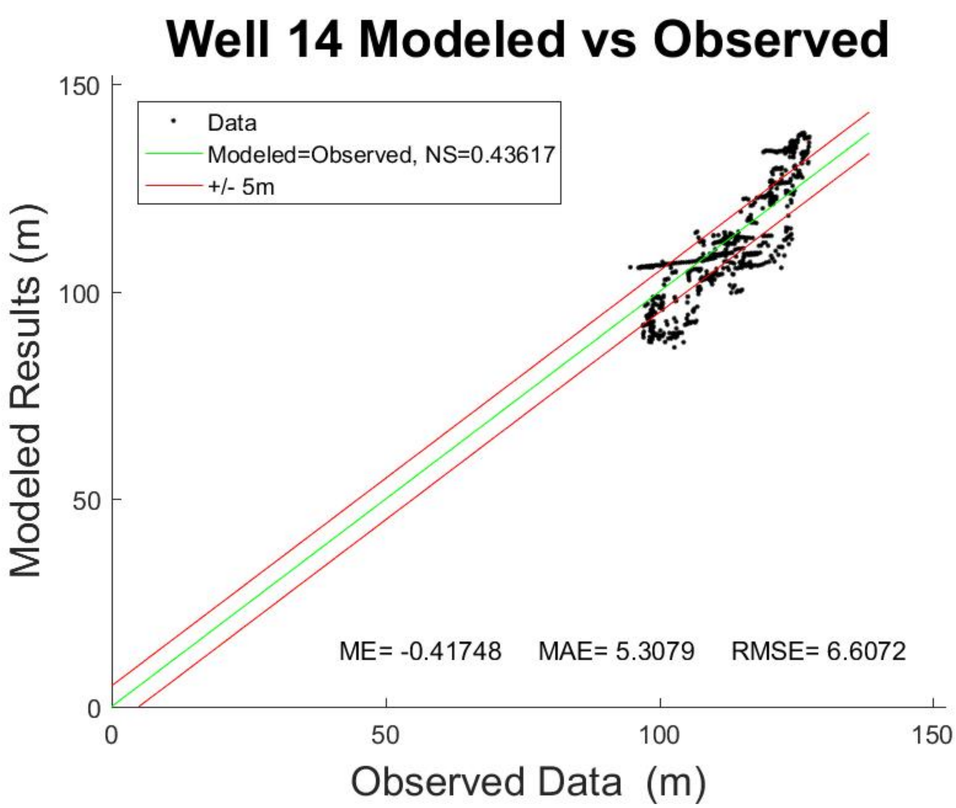
Well 14 Modeled vs Observed
Data
Modeled=Observed, NS=0.43617
+/- 5m
Modeled Results (m)
150
100
50
0
ME= -0.41748
MAE= 5.3079
RMSE= 6.6072
0
50
100
150
Observed Data (m)

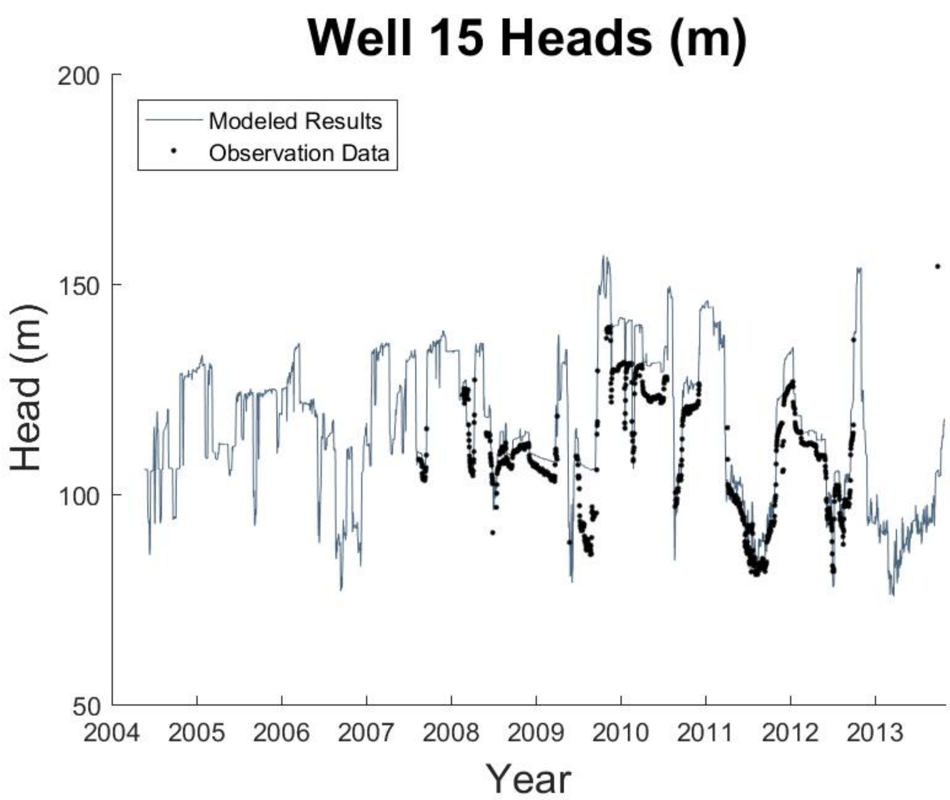
Well 15 Heads (m)
Modeled Results
Observation Data
Head (m)
Year
200
150
100
50
2004
2005
2006
2007
2008
2009
2010
2011
2012
2013

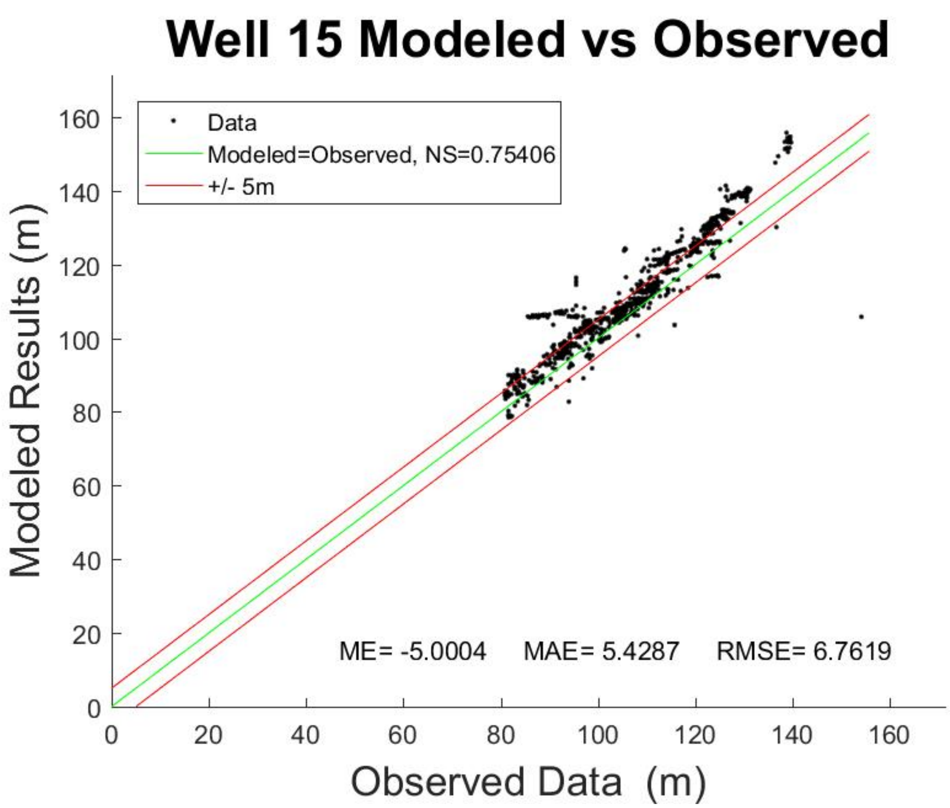
Well 15 Modeled vs Observed
Data
Modeled=Observed, NS=0.75406
+/- 5m
ME= -5.0004
MAE= 5.4287
RMSE= 6.7619
Modeled Results (m)
Observed Data (m)
0
20
40
60
80
100
120
140
160

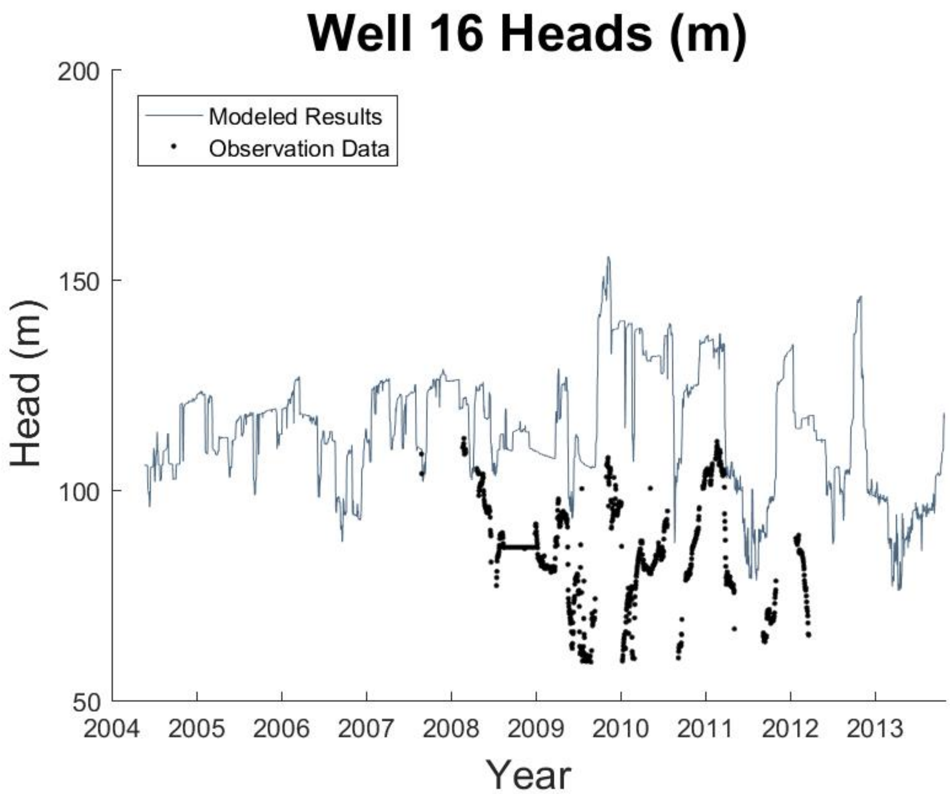
Well 16 Heads (m)
Modeled Results
Observation Data
Head (m)
Year
200
150
100
50
2004
2005
2006
2007
2008
2009
2010
2011
2012
2013

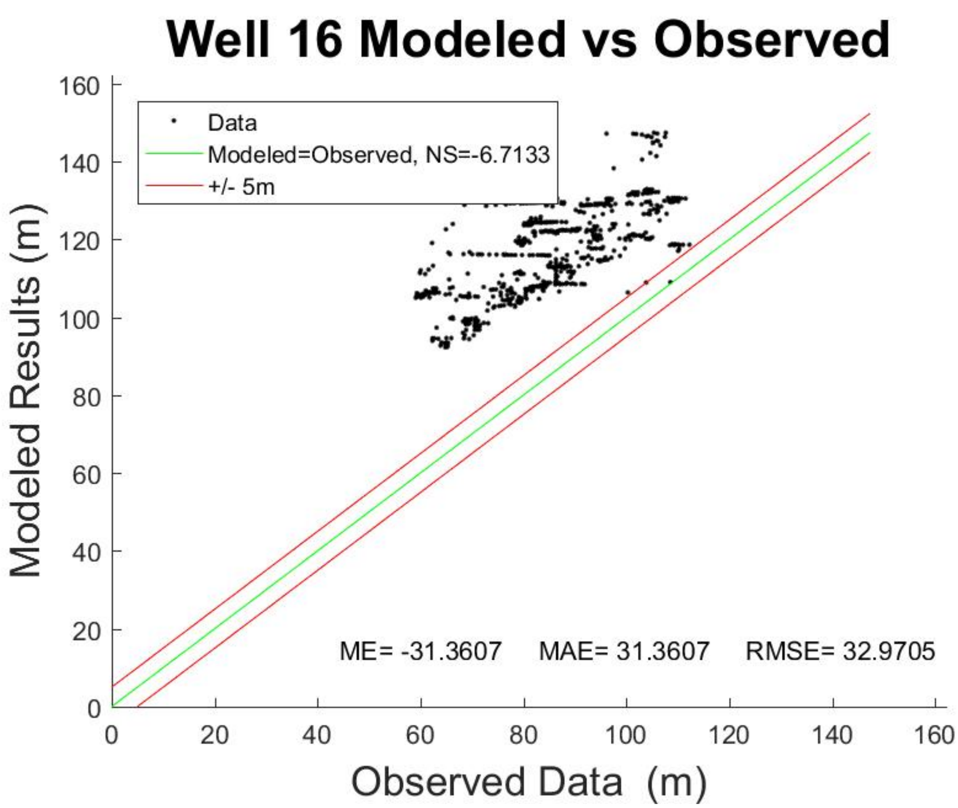
Well 16 Modeled vs Observed
Data
Modeled=Observed, NS=-6.7133
+/- 5m
Modeled Results (m)
Observed Data (m)
ME= -31.3607
MAE= 31.3607
RMSE= 32.9705
0
20
40
60
80
100
120
140
160

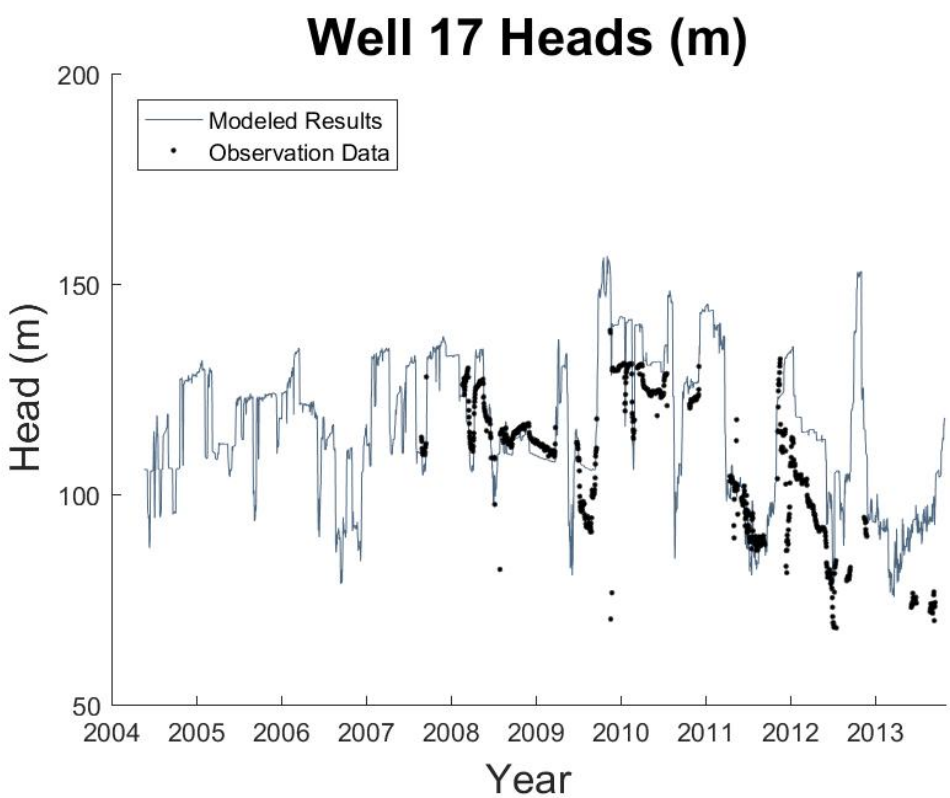
Well 17 Heads (m)
Modeled Results
Observation Data
Head (m)
200
150
100
50
2004
2005
2006
2007
2008
2009
2010
2011
2012
2013
Year

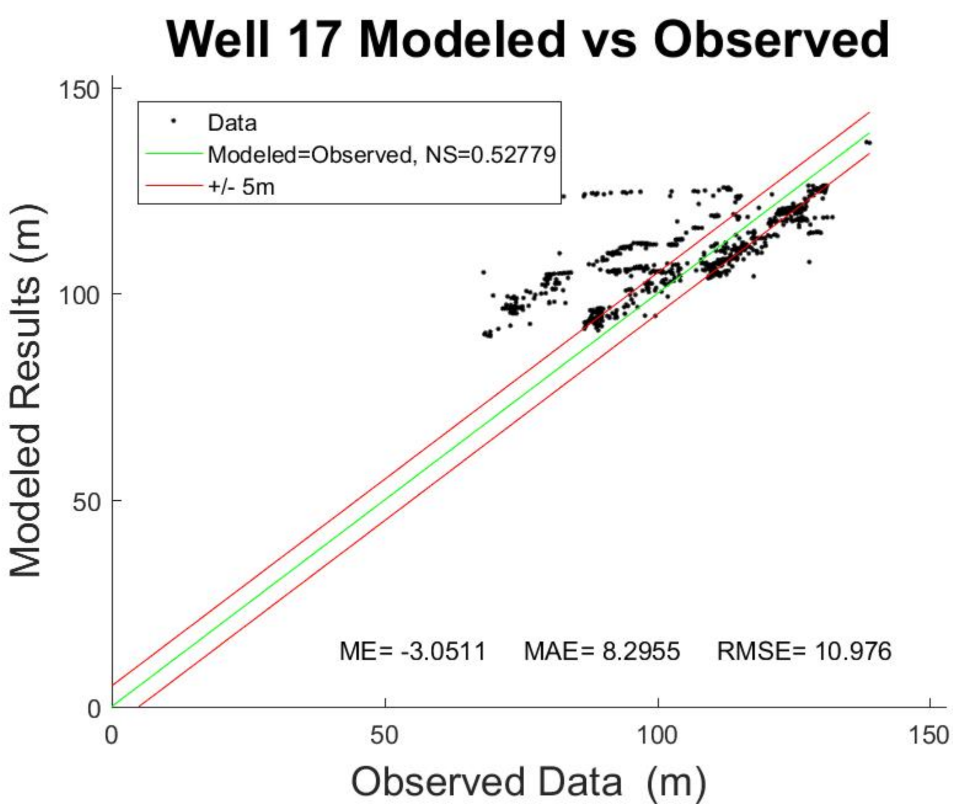
Well 17 Modeled vs Observed
Data
Modeled=Observed, NS=0.52779
+/- 5m
Modeled Results (m)
150
100
50
0
ME= -3.0511
MAE= 8.2955
RMSE= 10.976
0
50
100
150
Observed Data (m)

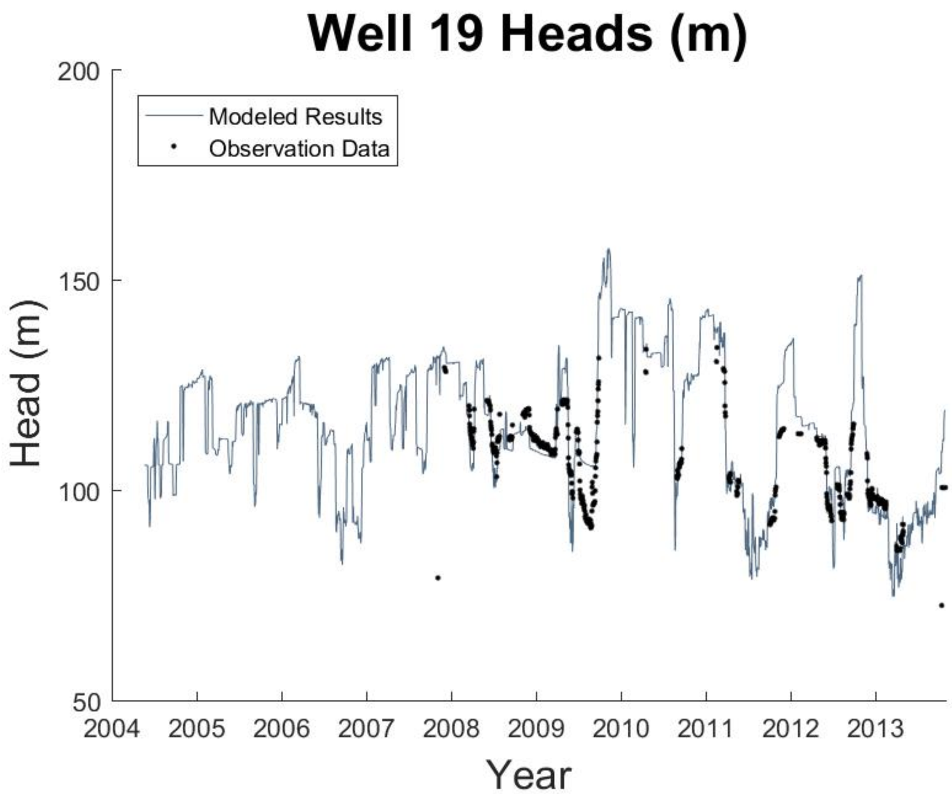
Well 19 Heads (m)
Modeled Results
Observation Data
Head (m)
200
150
100
50
2004
2005
2006
2007
2008
2009
2010
2011
2012
2013
Year

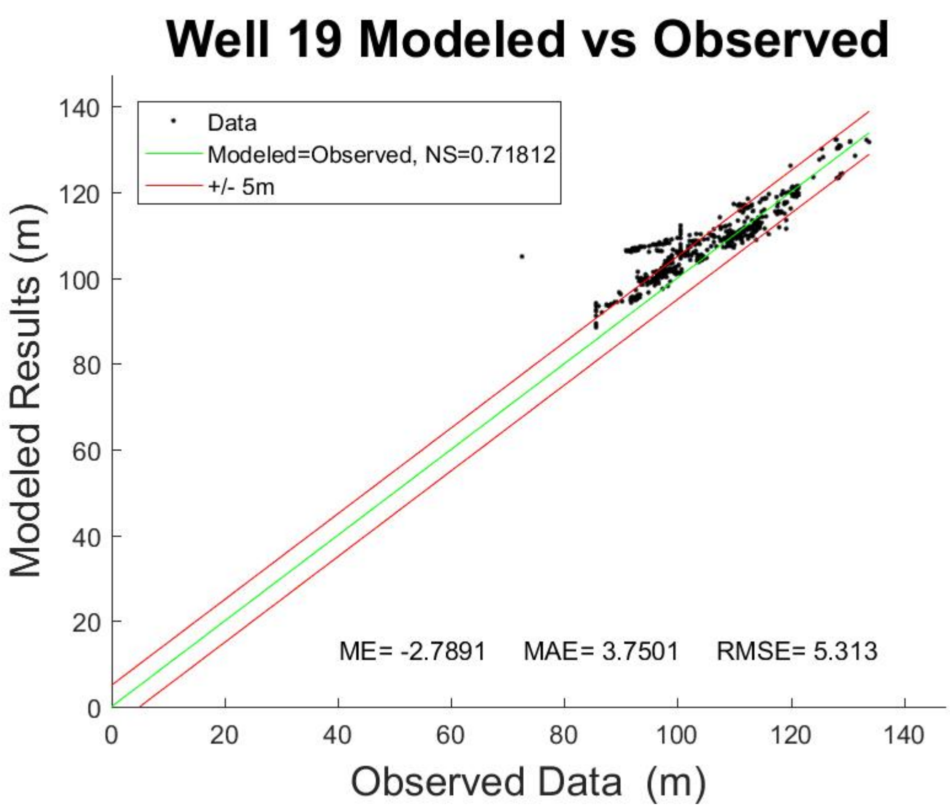
Well 19 Modeled vs Observed
Data
Modeled=Observed, NS=0.71812
+/- 5m
Modeled Results (m)
ME= -2.7891
MAE= 3.7501
RMSE= 5.313
0
20
40
60
80
100
120
140
Observed Data (m)

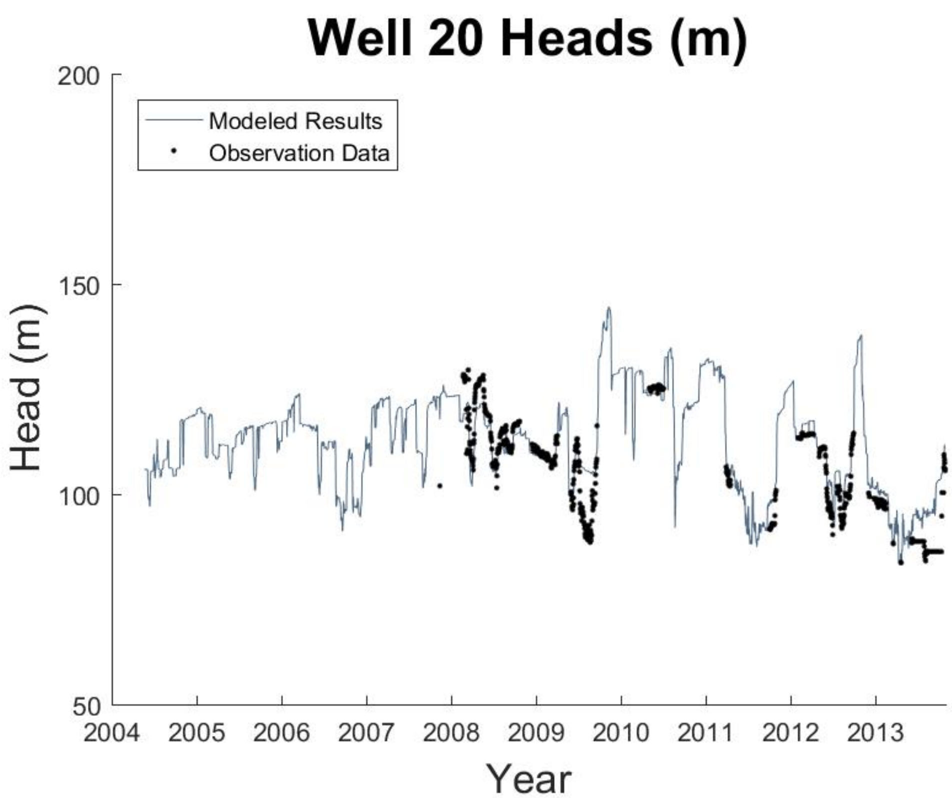
Well 20 Heads (m)
Modeled Results
Observation Data
Head (m)
Year
200
150
100
50
2004
2005
2006
2007
2008
2009
2010
2011
2012
2013

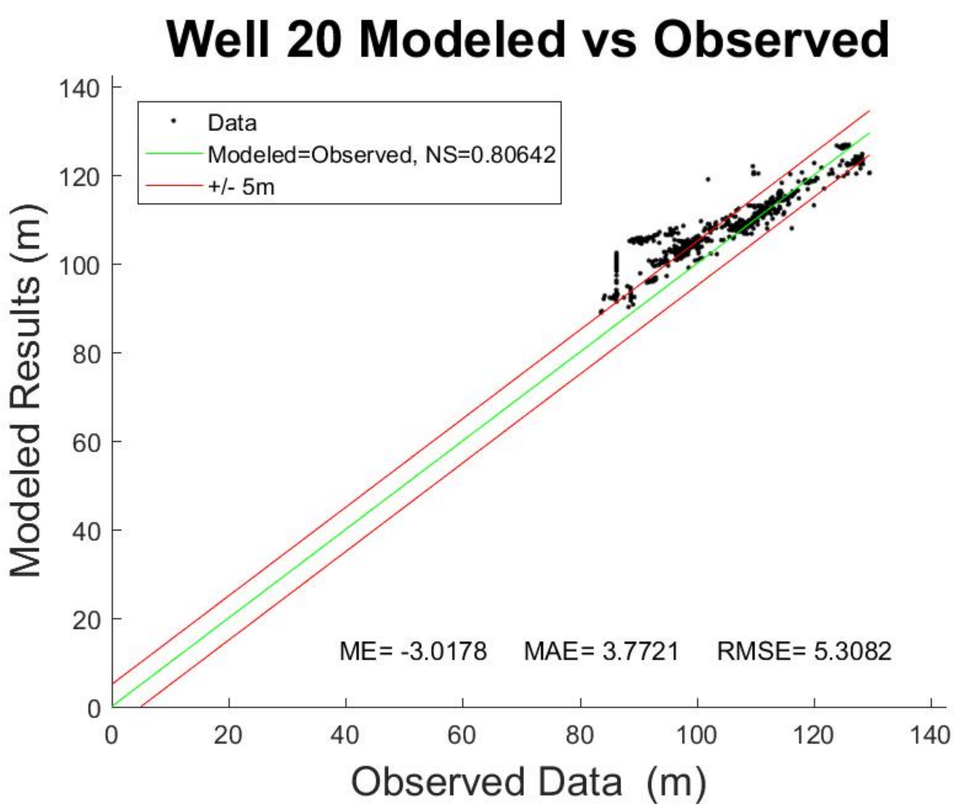
Well 20 Modeled vs Observed
Data
Modeled=Observed, NS=0.80642
+/- 5m
ME= -3.0178
MAE= 3.7721
RMSE= 5.3082
Modeled Results (m)
Observed Data (m)
0
20
40
60
80
100
120
140

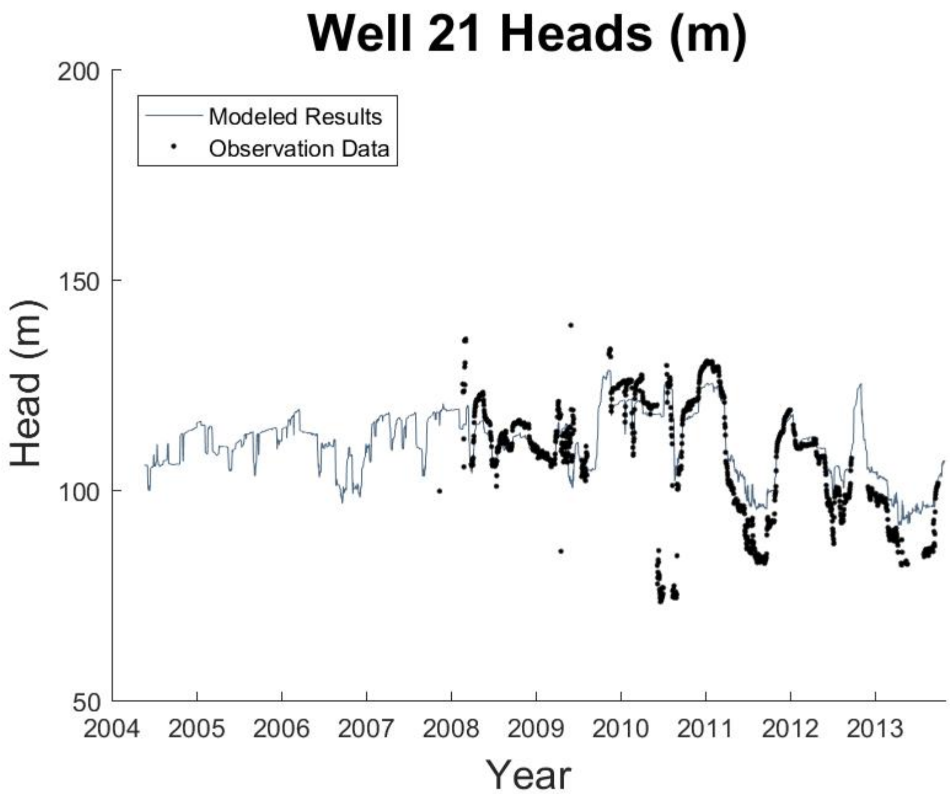
Well 21 Heads (m)
Modeled Results
Observation Data
Head (m)
200
150
100
50
2004
2005
2006
2007
2008
2009
2010
2011
2012
2013
Year

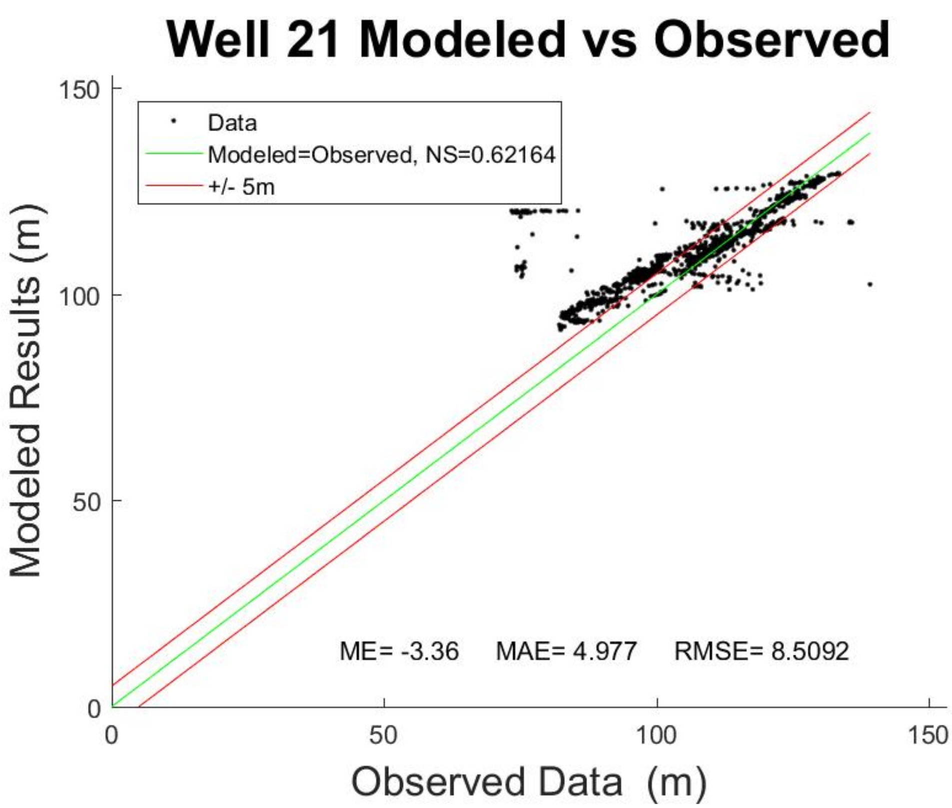
Well 21 Modeled vs Observed
Data
Modeled=Observed, NS=0.62164
+/- 5m
Modeled Results (m)
ME= -3.36
MAE= 4.977
RMSE= 8.5092
0
50
100
150
Observed Data (m)

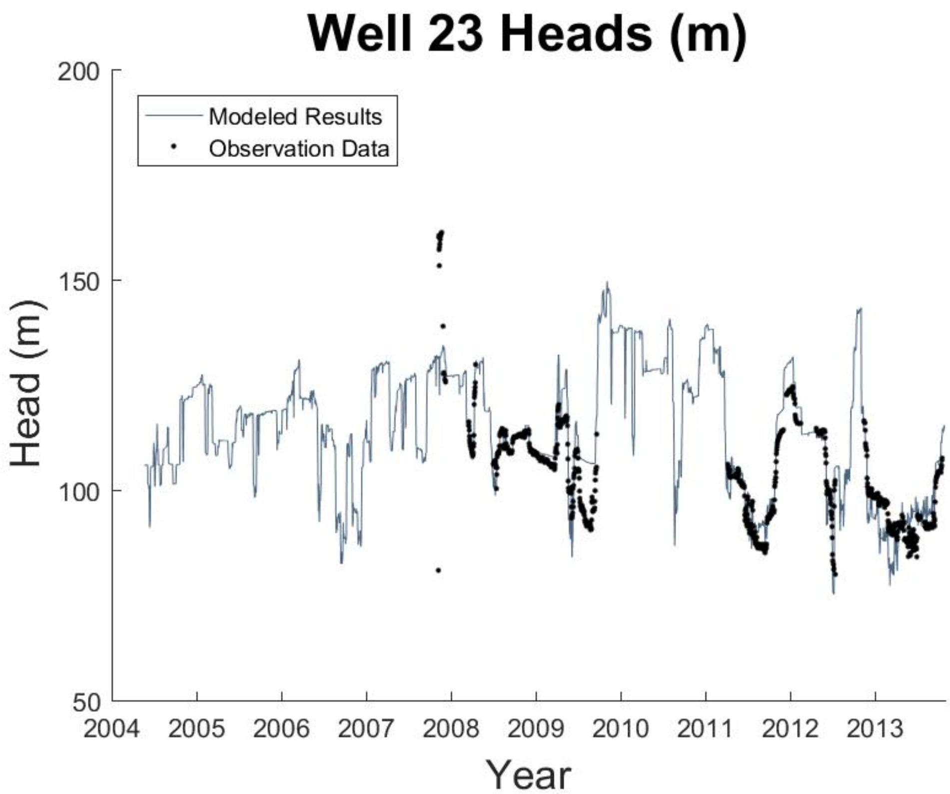
Well 23 Heads (m)
Modeled Results
Observation Data
Head (m)
200
150
100
50
2004
2005
2006
2007
2008
2009
2010
2011
2012
2013
Year

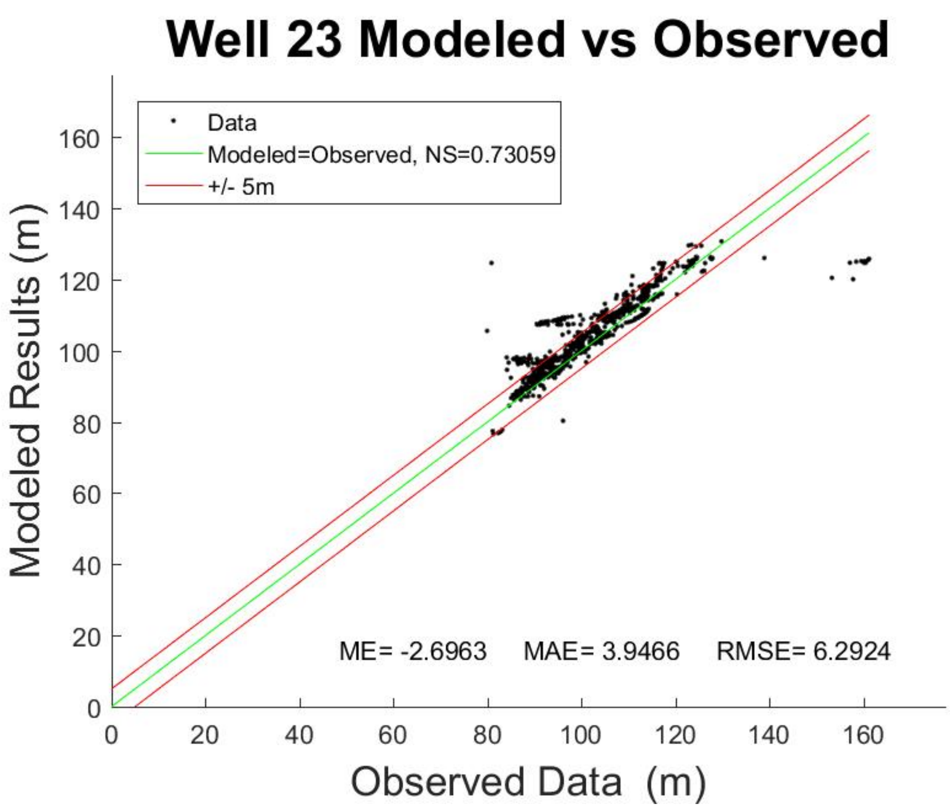
Well 23 Modeled vs Observed
Data
Modeled=Observed, NS=0.73059
+/- 5m
Modeled Results (m)
160
140
120
100
80
60
40
20
0
ME= -2.6963
MAE= 3.9466
RMSE= 6.2924
0
20
40
60
80
100
120
140
160
Observed Data (m)

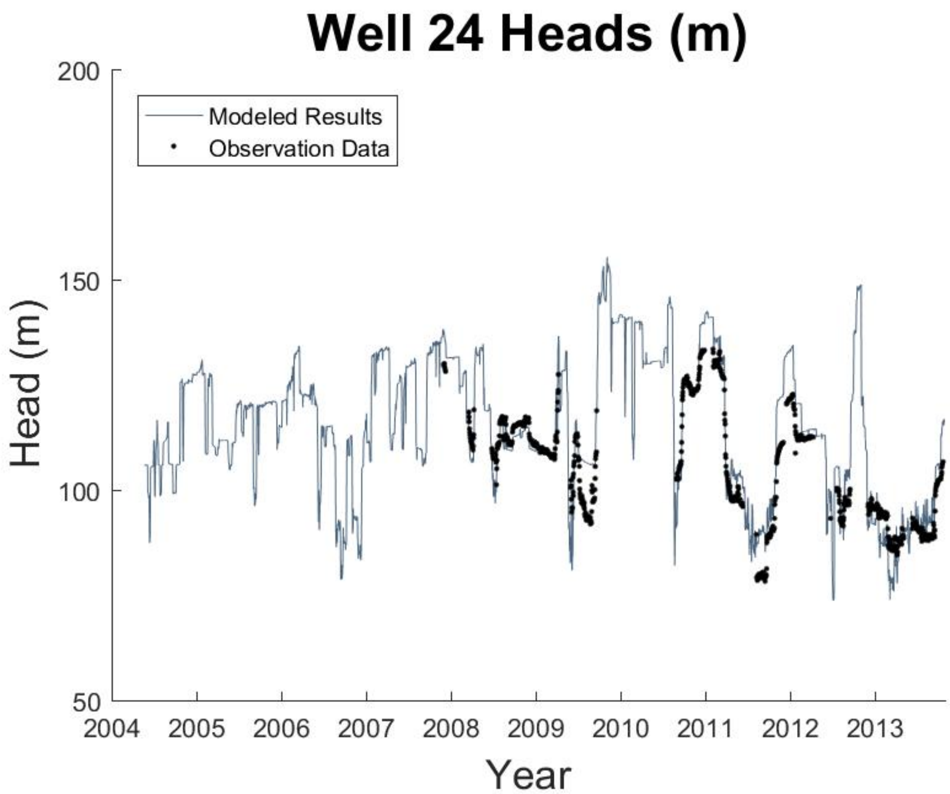

Well 24 Heads (m)
Modeled Results
Observation Data
Head (m)
200
150
100
50
2004
2005
2006
2007
2008
2009
2010
2011
2012
2013
Year

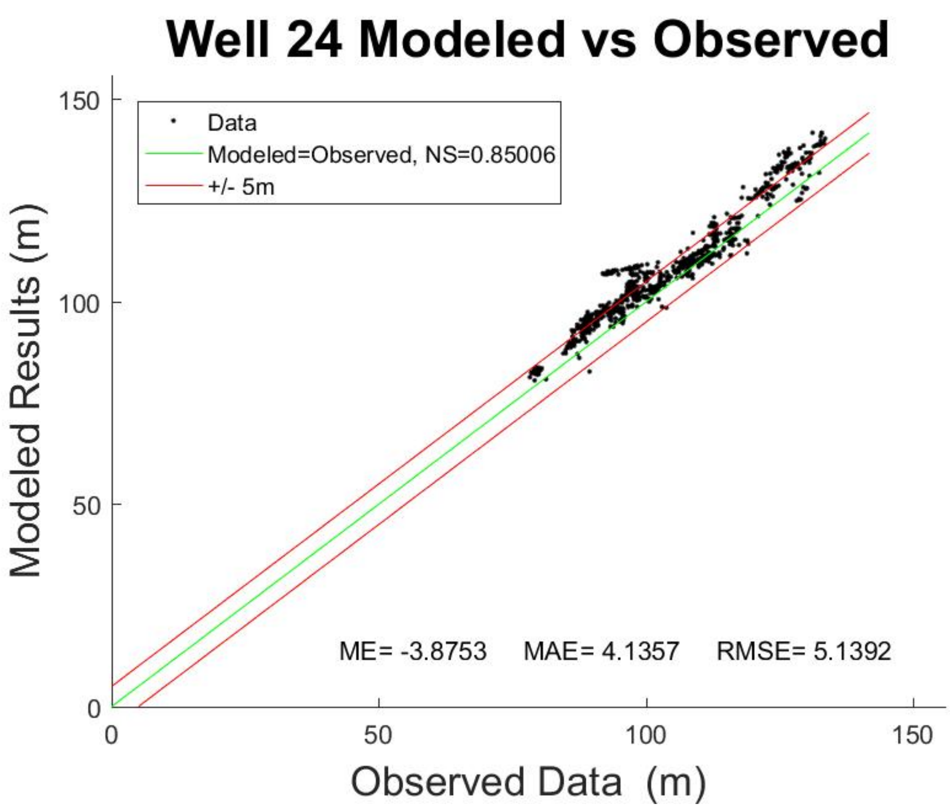

Well 24 Modeled vs Observed
Data
Modeled=Observed, NS=0.85006
+/- 5m
Modeled Results (m)
ME= -3.8753
MAE= 4.1357
RMSE= 5.1392
0
50
100
150
Observed Data (m)

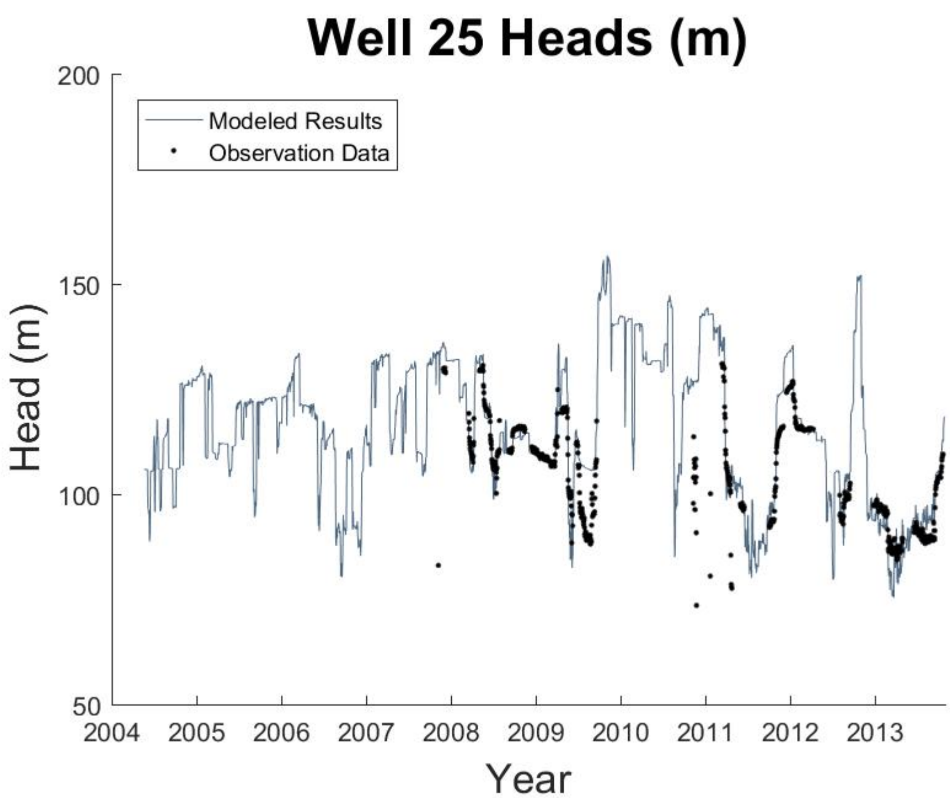
Well 25 Heads (m)
Modeled Results
Observation Data
Head (m)
200
150
100
50
2004
2005
2006
2007
2008
2009
2010
2011
2012
2013
Year

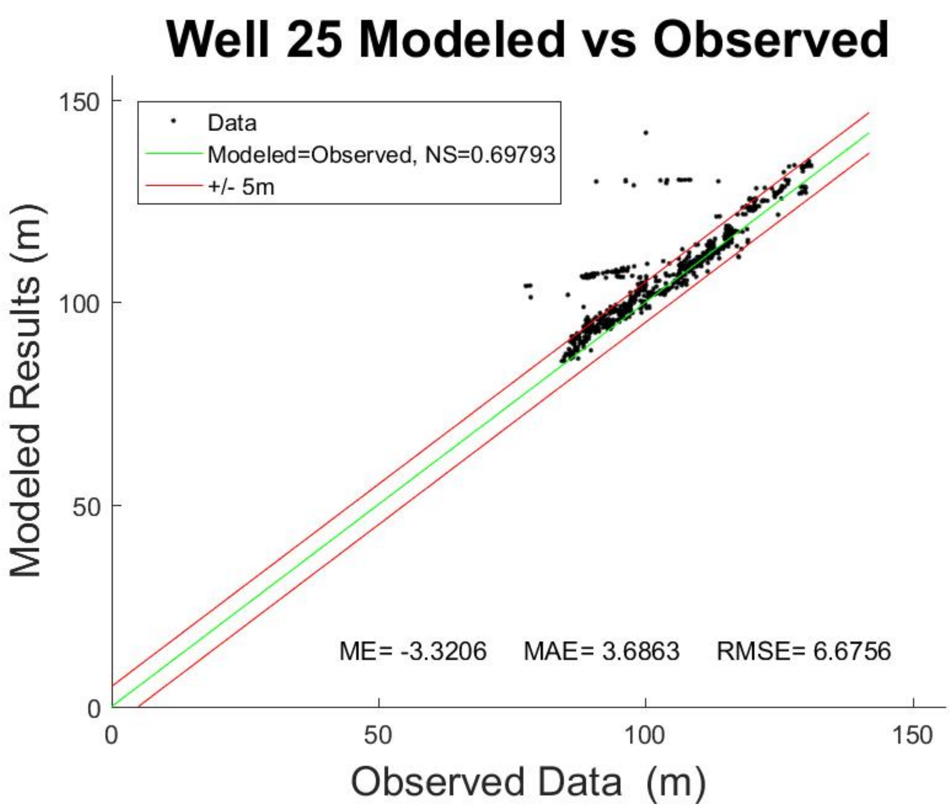
Well 25 Modeled vs Observed
Data
Modeled=Observed, NS=0.69793
+/- 5m
ME= -3.3206
MAE= 3.6863
RMSE= 6.6756
Modeled Results (m)
150
100
50
0
Observed Data (m)

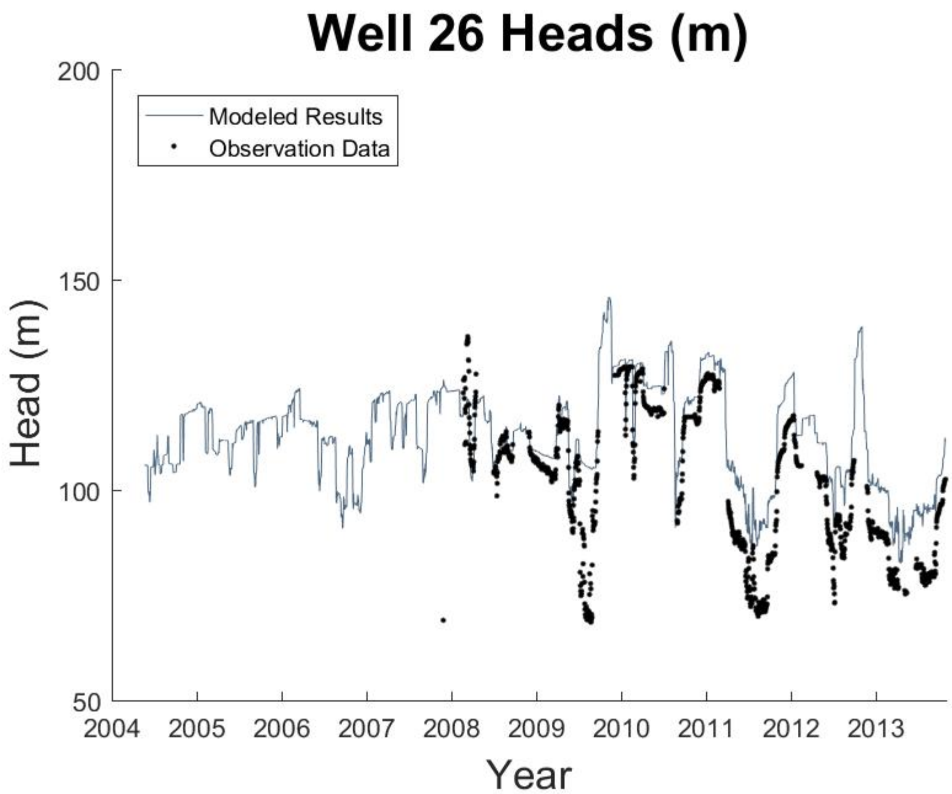
Well 26 Heads (m)
Modeled Results
Observation Data
Head (m)
Year
200
150
100
50
2004
2005
2006
2007
2008
2009
2010
2011
2012
2013

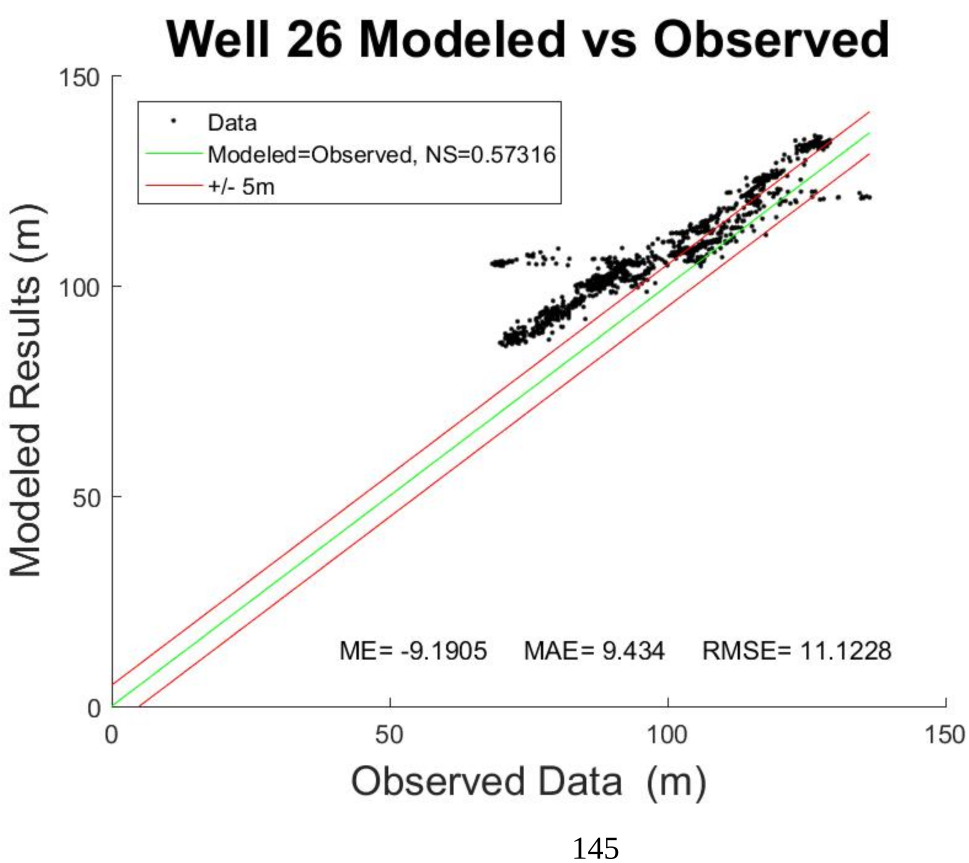
Well 26 Modeled vs Observed
Data
Modeled=Observed, NS=0.57316
+/- 5m
ME= -9.1905
MAE= 9.434
RMSE= 11.1228
Modeled Results (m)
Observed Data (m)
150
100
50
0

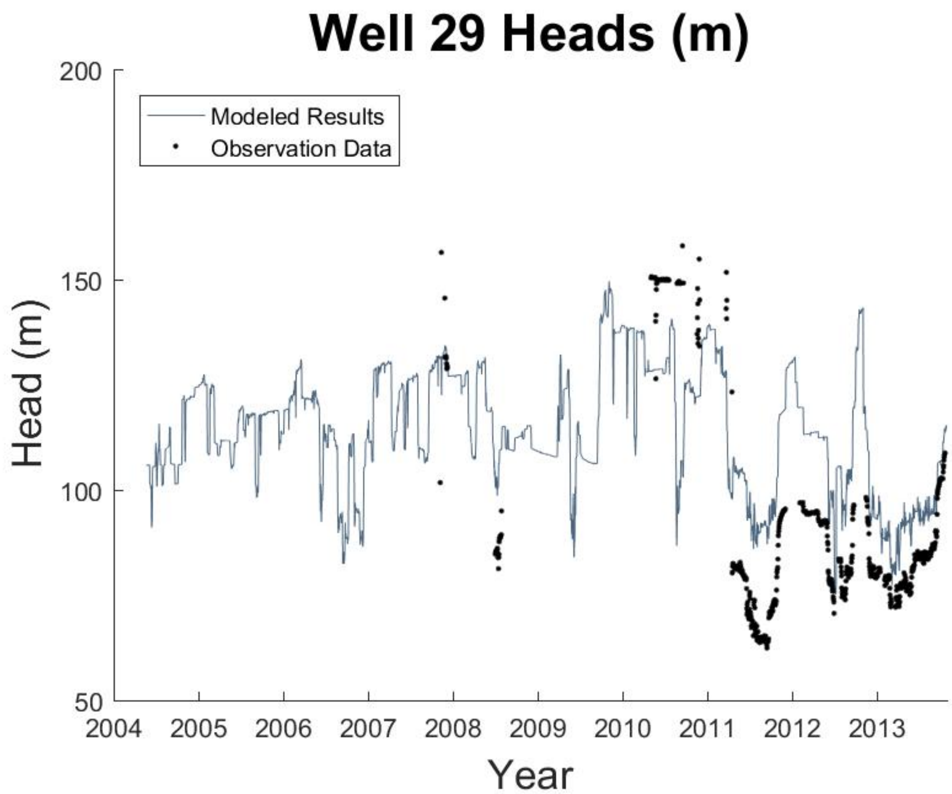

Well 29 Heads (m)
Modeled Results
Observation Data
Head (m)
200
150
100
50
2004
2005
2006
2007
2008
2009
2010
2011
2012
2013
Year

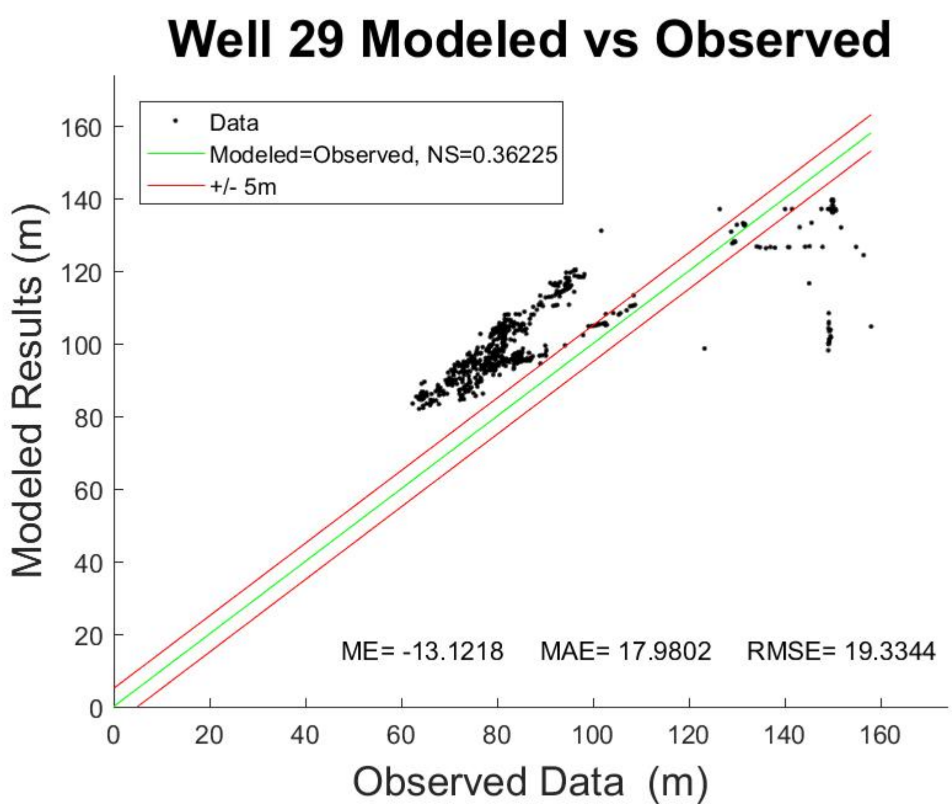

Well 29 Modeled vs Observed
Data
Modeled=Observed, NS=0.36225
+/- 5m
Modeled Results (m)
ME= -13.1218
MAE= 17.9802
RMSE= 19.3344
Observed Data (m)

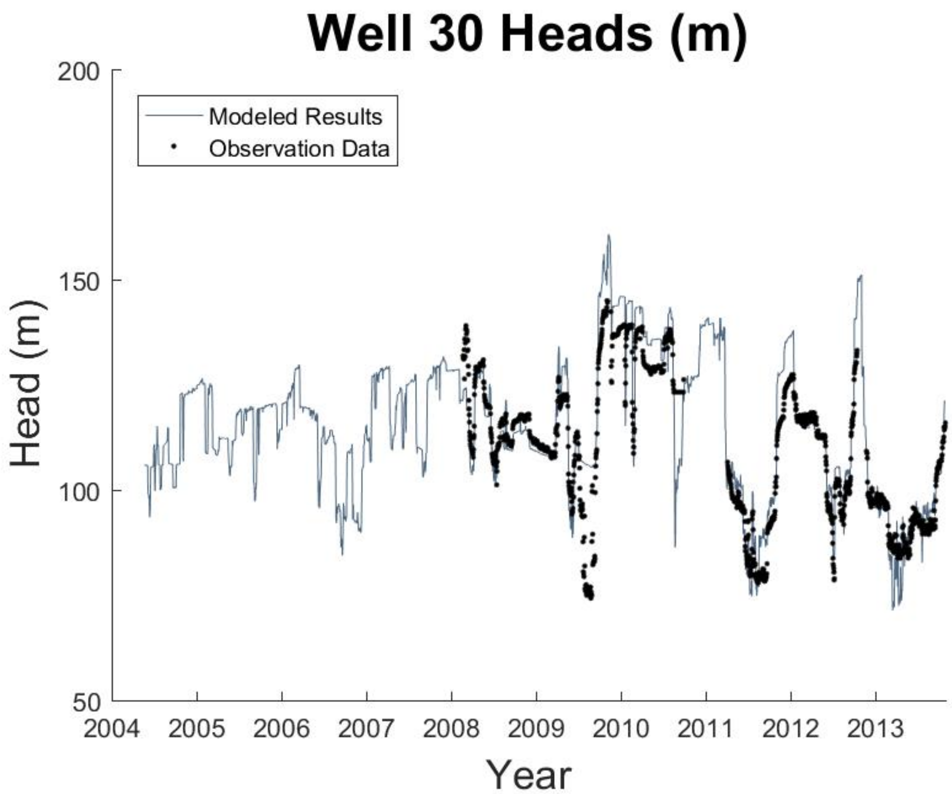
Well 30 Heads (m)
Modeled Results
Observation Data
Head (m)
200
150
100
50
2004
2005
2006
2007
2008
2009
2010
2011
2012
2013
Year

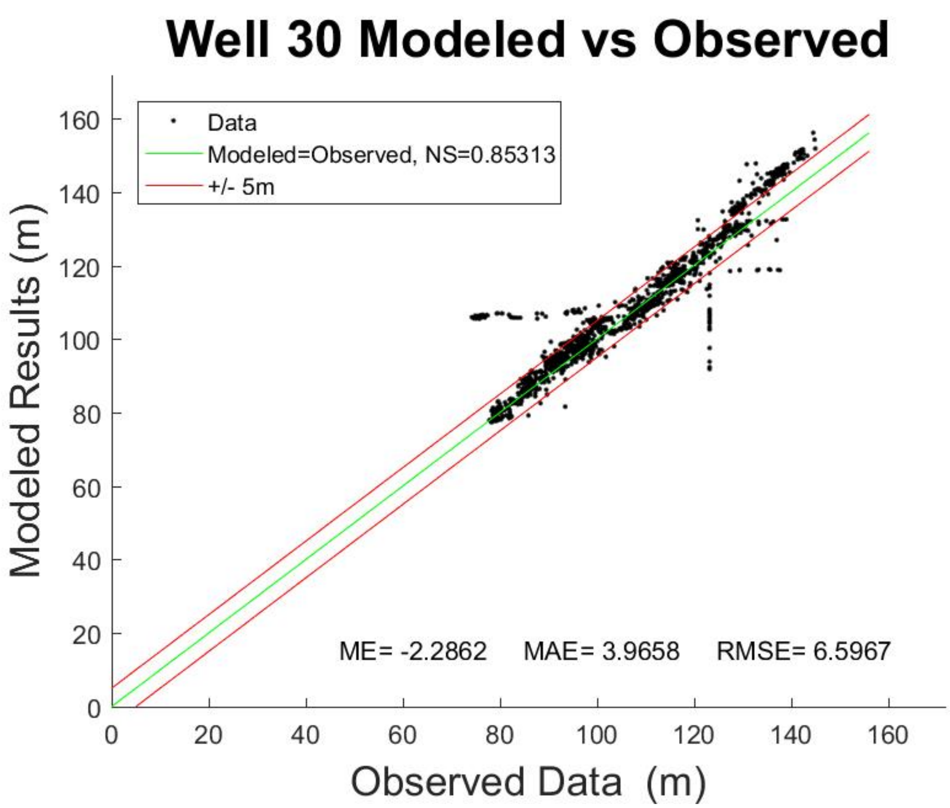
Well 30 Modeled vs Observed
Data
Modeled=Observed, NS=0.85313
+/- 5m
Modeled Results (m)
ME= -2.2862
MAE= 3.9658
RMSE= 6.5967
0
20
40
60
80
100
120
140
160
Observed Data (m)

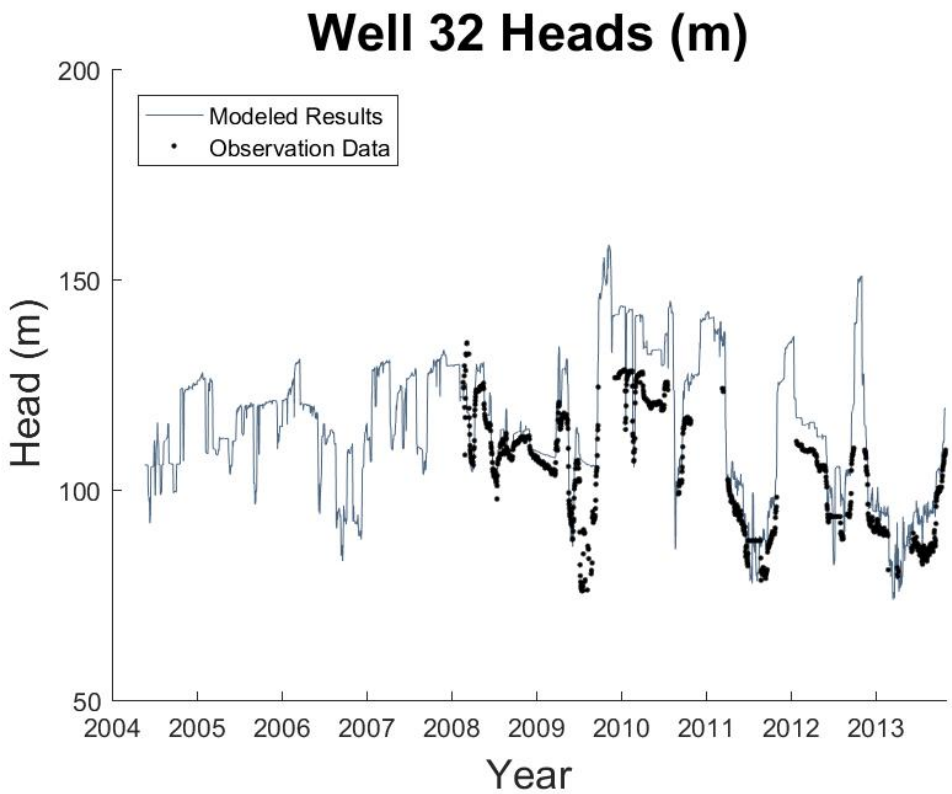
Well 32 Heads (m)
Modeled Results
Observation Data
Head (m)
Year
200
150
100
50
2004
2005
2006
2007
2008
2009
2010
2011
2012
2013

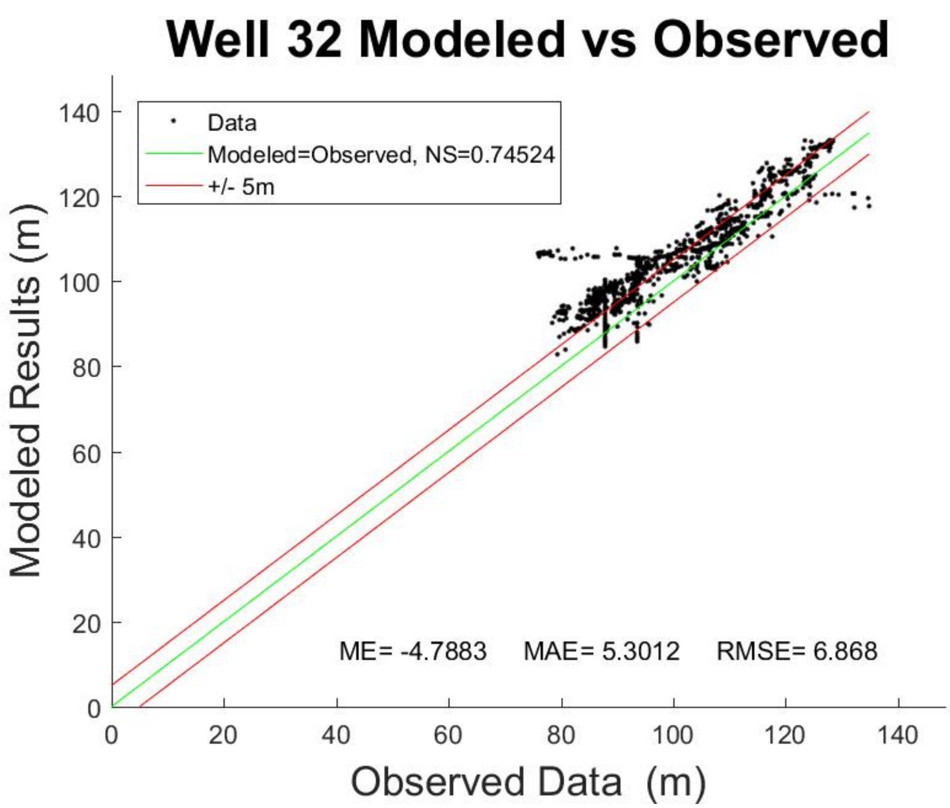
Well 32 Modeled vs Observed
Data
Modeled=Observed, NS=0.74524
+/- 5m
ME= -4.7883
MAE= 5.3012
RMSE= 6.868
Modeled Results (m)
Observed Data (m)
0
20
40
60
80
100
120
140

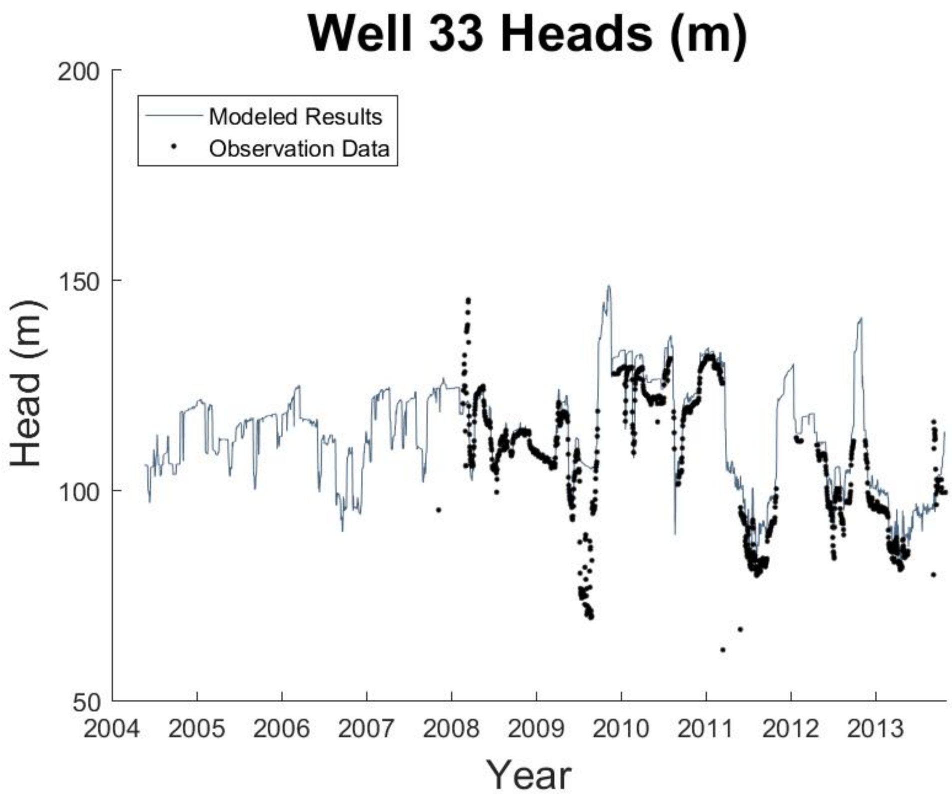
Well 33 Heads (m)
Modeled Results
Observation Data
Head (m)
200
150
100
50
2004
2005
2006
2007
2008
2009
2010
2011
2012
2013
Year

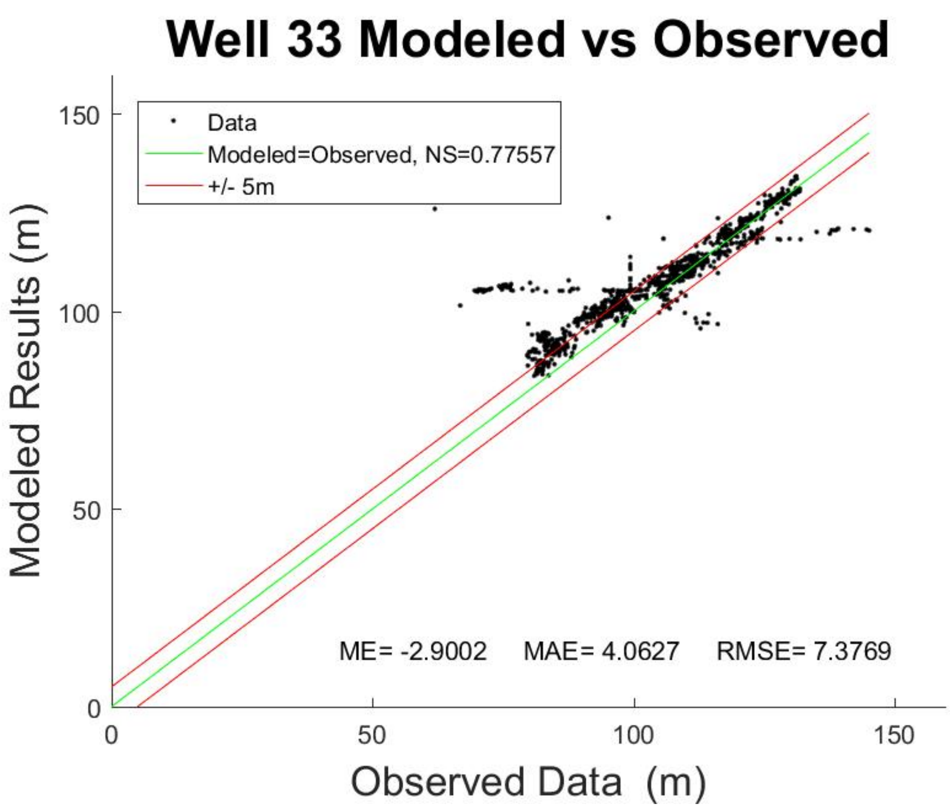
Well 33 Modeled vs Observed
Data
Modeled=Observed, NS=0.77557
+/- 5m
Modeled Results (m)
150
100
50
0
ME= -2.9002
MAE= 4.0627
RMSE= 7.3769
0
50
100
150
Observed Data (m)

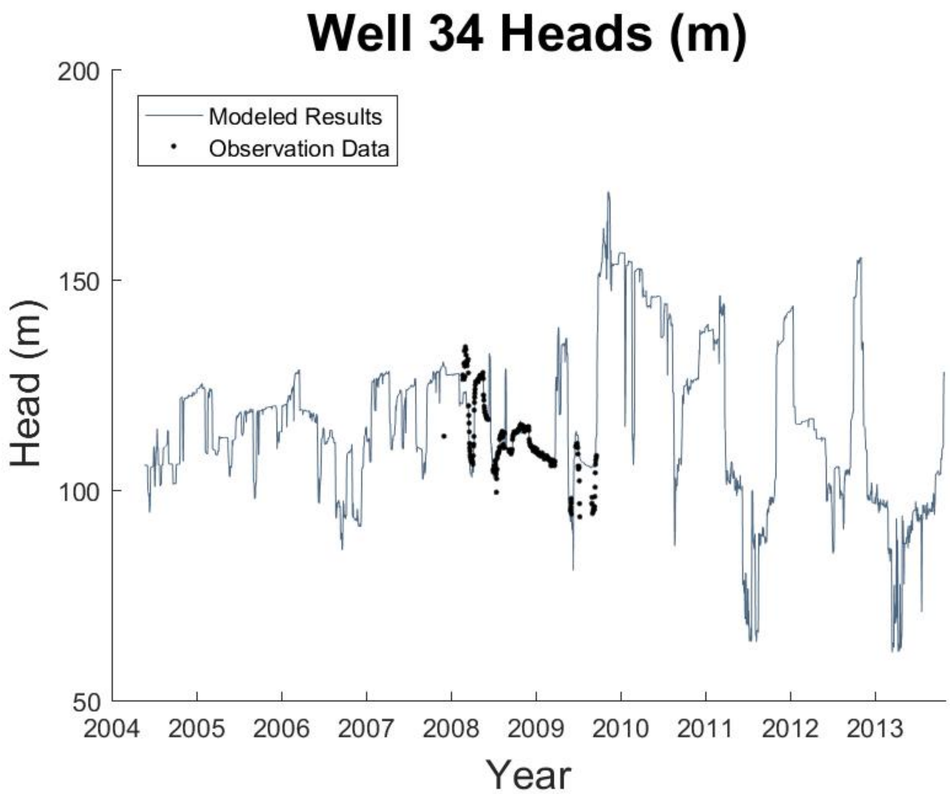
Well 34 Heads (m)
Modeled Results
Observation Data
Head (m)
200
150
100
50
2004
2005
2006
2007
2008
2009
2010
2011
2012
2013
Year

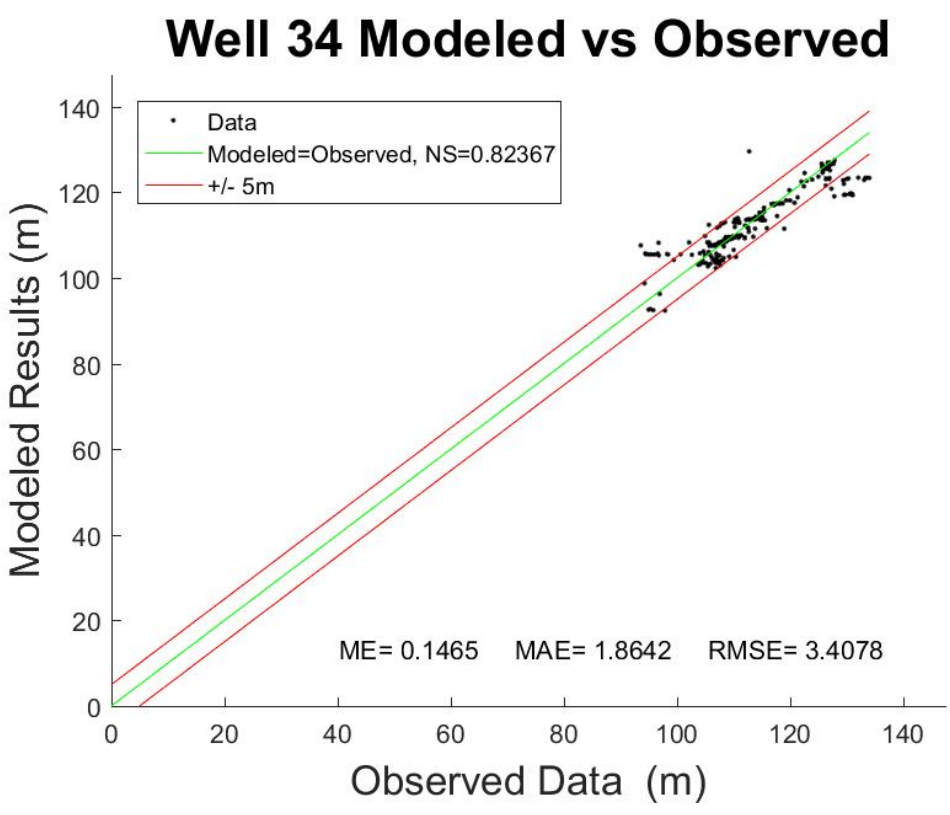
Well 34 Modeled vs Observed
Data
Modeled=Observed, NS=0.82367
+/- 5m
Modeled Results (m)
140
120
100
80
60
40
20
0
ME= 0.1465
MAE= 1.8642
RMSE= 3.4078
0
20
40
60
80
100
120
140
Observed Data (m)

APPENDIX C

ANIMATION OF MIXING FRACTION CONTOURS OVER TIME

The video presented in this appendix illustrates the transport and movement of the injected Edwards water in the H2Oaks ASR system. Contours of mixing fraction (f) throughout the wellfield are shown as they change over time. Locations of the ASR and extraction-only wells are indicated, with the color of the well indicating its state at that point in time (green represents an injecting well, yellow represents an idle well, and red represents a recovering or extracting well). A plot of f_d (the flow-weighted wellfield recovered fraction) over time is presented in the corner, with a red star that tracks along the plotted curve whenever any wells are in recovery mode (red). The animation helps to illustrate how and why f_d changes over time, including a few periods where it increases, and how f_d could be improved by selectively recovering from certain wells. Some decreases can be explained by long periods of recovery where the fraction of injected water surrounding recovering wells gradually decreases. However, many other decreases and increases are a result of simply switching recovery to wells that are more or less centered in their surrounding injected water plumes.

APPENDIX D

PLOTS OF MIXING FRACTION (*F*) OVER TIME FOR EACH ASR WELL.

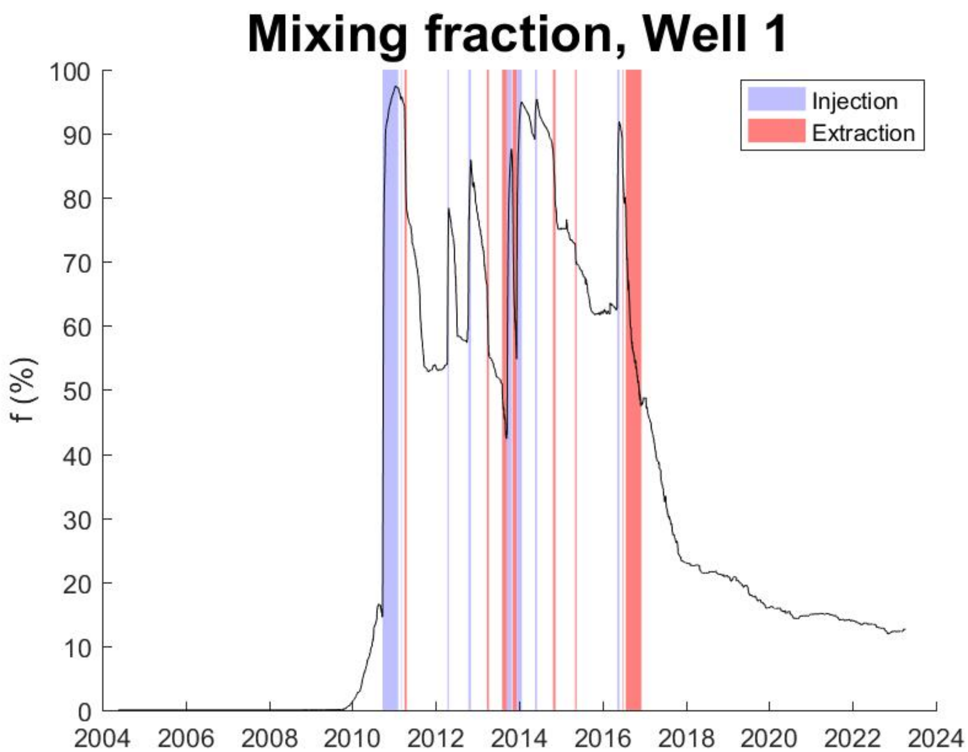

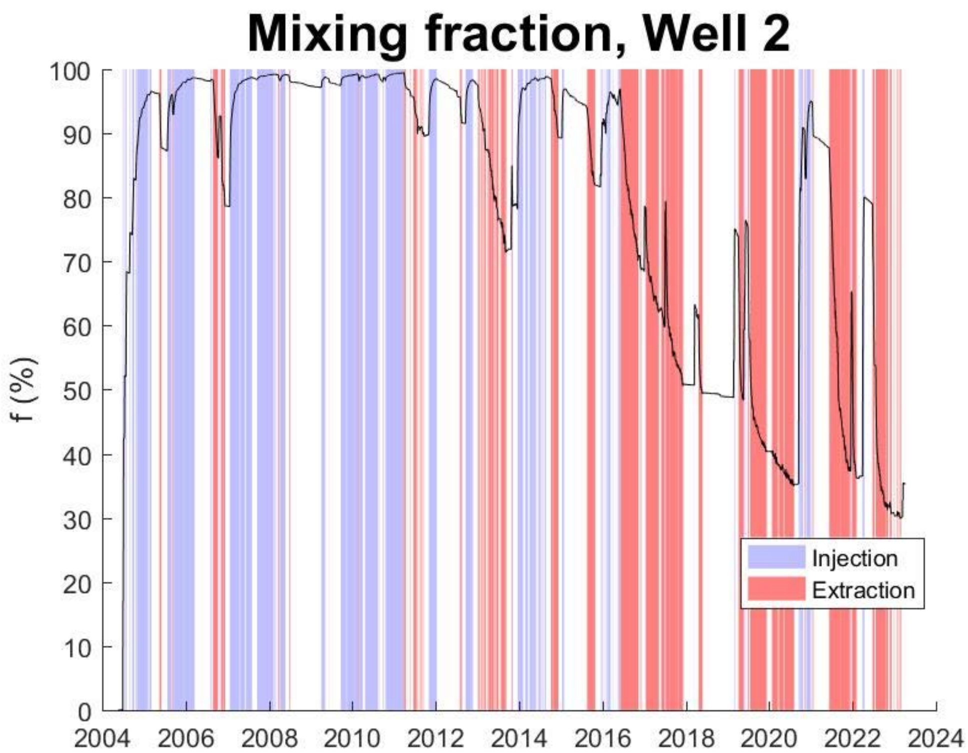
Mixing fraction, Well 2
f (%)
0
10
20
30
40
50
60
70
80
90
100
2004
2006
2008
2010
2012
2014
2016
2018
2020
2022
2024
Injection
Extraction

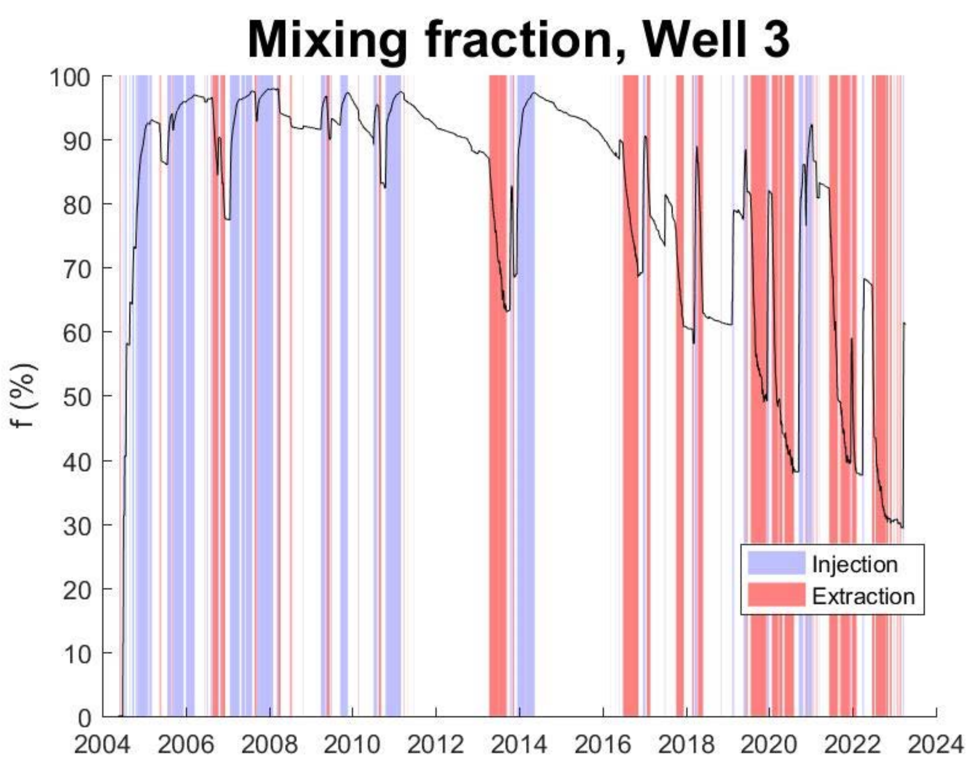
Mixing fraction, Well 3
f (%)
0
10
20
30
40
50
60
70
80
90
100
2004
2006
2008
2010
2012
2014
2016
2018
2020
2022
2024
Injection
Extraction

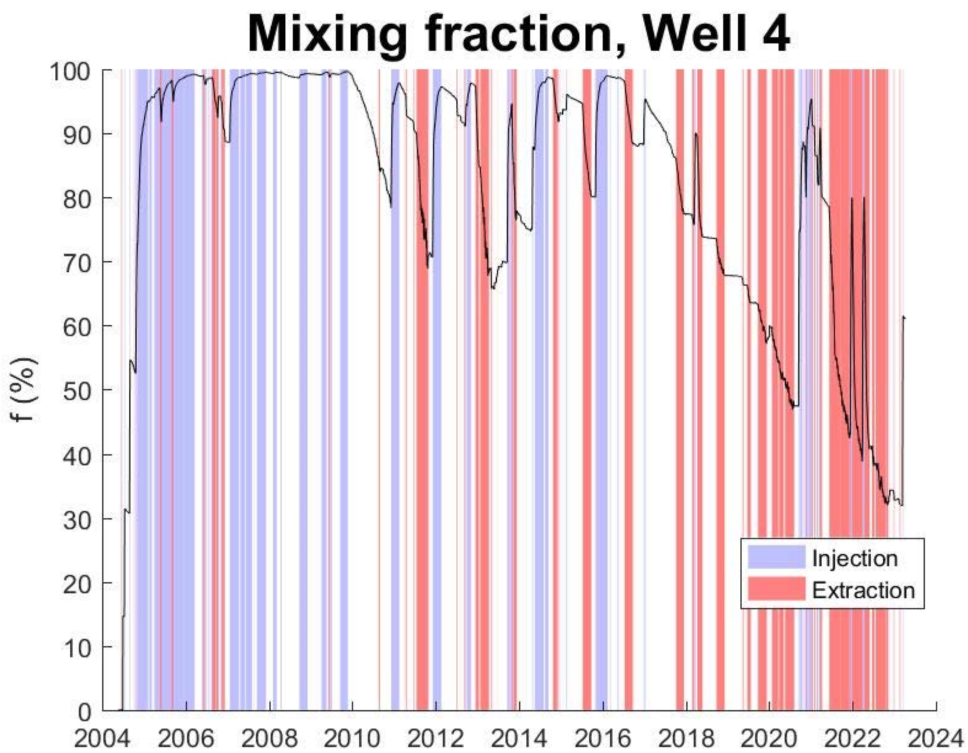
Mixing fraction, Well 4
f (%)
Injection
Extraction

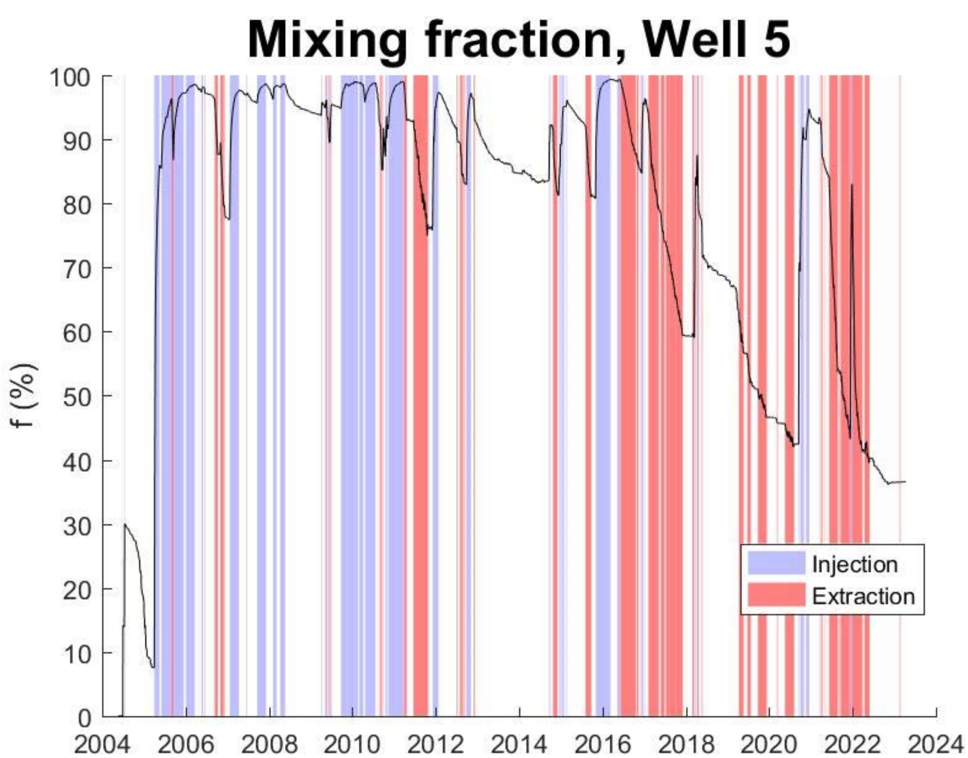
Mixing fraction, Well 5
f (%)
Injection
Extraction

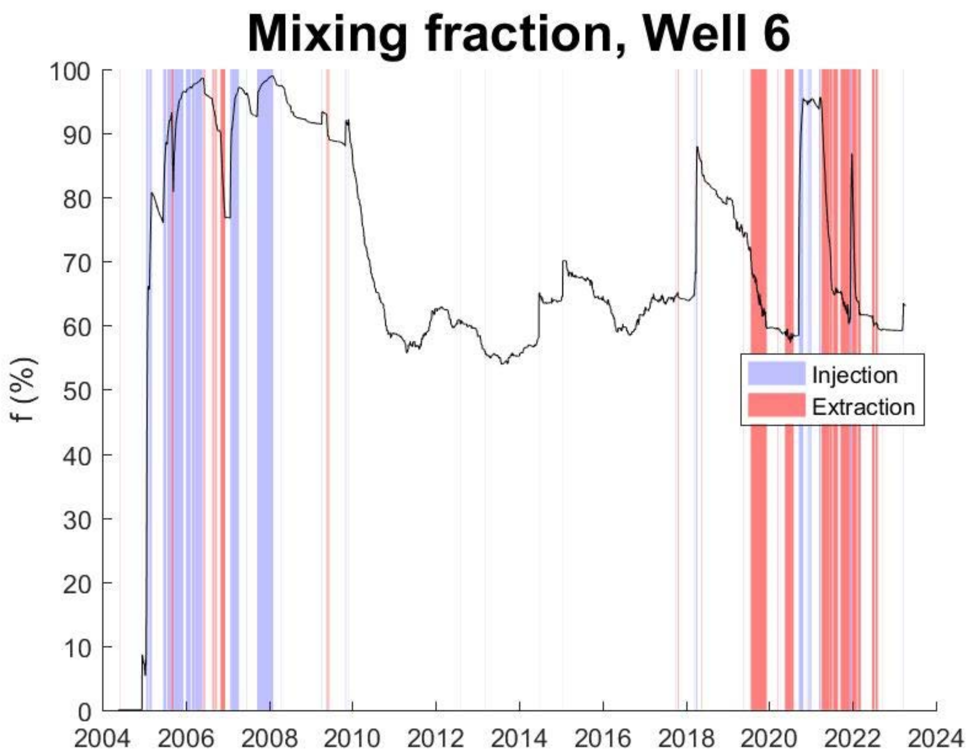
Mixing fraction, Well 6
f (%)
0
10
20
30
40
50
60
70
80
90
100
2004
2006
2008
2010
2012
2014
2016
2018
2020
2022
2024
Injection
Extraction

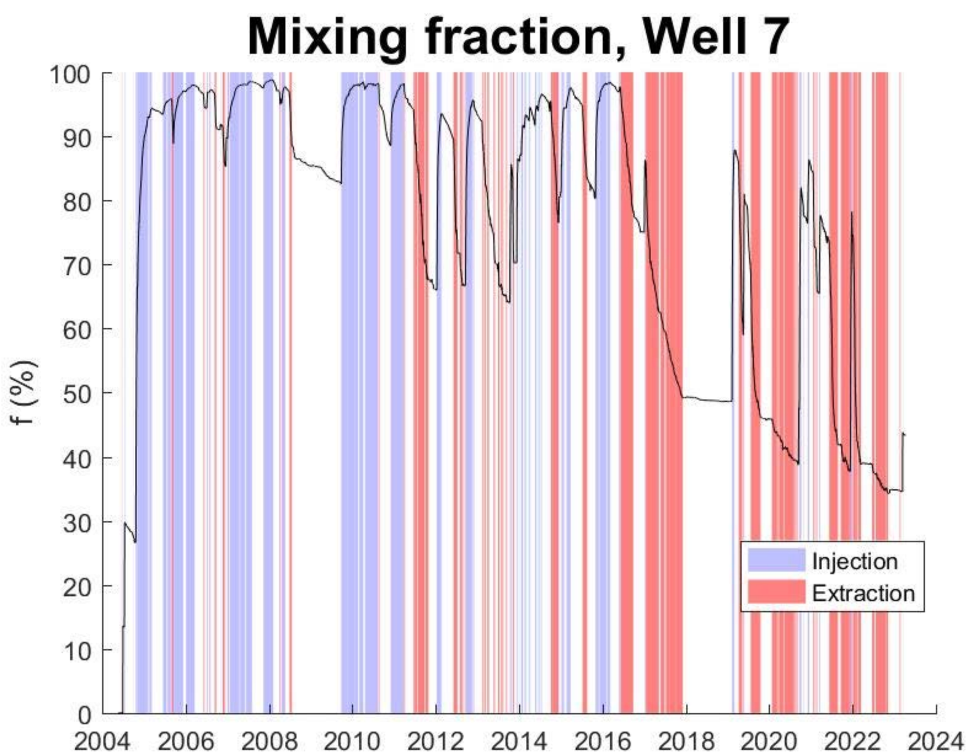
Mixing fraction, Well 7
f (%)
0
10
20
30
40
50
60
70
80
90
100
2004
2006
2008
2010
2012
2014
2016
2018
2020
2022
2024
Injection
Extraction

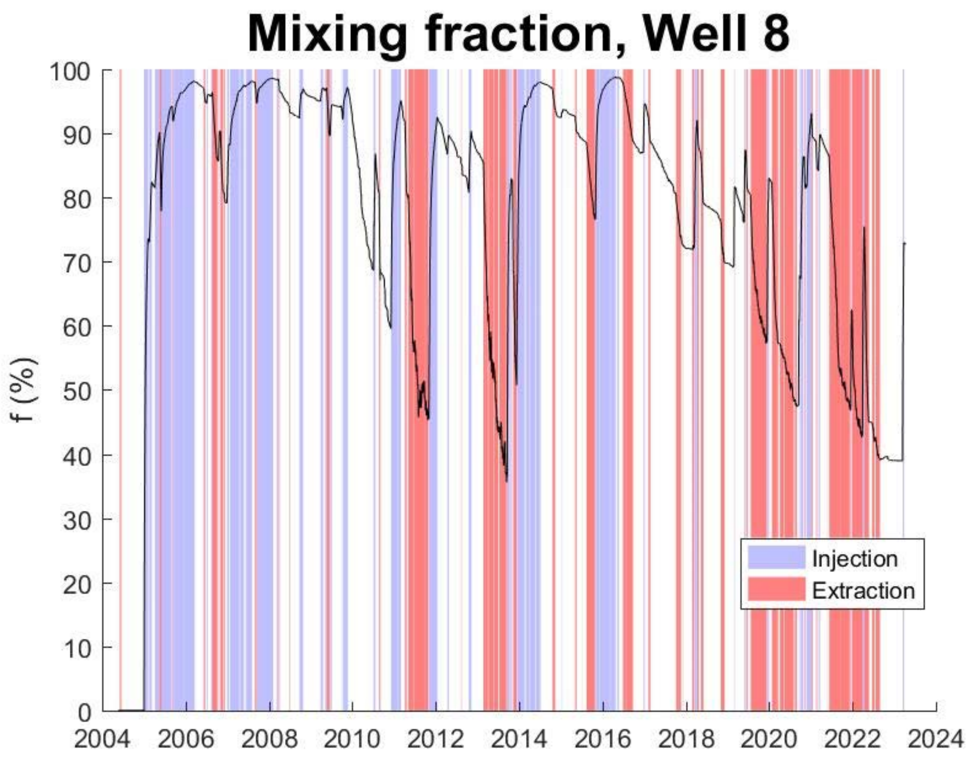
Mixing fraction, Well 8
f (%)
Injection
Extraction
0
10
20
30
40
50
60
70
80
90
100
2004
2006
2008
2010
2012
2014
2016
2018
2020
2022
2024

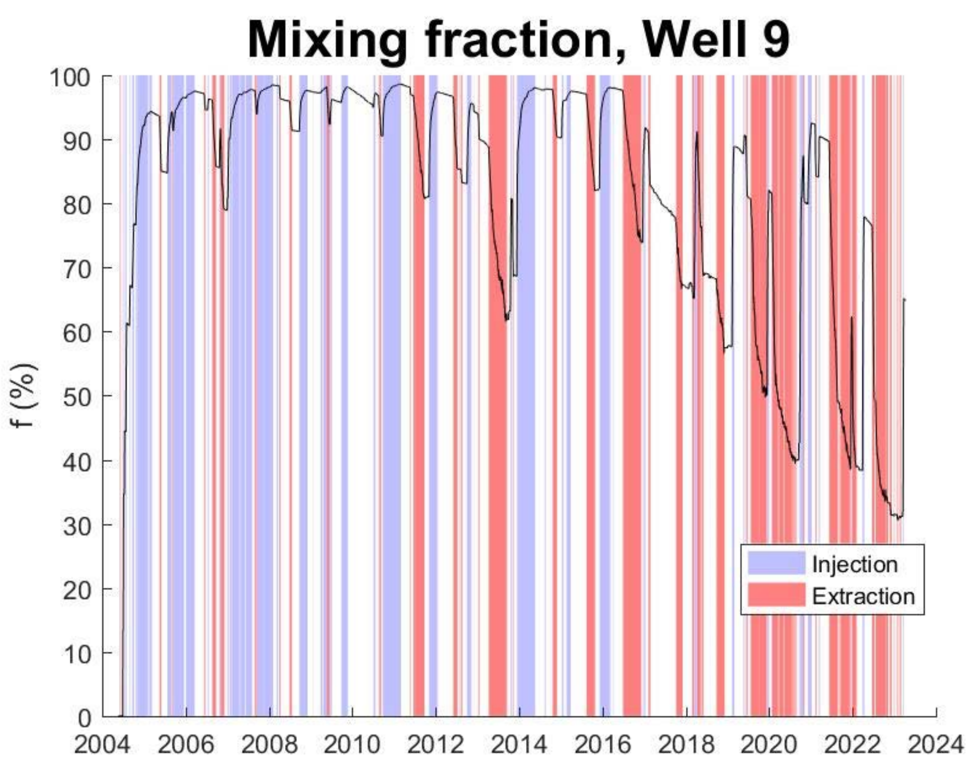
Mixing fraction, Well 9
f (%)
Injection
Extraction
0
10
20
30
40
50
60
70
80
90
100
2004
2006
2008
2010
2012
2014
2016
2018
2020
2022
2024

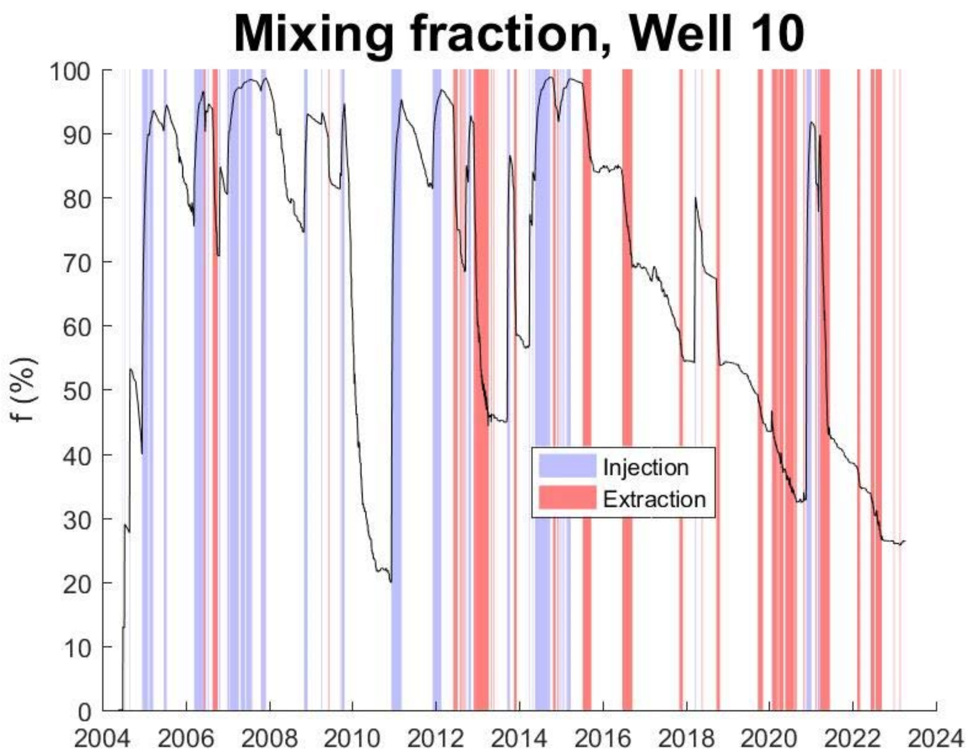

Mixing fraction, Well 10
f (%)
Injection
Extraction
0
10
20
30
40
50
60
70
80
90
100
2004
2006
2008
2010
2012
2014
2016
2018
2020
2022
2024

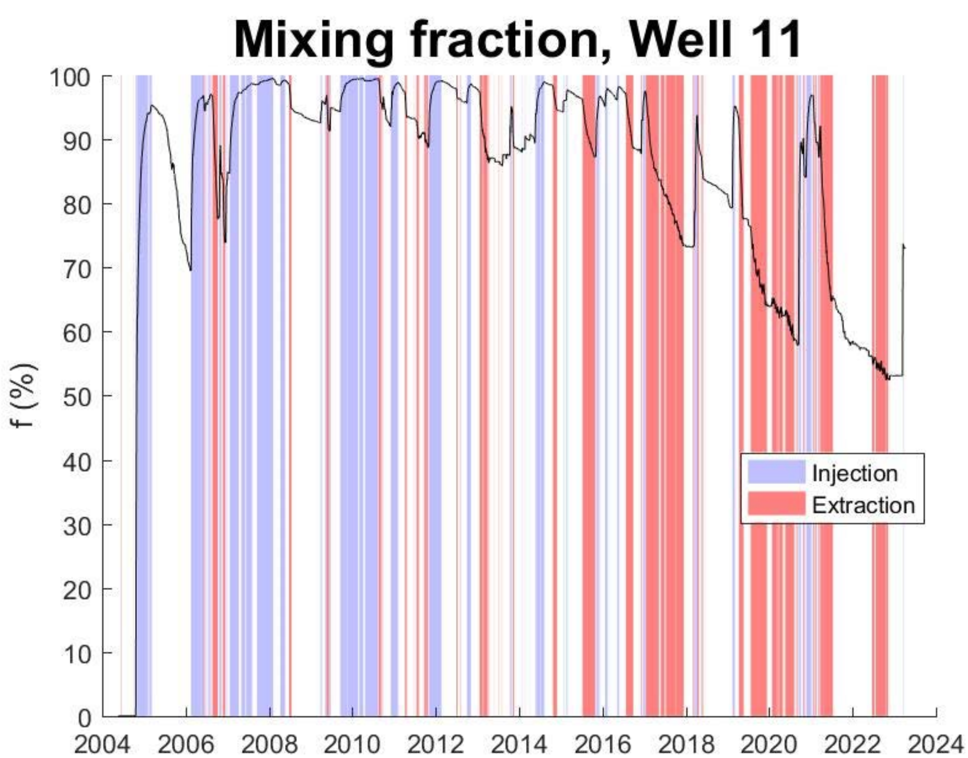

Mixing fraction, Well 11
f (%)
Injection
Extraction
0
10
20
30
40
50
60
70
80
90
100
2004
2006
2008
2010
2012
2014
2016
2018
2020
2022
2024

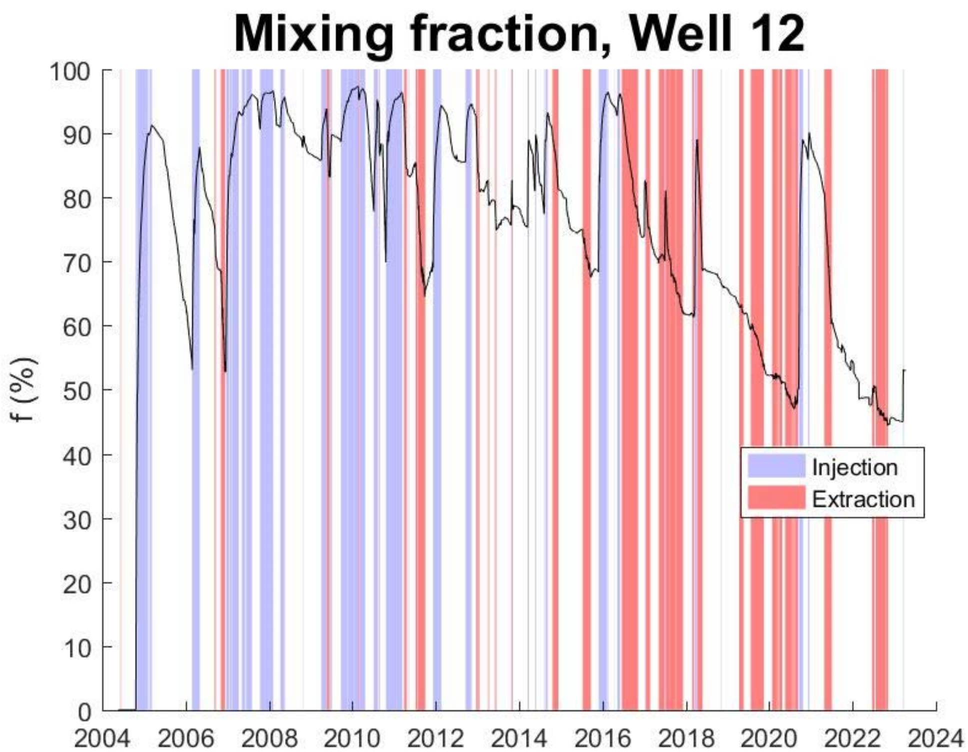
Mixing fraction, Well 12
f (%)
Injection
Extraction
0
10
20
30
40
50
60
70
80
90
100
2004
2006
2008
2010
2012
2014
2016
2018
2020
2022
2024

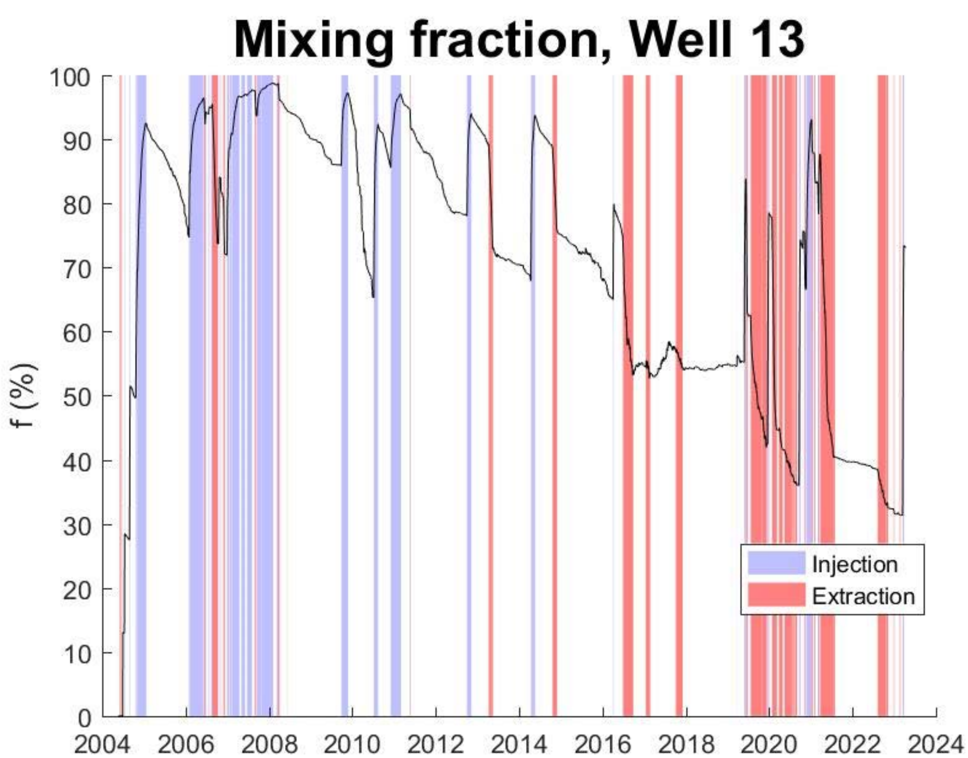
Mixing fraction, Well 13
f (%)
Injection
Extraction
0
10
20
30
40
50
60
70
80
90
100
2004
2006
2008
2010
2012
2014
2016
2018
2020
2022
2024

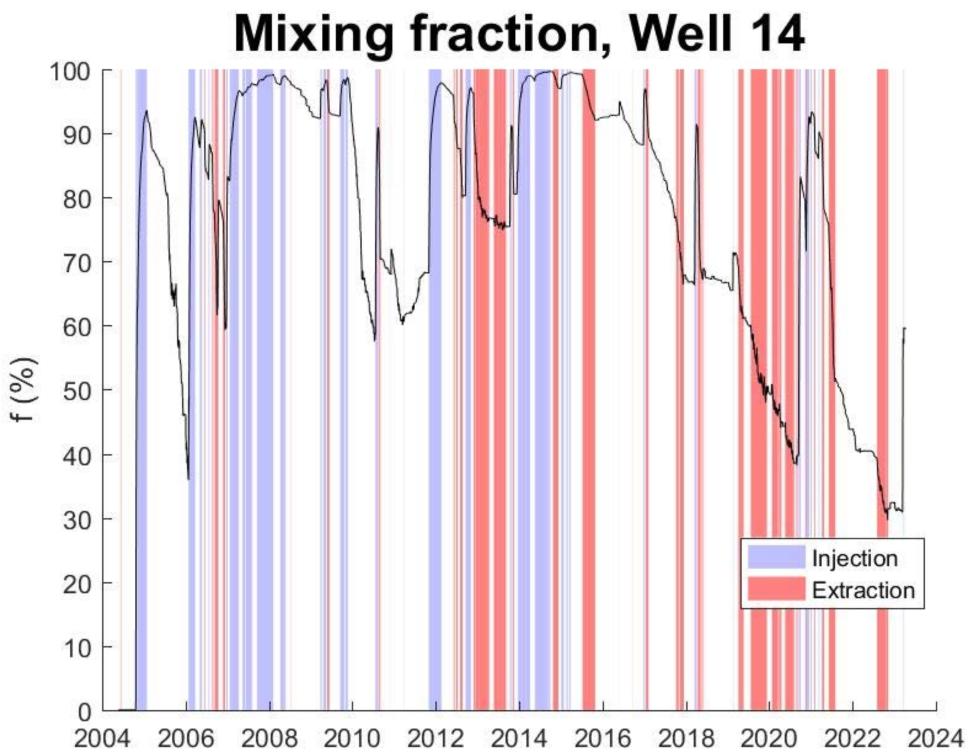

Mixing fraction, Well 14
f (%)
Injection
Extraction
0
10
20
30
40
50
60
70
80
90
100
2004
2006
2008
2010
2012
2014
2016
2018
2020
2022
2024

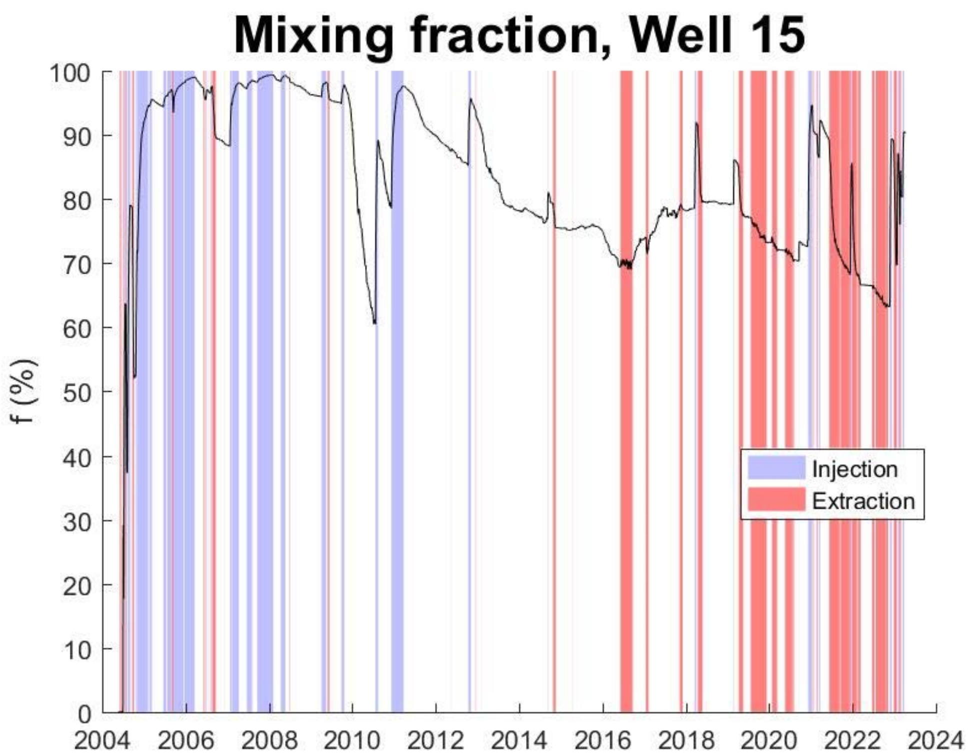

Mixing fraction, Well 15
f (%)
Injection
Extraction
0
10
20
30
40
50
60
70
80
90
100
2004
2006
2008
2010
2012
2014
2016
2018
2020
2022
2024

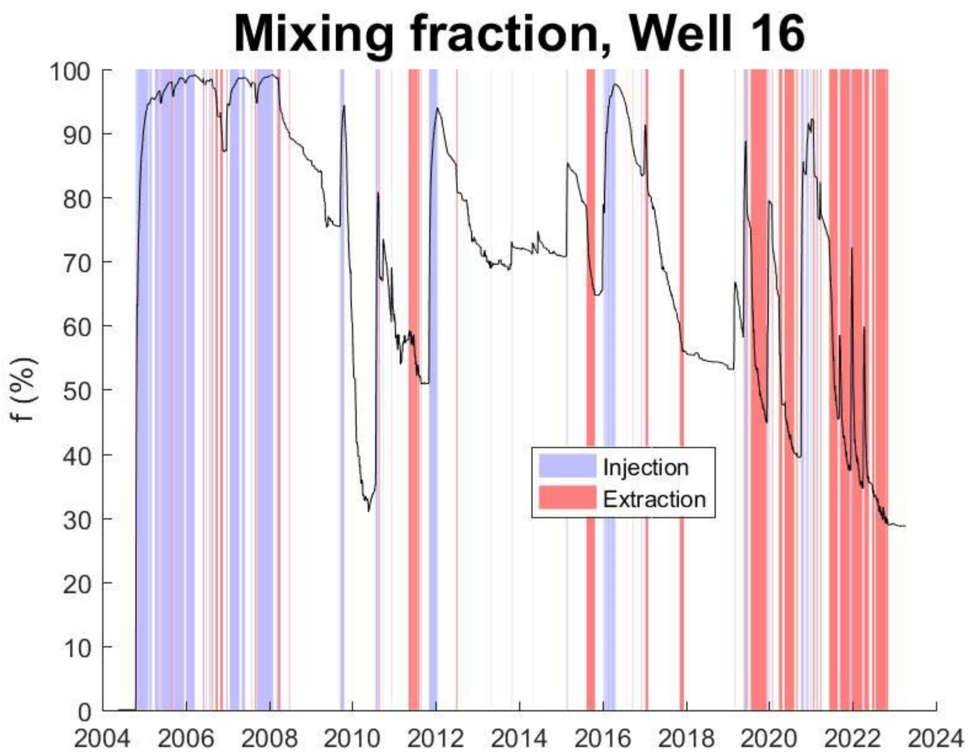
Mixing fraction, Well 16
f (%)
Injection
Extraction
2004
2006
2008
2010
2012
2014
2016
2018
2020
2022
2024

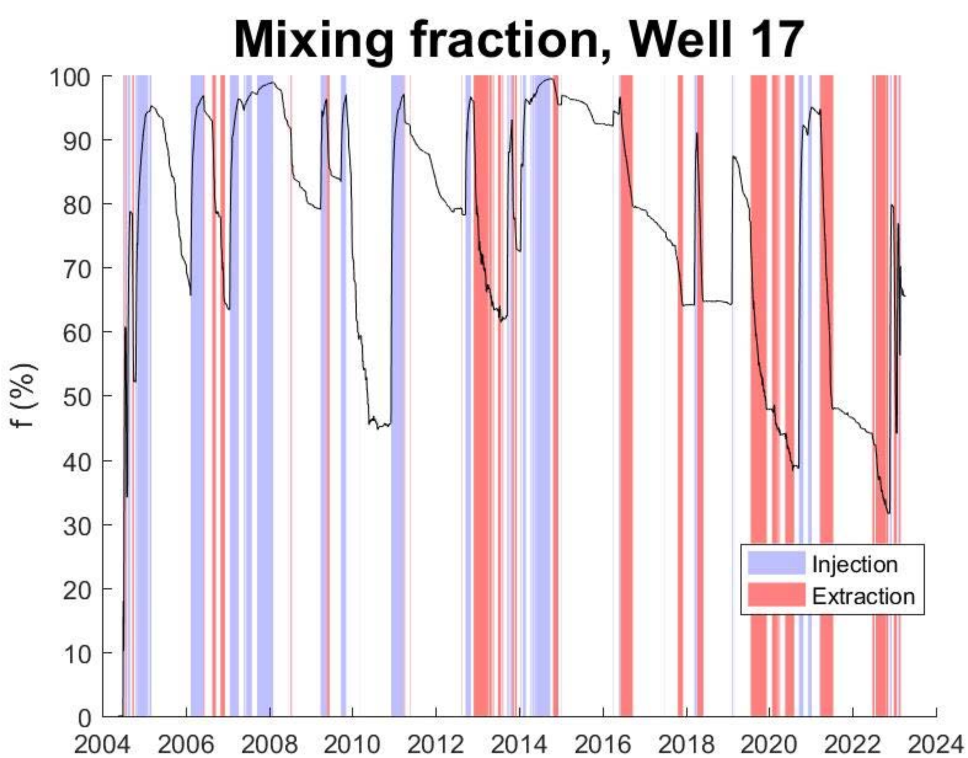
Mixing fraction, Well 17
f (%)
Injection
Extraction
2004
2006
2008
2010
2012
2014
2016
2018
2020
2022
2024

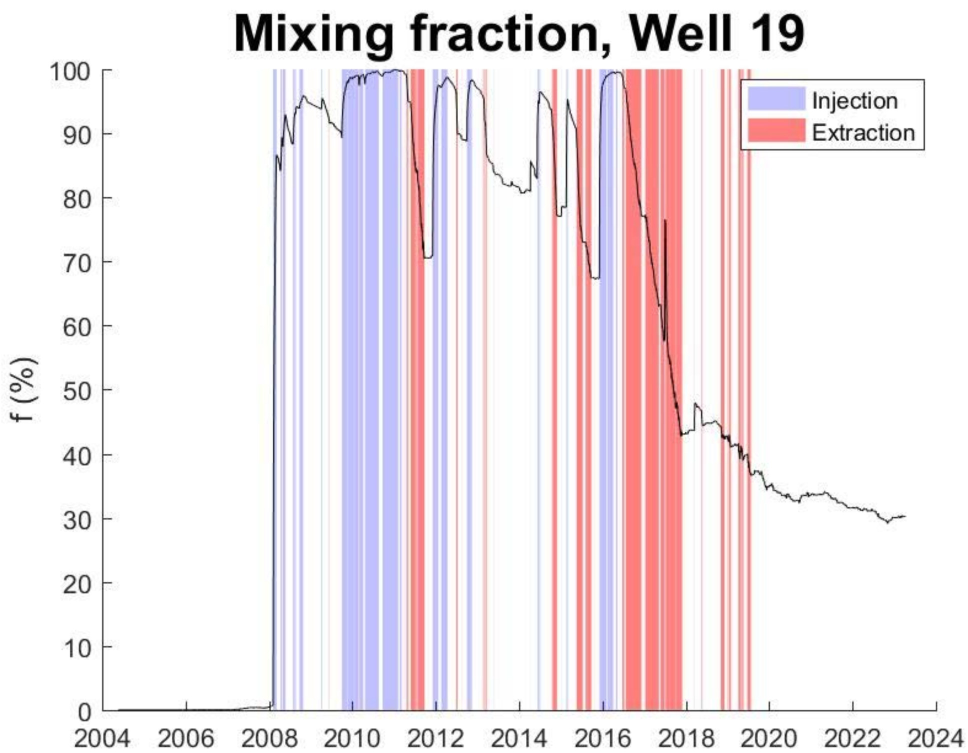
Mixing fraction, Well 19
Injection
Extraction
f (%)
100
90
80
70
60
50
40
30
20
10
0
2004
2006
2008
2010
2012
2014
2016
2018
2020
2022
2024

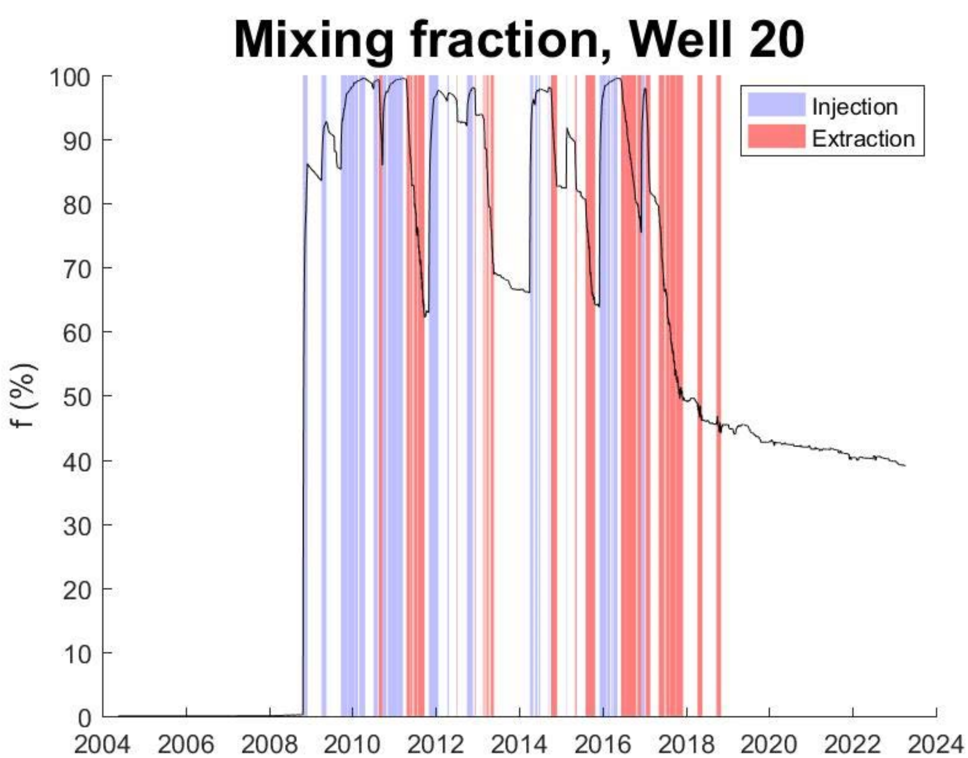
Mixing fraction, Well 20
Injection
Extraction
f (%)
100
90
80
70
60
50
40
30
20
10
0
2004
2006
2008
2010
2012
2014
2016
2018
2020
2022
2024

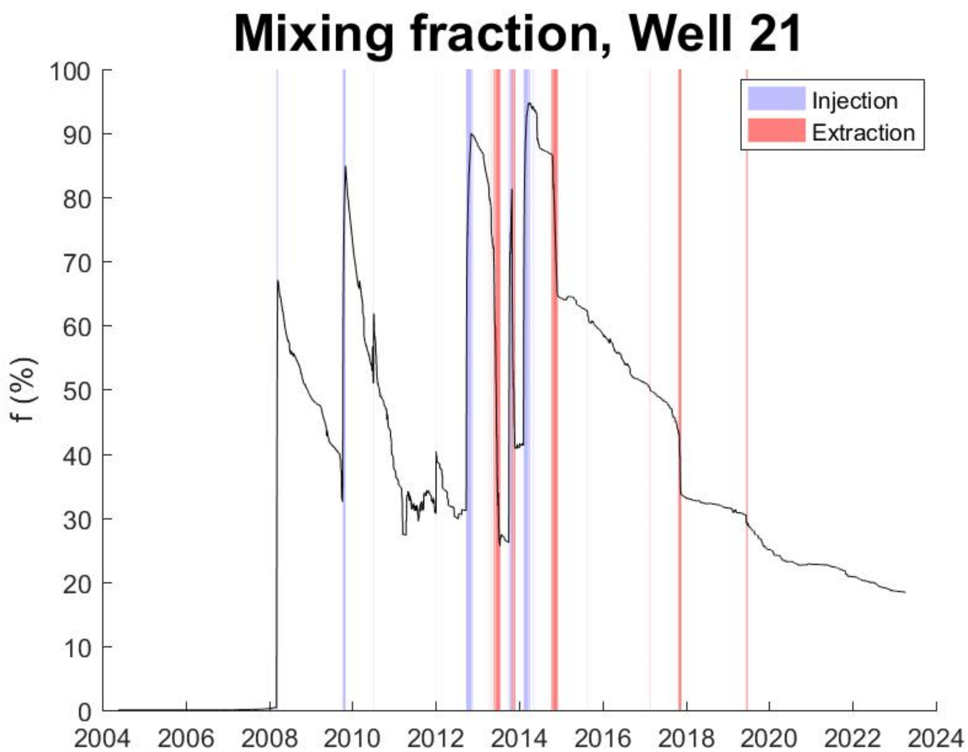
Mixing fraction, Well 21
Injection
Extraction
f (%)
100
90
80
70
60
50
40
30
20
10
0
2004
2006
2008
2010
2012
2014
2016
2018
2020
2022
2024

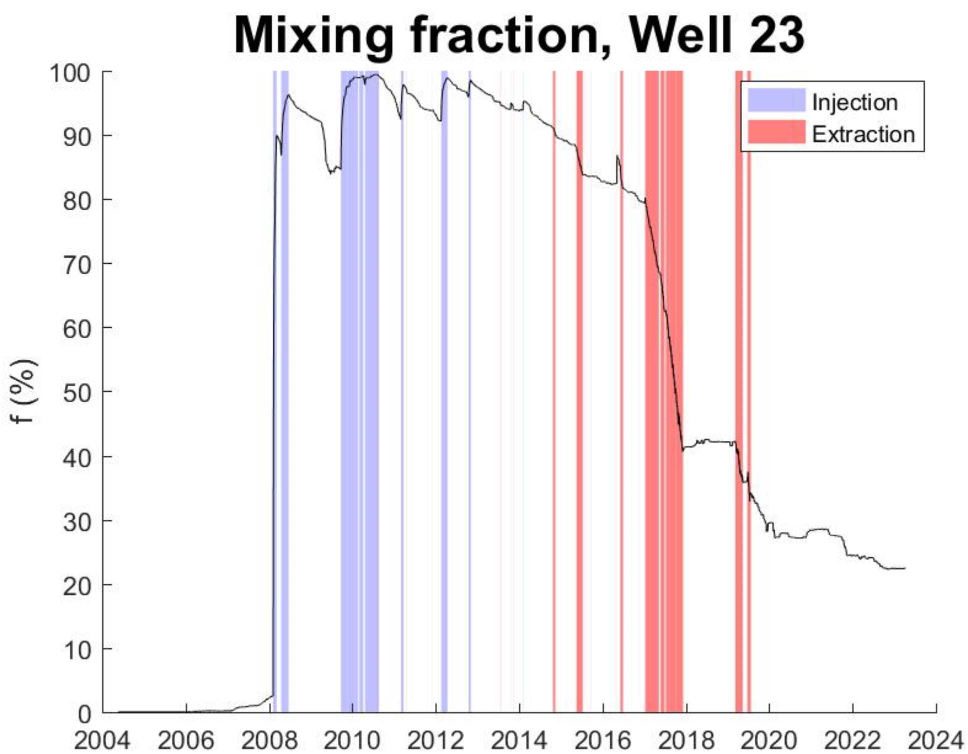
Mixing fraction, Well 23
Injection
Extraction
f (%)
100
90
80
70
60
50
40
30
20
10
0
2004
2006
2008
2010
2012
2014
2016
2018
2020
2022
2024

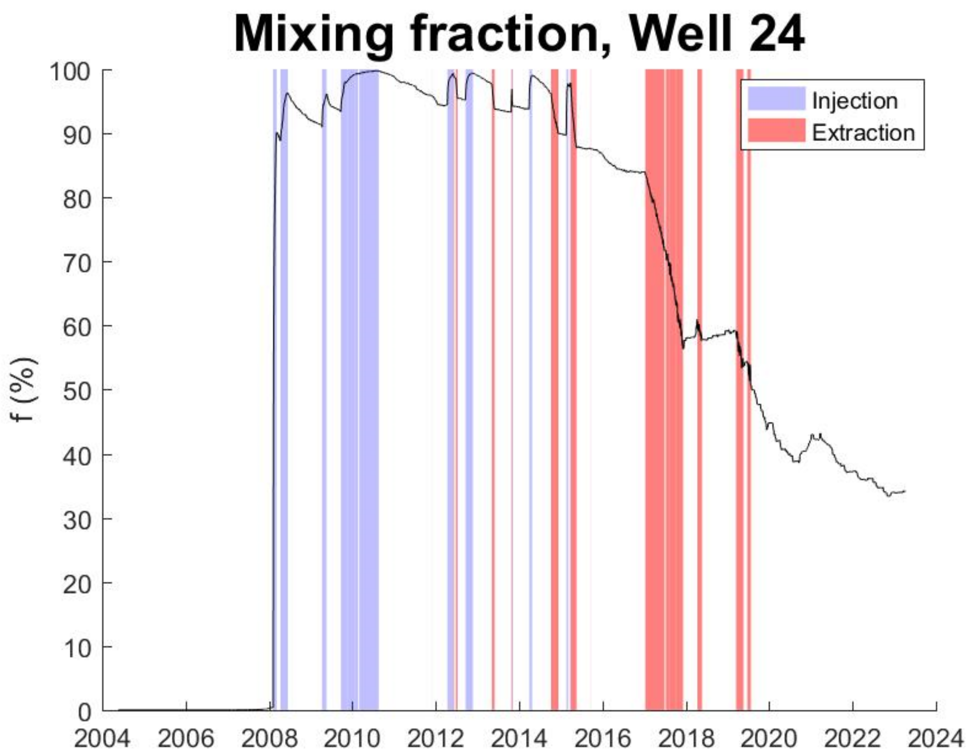

Mixing fraction, Well 24
Injection
Extraction
f (%)
100
90
80
70
60
50
40
30
20
10
0
2004
2006
2008
2010
2012
2014
2016
2018
2020
2022
2024

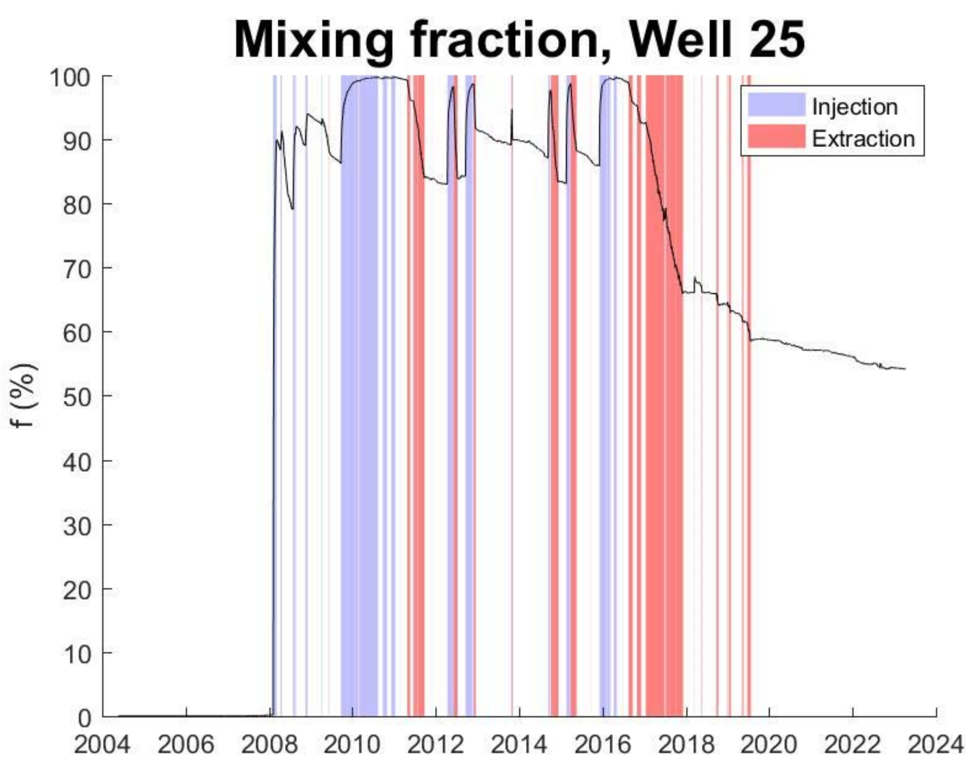

Mixing fraction, Well 25
Injection
Extraction
f (%)
100
90
80
70
60
50
40
30
20
10
0
2004
2006
2008
2010
2012
2014
2016
2018
2020
2022
2024

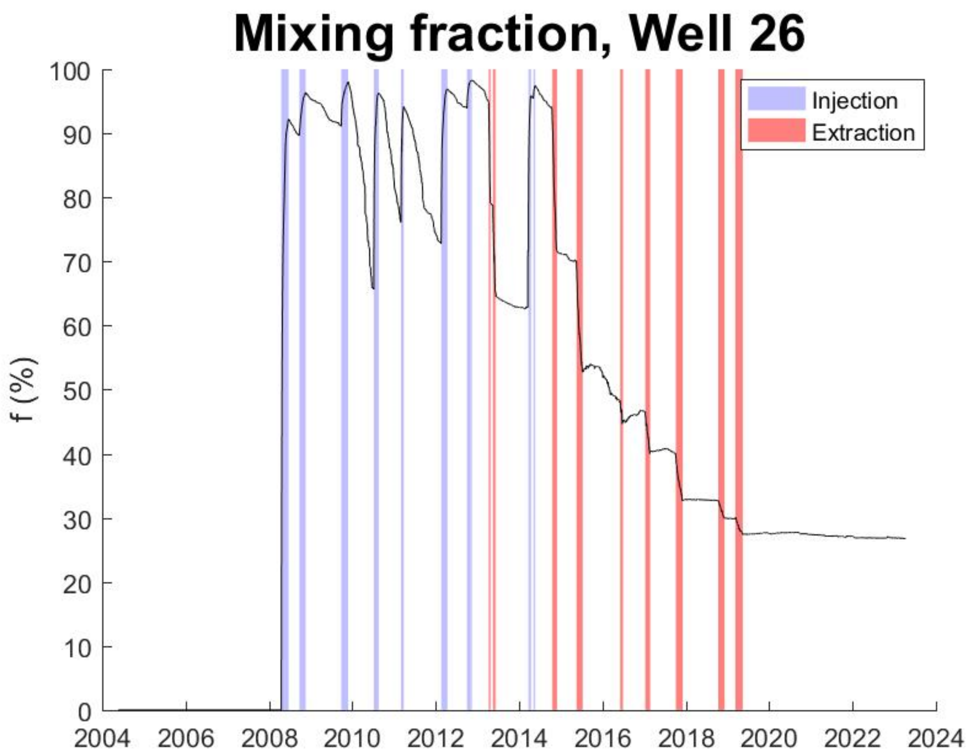
Mixing fraction, Well 26
f (%)
Injection
Extraction
0
10
20
30
40
50
60
70
80
90
100
2004
2006
2008
2010
2012
2014
2016
2018
2020
2022
2024

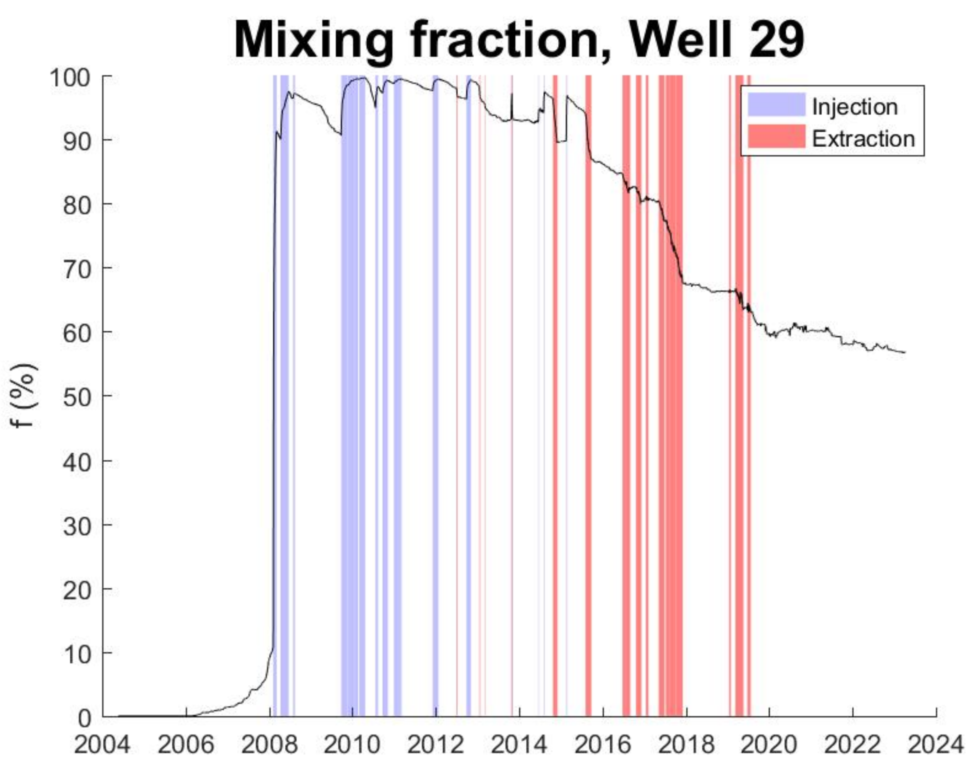
Mixing fraction, Well 29
f (%)
Injection
Extraction
0
10
20
30
40
50
60
70
80
90
100
2004
2006
2008
2010
2012
2014
2016
2018
2020
2022
2024

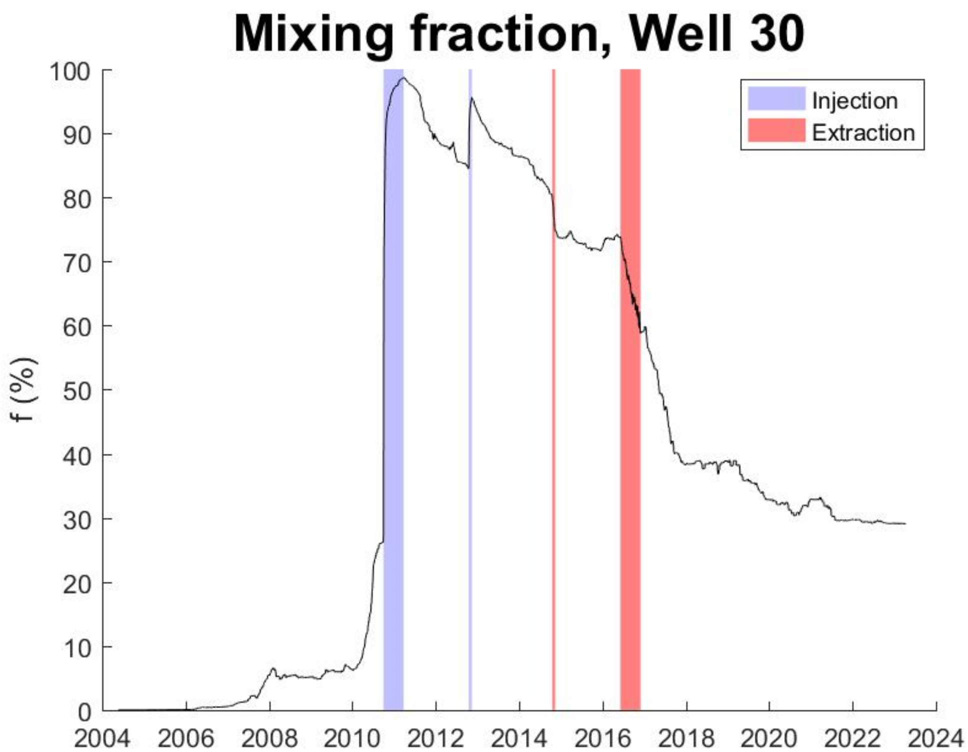
Mixing fraction, Well 30
Injection
Extraction
f (%)
100
90
80
70
60
50
40
30
20
10
0
2004
2006
2008
2010
2012
2014
2016
2018
2020
2022
2024

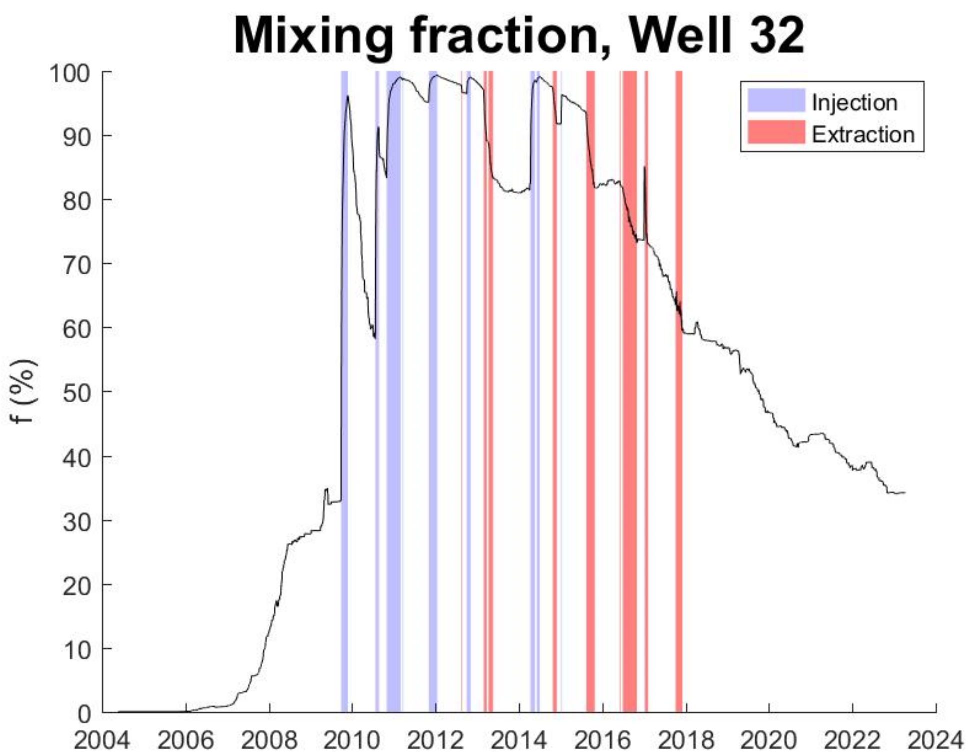
Mixing fraction, Well 32
Injection
Extraction
f (%)
100
90
80
70
60
50
40
30
20
10
0
2004
2006
2008
2010
2012
2014
2016
2018
2020
2022
2024

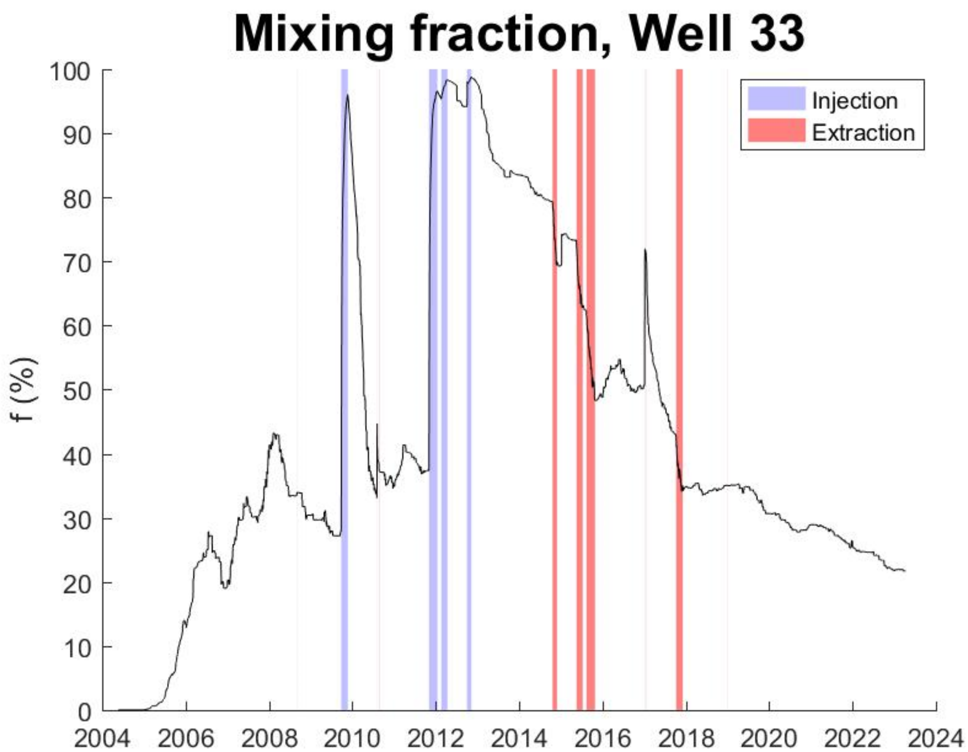
Mixing fraction, Well 33
f (%)
Injection
Extraction
0
10
20
30
40
50
60
70
80
90
100
2004
2006
2008
2010
2012
2014
2016
2018
2020
2022
2024

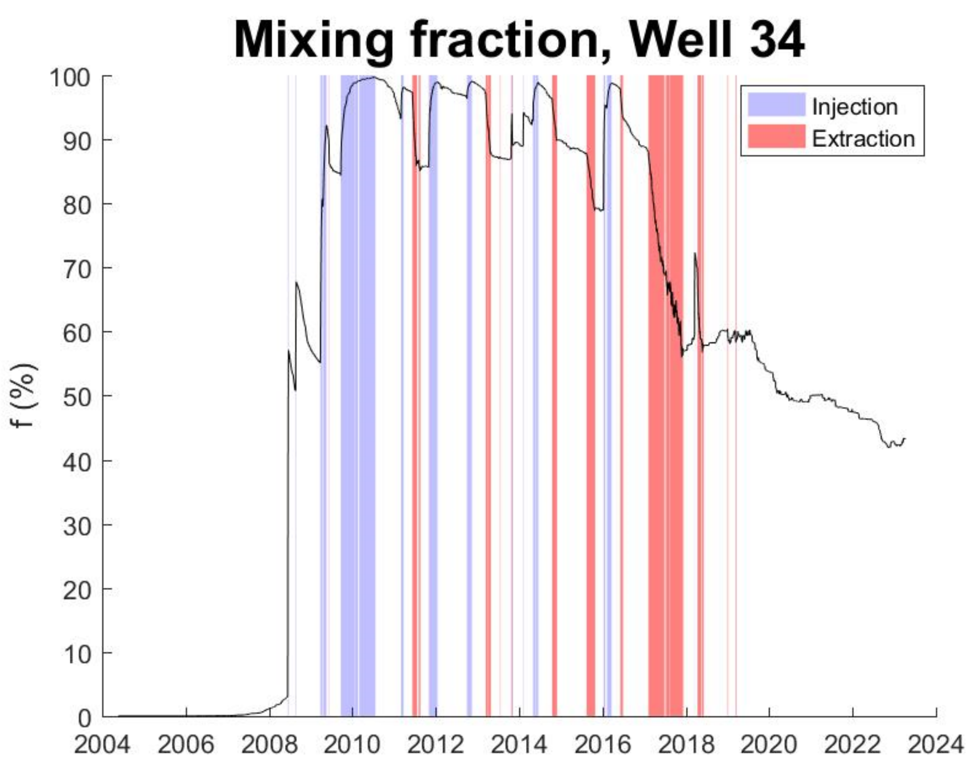
Mixing fraction, Well 34
f (%)
Injection
Extraction
0
10
20
30
40
50
60
70
80
90
100
2004
2006
2008
2010
2012
2014
2016
2018
2020
2022
2024

APPENDIX E

PROCEDURE FOR IMPLEMENTING OTHER REGIONAL GROUNDWATER PUMPING IN GROUNDWATER AVAILABILITY MODEL

1. Obtain raw data from TWDB from Groundwater Use surveys for 2000-2013. These are in monthly values, but some records are aggregated in December.
2. Delete records that are not in the following counties (these are the only counties with data that fall within the active model grid).
    a. BASTROP Or "FAYETTE" Or "caldwell" Or Or "gonzales" Or "bexar" Or "wilson" Or "karnes" Or "atascosa" Or "mcmullen" Or "medina" Or "frio" Or "la salle" Or "uvalde" Or "zavala" Or "dimmit" Or "webb"
3. Change name of following entries to "SOUTH TEXAS ELECTRIC CO OP-PEARSALL PLANT"
    a. SOUTH TEXAS ELECTRIC CO OP-PERSALL PLANT
4. Change name of two following entries to "SASPAMCO PLANT"
    a. MISSION CLAY PRDUCTS CORPORATION-SASPAMCO PLANT
    b. MISSION CLAY PRODUCTS LLC-SASPAMCO PLANT
5. Estimate monthly flows for those rows that only report yearly flows
    a. Estimate the average monthly ratios of flows based on the smallest unit available that matches that row where data is available
        i. County-Basin-Type-Year first
        ii. Basin-Type-Year
        iii. Basin-Year
        iv. Year
    b. Apply the ratios to the annual flow in the rows without monthly data
6. Delete records from SAWS (in Bexar, Atasocsa, or Wilson counties, leave the Gonzales records) – assuming these are the same records as ASR data already included in model
7. Combine monthly data into one row for each facility– don't separate each facility by year anymore.
8. Import Data just on facilities (not flows) into MSAccess TWDB Groundwater Database (GWDB)table called "**2000-2013_ WatSurvey_UniqueLocations** ".
9. Create new table called "**aquifer_layer_link**" to link aquifers codes used to the layers in the GAM
10. MakeTable (**2000_2013_WatSurvey_UniqueLocations_coords**) query = **2000_2013_automatch** by:
    a. Link SurveyName to Owner1 field from welldata table
11. AppendTable (**2000_2013_WatSurvey_UniqueLocations_coords**) query = **2000_2013_manualmatch** by:
    a. Link SurveyName to Owner3 (manually entered to match survey name where appropriate) field from welldata table

        i. Do this for large pumpers and as many pumpers as possible in surrounding counties of Bexar and Atascosa

12. AppendTable (**2000_2013_WatSurvey_UniqueLocations_coords**) query = **2000_2013_append_googled_records** by:
    a. For remaining users in surrounding counties, attempt to match as many as possible by searching for approximate locations on the internet (google maps, other sources)
    b. Reference these based on decimal degrees of latitude and longitude
    c. Not tied to a GWDB state well number
13. Spatial join wells/locations (399 total) to cells from model grid for Queen City / Sparta South GAM
    a. Use this to identify which grid cell each well falls in
14. Export a new table that has all wells from GWDB in Carrizo-Wilcox in correct counties – make sure this table has latitude, longitude, and associated model layer (from aquifer_layer_link).
    a. Create a Theissen polygon map from these wells that identifies which layer the closest well is in
15. Spatial join wells/locations (399 total) to Theissen polygons to identify layers of the unmatched locations (and to check/verify/cross-reference the layers from the GWDB)
16. Delete SWWC DIAMOND WATER COMPANY-RIM ROCK RANCH SYSTEM (Glen Rose and Cow Creek Limestone aquifer) and Cordi marian Villa (Edwards aquifer)
17. Delete the following since they don't fall within model grid: Name (County, River Basin)
    a. Lee County WSC (Bastrop, Colorado)
    b. City of Bastrop (Bastrop, Colorado)
    c. City of Elgin (Bastrop, Colorado)
    d. City of Smithville (Bastrop, Colorado)
    e. Aqua WSC (Bastrop, Colorado)
    f. Bastrop County WCID 1 (Bastrop, Colorado)
    g. Bastrop County WCID 2 (Bastrop, Colorado)
18. After deleting these records, only 324 wells/locations left
19. Associate flows with the correct cells
    a. Distribute flow equally among wells from same user
    b. Then go back and sum by unique wells (179 wells)
20. Need to generate points to implement in GMS
    a. Associate the unique cells with their x and y location and elevation of their centroid
    b. Find that 27 of the cells are actually inactive – discard these pumping rates
        i. Weatherford Engineered Chemistry Well is only in inactive zone by 1 cell (but it's a really small amount of flow, so ignore it anyways)
    c. Import point file into GMS (have x,y,z,FID,name)
    d. Import transient data
        i. Make sure it's in step-wise mode

ii. Associate the FID or name from point file with the correct flows
iii. Make sure these flows are only superimposed onto the existing flows and don’t replace them